Yallourn Rehabilitation Hydrogeological Modelling

Numerical Groundwater Model - Design, Construction and Calibration Report

EnergyAustralia Yallourn Pty Ltd

15 May 2025

→ **The Power of Commitment**

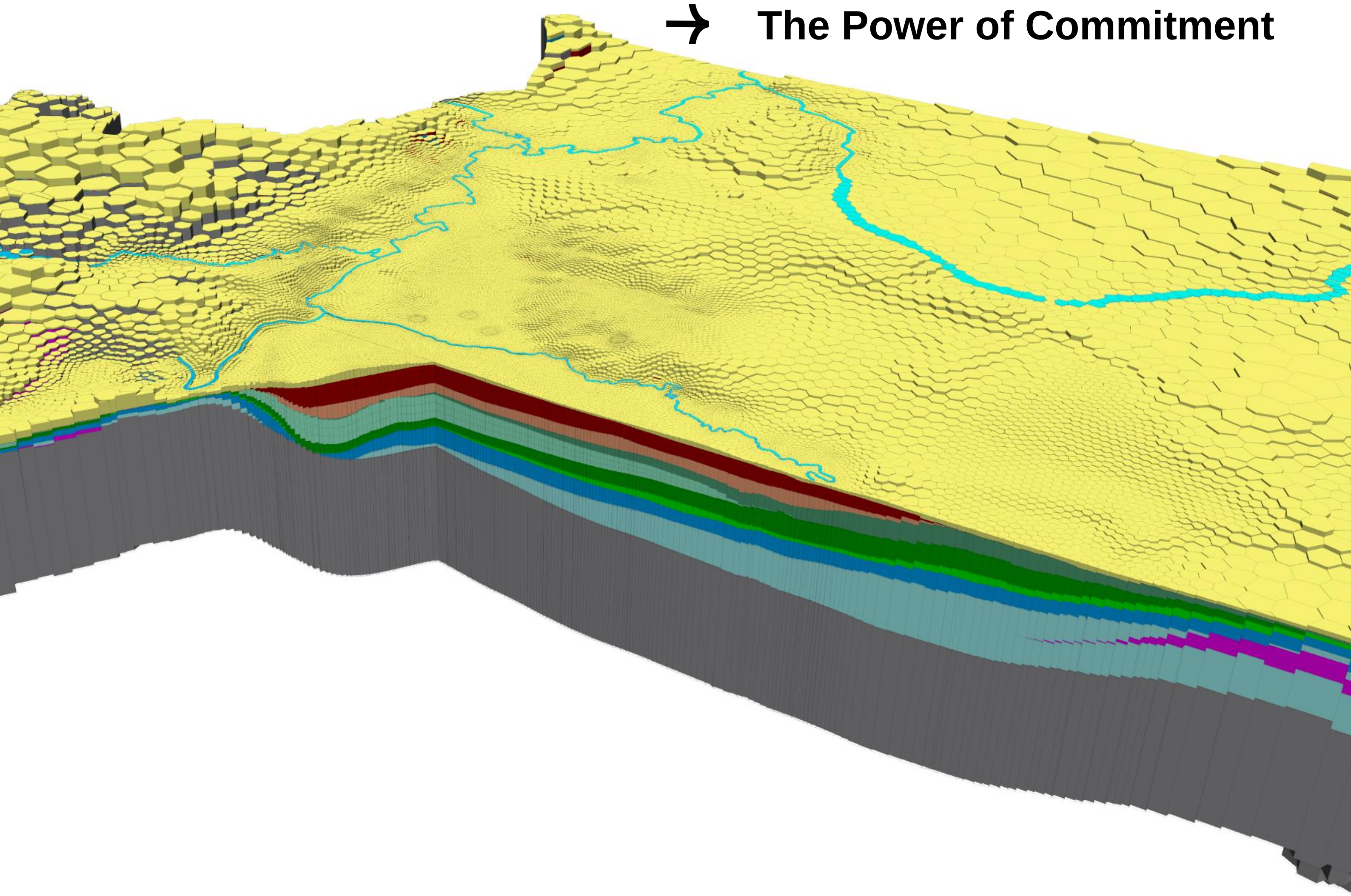

This “Yallourn Rehabilitation Hydrogeological Modelling – Numerical Groundwater Modelling Report” (Report) has been prepared by GHD Pty Ltd (GHD) for EnergyAustralia Yallourn under the “Umbrella (Fixed Period) Agreement – Geotechnical Services” (ref:CW2226566) and the associated “Supplementary Agreement – Geotechnical and Environmental Services Yallourn” (ref: CW2226569) and Purchase Orders (#11005439, #11031504 and #11039186) and relevant sections in this report, provides a list of the information relied upon in preparing this report, and any limitations/assumptions made. This report may only be used or relied upon by:

– EnergyAustralia Yallourn and its related bodies corporate; or
– Any third parties engaged by EnergyAustralia Yallourn or any of its related bodies corporate in respect of activities the subject of such engagement.

Project name	EAY-M Yallourn Mine Rehabilitation Hydrogeological Modelling
Document title	Yallourn Rehabilitation Hydrogeological Modelling | Numerical Groundwater Model - Design, Construction and Calibration Report
Project number	12521481
File name	12521484_REP-0_EAY_GWmodel_DC_Draft1.docx

Status Code	**Revision**	**Author**	**Reviewer**		**Approved for issue**		
			Name	**Signature**	**Name**	**Signature**	**Date**
S4	0	R. Gresswell	G. Foley	Genevieve Foley	G. Foley	Genevieve Foley	15/05/2025
[Status code]							
[Status code]							
[Status code]							
[Status code]							

GHD Pty Ltd | ABN 39 008 488 373
Contact: Rikito Gresswell, Technical Director Hydrogeology | GHD
180 Lonsdale Street, Level 9
Melbourne, Victoria 3000, Australia
T +61 3 8687 8000 | **F** +61 3 8732 7046 | **E** melmail@ghd.com | **ghd.com**

Contents

Table index

Figure index

Appendices

1. Introduction

1.1 Background

EnergyAustralia Yallourn (EAY) is planning for the closure and rehabilitation of the Yallourn Mine in mid-2028, located in the Latrobe Valley approximately 150 km east of Melbourne. The planned rehabilitation of the mine will involve filling of the void to form a pit lake, marking an important hydrogeological transition from the operational phase (involving the excavation of coal and aquifer depressurisation) to the post-mining phase (when the groundwater system reaches a new dynamic equilibrium with respect to the final pit lake level and prevailing climate conditions).

GHD has been engaged by EAY to undertake numerical groundwater modelling of the Yallourn Mine, to support its rehabilitation planning and subsequent implementation. The overarching objective of the modelling is to quantify potential changes to groundwater levels and quantity that may arise from the implementation of proposed rehabilitation, particularly those associated with the changes made to the groundwater extraction regime and the interaction between the pit lake and groundwater systems (during and after filling). Outputs from the numerical groundwater model are required to inform the aquifer depressurisation program (to ensure safe mining and rehabilitation conditions), pit water balance and water quality modelling (based on the volumes of pit water that may be lost to and gained from the groundwater systems) and potential changes to the shallow groundwater regime arising from the presence of a full pit lake (and how this may influence interactions with the surface water systems and ecosystems that are depended on these interactions).

1.2 Purpose of this report

The purpose of this report is to provide detailed descriptions of the design, construction and calibration of the numerical groundwater model developed to inform the rehabilitation planning for the Yallourn Mine. The hydrogeological conceptualisation or “conceptual model” that underpins the development of the numerical model is described separately in a GHD report titled: *Yallourn Rehabilitation Hydrogeological Modelling – Hydrogeological Conceptual Model* (dated September 2023). References are made to GHD (2023b) throughout this report to highlight linkages between the conceptual and numerical models and to provide the necessary context for translating hydrogeological concepts into a quantitative modelling framework. Detailed descriptions of the site setting and associated figures are included in GHD (2023b) and are not duplicated in this report except where these are deemed relevant for specific aspects of the model design, construction and calibration.

The design and construction of the groundwater model documented in this report have been preceded by the Design Basis memorandum prepared by GHD, dated July 2023 (GHD, 2023a). The purpose of the Design Basis memorandum was to clearly outline the assumptions and sources of information used to inform the model development, and to serve as a record of formal model planning process having taken place prior to the completion of the modelling. As stated in the memorandum, some of the assumptions made at the planning stage are subject to change and more detailed descriptions and discussions are provided in this report (based on the findings of the modelling and calibration).

There is a long history of groundwater modelling in the Latrobe Valley and a substantial amount of modelling has been undertaken to date to support the operation and rehabilitation planning for the Latrobe Valley coal mines using the Latrobe Valley Regional Groundwater Model (LVRGM) developed and maintained by GHD for the Latrobe Valley mines. The LVRGM was originally designed to simulate the significant aquifer depressurisation effects within the deep confined aquifers (particularly those associated with the Hazelwood and Loy Yang mines and to a smaller extent by the Yallourn Mine) and regional subsidence arising from them. The capability of the LVRGM has been greatly expanded in recent years to include more detailed simulations of near surface processes and effects of climate change (refer to Section 3.3.2 of GHD, 2023b for further details).

The main point of difference between the LVRGM and the modelling required to inform the rehabilitation planning for the Yallourn Mine is that the aquifers (both confined and unconfined) and hydrogeological processes of interest for the Yallourn Mine are associated with parts of the Latrobe Valley groundwater systems that are shallower than those affected by the neighbouring Hazelwood and Loy Yang mines. The significant depressurisation of the deep confined aquifers at Hazelwood and Loy Yang, while relevant, is not the main focus of the modelling at Yallourn and there is a greater need to understand the effects of rehabilitation on the shallow groundwater system due to the mine's proximity to major surface water features (such as the Morwell River and Latrobe River). Furthermore, the location of the mine adjacent to major geological structures such as the Haunted Hills Fault/Yallourn Monocline and Moe Swamp Basin means the modelling for the Yallourn Mine is required to consider a spatial extent that is different to the domain of the LVRGM (refer to Figure 1, showing the conceptual model domain defined in GHD, 2023b).

For these reasons, the groundwater modelling for the Yallourn Mine needs a more targeted approach focusing on specific processes that are relevant to its rehabilitation planning (necessitating a separate model that is locally refined at the Yallourn Mine and relevant hydrological features). The main advantage of the LVRGM is that the outputs from the regional scale modelling can be readily extracted and used to set the boundary conditions for the more localised Yallourn Mine model, enabling the effects of aquifer depressurisation from the adjacent mines to be simulated in a highly efficient manner. This minimises the computational burden and model pre-processing time, allowing more effort to be directed at modelling mine-scale processes of interest for rehabilitation of the Yallourn Mine. The outputs from the 2020 version of the LVRGM, updated for the Latrobe Valley regional committee (as part of the 2015 to 2020 5-year update), have been used for the calibration of the Yallourn Mine model.

1.3 Modelling approach

1.3.1 Staged approach

Groundwater modelling described in this report has been undertaken in a staged manner, consistent with the recommendations of the Australian Groundwater Modelling Guidelines (AGMG; Barnett et al, 2012). The model planning stage involved a workshop with EAY and the independent peer review team in December 2019 to identify key rehabilitation issues relevant to groundwater and set out expectations for the modelling (GHD, 2020). The model planning was followed by the development of a hydrogeological conceptual model, which commenced in 2020 and involved several iterations based on the feedback from the independent peer review process and as additional data became available. The findings of this conceptualisation stage are documented in GHD (2023b), describing the essential features of the groundwater system and its behaviour before, during and after mining.

This report describes the design, construction and calibration of the numerical groundwater model, building on the prior works completed as part of the planning and conceptualisation stages. The report has been structured to follow the key stages of the AGMG so that the findings of the modelling are presented in a clear and logical order. The report includes:

– Section 2, describing the design and construction of the model including the model grid, model layers, boundary conditions and parameterisation (stages 3 and 4 of the AGMG)
– Section 3, describing the calibration of the model to available data (stage 5 of the AGMG)
– Section 4, describing the results of post-calibration verification of the model (stage 5 of the AGMG)

1.3.2 Target confidence level

When a groundwater model is used to inform the outcome of a particular future scenario, the level of confidence in the model's outputs depends fundamentally on the data used to calibrate the model and their relevance to the hydrological processes of future scenarios. It follows that a model that is required to predict responses to hydrological stresses that are similar to those of the past and for a period of time similar to the period of historical observations would have high confidence in its predictions, provided that the model has been adequately calibrated and the results of the model are mathematically sound. This forms the basis of the confidence level classification of the AGMG (Barnett et al., 2012).

The groundwater modelling for the Yallourn Mine benefits from the knowledge gained over more than 100 years of mining and the substantial amount of hydrogeological data collected over that time, particularly in the last 40 years (GHD, 2023b). The depressurisation of the confined aquifers beneath the floor of the mine has resulted in up to around 100 m of drawdown in piezometric heads, with the stress-response (cause and effect) relationships clearly reflected in the measurements of groundwater levels and record of pumping rates. The monitoring adjacent to surface water features provides insights into the nature of interaction between the shallow groundwater and surface water systems. On the basis of information available, a target confidence level of two with some attributes of three is considered appropriate (moderate to high confidence).

The uncertainty guidelines recently revised by the Independent Expert Scientific Committee (IESC) (Peeters and Middlemis, 2023) suggest the confidence level classification is no longer a useful measure of whether or not the model is fit for purpose, and more efficient and effective uncertainty analysis should be undertaken to address recognised data gaps and limitations of groundwater models. Model calibration and associated findings, as documented in this report, would inform the future uncertainty analysis of the rehabilitation scenarios.

1.4 Model expectations and limitations

The groundwater model described in this report is of regional scale, extending beyond the footprint of the Yallourn Mine to account for the larger area of influence of aquifer depressurisation at the mine and the cumulative effect arising from the operation and rehabilitation of the neighbouring Hazelwood and Loy Yang mines. The model uses the unstructured grid capability of MODFLOW-USG to improve accuracy in areas of interest and to simulate mine scale processes within a regional domain.

The design, construction and calibration of the model described in this report are based on the requirement of the groundwater model to ultimately assist with the rehabilitation planning (and beyond, to assess the performance of rehabilitation following implementation). The key mine-scale hydrogeological processes of interest for mine rehabilitation are ongoing aquifer depressurisation and subsequent recovery, pit lake and groundwater interactions (and volume of water exchanged between the two systems), groundwater flow within and across hydrostratigraphic units (inter-aquifer connections) and shallow groundwater dynamics (and interactions with the surface water systems). The outputs from the model are required to assist with other technical studies undertaken in parallel to inform the planning and implementation of rehabilitation (e.g. pit lake water balance and quality modelling).

As with all numerical groundwater modelling studies, there are some practical constraints and limitations with the model described in this report. All groundwater models are fundamentally a mathematical representation of natural physical systems, using a finite number of cells and parameters to simulate the movement of groundwater through layers of rocks and sediments. This simplification inherent in modelling means it is not possible for a single model to simulate hydrogeological processes (and groundwater behaviour) occurring at all spatial scales, particularly those at scales smaller than the resolution of the underlying model. Equally, it is not possible for a model to perfectly replicate the real-world observations of groundwater systems, which are often complex and highly variable. Uncertainty is therefore inherent in modelling and the outputs of the modelling presented in this report should be considered in this context.

The groundwater model described in this report has been primarily designed to simulate the groundwater behaviour in transmissive aquifer units, where the effects of hydrogeological stresses such as pumping are transmitted and where the groundwater systems are sensitive to near surface processes (such as recharge and interactions with the surface water systems). The intervening coal layers are conceptualised and simulated as aquitards that generally limit the hydraulic connections with the adjacent aquifer layers except near the mine, where the coal material properties are enhanced (increased hydraulic conductivity) to simulate the effects of joints and fractures due to ground movement. The model is not designed to accurately simulate the pore pressure behaviour within the coal batters, which is complex and locally variable depending on the presence of discrete joints and how these are connected with hundreds of horizontal drains used to drain the coal. This does not fundamentally affect the model's intended use, as the groundwater behaviour in the transmissive aquifers are controlled primarily by pumping, mine drainage and near surface hydrological processes (such as recharge that maintains the water table above the coal batters) and the net fluxes exchanged between the future mine pit lakes and groundwater systems depend on the bulk (average rather than local) aquifer properties.

As stated in GHD (2023b), the rehabilitation of the Yallourn North Open Cut (YNOC) will be driven by the EPA Landfill Licence process and is not the focus of the modelling detailed herein. The YNOC is located to the north of the Haunted Hills Fault/Yallourn Monocline and is hydraulically poorly connected with the mine (refer to Section 4.8.2.3 of GHD, 2023b). The presence of this landfill and local scale pumping are therefore simulated in the model in a simplified manner (using a fill material property zone and a well boundary condition).

Groundwater modelling is an iterative process, with feedback expected between data collection, conceptualisation and simulations (calibration, prediction and verification). Ongoing updates to the model before, during and after rehabilitation would improve the model confidence over time as additional data become available. The groundwater model for the Yallourn Mine has been designed to facilitate this process, using PEST utilities and custom scripts (written in python and fortran) to automate key modelling tasks and enable progressive assimilation of additional data in an efficient manner.

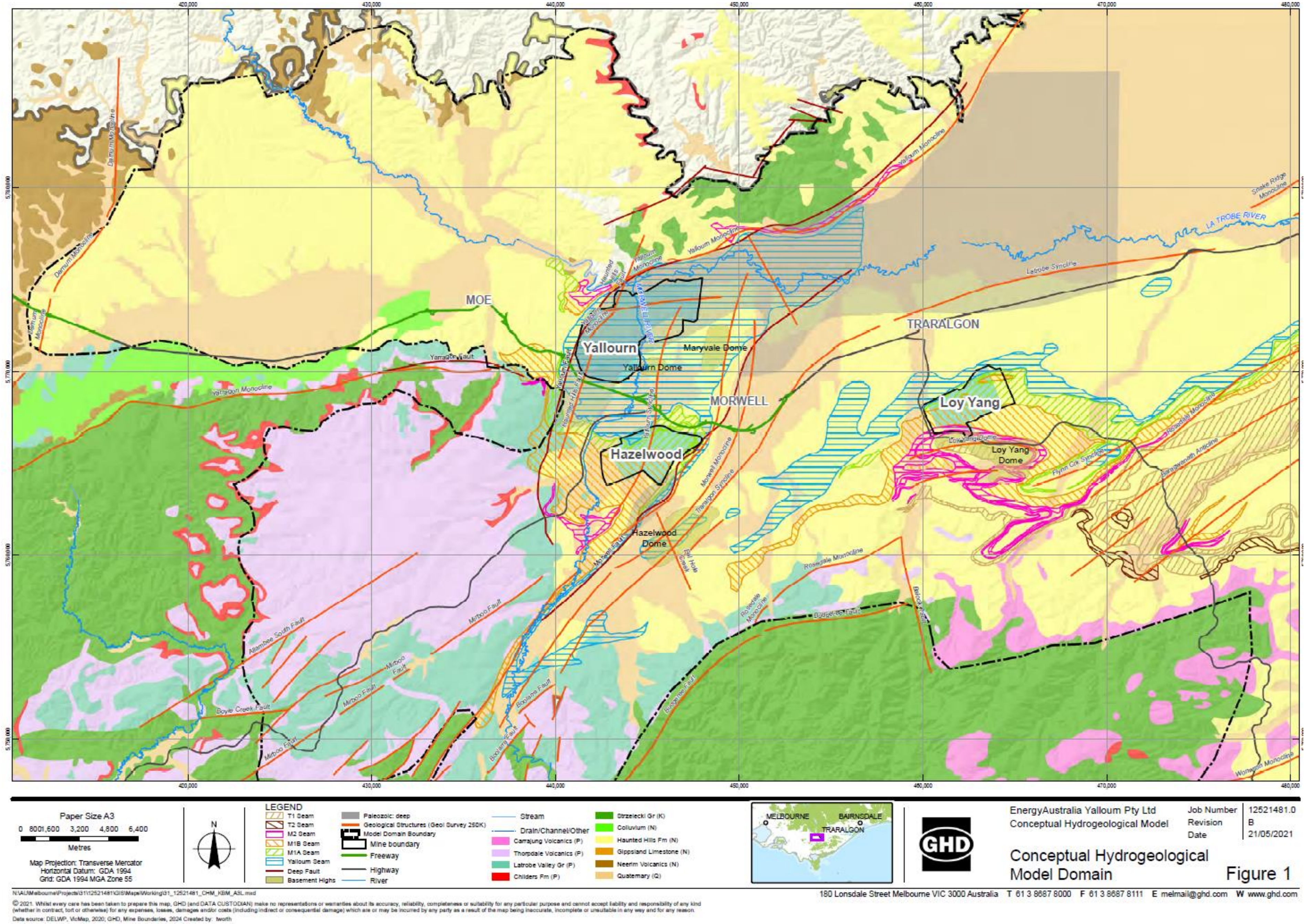

Figure 1 ***Conceptual Hydrogeological Model Domain (after GHD, 2023b)***

2. Model design and construction

2.1 Modelling software

For this project, an unstructured grid version of MODFLOW called USG-Transport version 2.2.1 (Panday, 2023) has been chosen as the most appropriate modelling platform. The USG-Transport code is based on the MODFLOW-USG code (Panday et al., 2013) developed by the United States Geological Survey and includes several enhancements (such as adaptive time stepping) that are frequently updated by the code's lead developer. The MODFLOW6 code was considered as a possible alternative at the time of model planning (GHD, 2023a), although the USG-Transport code has been selected as the preferred code due to its extensive use and successful prior application to the modelling of the Latrobe Valley groundwater systems.

Features of USG-Transport that are particularly suited to this project include:

– Flexible meshing, supporting a range of cell shapes, that allows the model cells to closely follow the geometry of hydrological features (such as the Morwell River), enabling more accurate representation of the physical system.
– Efficient local mesh refinement around features of interest within a regional model domain while retaining larger cells elsewhere, enabling an optimal balance between model size (total cell count) and run times without compromising resolution in critical areas. The model layers can also be 'pinched out' or "by-passed' where hydrostratigraphic units (HSUs) are not present and cells are not required in the model domain, reducing the number of active cells and improving numerical stability. This has flow-on benefits to the modern requirements of modelling projects such as run-intensive calibration and uncertainty analysis.
– Robust handling of de-saturation and re-saturation of model cells for tracking the water table across multiple model layers, based on the Upstream Weighting scheme of MODFLOW-NWT (Niswonger et al., 2011). In this case, all model layers are of the Upstream Weighting type.
– The capability to simulate changes in material properties over time, using the Time-Variant Materials (TVM) package.
– The capability to simulate the formation of a pit lake and its interaction with the groundwater system based on accurate accounting of pit water balance and stage-storage relationship, using the Lake (LAK) package.
– Extraction of local water balance, such as in and out of groups of cells, which can be implemented easily using the utility ZONBUDUSG (the ZONEBUDGET program for MODFLOW-USG).
– Interface with the parameter estimation code PEST, including a suite of utilities for facilitating pre- and post-processing of model files.

The unstructured mesh of the USG-Transport model has been generated using AlgoMesh 2.0 (HydroAlgorithmics, 2020) and model input files have been prepared using a combination of AlgoMesh, Geographic Information Systems (GIS) and a range of in-house and third-party utilities (written in python and fortran). All model runs have been undertaken using the PCGu linear solver of the Sparse Matrix Solver package of USG-Transport (with the Bottom Dampening and Truncated Newton options used as required to overcome convergence issues in some model runs).

2.2 Model domain and unstructured grid

A hydrogeologically sensible model domain has been delineated, broadly aligned with geological and hydrological boundaries and covering an area large enough to minimise boundary-induced effects at the Yallourn Mine while maintaining a sensible model size. The model domain is based on the conceptual domain described in GHD (2023b) and shown in Figure 1, incorporating the part of the Gippsland Basin where the Yallourn Mine and Hazelwood Mine are located and extending out into the Moe Swamp Basin to the northwest of the Yallourn Mine and across the Narracan Block to the south of the Yallourn Mine (west of the Hazelwood Mine).

The northern and southern boundaries of the model domain follow the edge of the basin, where the basement outcrops and the overlying younger sedimentary units pinch out. Elsewhere, the extent of the model domain is reduced relative to the conceptual domain (except for a small area southwest of the mine). This is based on the recognition that the effects of aquifer depressurisation do not extend far beyond the Haunted Hills Fault/Yallourn Monocline, into the Moe Swamp Basin, and across the Narracan Block, rendering a larger model domain unnecessary (and less optimal for a model where higher grid resolution and accuracy are required at the mine and along hydrological features of interest).

The eastern boundary of the groundwater model is located around 8.5 km east of the Yallourn Mine and intentionally excludes the Loy Yang Mine. This is because the effect of regional depressurisation from the Loy Yang Mine can be simulated by prescribing heads along this boundary using the outputs from the LVRGM. This practical approach allows the effect of regional depressurisation within the deep confined aquifers to be incorporated into the model without having to explicitly simulate the presence of Loy Yang Mine (and complex hydrogeological processes associated with the mine). The efficiency gained from this approach allows the modelling efforts to be directed at the Yallourn Mine, where detailed simulations of mine-scale processes are the focus of this project.

Figure 2 shows the model domain and features used to generate the unstructured grid. The unstructured grid for the entire domain is shown in Figure 3 (including the topography and the larger conceptual model domain). The model grid uses Voronoi-shaped (tessellated) cells, which are considered numerically ideal for meeting the requirements of the controlled volume finite difference formulation (a line connecting the centres of two adjacent cells intersects the shared face at or close to a right angle). The level of refinement introduced into the model grid is balanced by the need to maintain a sensible model size (and ultimately model run times). The grid refinement is summarised as follows and shown in Figure 4:

– The model grid is refined along major water courses, which include the Morwell River, Latrobe River and Tyers River and creeks such as Anderson Creek, Narracan Creek, Ten Mile (Wilderness) Creek and Waterhole (Wades) Creek. The Morwell River Diversion (MRD) through the mine and Latrobe River to the north of the mine are accurately delineated using a curvilinear gridding approach with cell lengths of around 20 m (and cell widths adjusted based on the typical river width). Coarser cell edge lengths are used elsewhere, with the cell size increasing further away from the mine.
– The model grid is refined over the footprint of the mine void and mine batters, with a cell size of around 50 m. A buffer zone is defined outside of the mine to control the level of refinement, with a cell size of around 80 m, and increasing to 200 m cells away from this buffer zone. The grid is also refined over the Yallourn North Open Cut (YNOC), with a cell size of around 60 m, and the adjacent Hazelwood Mine (with a cell size of around 120 m).
– Within the mine area, the grid is further refined at the location of pumping bores. A radial zone of refinement of around 200 m diameter is introduced over the key pumping bores, to account for the radial flow effect of pumping, with the pumping bore located in the centre. The size of cells within the refined zone is around 20 m.
– The model grid is refined at the location of major water areas (outside of the mine void) such Blue Lagoon, Lake Narracan, Morwell River Wetlands, Witts Gully Reservoir, Pine Gully Reservoir, Hazelwood Cooling Pond (HCP) and aeration pond/lagoon associated with the Australian Paper Mill (APM). The smallest cell size is around 20 m at the Morwell River Wetlands and Blue Lagoon, increasing to around 60 to 80 m at Witts Gully Reservoir, Pine Gully Reservoir, Lake Narracan and APM lagoon. Larger cell sizes of 200 to 250 m are used for the HCP and APM aeration pond located further away from the Yallourn Mine.
– The model grid is refined along the Haunted Hills Fault/Yallourn Monocline (show as a fault line in Figure 2 and fault refinement in Figure 4), where the geological layers are steeply dipping. The cell size is around 40 m, which is applied along the fault alignment mapped by EAY, across a width of around 250 m.

The model domain covers an area of 774.4 km^2 and the total number of cells within a 2d unstructured grid is 38,981.

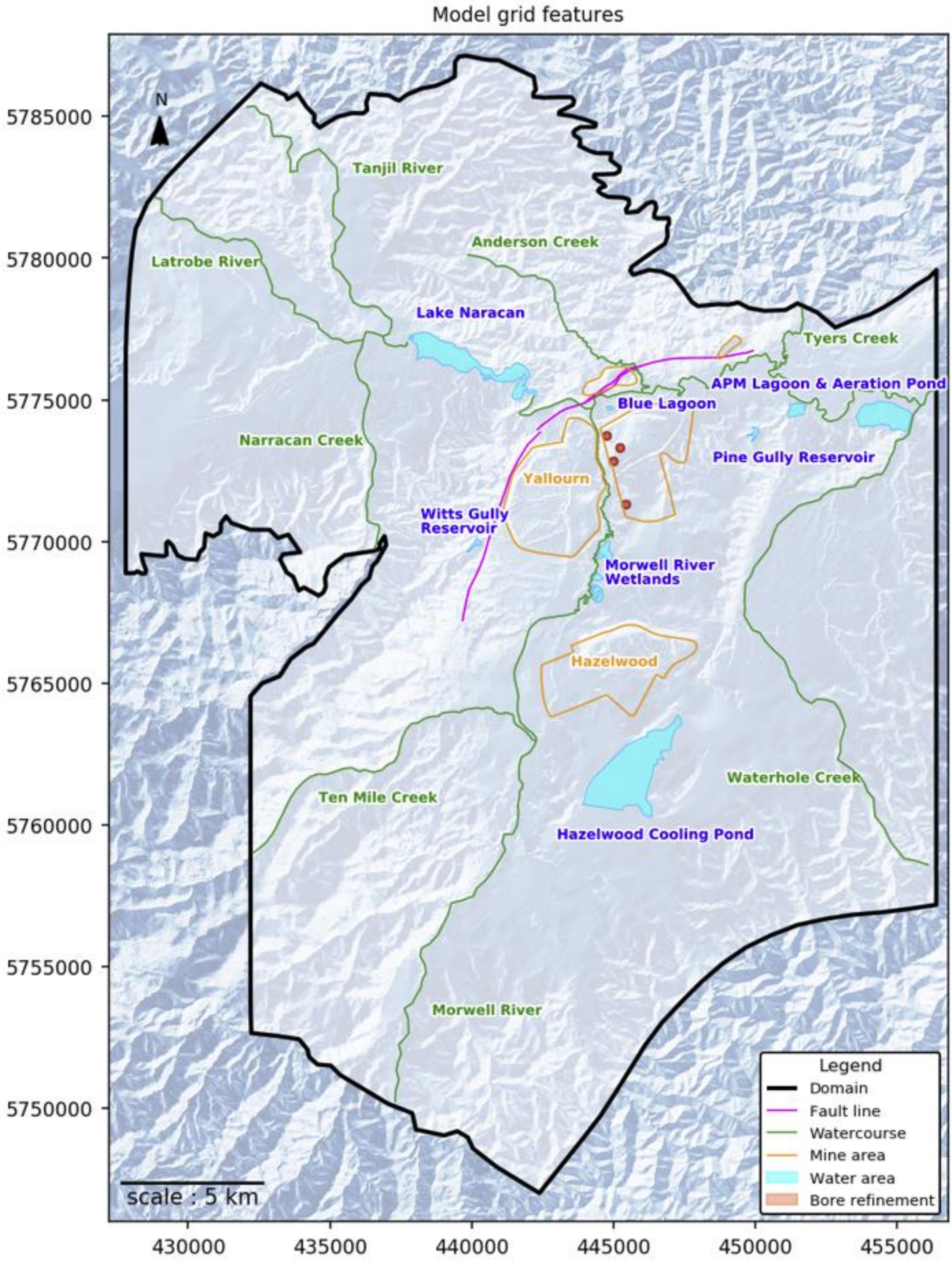

Figure 2 *Model grid features*

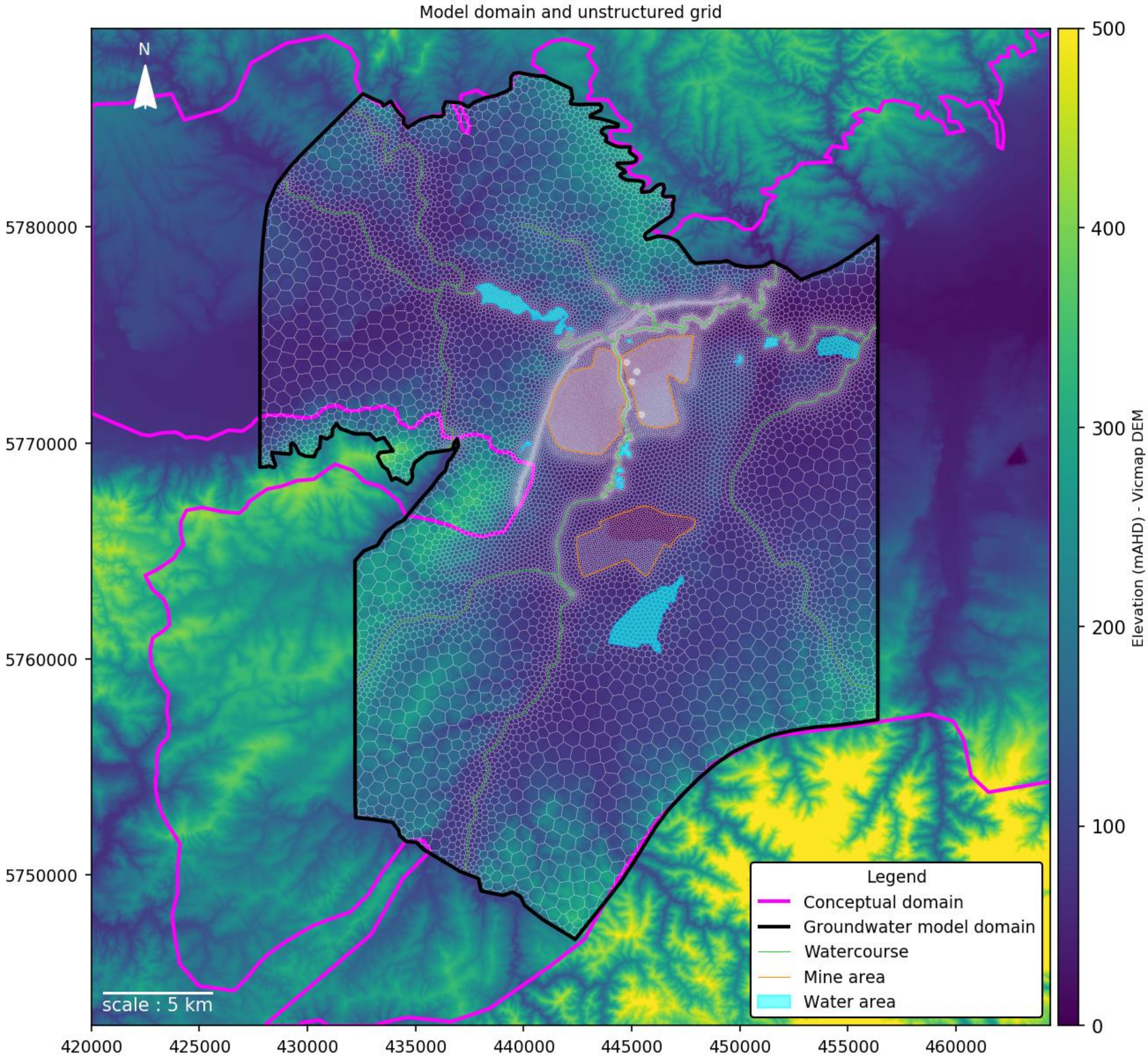

Figure 3 ***Model domain and unstructured grid***

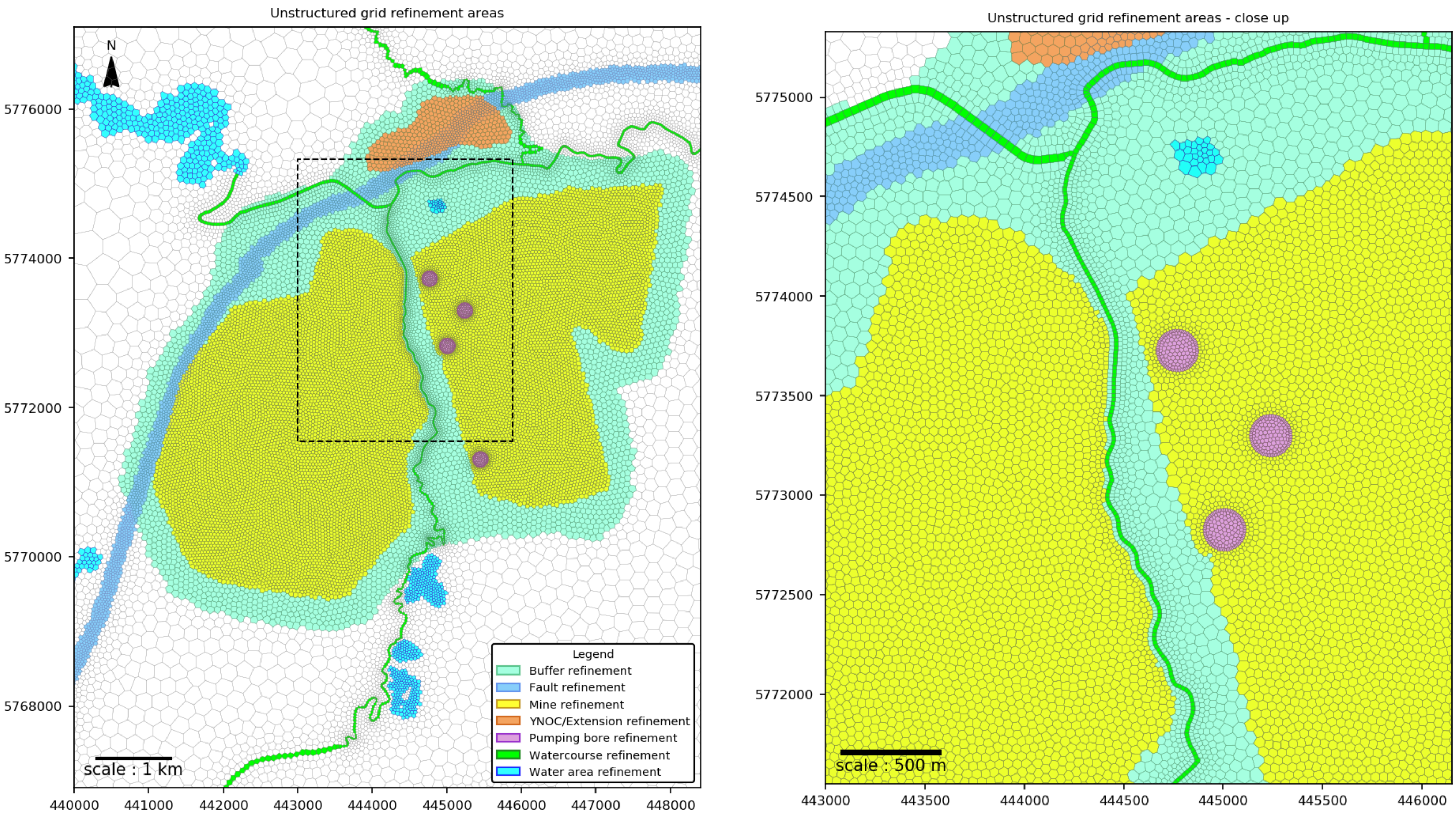

Figure 4 *Unstructured grid refinement areas at and near Yallourn Mine*

2.3 Model layers

2.3.1 Leapfrog hydrostratigraphic model

2.3.1.1 Objective

Defining the spatial distribution of hydrostratigraphic units within the groundwater model domain is complex due to the presence of significant geological structures such as the Haunted Hills Fault/Yallourn Monocline and the large spatial extent of the model requiring integration of geological data from several difference sources (with a varying degree of resolution and accuracy). To facilitate this process, a 3D hydrostratigraphic model has been developed using the software program Leapfrog Works (Version 2022.1.1).

Given the substantial amount of geological modelling already completed within the Latrobe Valley (GHD, 2023b), the goal of the Leapfrog modelling was not to recreate the geological models but to integrate the existing geological datasets into a single geological modelling platform for efficiently building the layers in the numerical groundwater model (similar to the approach adopted for the LVRGM except using Leapfrog in this instance to enable the complex geology to be represented across the Haunted Hills Fault/Yallourn Monocline). This method of modelling, in which the geological contacts within the Leapfrog model are forced to respect the surfaces from pre-existing models, is different from a more traditional approach using borehole logs as the primary input dataset. This led to some practical challenges, particularly when the surfaces from different models with different resolution (both horizontally and vertically) were merged and extrapolated over the broader area (overcoming known limitations with Minescape models such as unmodelled interseams and discontinuous layers), necessitating several iterations, adjustments and verifications against key borehole logs and regional cross-sections.

The Leapfrog model domain covers an area of 1,125 km² (Figure 5) and is large enough to fully encompass the groundwater model domain. The resolution of the Leapfrog model is adaptive, featuring a general cell size of 200 by 200 m that reduces to 50 by 50 m in the mine areas where higher-resolution data are available.

2.3.1.2 Model surfaces and key input datasets

The topography (model top) of the Leapfrog model has been defined using several sources. Due to the presence of the mine voids (early excavations) in Vicmap's Digital Elevation Model (DEM), the pre-mining surface has been estimated by digitising contours extracted from a historical elevation map (Narracan Map 121b, Maryvale Map, 1927). In addition, the recorded collar elevations from old bores are used to provide spot measurements of approximate pre-mining elevations. These elevation datasets were merged with the Vicmap DEM (along with more accurate 1 m elevation contours available at the Hazelwood Mine area) to generate the model top.

The hydrostratigraphic units (HSUs) are defined based on the key aquifer and aquitard units described in GHD (2023b), which form the basis of layers in the numerical groundwater model. The stratigraphic units from the existing mine-scale geological models (Yallourn Minescape and Hazelwood Vulcan models) and regional coal model have been correlated with the HSUs, with a priority given to the mine models due to higher resolution and more detailed representation of local geology. Beyond the extent of the regional coal model, the hydrostratigraphy is interpreted from the surfaces of the Victorian Aquifer Framework (VAF), which has the lowest resolution and treated with the lowest priority (although the floor of the Haunted Hills Formation and roof of the Basement showed reasonable correlations with the surfaces from the mine scale models). Regionally, the Hazelwood Formation (clay-rich coal deposits within the Traralgon Syncline, between the base of the Haunted Hills Formation and the top of the Yallourn Coal) becomes thicker, particularly in the southern part of the model (refer to Figure 12 and Figure 14 of GHD, 2023b). Given the distance from the Yallourn Mine, the hydrostratigraphy has been simplified by lumping the Hazelwood Formation with the Haunted Hills Formation. Appendix A shows the surfaces of HSUs derived from different geological models (areas marked as "Yallourn" and "Hazelwood" are mine-scale models while "Regional" and "VAF" represent the regional coal model and VAF, respectively).

Outcrops of the Thorpdale Volcanics and the Basement (Strzelecki Group) have been delineated from published geological maps to constrain the extrapolation of model surfaces towards the edge of the basin. Due to the erosive nature of some layers overlying the Basement, it was not possible to uniformly apply erosive contacts to accurately simulate the pinch outs of selected layers (since no spatial constraints could be imposed, resulting in little control on erosion)[1]. To overcome this issue, a refined two-layer model (comprising the Basement and basin fill above) was first constructed and the basin fill was subsequently refined by incorporating the coal and interseams layers (thereby restricting the erosion processes of the basin fill and preserving the outcrops).

The Thorpdale Volcanics unit, which covers a limited extent, has been incorporated into the model as a vein. The surfaces of the Thorpdale Volcanics from the VAF have been used for this purpose, due to the VAF having most regionally extensive coverage (extending into the Moe Swamp Basin and outcropping over the Narracan Block west of the Hazelwood Mine), consistent with the outcrops shown on geological maps (Figure 1) and the distribution shown in schematic geological cross-sections (such as Figure 12 and Figure 14 in GHD, 2023b). Where the Thorpdale Volcanics directly overlie the Basement in the outcropping area, a uniform thickness of 50 m has been applied due to limited data (noting that this area is far from the Yallourn Mine and does not materially impact mine scale hydrogeological processes).

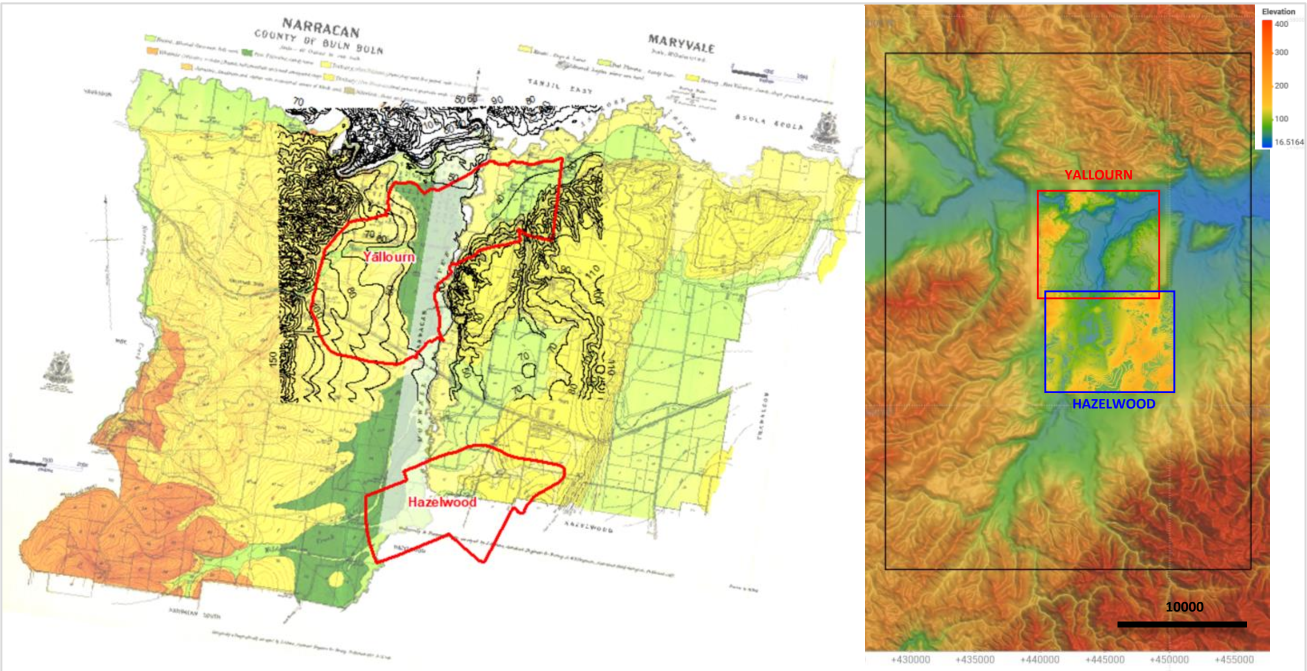

Figure 5 *Digitised pre-mining contours (left) and merged topographic surface (right)*

[1] The term erosion in Leapfrog refers to a contact surface where the existing lithologies on the older side of the erosion are removed (pinched out against the erosion contact). This function could not be applied uniformly to simulate the necessary pinch outs on a layer by basis; therefore, a simple model consisting of the basement and overlying material was first constructed and individual layers (contacts) were subsequently added (with erosion control applied on a layer by layer basis).

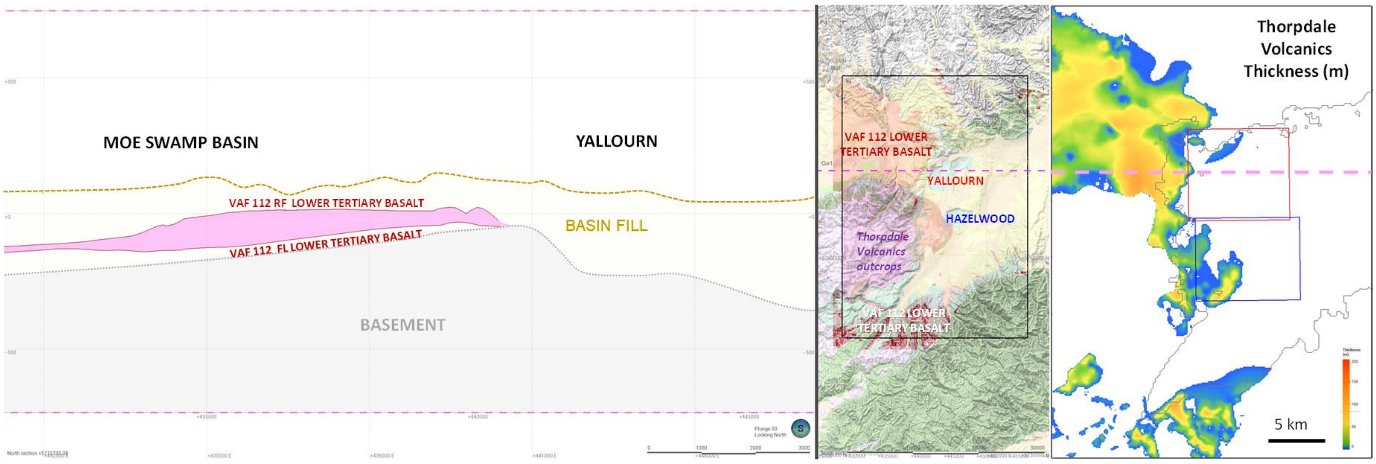

Figure 6 Thorpdale Volcanics in Moe Swamp Basin

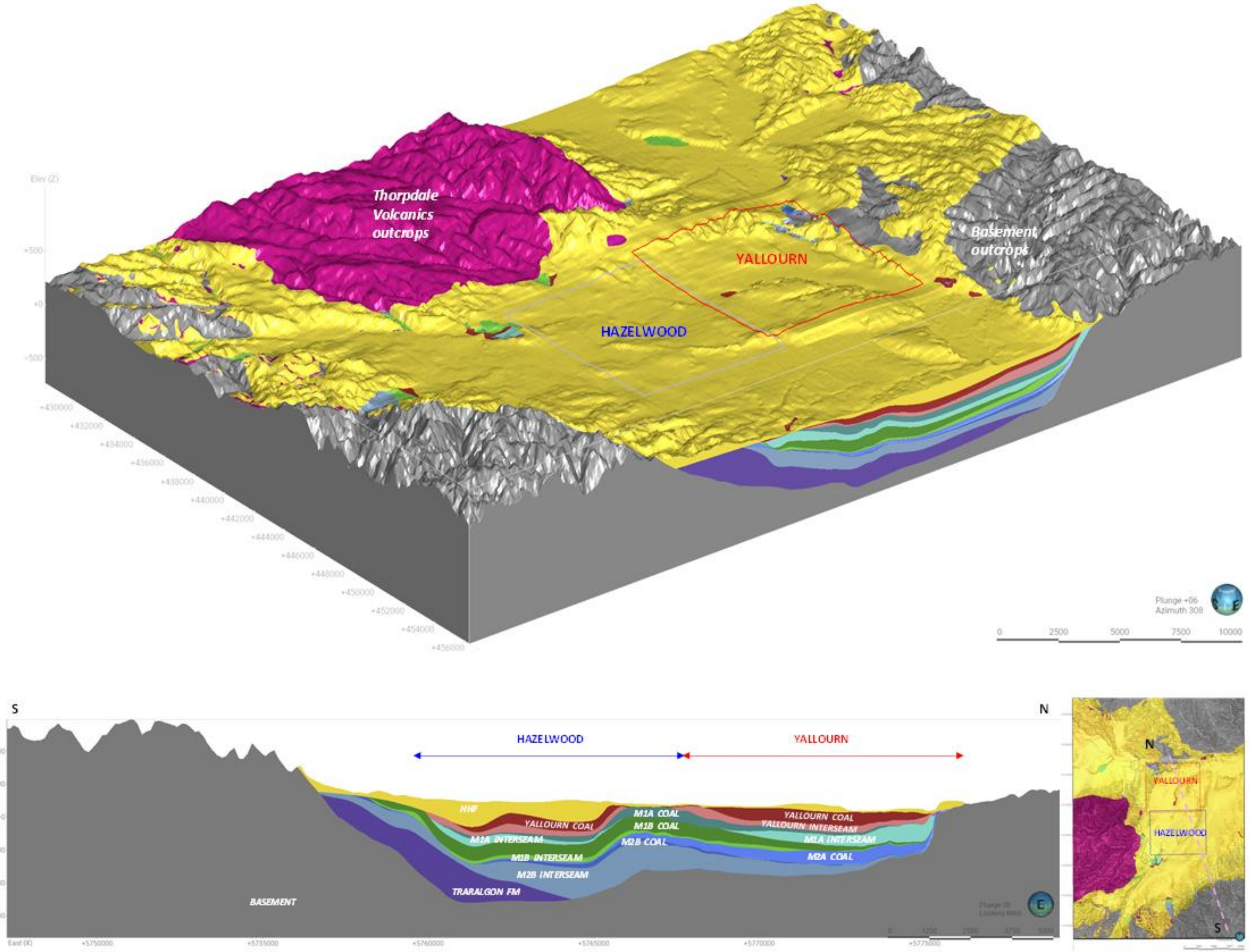

Figure 7 ***Leapfrog model image and cross-section***

2.3.2 Model layering and cell connections

2.3.2.1 Model layers

The relationship between the model layers and HSUs is summarised in Table 1. The Yallourn Coal is the main coal unit that is exposed in the mine batters and will directly interact with the future pit lake. This unit is split into four model layers of equal proportion, to increase the vertical resolution in areas of steep vertical hydraulic gradients and to assist with the simulation of a future pit lake (for void volume and stage-storage relationship).

The M1A Interseam is the main confined aquifer depressurised by the pumping bores at the Yallourn Mine. This unit is also split evenly into three model layers, to account for the variations in the abundance of sand with depth and to simulate subtle vertical differences in groundwater levels observed at nested piezometers. As described in GHD (2023b), the M1A Interseam consists of four distinct (albeit discontinuous) sand aquifers, which cannot be simulated individually due to an impractically large number of model layers required to do so (four layers for the sand aquifers plus five layers for the intervening coal/clay layers). The splitting into three model layers is considered a reasonable compromise, providing some flexibility for capturing the differences in sand abundance without incurring excessive run time from having a large number of layers.

The Thorpdale Volcanics is represented by a single model layer (model layer 15). The M2 Interseam is split into two layers, above and below layer 15, to simulate the intrusion of the Thorpdale Volcanics into this unit. Where the Thorpdale Volcanics locally cut through the overlying layers, this effect is simulated by truncating the overlying layers against the top of the volcanics (model layer 15).

The top and bottom elevation of the layers are derived from the surfaces of the Leapfrog model, with minor adjustments made within the groundwater model e.g. to remove localised holes created in the Leapfrog model due to artefacts in the exported surfaces from the Minescape geological model. In areas where the HSUs are absent, a minimum thickness of 0.1 m is assigned. Figure 9 and Figure 10 include several model cross-sections, showing the distribution of model layers and their relationship with the HSUs. The locations of cross-sections are shown in Figure 8. Maps showing the elevation of each model layer are included in Appendix B.

Table 1 Model layers and corresponding HSU

Layer	HSU	Active cells	Inactive cells
1	Haunted Hills Formation (Hazelwood Formation)	36,757	2,224
2	Yallourn Coal	28,565	10,416
3	Yallourn Coal	28,567	10,414
4	Yallourn Coal	28,566	10,415
5	Yallourn Coal	28,566	10,415
6	Yallourn Interseam	27778	11,203
7	M1A Coal	26,192	12,789
8	M1A Interseam	27,143	11,838
9	M1A Interseam	27,142	11,839
10	M1A Interseam	27,144	11,837
11	M1B Coal	29,896	9,085
12	M1B Interseam	29,727	9,254
13	M2 Coal (M2A and M2B Coal combined)	32,011	6,970
14	M2 Interseam	1,102	37,879
15	Thorpdale Volcanics	4,553	34,428
16	M2 Interseam	35,283	3,698
17	Basement	38,981	0

Although the Basement is conceptualised as an effective hydraulic base of the Latrobe Valley groundwater systems, it is incorporated as a layer in the model (with a uniform thickness of 400 m) to improve numerical stability, particularly towards the edge of the basin where the overlying layers are thin and the application of recharge at surface can lead to convergence issues (without the underlying Basement to allow some of that flow to be absorbed and drained away).

2.3.2.2 Cell connections

The use of USG-Transport's LAK package (for the future pit lake simulation) requires the model layers to be continuous throughout the model domain, with the same grid refinement in all 17 model layers. A common approach to mimicking the effect of pinch outs within continuous model layers is to reduce the layer thicknesses to a small value where the HSUs are not present. In a complex geological setting with multiple model layers, this approach results in a large number of vertically stacked thin cells that can lead to numerical instabilities particularly in areas of steep changes in layer elevations (e.g. towards the edge of the basin where multiple HSUs pinch out).

To overcome this constraint, the pinch out cells have been reduced to a minimum thickness of 0.1 m and made inactive (through the IBOUND array of USG-Transport). The connectivity of individual model cells within the unstructured grid is modified to ensure the cells above and below the pinch out cells are vertically connected, with connection lengths corrected for the inter-nodal distance. This approach effectively bypasses the pinch out (minimum thickness) cells while retaining continuity in model layers, providing a more numerically stable model without compromising the representation of the geology and model's ability to simulate mine pit lakes. The overall effect is the same as the standard implementation of pinch outs in USG-Transport, except that the layer continuity is retained to preserve the functionality of the LAK package. This approach is similar to the "vertical pass-through cells" implemented in MODFLOW6 (Langevin et al, 2017).

The model has a total of 701,658 cells, with 457,973 active cells. The total number of active cells is below the target threshold of 500,000 active cells, which is considered a sensible practical limit for a regional scale model with complex boundary conditions, long simulation time and run intensive automated calibration (requiring many model runs).

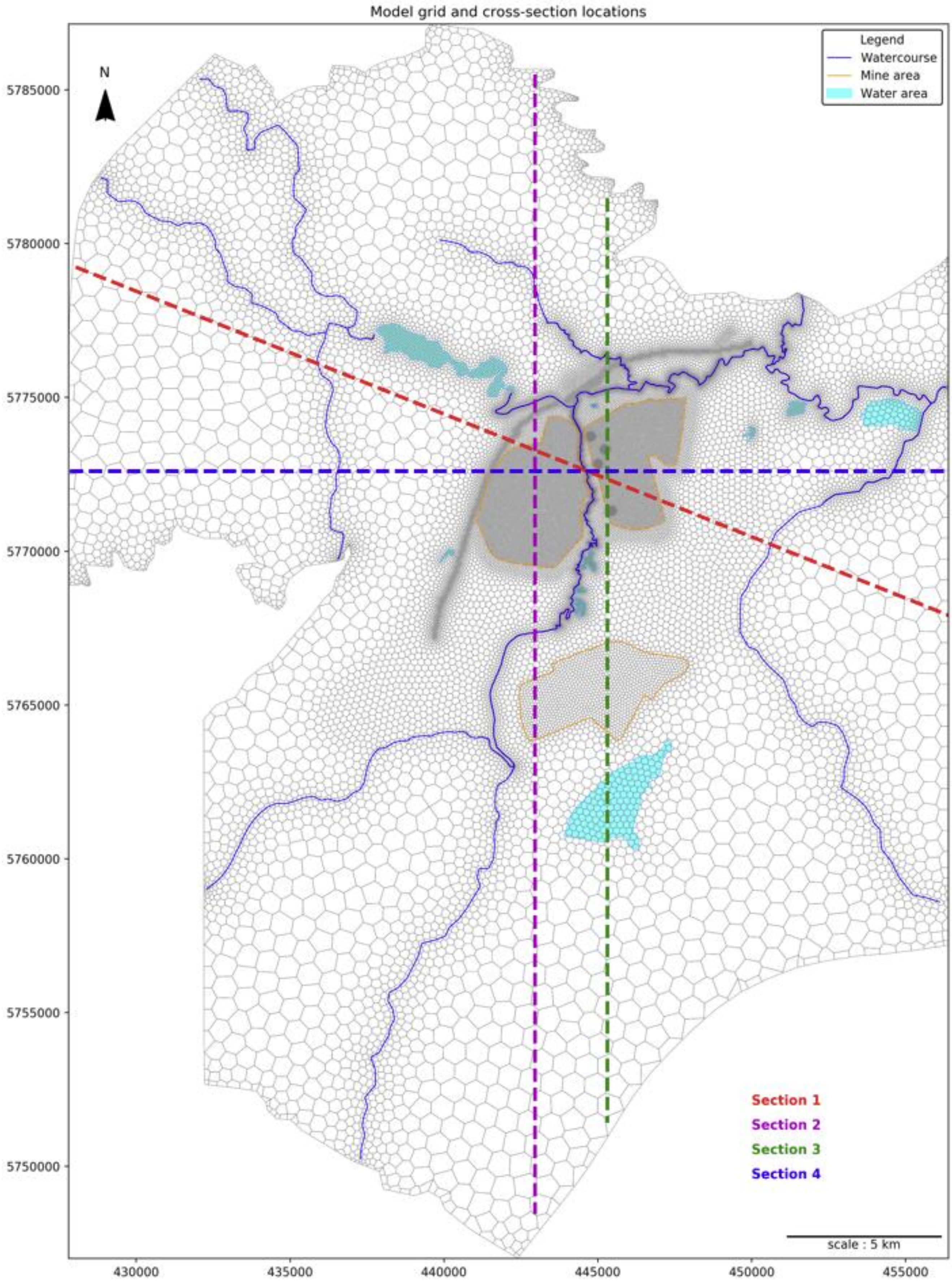

Figure 8 *Model grid and cross-section locations*

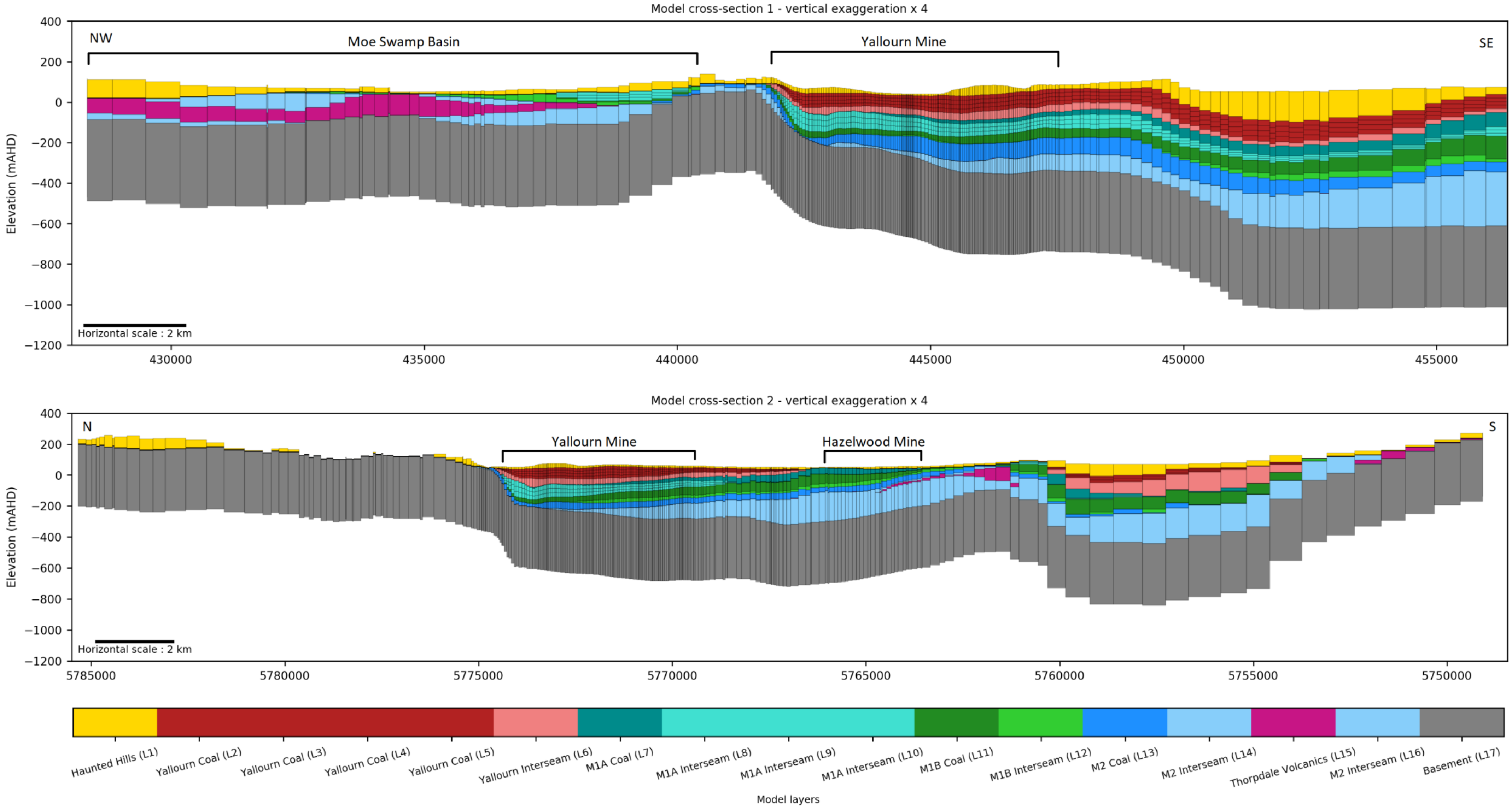

Figure 9 Model cross-sections 1 and 2

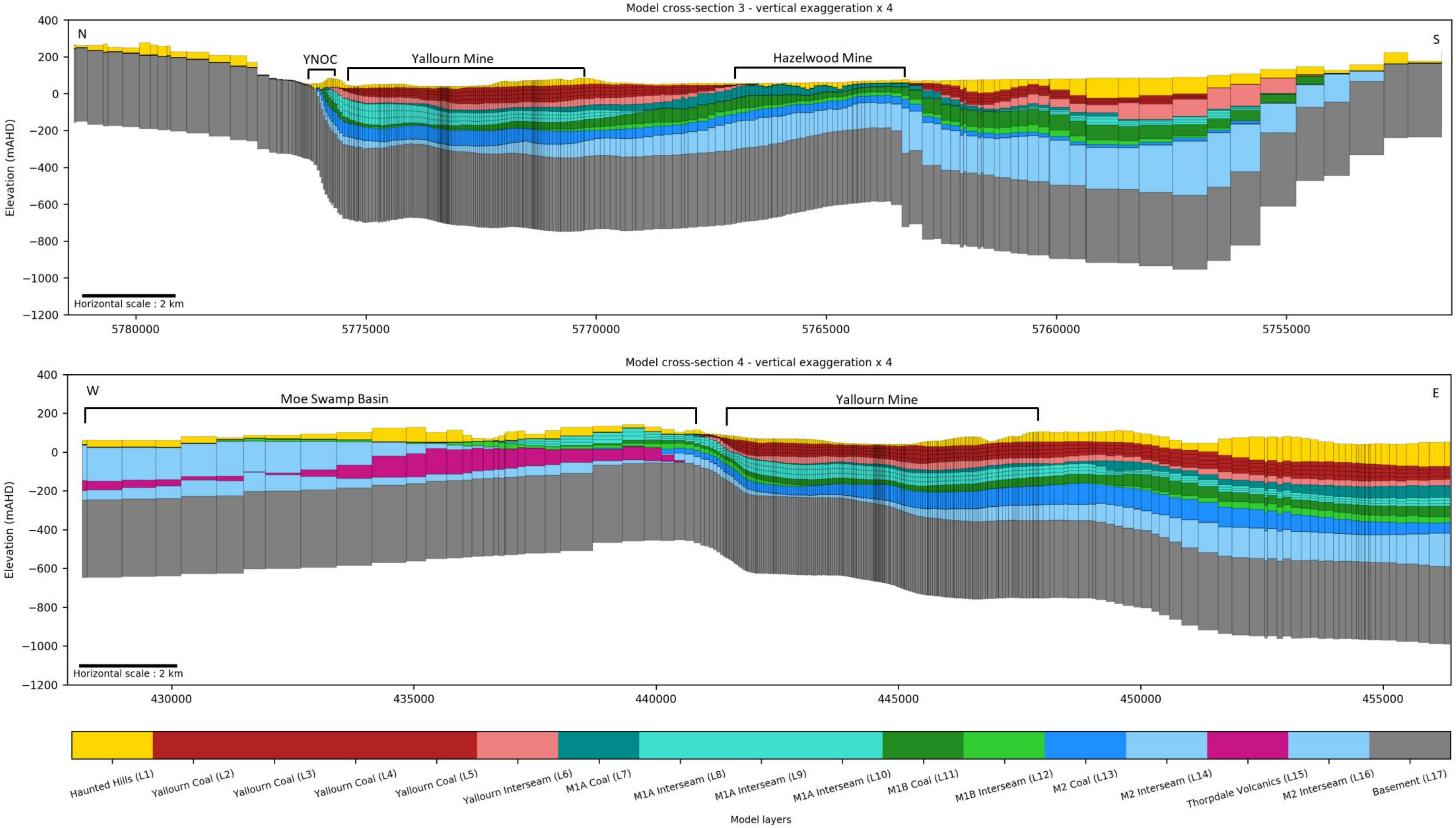

Figure 10 ***Model cross-sections 3 and 4***

2.4 Precipitation Runoff Modelling System

2.4.1 Integrated approach

The numerical groundwater modelling for the Yallourn Mine rehabilitation adopts an integrated modelling approach, using a physical-based distributed rainfall-runoff model to derive spatially and temporally varying recharge, evapotranspiration and lateral flow (runoff and interflow) for the groundwater model. The main benefits of the integrated modelling approach are:

– A realistic representation of recharge and evapotranspiration mechanisms that accounts for the total water balance and the influence of topography, vegetation type, soil zones, land use and spatial variability in climate (using physically-based processes).
– The ability to account for the total stream flow and time-varying stream levels, which is considered important for modelling surface water-groundwater interactions in detail along major watercourses near the Yallourn Mine.
– The use of daily climate data, which is well suited to incorporating the effects of climate change based on the scaling factors of the Victorian government's climate change guidelines (DELWP, 2020) that are applied directly to the underlying climate data (such as rainfall and evaporation).

The distributed rainfall-runoff model used in this study is the Precipitation Runoff Modelling System (PRMS) version 5.2.1 developed and maintained by the USGS (Markstrom et al, 2015, February 2022 release). The hydrological processes simulated by PRMS are similar to the PERFECT model (Littleboy et al, 1989) adopted for the LVRGM with some key differences that make PRMS better suited to meeting the needs of the Yallourn Mine rehabilitation modelling. These include the following:

– The capability to account for cascading flows, using the Cascade Routing Tool (Henson et al, 2013). The flow cascades allow routing of flow that accounts for changes in hydrologic drainage patterns as water moves from upslope to downslope areas, enabling a more realistic simulation of the topographical influence on recharge, evapotranspiration and stream flow.
– The ability to distribute daily climate data using several options, such as the inverse distance elevation interpolation that allows the climate data from multiple weather stations to be distributed in a more realistic manner (compared to traditional methods such as the nearest neighbour grids).
– A single RRMS model can contain many cells/flow areas referred to as Hydrologic Response Units (HRU). In contrast, modelling with PERFECT requires a separate PERFECT model for every cell/flow area (necessitating many individual PERFECT models). This makes the PRMS modelling workflow more streamlined and efficient, with linkages between HRUs that allow for processes such as cascade routing and climate distribution to be simulated effectively.
– PRMS has been enhanced over the years to enable better integration with the MODFLOW-based codes (including the GSFLOW code, which couples PRMS with a structured grid version of MODFLOW). This means there are features of PRMS that make the post-processing of outputs more straightforward for preparing inputs to a MODFLOW model. These include:
    - The ability to incorporate streams into the PRMS model with the same segment numbering used in the MODFLOW model, allowing the lateral flow component (runoff and interflow) calculated by PRMS on a segment basis to be easily incorporated into MODFLOW's stream boundary condition.
    - The ability to export selected outputs (recharge, evapotranspiration) at different output frequencies (e.g. daily, mean monthly…etc) to assist with the preparation of MODFLOW input files.
    - The ability to export outputs from a group of HRUs (as sub-basins), which can be useful for verification and calibration.
– The input and output file structures of PRMS are better suited to integrating the rainfall-runoff modelling processes into the automated calibration workflow, enabling the recharge, evapotranspiration and lateral flow components to be calibrated with the groundwater model at the same time (based on the groundwater model response). Testing has also shown that PRMS models generally run quickly, making it suitable for run-intensive automated calibration procedures and uncertainty analysis.

There are some features of PERFECT that are more advanced than PRMS e.g. capability to simulate various crop types, which may be important for certain modelling applications (such as detailed modelling of land use changes based on vegetation types). This is not the focus of the mine rehabilitation modelling.

2.4.2 PRMS model domain and grid

The PRMS model domain fully encloses the groundwater model domain, with a larger upstream area to account for the contribution of lateral flow (runoff and interflow) from the wider catchment. Similar to MODFLOW's stream boundary condition, stream flows originating from the upstream catchments can be simulated by directing gauged flows into the model (using the flow gauges located outside of model domain, see Section 2.5.2.2). This allows the PRMS model domain to be smaller than the entire catchments of the major water courses, which is necessary for preventing excessive model size and run time.

The PRMS grid uses a regular structured grid, which is required for incorporating the cascading flow effects. A cell size of 250 m by 250 m is used, with a total of 16,861 active cells covering an area of around 1,054 km^2. The surface elevation of the model grid is derived from the Vicmap DEM, which is converted into a "hydrologically correct" DEM by the Cascading Routing Tool (CRT) to fill local depressions and enforce downward drainage (preventing circular flow paths). Up to four flow cascades are defined for each HRU, with the proportion of flow splits calculated by the CRT based on the elevation differences relative to the four adjacent HRUs. The stream network is incorporated using the segment numbering consistent with the stream boundary condition of the groundwater model (see Section 2.5.2 for more details). Where multiple stream reaches exist within a single HRU, the CRT splits the flow cascades to allow lateral flow into that HRU to be apportioned to each stream reach.

Figure 11 shows the PRMS grid, the filled DEM and flow cascades in the area of the mines. For the majority of the HRUs, the proportion of flow split assigned to the cascade links ranges from 1 (only one flow cascade, in the dominant direction of flow) to 0.25 (four flow cascades, with even flow splits). Where there are multiple stream reaches within the same HRU, more than four cascade links can be defined depending on the connections with the surrounding HRUs (reducing the flow split to as little as 0.2 per cascade link).

2.4.3 PRMS input parameters

The datasets used to parameterise the PRMS model are similar to those used for the PERFECT model of the LVRGM, with some differences to account for the different input parameters required by the two models. The PRMS model parameters are summarised as follows:

- The daily climate data are sourced from the SILO database, using the continuous data from 18 Bureau of Meteorology (BoM) weather stations located within (16) and near (2) the PRMS model domain. The daily rainfall and temperature (minimum and maximum) from the weather stations are interpolated to the PRMS grid using the inverse distance elevation (IDE) module, which provides realistic spatial distributions of climate data that accounts for the effect of elevation differences. The potential evapotranspiration (PET) is also derived from the SILO database (rather than attempt to calculate this using PRMS modules, which requires other inputs such as solar radiation and would be less straightforward for incorporating climate change effects using the published scaling factors). As the IDE module is not available for distributing pre-defined PET, the pan evaporation distribution module has been selected. This uses the nearest neighbour interpolation, albeit with a multiplier grid that can be used to further adjust (smoothen) the PET distribution. When pre-defined PET is distributed, rather than calculated, the PRMS model outputs become largely insensitive to the minimum and maximum temperature values (although they are still required as inputs, for example, to calculate the start of the period of active transpiration). Appendix C includes a map showing the long term average historical climate data distributed to the PRMS grid (from 1960 to end of 2021) and the location of BoM stations.
- The land use is simplified into a broad classification of grass and trees. These zones have been delineated accurately from aerial imagery. PRMS also allows the effect of impervious surfaces to be simulated in the model. The impervious zones have also been delineated from aerial imagery based on the presence of buildings and paved areas (limited to areas larger than one HRU). The fraction of HRU area within these zones that consists of impervious surfaces is further adjusted during model calibration.

– The vegetation cover density is required for the summer and winter periods. This data has been sourced from the MODIS fractional cover images (*https://eo-data.csiro.au/fc_images.html*). For the purpose of modelling, the fractional covers from January (month of highest PET and lowest rainfall) and June (month of lowest PET and highest rainfall) have been used for the summer and winter periods respectively (taking average values calculated from 2004 to 2020, when the data is available). This simplification is considered valid, as the PRMS outputs are only moderately sensitive to the subtle differences in the vegetation cover density.
– Recharge and evapotranspiration computed by PRMS are highly sensitive to a parameter called "soil_moist_max", which represents the maximum water holding capacity of the capillary reservoir from ground surface to the root depth of major vegetation types. It represents the volume of soil moisture store available for plants to access for evapotranspiration from within the soil/unsaturated zone. Conceptually, this parameter can be considered to represent a combination of the soil/subsurface material property (effectively the difference between the field capacity and wilting point of the unsaturated zone) and vegetation type (the depth of root zone that can access moisture from within the unsaturated zone). In this study, the soil moisture maximum zones have been defined based on the major soil zones from the Atlas of Australian Soils (McKenzie et al, 2000) and the broad classification of vegetation type (grass and trees). The field capacity and wilting point for each soil zone are used in combination with the plausible range of rooting depth of grass and trees to define a range of soil moisture maximum values for each zone (which are further adjusted during calibration). For the same soil zone, this means there is greater potential for soil zone evapotranspiration in areas of dense forest (which would reduce deep drainage/recharge to the underlying water table). PRMS sets an upper limit of 20 inches (508 mm) for this parameter. To put this into context, a loam soil type with the typical field capacity and wilting point difference of around 2 inches per feet would imply an effective maximum depth of soil evapotranspiration of around 3 m. For sandy soils with much smaller soil stores, the equivalent depth would be higher (noting, however, that PRMS only considers the soil moisture volumetrically).
– The capillary reservoir zones, land use and vegetation cover density maps are included in Appendix C. Other PRMS parameters have been adjusted during model calibration on a model-wide basis (see Section 3.1.3.1 for further information).

2.4.4 Linkage with USG-Transport

The outputs from the PRMS model are used to generate the following inputs to the USG-Transport model:

– Runoff assigned to each segment of the stream boundary condition, using the lateral flow (runoff and interflow) computed by PRMS.
– Evapotranspiration, using the unused PET computed by PRMS. This represents the portion of PET not used (lost) by the surface processes above the water table such as interception and soil (unsaturated) zone evapotranspiration, which is available for plants to uptake directly from the water table (where the root depth is within the saturated zone).
– Recharge, using recharge (deep drainage) computed by PRMS.

Although the PRMS model is run using daily climate data, the outputs have been generated on a mean monthly basis to facilitate the subsequent lumping and averaging of the outputs to match the longer stress period lengths of the USG-Transport model. Recharge and evapotranspiration computed for each HRU is linearly interpolated to the cells of the unstructured grid, with spatial averaging occurring where the USG-Transport cells are larger than the PRMS HRUs (while preserving the original PRMS distribution where the USG-Transport cells are smaller). The PRMS units are converted to the correct USG-Transport units prior to undertaking interpolation.

Figure 12 shows the graphical representation of the linkage between the PRMS and USG-Transport models. The loose coupling method involves running the PRMS and USG-Transport model in sequence, which allows the PRMS model parameters to be calibrated based on the response simulated in the USG-Transport model. Feedback from the USG-Transport model to the PRMS model is not allowed, which would require more complex linkages and iterative coupling that would be impractical for meeting the requirements of the rehabilitation modelling. The loose coupling method is intended to provide a practical approach to estimating hydrologically sensible recharge, evapotranspiration and lateral flow for a complex groundwater model, which can be readily integrated into a rigorous automated calibration procedure without incurring excessive model run times.

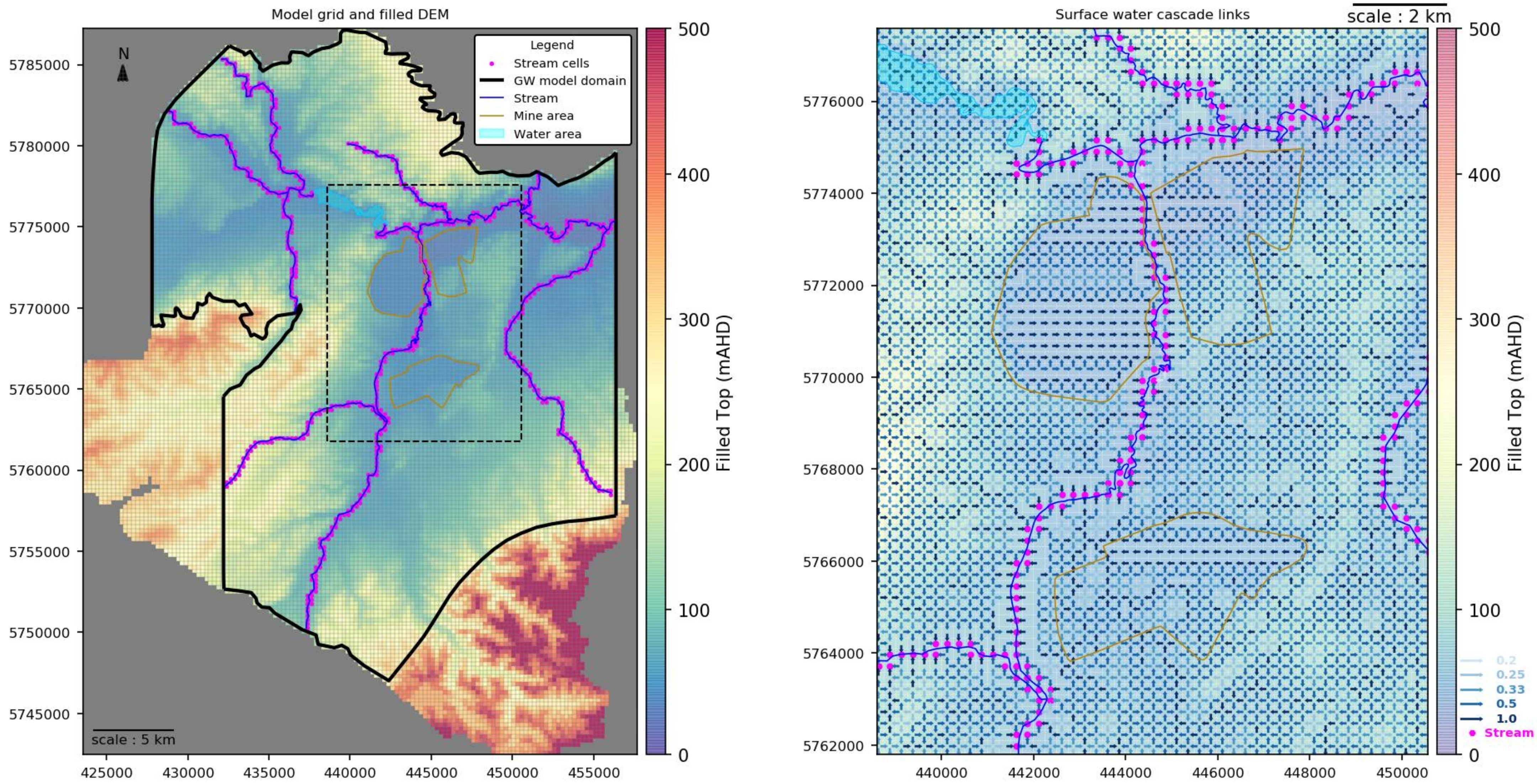

Figure 11 ***PRMS model grid and flow cascades***

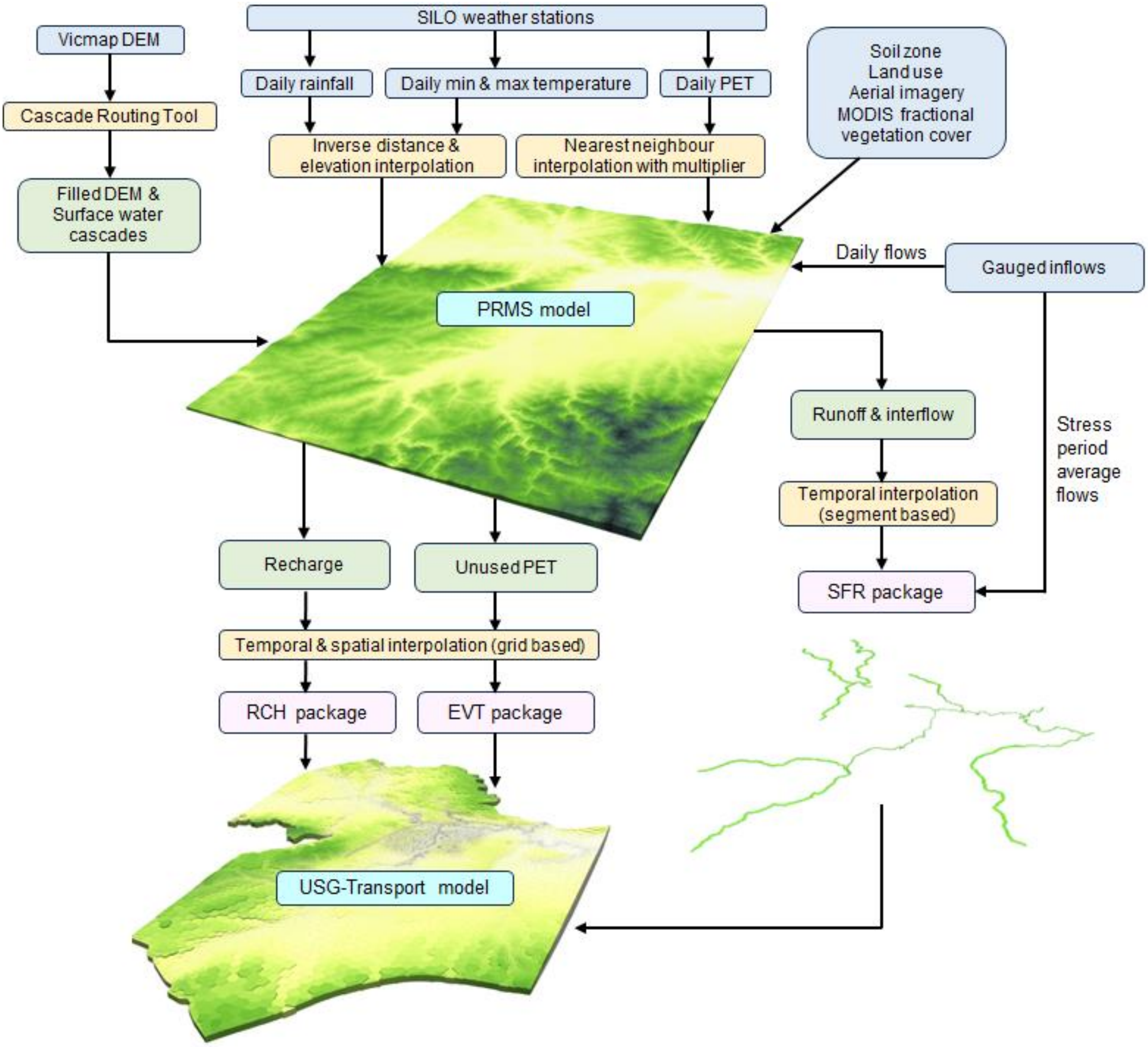

Figure 12 *PRMS and USG-Transport model coupling*

2.5 Model boundary conditions

2.5.1 Recharge and evapotranspiration

Recharge and evapotranspiration are assigned using USG-Transport's Recharge (RCH) and Evapotranspiration (EVT) packages respectively. The recharge and evapotranspiration rates are derived from the PRMS model, as described in Section 2.4. Option 3 of the RCH package is used to automatically assign recharge directly to the uppermost active cells. For the EVT package, Option 2 is used to apply EVT to the uppermost active nodes by explicitly specifying the EVT nodes.

The EVT package requires the specification of EVT surface and extinction depth. The EVT is assumed to occur at the prescribed rate when the modelled heads are at or greater than the elevation of the EVT surface. The EVT rate is assumed to decrease linearly with depth, reducing to zero when the modelled heads are at or below the extinction depth (calculated relative to the EVT surface). The EVT surface is set equal to the model top elevation (ground surface). The EVT extinction depth is parameterised based on the broad classification of grass and trees (two zones), as per the PRMS model (see Appendix C), and the calibrated depths are discussed further in Section 3.2.2.

Both recharge and EVT are set to zero at the stream and river cells, to avoid duplicating the fluxes.

2.5.2 Stream boundary condition

2.5.2.1 Stream cells

The Stream Flow Routing (SFR2) package of USG-Transport is used to simulate the major watercourses within the model domain (Figure 13). There are several advantages with this boundary condition compared to standard head boundaries such as the river boundary condition for simulating surface water-groundwater interaction. These include:

– The volume of water available for interaction with the modelled groundwater system is limited to that which has accumulated from upstream within the defined stream channel network (from baseflow, and/or any runoff and artificial discharges, less any diversions). In dry times, there may be no or little water flowing down the stream network, thus avoiding unrealistic leakage of water into the model from these boundaries. This can be particularly important close to the mines where the aquifers are drained/depressurised.
– The ability to dynamically calculate stream stage based on flow volumes and stream geometry. Although this can lead to numerical instability (particularly during wet/high flow periods), the time-varying stream stage can improve the accuracy of surface water-groundwater interactions, particularly adjacent to the Latrobe River where data from shallow monitoring bores are available to assist with model calibration. In this case, the Mannings equation is used to compute the stream stage assuming wide rectangular channels.
– The model can be calibrated to both stream flow and stream stage, which aids in narrowing the uncertainty in groundwater recharge rates and hydraulic conductivity.
– The SFR package can be linked to MODFLOW-USG's Lake (LAK) package, with flow transfers between streams and lakes depending on hydraulic constraints. This capability is useful for the rehabilitation scenario modelling e.g. water flowing down streams can be diverted into the lakes and/or lake water can spill (or be pumped) to the SFR network.

Stream bed elevations are defined based on the 20 m resolution Vicmap DEM, with enforced topographic fall down the stream network. Channel widths are varied based on broad inspection of aerial imagery. Stream bed thickness is set to 0.5 m except along sections of the Morwell River Diversion (MRD) underlain by clay and geosynthetic liners, where a thicker stream bed of 3 m is assumed (a representative thickness of the constructed liners across the width of the channel). Stream length within each model cell is calculated rigorously based on the mapped stream geometries from Vicmap (and refined using aerial imagery). Hydraulic conductivity of the bed material (and hence the stream bed conductance) is adjusted during model calibration using discrete zones (see Section 3.1.3.2).

It is currently not possible to activate and deactivate sections of the SFR boundary condition to simulate the diversion of the Morwell River over time without breaking up the model simulation into separate model runs or incorporating all historical segments and creating complex diversions to direct flows to the correct segments. This level of complexity is not considered necessary, given little to no historical groundwater data are available along the prior courses of the Morwell River to enable meaningful calibration and that most of the aquifers in the area have since been excavated out by mining. The third MRD, completed in 1987 (after the earlier diversion around the Hazelwood Mine and minor diversion in the upstream section of the Yallourn Mine), also consisted of a buried low flow pipeline with limited potential for interaction with the shallow groundwater system. For this reason, the location of SFR cells along the MRD has been maintained constant based on the current alignment (the fourth MRD commissioned in 2005). Although simplified, this approach enables correct volumes of stream flow to be routed from the upstream area of the Morwell River to the Latrobe River, resulting in negligible changes to the flow and stage simulated in the downstream area. Similarly, the Morwell River diversion further upstream at the Hazelwood Mine is based on the current alignment as the changes in the river position do not materially affect the volume of flow that ultimately reaches the Yallourn Mine further downstream (especially when correct inflow and return flows are assigned to the stream segments, as discussed in Section 2.5.2.2 below).

2.5.2.2 Inflows and return flows

As the groundwater model domain covers only a portion of the Latrobe Valley surface water catchment, flows from inflowing streams have been assigned using the gauged historical daily flow data on the main inflowing rivers and creeks (the same approach adopted for the PRMS model). These include the Latrobe River (226204A, western boundary), Morwell River (226407, southern boundary), Narracan Creek (226218A, southern boundary) and Tyers River (226028/226007, northern boundary). In many cases the flow data had to be extended in time (back to 1960) and/or infilled using regressions developed between relevant nearby gauges.

Surface water diversions for mining operations occur from the Latrobe River downstream of Lake Narracan (adjacent to the power station). These have been incorporated into the modelled Latrobe River inflows based on the flows recorded at two gauges downstream of the intake point (226401A and 226400B). The benefit of this approach is that the flow takes are already accounted for in the inflow data, enabling correct volumes of surface water to be routed downstream of the Latrobe River without having to explicitly simulating the diversions.

Discharge of mine water to the Morwell River (via floc pond) is assigned as a flow component to the stream segment closest to the discharge point (west of floc pond). The measured discharge rates are available from 2006, which are used to assign flow returned to the Morwell River. For the period prior to 2006, the modelled discharge is based on that used in the LVRGM, which is derived from the Latrobe Valley REALM model (GHD, 2013a,b). Surface water discharges ('returns') from the Morwell Wastewater Treatment Plant and industry (Hazelwood Mine and EnergyBrix) are also added to the stream network at their relevant locations based on the information used in the LVRGM. A summary of return flows is provided in Table 2.

Figure 13 shows the location of SFR cells, segment number and flow gauges located outside of the model domain (used to direct flow into the stream segments). The stream bed elevation is also shown along the MRD and Latrobe River north of the mine.

Table 2 SFR stress period return flows

Return flows	Segment	Min (ML/d)	Max (ML/d)	Average (ML/d)
Yallourn Morwell River	13	0	63	41
Hazelwood Morwell River	9	0.0033	157	33
Morwell Wastewater Treatment Plant	12	0.4	2.3	1.5
EnergyBrix (ceased in 2014)	20	0	14	5.2

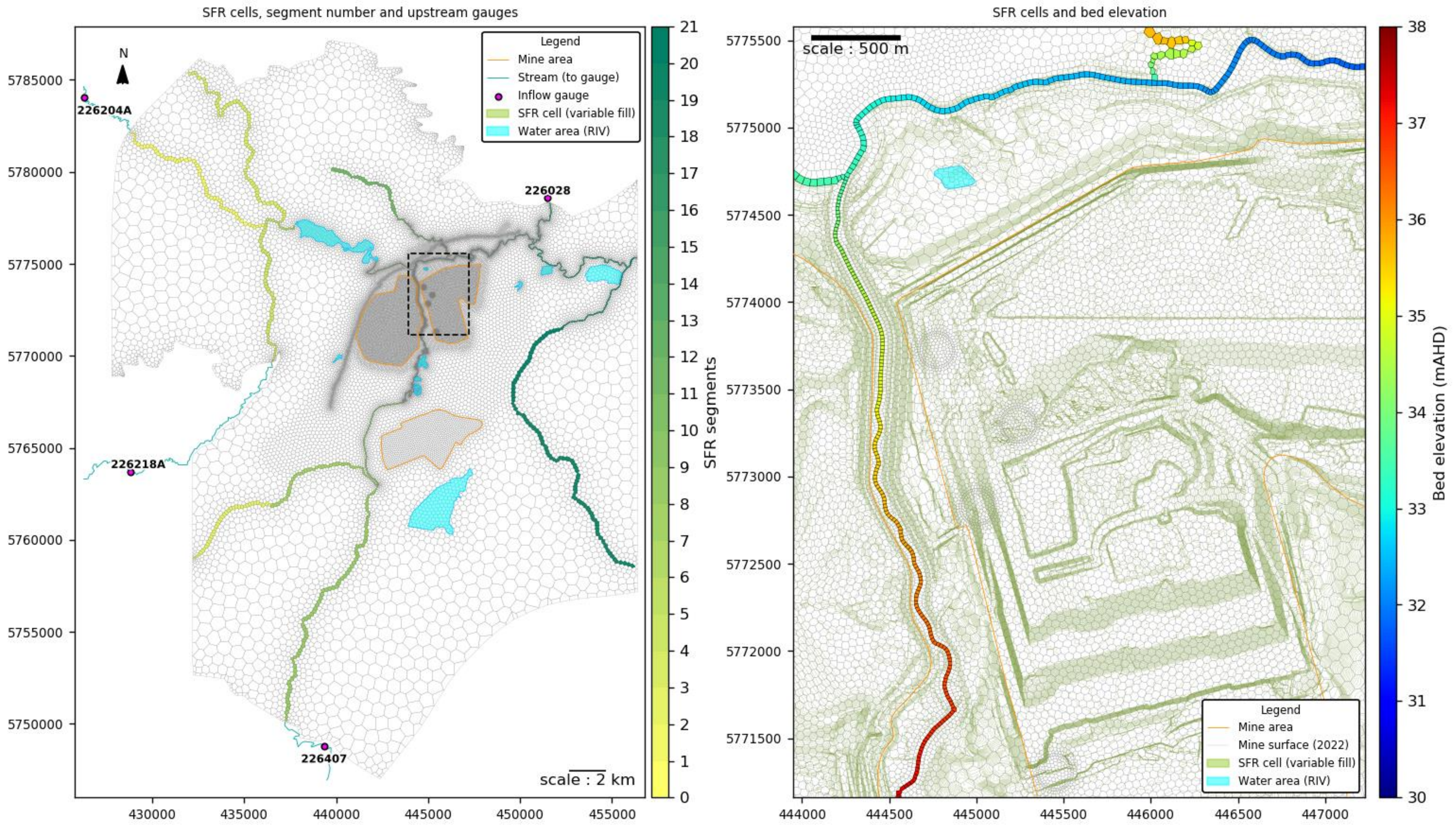

Figure 13 *SFR boundary condition*

2.5.3 River boundary condition

The River (RIV) package of USG-Transport is used to simulate features within the model domain that hold surface water either permanently or temporarily.

Water features outside of the Yallourn Mine void include Blue Lagoon, Lake Narracan, Witts Gully Reservoir, Pine Gully Reservoir, Morwell River wetlands, Hazelwood Cooling Pond (HCP) and APM lagoon and aeration pond. With the exception of the Morwell River wetlands, which were constructed around 2001, all these water features have been present for the majority of the historical calibration period (commencing in 1960) and are simulated using time-constant RIV stage estimated from Vicmap DEM and other publicly available information (except for Lake Narracan, where time-varying RIV stage has been applied from 2001 based on the storage level recorded at gauge 226236A). The RIV cells representing the Morwell River wetlands are activated in 2001, when these wetlands were first flooded. The approximate depth of these water features (RIV bed elevation) has been estimated from the information collected by EAY (including historical elevation maps) and other publicly available information (de Kretser et al; 2002, PB; 2014).

The water features within the Yallourn Mine void (in-pit water features) include Township Lake (Lake Placid), Fire Service Pond, Floc Pond, Dewatering Pond, Eastfield Sump, North East Pond and Marval Field Sump (see Figure 15). The RIV cells representing these features are activated in accordance with the timing of formation of these features, with the extent of each water feature adjusted over time based on the estimated and measured water levels supplied by EAY (see Figure 14). The RIV cells are assigned to the layer representing the floor of the mine (lowest DRN cell), with the RIV bed elevation set equal to the mine floor elevation (with a nominal bed thickness of 0.1 m).

All of the DRN cells at the location of RIV cells are deactivated (removed) when the RIV cells are activated, to prevent conflicting boundary conditions. This works well because all of the cells occupying the volume of the void are dewatered first by the DRN cells and leakage from the in-pit water features is only initiated when the RIV cells are first activated (with the RIV cells only allowing leakage in the vertical direction, based on the difference between the RIV stage and head in the underlying aquifer or RIV bottom elevation if disconnected).

The RIV conductance value for each RIV cell is calculated from the cross-sectional cell area (which varies for every Voronoi cell), assuming a RIV bed thickness of 0.1 m and hydraulic conductivity adjusted during calibration. The calibrated range of RIV conductance values are further discussed in Section 3.2.2.1.

Figure 15 shows the location of RIV cells simulated at the end of calibration, corresponding to the end of year 2021 (Section 3.1.1 provides further details on the calibration timeframe and associated stress periods).

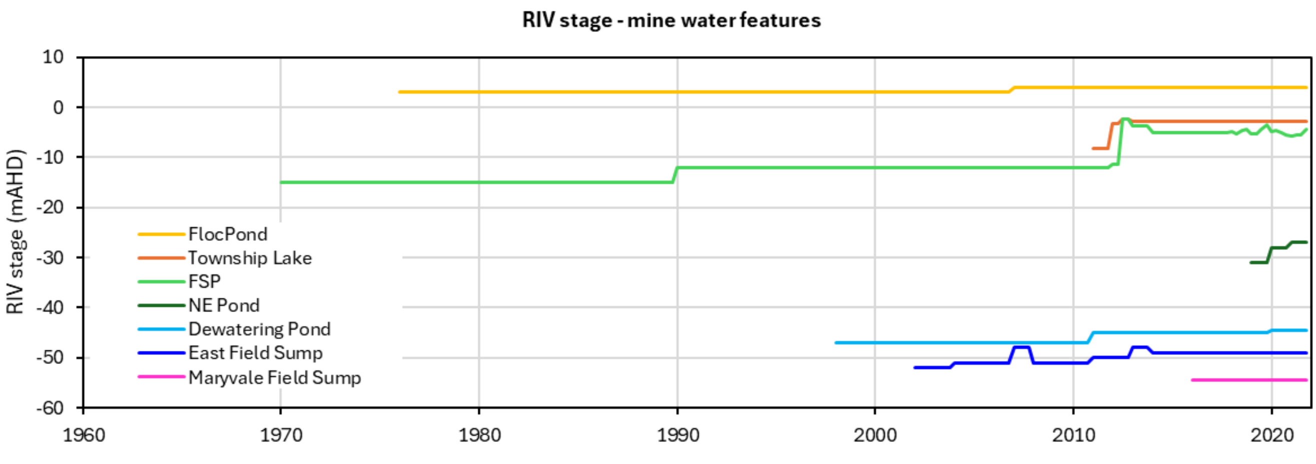

Figure 14 *RIV stage for mine water features*

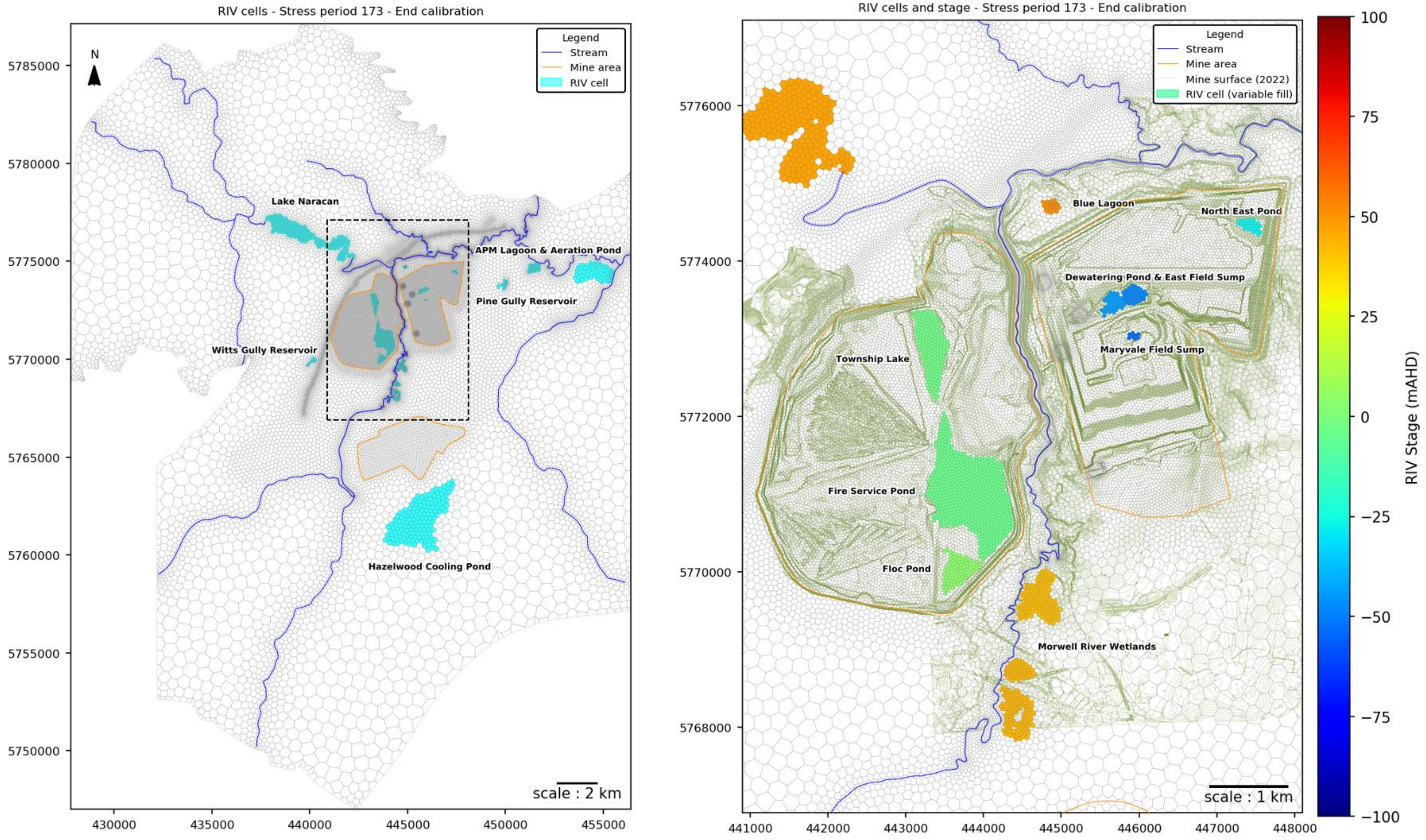

Figure 15 *RIV boundary condition*

2.5.4 Drain boundary condition

The Drain (DRN) package is used to simulate the excavation of overburden and coal at the Yallourn Mine, in accordance with the historical mine development (GHD, 2023b). The location and elevation of DRN cells have been derived from a series of historical mine survey drawings and digital mine plans supplied by EAY. For periods prior to 1994, the mine progression in Yallourn Open Cut and Township Field has been interpreted from the mine development plan published in 1989 (refer to Appendix A and Figure 15 of GHD, 2023b) with the DRN elevation set equal to the bottom of the Yallourn Coal (assuming excavation of the full thickness of the coal). From 1994 onwards, detailed digital mine surfaces from 1994, 1999, 2004, 2009 and annually from 2014 to 2022 have been used to accurately define the DRN elevations and mine progression. The elevation of DRN cells has been linearly interpolated between the mine surfaces that are more than one year apart, to simulate the mine progression on annual increments. Figure 16 shows the elevation of the DRN cells mapped to the model grid for selected time periods.

The DRN cells are assigned to the lowest layer within which the base of the mine is located. The DRN cells are also assigned to all of the overlying layers, with the DRN elevation set equal to the cell bottom to fully dewater the cells that occupy the void space. As mining progresses over time, the total number of DRN cells increases as the mine floor deepens over an increasingly wider area. For each DRN cell, a conductance value of 100 m^2/d is applied, high enough to fully DRN the cells to the specified DRN elevations.

As discussed in Section 2.5.3, the River (RIV) boundary condition is used to simulate the presence of water features within the mine void. When the RIV cells are activated, the DRN boundary condition is deactivated (deleted) to prevent conflicting boundary conditions within the same model cells.

In addition to the Yallourn Mine progression, the DRN boundary condition is used to simulate the hydraulic head changes at the Hazelwood Mine from mining and aquifer depressurisation. In this case, the DRN cells are assigned over the footprint of the Hazelwood Mine, from layer 1 to 17, and the DRN elevations are set based on the hydraulic heads extracted from the LVRGM (with each DRN cell effectively representing the time series of hydraulic heads computed at that location). This provides a highly efficient means of simulating the major aquifer depressurisation effect at the Hazelwood Mine without having to explicitly simulate the mining and depressurisation processes at this mine. The DRN boundary condition only allows fluxes out of the model, which makes it well suited to simulating the net loss of groundwater due to mining at Hazelwood. The extent and elevation of DRN cells used to simulate the aquifer depressurisation of the confined M2 aquifer are shown in Figure 17, for selected time periods (showing the effect of pumping and how this has changed over time).

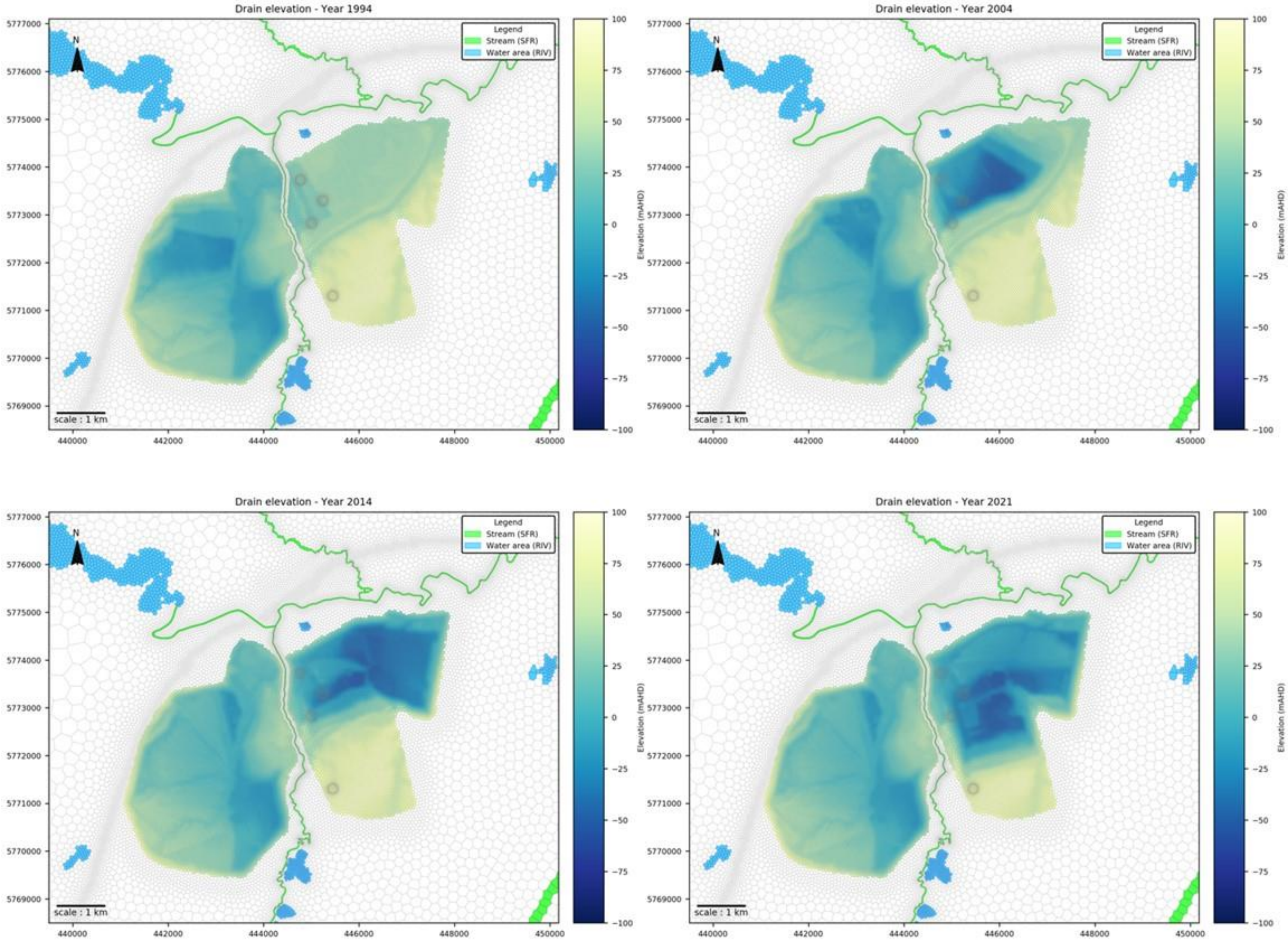

Figure 16 ***Yallourn mine DRN surface elevation***

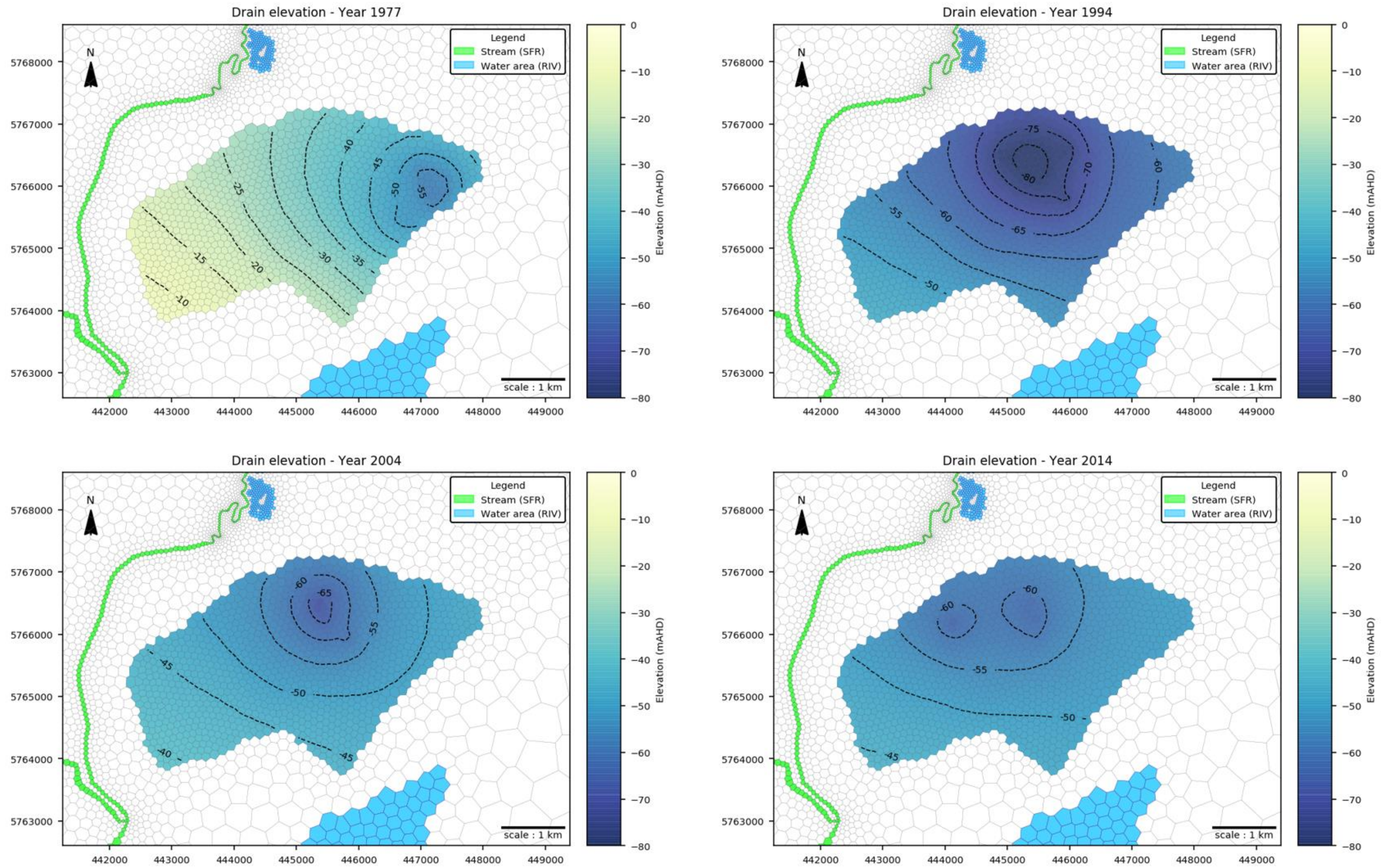

Figure 17 ***DRN elevation at Hazelwood Mine***

2.5.5 Well boundary condition

The Well (WEL) package of USG-Transport is used to simulate the extraction of groundwater by pumping bores at the Yallourn Mine, YNOC and for other non-mining uses. The location of pumping bores and the groundwater extraction rates used in the modelling are based on those described in GHD (2023b) and are shown in Figure 19. These include:

– Groundwater extraction from the M1A Interseam at the Yallourn Mine, commencing in 1996. Up to 12 pumping bores are incorporated to simulate the historical groundwater extractions at the mine in accordance with the pumping record. The two active pumping bores (at the time of reporting) and one additional ex-pit pumping bore (commissioned in 2024) are shown in Figure 19[2].

– Groundwater extraction at the YNOC, which includes pumping from ash fill and underlying coal, interseams and basement. Although there are large number of pumping bores at the YNOC, not all bores are operational or pumping continuously, and detailed simulation of pumping schedule and local scale processes within the YNOC is beyond the scope of this modelling (also noting that the YNOC is hydraulically poorly connected with the mine, as discussed in Section 4.8.2.3 in GHD, 2023b). The pumping effect has been simplified by assigning extraction rates to 10 main pumping bores where reliable flow records are available (from 2016 onwards).

– Other (non-mining) groundwater extraction, derived from the LVRGM and regional groundwater usage data. These pumping bores are based on the licence data supplied by SRW, which include bores within the Moe Groundwater Management Unit (GMU), and unmetered stock and domestic bores (for which a nominal usage of 2 mega litres per year is applied). The groundwater extraction rates are based on the actual and estimated usage (the latter derived from the licensed allocation per bore multiplied by a typical usage factor for the corresponding GMU). The annual extraction rates are apportioned into quarterly extraction rates to reflect expected seasonal variations in demand, with pumping assumed to commence based on the date of bore completion recorded in the Water Management Information System (WMIS) database.

The pumping bores have been mapped to the nearest node based on their location and screen interval/aquifers. A total of 51 bores are incorporated into the model to simulate the historical extractions. For the pumping bores in the M1A Interseam at the mine, the WEL node has been assigned to the correct model layers (8,9,10) based on the intersection of the screen interval with the model layers representing this aquifer. Pumping bores N6899 and M4203 have multiple screen intervals, intersecting more than one model layer. In this case, two WEL nodes are used to simulate the effect of pumping from each bore with the pumping rate split evenly between the two nodes (model layers 9 and 10 for N6899 and 8 and 10 for M4203).

All pumping rates are apportioned in accordance with the length of model stress periods. USG-Transport's automated flux reduction capability is activated to automatically adjust the pumping rates and prevent well cells from becoming dry as a result of pumping. This prevents the Upstream Weighting scheme of MODFLOW-NWT from simulating unrealistic negative heads in dry well cells when pumping is allowed to continue at the full rate irrespective of the amount of drawdown.

Figure 18 shows the annualised groundwater extraction rates applied using the WEL package for the model calibration period, comparing the groundwater extraction rates of the Yallourn Mine with other groundwater uses for context. The extraction rates are presented since 1995, coinciding with the timing of the aquifer depressurisation program commencing at the Yallourn Mine (note many of the stock and domestic bores are assumed to start pumping before 1995, based on their bore completion date). The groundwater extraction at the Hazelwood Mine is not included, as the effect of aquifer depressurisation is simulated using the DRN package (as discussed in Section 2.5.4).

[2] The model grid has been locally refined around the three existing/historical pumping bores that have accounted for the majority of bore yields (bores N5056 and N6899, as shown in Figure 19 and bore N4934 to the north; refer to Figure 15 of GHD, 2023b). The grid was also refined around the original (planned) location of bore M4203 (at the time of the model construction); however, this bore was subsequently relocated further to the north (as shown in Figure 19).

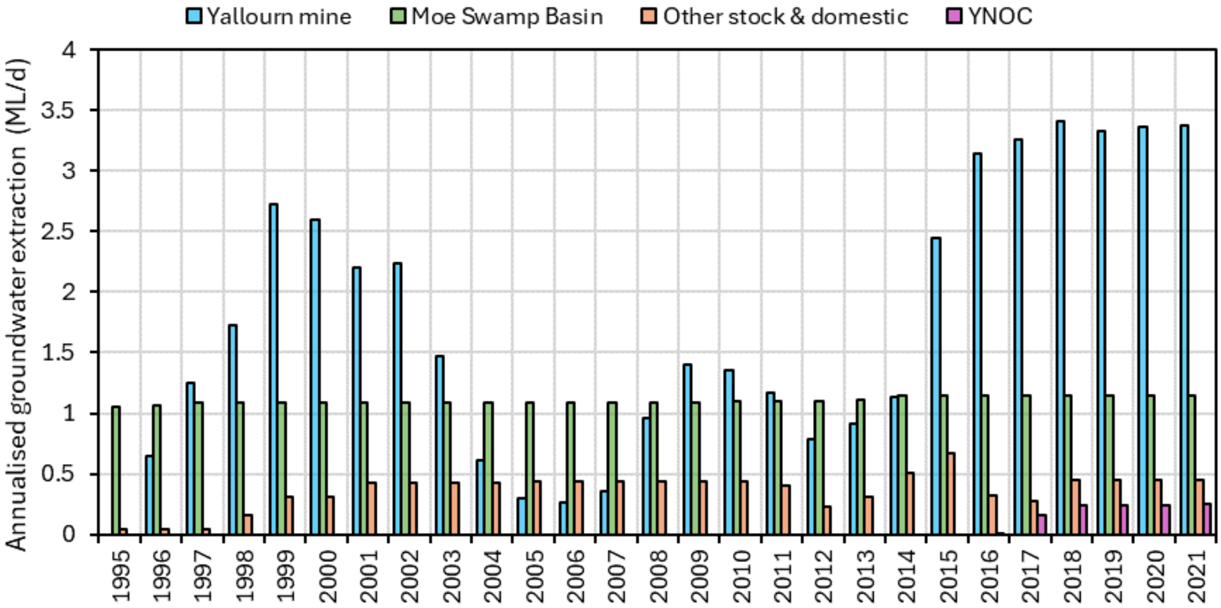

Figure 18 Modelled annualised groundwater extraction rates

2.5.6 General head boundary condition

The General Head Boundary (GHB) package of USG-Transport is used to simulate the throughflow of groundwater across the model boundaries (outer edges of the model) based on groundwater levels specified along the boundaries. The GHB boundary condition is assigned along:

– The entire length of the eastern boundary to simulate regional changes in piezometric heads, primarily due to the cumulative effect of the confined aquifer depressurisation at the Loy Yang Mine. The time-varying heads are extracted from the LVRGM (from cells located along the length of the eastern boundary) and assigned to the nearest GHB cells.
– The western boundary across the Narracan Block to simulate the head changes within the outcropping Thorpdale Volcanics and throughflow of shallow groundwater. The time-varying heads are extracted from the LVRGM along the length of the boundary and assigned to the nearest GHB cells.
– The western boundary along the Moe Swamp Basin to simulate the throughflow of groundwater into the basin. Given the substantial distance of this boundary to the Yallourn Mine and Haunted Hills Fault/Yallourn Monocline, a time-constant value of 68 mAHD has been assigned to simulate the regional throughflow (based on the groundwater levels recorded in regional monitoring bores near this boundary).

The conductance term for each GHB cell is calculated from the cross-sectional area of the cell (perpendicular to the horizontal flow direction) and the horizontal hydraulic conductivity assigned to the cell. The location of GHB cells is shown in Figure 19 and the calibrated range of conductance values are discussed in Section 3.2.2.1.

2.5.7 Horizontal flow barrier

The Horizontal Flow Barrier (HFB) package of USG-Transport is used to simulate the resistance to flow that occurs along the Haunted Hills Fault/Yallourn Monocline, which limits hydraulic connections between the aquifers of the mine and those associated with the Moe Swamp Base and YNOC (refer to Sections 4.8.2.2 and 4.8.2.3 of GHD, 2023b). The HFBs are simulated by reducing the conductance between two horizontally connected cells (in this case, by assigning a low hydraulic conductivity value of 1×10^{-6} m/d assuming a metre thickness). The location of HFBs is based on the fault alignment mapped by EAY and that interpreted by GHD from the analysis of seismic data (see Figure 20). Adjustments were made during model calibration based on the piezometric head differences observed and simulated at monitoring bores located on either side of the fault. The HFBs assigned to the southwest of the Yallourn Mine are based on those included in the LVRGM, using the data from regional monitoring bores. The effect of HFBs on model outputs is discussed further in Section 3.2.3.

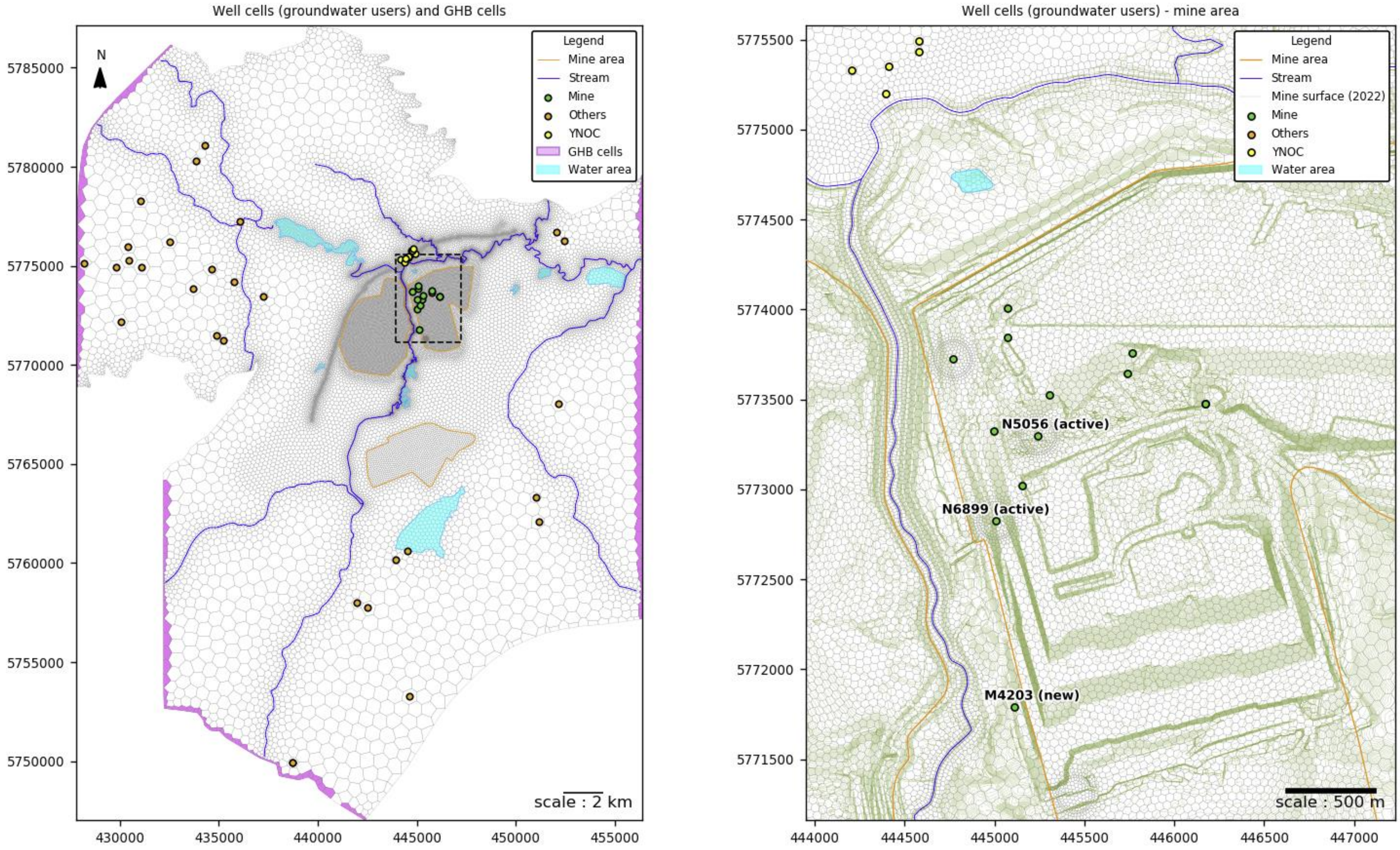

Figure 19 ***Well and GHB boundary conditions***

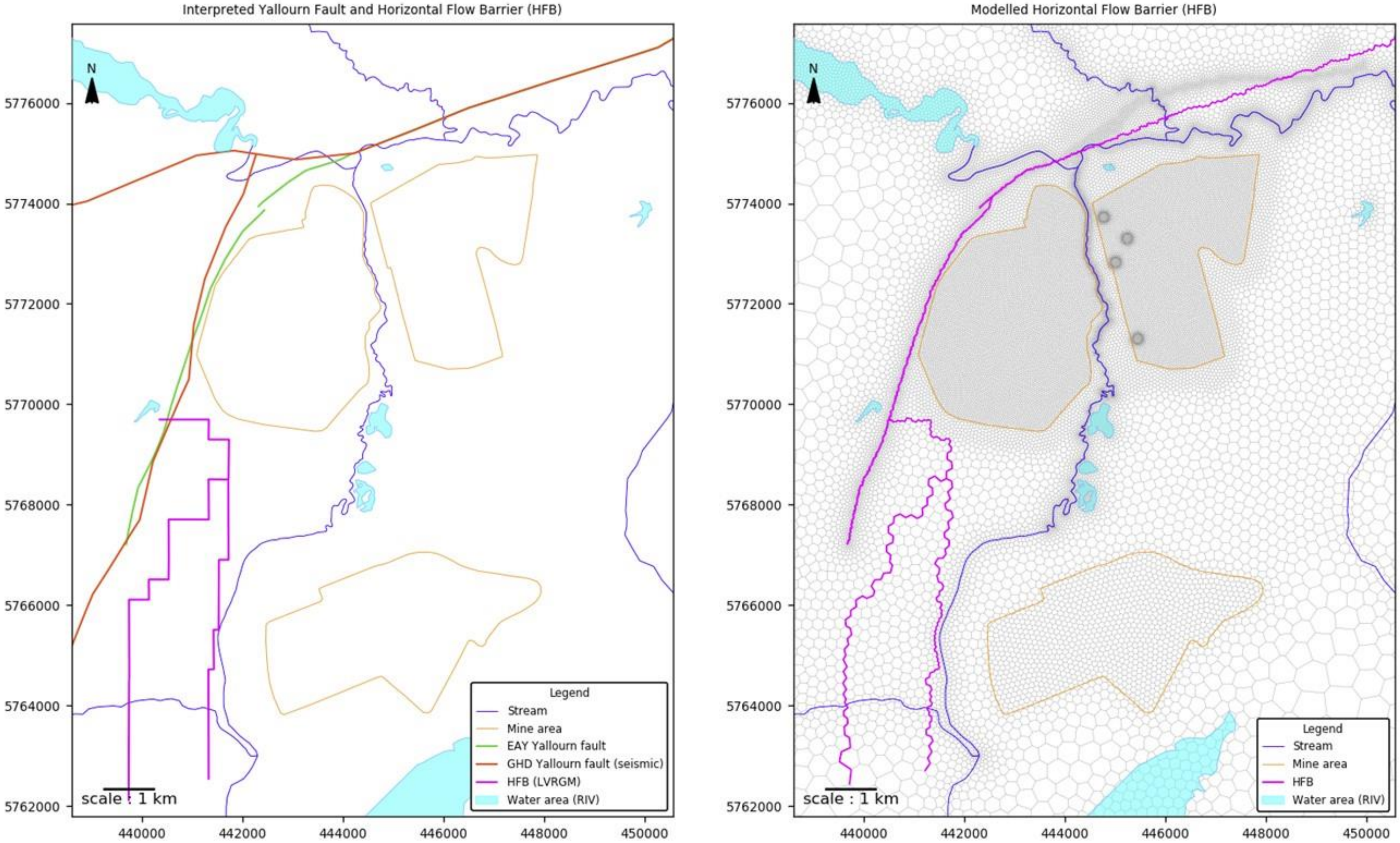

Figure 20 ***Horizontal flow barriers***

2.6 Model parameterisation

2.6.1 Parameterisation approach

Parameterisation involves making choices about how the spatial distribution of aquifer properties will be represented in the model (Barnett et al, 2012). Models with the smallest number of parameters possible are described as parsimonious whereas models with a large number of spatially varying parameters are described as highly parameterised. In modelling studies, a balance is sought between parsimony and complexity (highly parameterised spatial variability) that is consistent with the objective of modelling, the physical system of interest and supporting data.

For this project, the model is parameterised on an HSU basis; however, hydraulic conductivities are varied spatially within each aquifer unit through the use of percent sand grids (sand fractions) generated for the relevant model layers (in this case, model layers 1,6,8,9,10,12,14 and 16 representing the aquifer units). The percent sand grids provide an efficient means of incorporating hydrogeologically sensible distributions of hydraulic conductivity based on the sand abundance derived from the borehole data. Experience with the LVRGM has shown that this parameterisation approach works well for the Latrobe Valley groundwater systems, facilitating the model calibration process without having to rely on a large number of parameters to infer spatial variability (for example, using pilot points).

The percentage sand grids used for the model are derived from the LVRGM except for the Haunted Hills Formation and M1A Interseam at the Yallourn Mine, where more detailed percent sand grids have been calculated from sand thickness maps derived from the Minescape geological model (based on the site specific borehole data). For the M1A Interseam, the percent sand grid has been generated for each of the three model layers representing this aquifer (8,9 and 10) by calculating the total thickness of sands intersecting each model layer and dividing this by the layer thickness (as shown schematically in Figure 21). This approach allows the spatial differences in sand thickness (and hydraulic conductivity) to be simulated in horizontal as well as vertical directions without having to explicitly model the individual sand lenses and interburden layers. The percent sand grids adopted for the key aquifer layers are presented in Appendix D.

The percentage sand grids are converted into horizontal hydraulic conductivity grids using a multiplier for each parameter zone. Two parameter zones (mine and regional) are defined for the Haunted Hills Formation, Yallourn Interseam and M1A Interseam, based on the extent of the Minescape geological model (for the Haunted Hills Formation, the mine parameter zone is based on the extent of a well defined basal sand unit that exists along the floor of this unit, which has been delineated from the borehole logs). Using two separate parameter zones ensures the different underlying data (and method) used to generate the percentage sand grids at the mine and elsewhere are accounted for in the model calibration (also recognising the different amount of observation data available to inform the model calibration). A minimum sand percent of 0.1 % is used, so the hydraulic conductivity does not vary by more than three orders of magnitude within each aquifer unit (thereby preventing unrealistic range of values). The aquitard (coal and Thorpdale Volcanics) units are parameterised as zones of uniform (albeit anisotropic) property.

The model parameters are further discussed in Section 3.2.2 based on the results of model calibration.

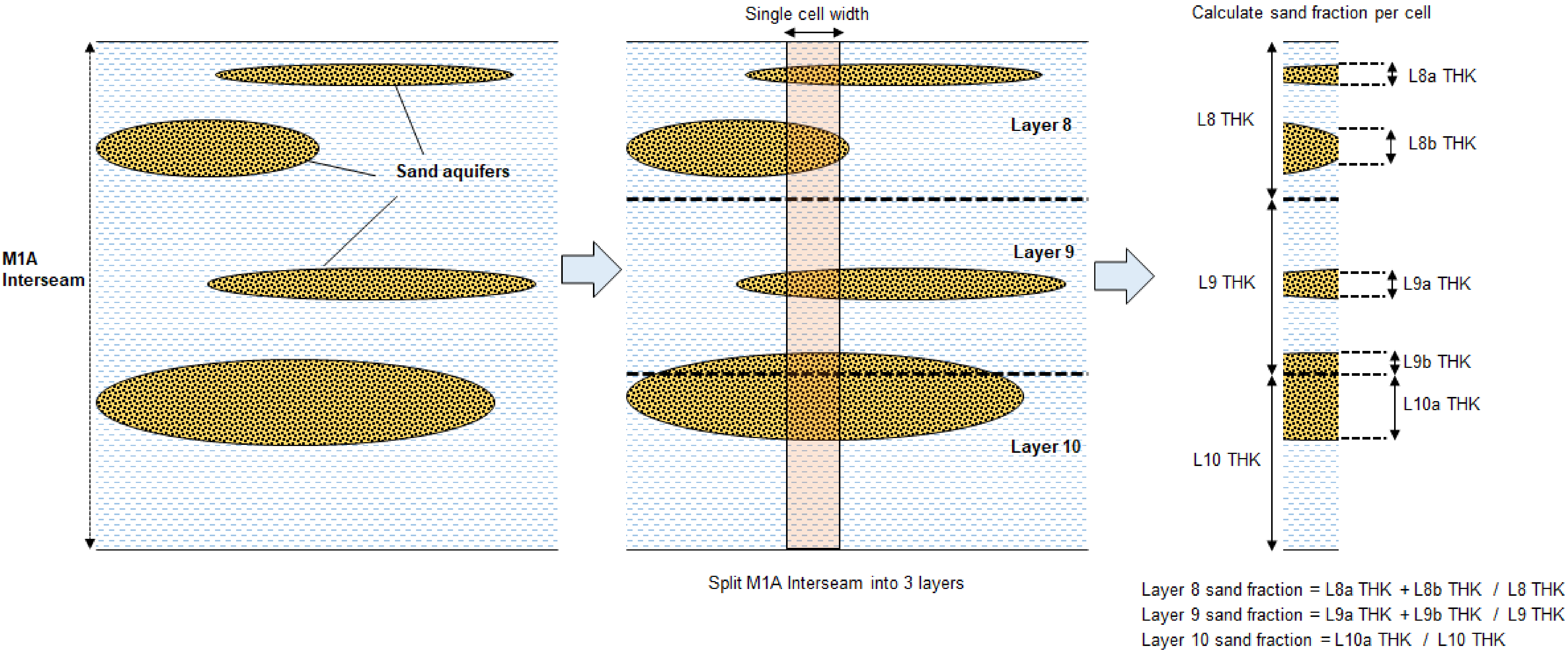

Figure 21 Schematic representation of sand fraction calculation of M1A Interseam model layers

2.6.2 Time-variant materials

During mining, the material properties of the Yallourn Coal experience changes within the batters and along the floor of the mine due to ground movement that leads to the formation of fractures and opening of pre-existing joints. As described in GHD (2023b), steeply dipping joints and fractures have been observed in numerous locations, which are often closed in-situ but can open up during mining due to pressure relief as the weight of the adjacent material is removed. The sub-vertical joints and faults can locally increase hydraulic conductivity of the coal by providing preferential groundwater pathways, resulting in rapid pore pressure changes such as those observed in response to the June 2021 flood event (refer to Section 4.8.1 of GHD, 2023b). In addition to the fracturing of coal, the overburden material excavated during mining has been placed within the mine void to form internal overburden dumps with thicknesses of up to around 70 m (refer to Section 4.3.4 and Figure 27 of GHD, 2023b). Both of these material property changes occur over time due to the progressive nature of mining.

The Time-Variant Materials (TVM) package of USG-Transport is used to simulate the transient material property changes of the Yallourn Coal layers (model layers 2 to 5). For the fracturing of the coal, two broad zones of material property changes are defined based on the information supplied by EAY. These include:

– A zone of highly fractured coal along the floor of the mine and coal batters, where open joints, many with large apertures, are present and the hydraulic conductivity is most enhanced.
– A zone of moderately fractured coal, extending 100 to 700 m from the batter crests, where open joints are present albeit with smaller apertures and larger spacing (lower density) compared to the highly fractured zone. Beyond this zone, the undisturbed (in-situ) coal material properties are assumed based on no movement mechanisms to open the coal joints.

For the placement of the overburden, a zone of material property changes is defined over the mapped footprint of the internal overburden dumps (such as that presented in GHD, 2023b). The extents of all TVM zones are shown in Figure 22. The zone of moderately fractured coal was initially delineated based on the expected area of influence of the movement mechanisms and subsequently adjusted during model calibration (based on the simulated influence of fracturing at observation bores). The material property changes within each zone are applied progressively, to reflect the progression of mining and overburden placement. This has been achieved by dividing the TVM zones into discrete sub-zones and incorporating the material property changes when the mine surface (drain elevation) reaches full depth in each sub-zone (to represent the material property changes that would occur once the coal has been excavated). The timing of material property changes is shown in Figure 22, using the stress period numbers of the model calibration period (which are further discussed in Section 3.1.1).

The implementation of material property changes is schematically presented in Figure 23. The drain (DRN) cells are activated first to simulate the excavation of the Haunted Hills Formation/overburden and Yallourn Coal (creating dry or dewatered cells where the DRN cells are assigned). After the DRN elevation reaches the full depth, the material property changes (fracturing of coal) are activated in the Yallourn Coal layers (at the start of the next stress period). This means the movement mechanisms and associated fracturing of coal are assumed to have taken place after the void (within each TVM sub-zone) has reached full depth.

Where the internal overburden dumps are present, the overburden material properties are assigned. This occurs initially in dry cells (drained by the DRN cells) and the overburden material properties only become effective when the DRN elevation is subsequently raised to simulate the placement of the overburden dumps. This ensures that the re-saturation of the previously drained cells occurs in response to the changed material properties, thereby correctly accounting for the influence of the dumped overburden.

The linear interpolation option is used instead of the step function option to introduce material property changes between stress period boundaries in a gradual manner. However, given the large areas of TVM zones, the modelled material property changes typically result in short term piezometric head changes that are more abrupt than those observed (in response to more complex and variable material property changes that would occur in reality). This effect is further discussed in Section 3.2.1.1.

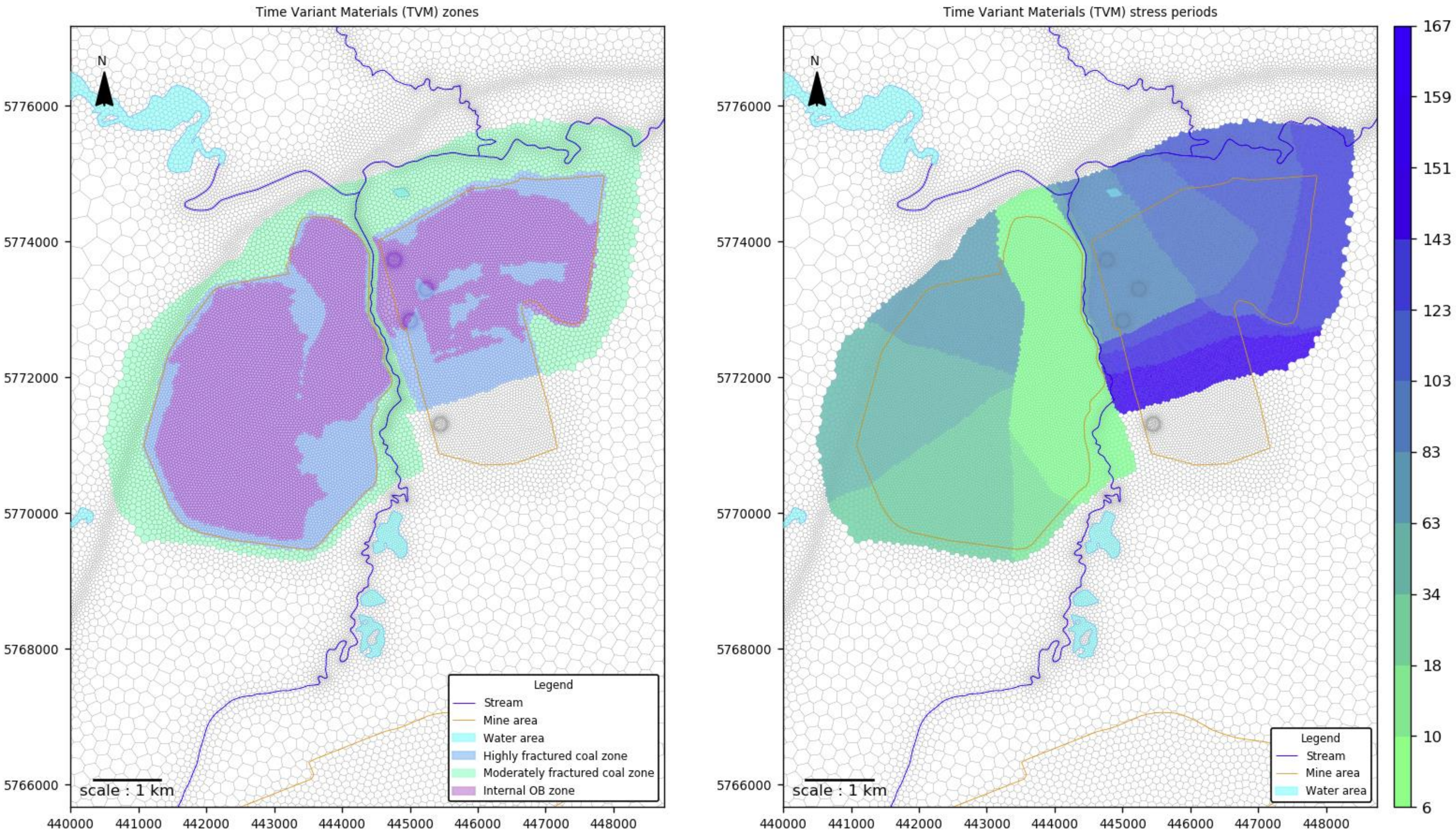

Figure 22 *Time-variant material zones*

Stress period years are: 6 (1965), 10 (1969), 18 (1977), 34 (1987), 63 (1994), 83 (1999), 103 (2004), 123 (2009), 143 (2014), 151 (2016), 159 (2018), 167 (2020). Refer to Section 3.1.1.

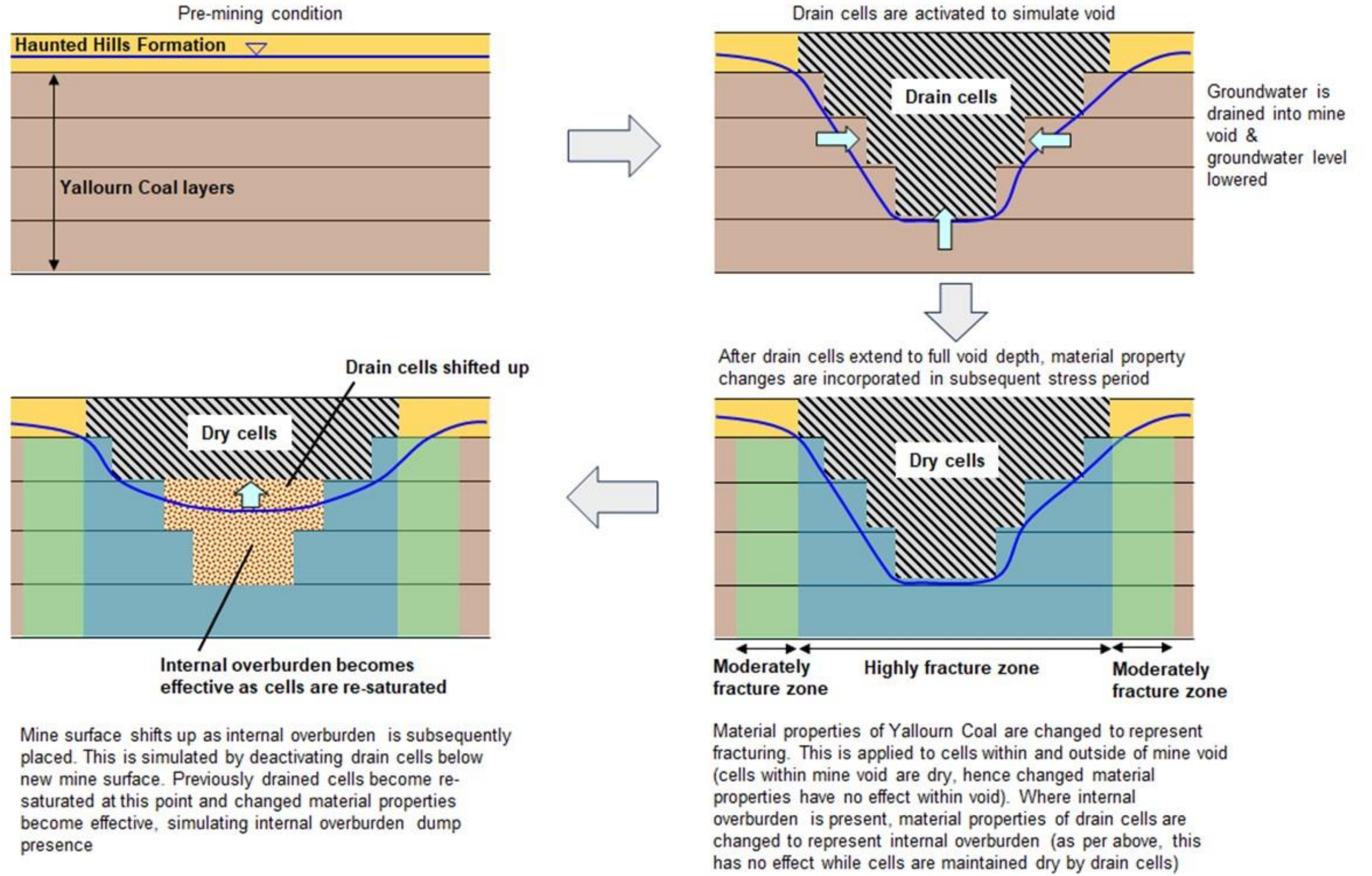

Figure 23 Time-variant materials implementation

3. Model calibration

3.1 Calibration approach

3.1.1 Calibration period

The model calibration period commences in January 1960 and extends to the end of 2021, capturing over 60 years of historical mining activities. While mining at Yallourn pre-dates this period, the drainage of groundwater was localised (including the YNOC) and the major aquifer depressurisation program at the Hazelwood Mine did not commence until after 1960 (leading to regional significant cumulative hydrogeological effects). Setting the start of calibration to 1960 provides a sufficient "warm up" period for the model to accommodate the early time mining effects, before the groundwater observations became more readily available at the Yallourn Mine to enable targeted calibration (refer to Section 3.1 and Section 3.2.4 of GHD, 2023b for the mine history and data availability). The model calibration period is also aligned to that of the LVRGM, which streamlines the transfer of information between the two models, allowing the LVRGM outputs to be efficiently translated into relevant model boundary conditions for the Yallourn model.

The transient calibration utilises annual stress periods (SP) from 1960 to the end of 1984 (SP1 to SP25), reducing to quarterly stress periods from 1985 to end 2021 (SP26 to SP173) to allow seasonal variations and temporal effects of mining to be more accurately simulated (as the number and accuracy of observation and mining related data increases over time). A steady state simulation of an average pre-mining condition is undertaken to provide initial heads to the transient simulation.

3.1.2 Calibration targets

3.1.2.1 Head targets

The primary calibration targets are time series of piezometric heads measured in observation bores and vibrating wire piezometers (VWPs) distributed throughout the model domain and across model layers. There is a significant amount of groundwater level data available from the Yallourn Mine bore database; however, not all bore data are deemed reliable or suitable for the purpose of calibration (e.g. anomalous trends, often caused by localised effects that are not possible to replicate in the model). Based on a rigorous review of the bore data, a total of 418 bores/piezometers from the Yallourn Mine bore database have been selected for model calibration. These are primarily from the key aquifer layers (Haunted Hills Formation, Yallourn Interseam and M1A Interseam) although representative bores/piezometers from the Yallourn Coal and internal overburden dumps are also included. Some of the piezometers are nested, measuring groundwater levels in multiple HSUs (model layers) at the same location.

For areas outside of the Yallourn Mine, regional calibration targets from the LVRGM as well as bores from the Moe Swamp Basin are used for calibration and to ensure the model performance is reasonable across the broader area of the model domain (specifically, the regional aquifer depressurisation effects from the Hazelwood and Loy Yang Mines, and stable trends observed in the Moe Swamp Basin due to the effect of the Haunted Hills Fault/Yallourn Monocline). A total of 53 regional bores with long term monitoring data have been selected for model calibration.

The measurements of piezometric heads from the 471 bores/piezometers have been reviewed and anomalous/erroneous measurements have been removed from the calibration dataset. Where a very large number of measurements are available (e.g. daily), these have been converted into average monthly measurements that are more in line with the length of the model stress periods (quarterly), ensuring the number of head targets used in the calibration is not excessive.

The measurements of piezometric head from the monitoring bores have been used to derive:

– 34,778 absolute head targets, representing the actual elevation of piezometric heads in mAHD.
– 34,872 head differences targets, representing the change in piezometric heads from the initial reading (temporal trends, in metres).
– 1,858 vertical head difference targets between 25 nested/closely spaced monitoring bores/VWPs (in metres).

3.1.2.2 Stream stage and flow targets

The SFR2 package is used to simulate total stream flow as well as stream stage (calculated using Manning's equation assuming a wide rectangular channel). To ensure realistic stream behaviour and interactions with the shallow groundwater system, stream flow and stream stage measured at key stream gauges located within the model domain are used as calibration targets.

The stream stage targets are derived from the water level measurements recorded at the following locations:

– MRD southern (upstream) crossing (gauge 26737) and northern (downstream) crossing (gauge 26736). Daily stage measurements are collected at these two locations by EAY and are available from mid-2014 (with spot measurements available from earlier periods).
– Morwell River at Yallourn (gauge 226408), providing measurements of water level in the Morwell River upstream of the MRD (and downstream of the Morwell River wetlands). Daily stage measurements are available from 1986 to 2018.
– Latrobe River at Thoms Bridge (gauge 226005A), providing measurements of water level in the Latrobe River downstream of the Yallourn Mine. Long term daily measurements are available since 1962.

The stream flow targets are derived from the flow data recorded at gauge 226408 (Morwell River at Yallourn) and at gauge 226005A (Latrobe River at Thoms Bridget). As per the stage data, daily flow measurements are available at these gauges over the corresponding periods (1986 to 2018 for 226408 and since 1962 for 226005A). Daily flow measurements recorded at gauge 226033A, located in the Latrobe River at Scarnes Bridge, are also used for flow calibration. Although this gauge is located outside of the model domain (around 4.3 km downstream), the flows recorded at this location can be checked against the flow recorded at the last stream reach of the Latrobe River, to ensure the flow volumes exiting the model are sensible.

The daily stage and flow measurements are converted into quarterly average targets, to align with the length of the model stress periods (and the average stages and flows computed by the model in each stress period). In total, 356 quarterly stage targets and 279 quarterly flow targets are used in the model calibration.

In addition to the stage and flow measurements, estimates of baseflow derived from the electrical conductivity (EC) mass balance method (GHD, 2013a,b) at the Morwell River gauge (226408) are used in calibration. As discussed in GHD (2023b), there is considerable uncertainty in the estimates of baseflow due to uncertainties associated with the significant discharge rates and EC of water returned from the industries. Experience with the LVRGM suggests that the actual baseflow is likely to be at or below the lower end of the estimated range. For this reason, the estimated baseflow rates are used only as loose calibration targets, to ensure that some quantifiable baseflows are simulated by the model along the Morwell River and that the simulated baseflow characteristics are broadly consistent with those inferred from the prior baseflow studies (slightly gaining to baseflow neutral along the Morwell River and Latrobe River, as discussed in Section 4.9.1 of GHD, 2023b).

3.1.2.3 Groundwater extraction targets

The automated flux reduction capability of USG-Transport is used to adjust the pumping rates to prevent unrealistic dry cells from developing in the model when the rates are large relative to the capacity of the model to supply the necessary flow (Section 2.5.5). This could lead to pumping rates that are much lower than the measured and estimated rates as the model parameter values are adjusted during calibration. To minimise the potential for excessive reductions in the pumping rates (leading to unrealistic water balance), the prescribed pumping rates are used as loose calibration targets by converting them into average pumping rates per model layer for the entire transient calibration period. This serves as a constraint to prevent unrealistic parameter realisations from developing during automated calibration that are insufficient to sustain the measured pumping rates.

Aquifer depressurisation at the Hazelwood Mine is simulated in an efficient manner using the DRN boundary condition (Section 2.5.4). In this case, the net measured groundwater extraction rates at the Hazelwood Mine are incorporated as flow calibration targets to ensure realistic volumes of groundwater are removed by the DRN boundary condition. For each stress period, the extraction rate from all active extraction wells is aggregated to give average net extraction, which is compared against the outflow from the DRN cells assigned over the Hazelwood Mine footprint.

3.1.3 Calibration parameters

3.1.3.1 PRMS model parameters

The PRMS model parameters that are adjusted during model calibration include the following:

– The parameter “soil_moist_max”, representing the maximum water holding capacity of the capillary reservoir (from ground surface to the root depth of the major vegetation type) is parameterised on the basis of soil zones and vegetation type (grass and trees). There are 18 soil moisture parameters (nine soil zones for each of the two vegetation types), with the minimum and maximum values calculated from the published range of field capacity and wilting point for each soil zone (from the Atlas of Australian Soils) and the expected range of root depths for grass (0.2 to 2 m) and trees (from 2 to 7 m or up until reaching the maximum soil moisture value of 20 inches, as permitted by PRMS). For each soil zone, the areas of grass cover have a lower maximum value than the areas of tree cover (representing the lower potential loss of soil moisture via soil zone transpiration). Recharge is most sensitive to these soil moisture parameters.

– The parameter preferential flow density (referred to as “pfloden” in this report) is used to control the size of the preferential flow reservoir through which fast interflow takes place. A single parameter value is assigned to the whole model, noting that recharge is only slightly sensitive to this number (especially when applied on a model-wide basis). The parameter values are allowed to vary from 0.01 to 0.5, as per the recommendations of the PRMS manual.

– The parameters representing the influence of impervious areas, including Hortonian runoff from impervious surfaces and water retention on the surface (and evaporation loss from ponded water). These parameters are the impervious fraction and maximum impervious area water retention storage (referred to as “impervf” and “impervstr” in this report, respectively). The default range of parameter values are used, as per the recommendations of the PRMS manual.

– The parameters that control surface runoff, specifically the computation of the contributing area of runoff i.e. the fraction of pervious areas that contributes to runoff, which varies dynamically as a function of the soil moisture content. These include the coefficient and exponent of the non-linear contributing area algorithm used by PRMS, referred to as “smidxcf” and “smidxexp” in this report. These are parameterised on a model-wide basis, using the default range of parameter values recommended by PRMS.

– The parameters that control the summer and winter rain interception storage capacity for the major vegetation type, referred to as “sintcp” and “wintcp” respectively. These are parameterised on a model-wide basis, using the default range of parameter values recommended by PRMS.

The PRMS model requires many other input parameters; however, extensive testing has shown that the model outputs, particularly with reference to recharge, are not sensitive to these parameters. The default values recommended by the PRMS manual are used for these insensitive (and fixed) parameters.

3.1.3.2 USG-Transport model parameters

The USG-Transport model parameters that are adjusted during model calibration include the following:

– Multipliers that convert percentage (fractional) sand grids to horizontal hydraulic conductivity. As discussed in Section 2.6.1, these multipliers are applied to the HSUs that are classified as “aquifers”. For the Haunted Hills Formation (layer 1), Yallourn Interseam (layer 6) and M1A Interseam (layers 8,9 and 10), separate multiplier zones are defined over the footprint of the Yallourn Mine and regionally. This is to account for the different data sources used to generate the percentage sand grids and to enable more targeted calibration at the mine i.e. within the Minescape geological model area, the percentage sand grids are derived from a large number of borehole logs and more accurate delineation of sand thicknesses compared to the regional dataset outside of the mine. For the Haunted Hills Formation (layer 1), the multiplier zone at the mine is based on the extent of the sand lens delineated from historical borehole logs (also referred to as the Haunted Hills Formation Aquifer in the geological model), which has been incorporated into the percentage sand grid. Figure 24 shows the extent of percent sand multiplier zones for the three aquifer units. A total of 10 multiplier parameters are used (referred to as “pckx” parameters), with different multipliers used for each of the three M1A Interseam layers.

- Horizontal hydraulic conductivity assigned for HSUs that are classified as “aquitards”, with a single representative value for each HSU i.e. the aquitards are assumed to be homogeneous with a spatially constant hydraulic conductivity value representative of the bulk average. A total of 6 horizontal hydraulic conductivity parameters are defined for the aquitards layers (referred to as “kx” parameters). While not classified as an aquitard, the fill material of the YNOC is also simulated using a single representative horizontal hydraulic conductivity value (referred to as “ynocx” parameter). The fill material of the YNOC appears in both the aquifer and aquitard layers as the YNOC intersects multiple model layers (where the layers approach ground surface on the northern side of the Haunted Hills Fault). For the aquifer layers, the horizontal hydraulic conductivities derived from the percentage sand grids are locally replaced by the correct fill hydraulic conductivity value at the location of YNOC. This is achieved by setting the sand fraction to 1 at the YNOC cells and assigning the correct fill hydraulic conductivity value to the multiplier grid. Figure 24 shows the location of YNOC cells intersected by the Haunted Hills Formation (layer 1), Yallourn Interseam (layer 6) and M1A Interseam (layers 8,9 and 10).
- Multipliers that convert horizontal hydraulic conductivity into vertical hydraulic conductivity (representing the ratio of vertical to horizontal hydraulic conductivities). These are referred to as “kzfac” parameters (vertical hydraulic conductivity factors). The maximum value is constrained at 1 based on the recognition that the hydraulic conductivities in the vertical direction are typically less than those in the horizontal direction for layered aquifer systems, thereby preventing physically unrealistic anisotropy from developing during model calibration. A total of 17 vertical hydraulic conductivity factors have been adjusted during calibration.
- Specific yield and specific storage, with a single representative value for each HSU. In total, 17 specific yield (“sy”) and 17 specific storage (“ss”) parameters are defined as adjustable parameters.
- Time variant material (TVM) properties for the two fractured coal zones and internal overburden dump. For each of the three TVM zones, the parameters are defined for horizontal hydraulic conductivity (“tvm_kx”), vertical hydraulic conductivity factor (“tvm_kzf””), specific yield (“tvm_sy”) and specific storage (“tvm_ss”). A total of 12 adjustable TVM parameters are defined.
- Stream bed hydraulic conductivity of SFR cells (referred to as “sfrk” parameters). For the Morwell River SFR cells, three bed hydraulic conductivity parameters are defined to differentiate sections of the river underlain by natural bed sediments from those of the MRD with constructed clay and geosynthetic liners. The SFR bed hydraulic conductivity parameter is also defined along the Latrobe River, while applying the same parameter for all other (regional) SFR cells. A total of five adjustable SFR bed conductivity parameters are used (refer to Figure 24 for the location of SFR bed conductivity zones).
- River bed hydraulic conductivity of RIV cells, referred to as “rivk” parameters which are assigned to the in-pit mine water features (using one representative parameter value) and all other ex-pit water features (separate parameter values for Blue Lagoon, Witts Gulley Reservoir, Lake Narracan, Morwell River Wetlands, Pine Gulley Reservoir, AMP lagoons and Hazelwood Cooling Pond), resulting in eight river bed hydraulic conductivity parameters. For each RIV cell, a unique conductance value is calculated from the bed hydraulic conductivity, cell surface area and bed thickness (assumed a nominal 0.1 m bed thickness for all RIV cells). This is necessary to account for the unique surface area of each cell within the unstructured grid, ensuring that the resistance to flow represented by the conductance value is consistent with the surface area of each RIV cell.
- Evapotranspiration extinction depth, which is required by the EVT package of the USG-Transport model but not calculated by the PRMS model. Two extinction depth parameters (“exdp”) are defined for areas covered predominantly by trees and grass, consistent with the broad classification of vegetation type assumed in the PRMS model (see Appendix C).

A total of 120 adjustable parameters have been calibrated for the coupled PRMS-USG-Transport model. The minimum, maximum and initial values for each parameter are based on a realistic range of values informed by their material properties, field data and previous modelling experience. These are summarised and discussed further in Section 3.2.2, along with the results of model calibration.

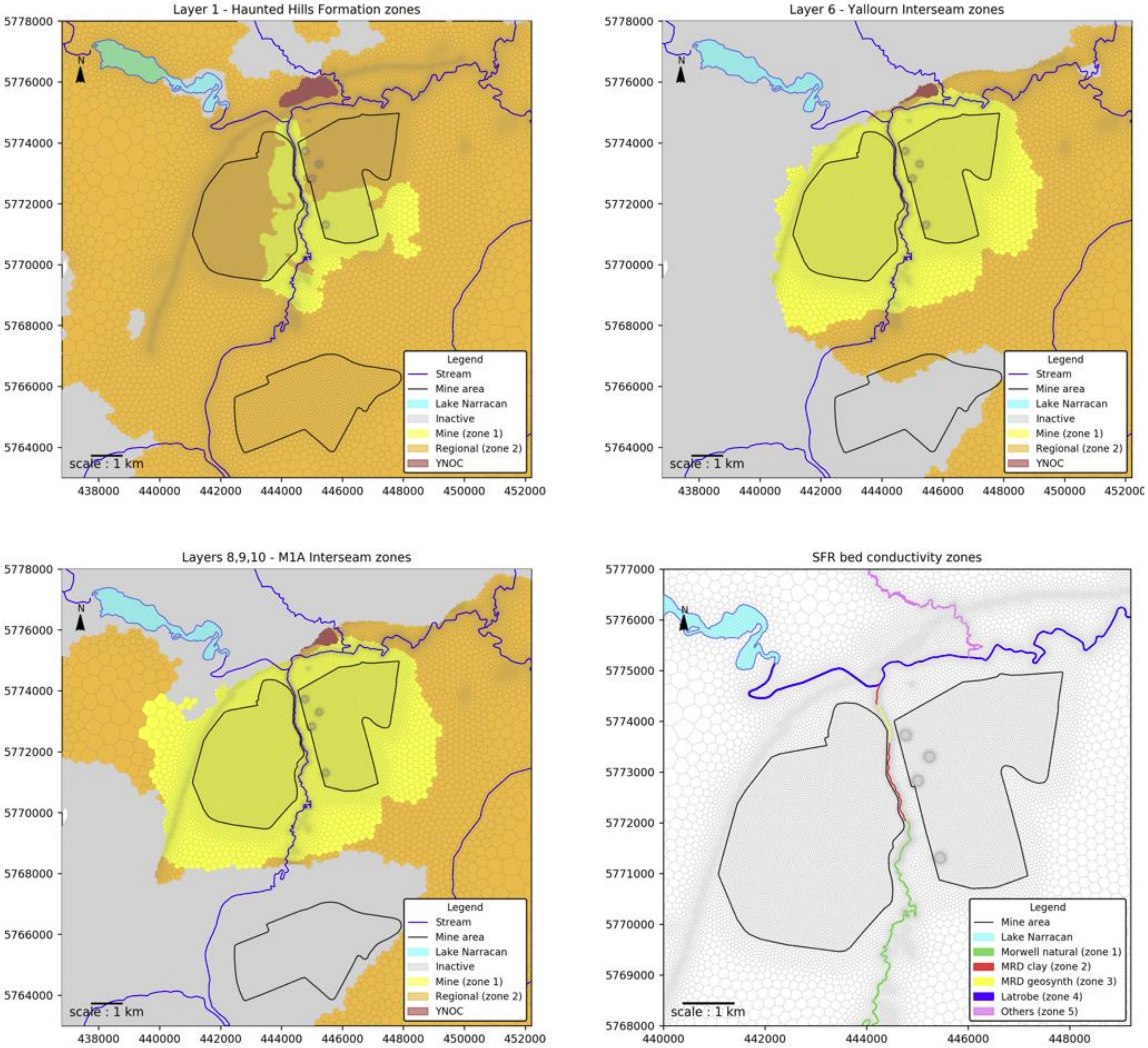

Figure 24 Percent sand multiplier and SFR bed conductivity zones

3.1.4 Calibration workflow

The calibration has been undertaken using a combination of manual (trial and error) and automated methods. The rigorous automated parameter estimation procedure utilised PEST_HP (Doherty, 2017) in a highly parallelised computing environment (a large number of simultaneous runs distributed across multiple cores on a virtual desktop). The PEST_HP calibration has been undertaken in the regularisation mode, using the preferred parameter values as prior information (to ensure the parameters estimated by PEST_HP are not deviated from their preferred values unless deemed necessary to improve model calibration).

A schematic representation of the automated calibration workflow is shown in Figure 25. The PRMS model and USG-Transport model are run in sequence, with the outputs of the PRMS model used to generate the recharge, evapotranspiration and stream input files for the USG-Transport model. This allows the two models to be calibrated simultaneously, taking into account the influence of the PRMS model parameters on the outputs of the USG-Transport model and calibration with respect to key groundwater observation targets. The USG-Transport model includes a steady-state run, which supplies initial heads to the subsequent transient run.

Some of the model inputs files are updated directly by PEST_HP while others are generated by PEST utilities and custom scripts using parameter files updated by PEST_HP. These include utilities that:

- Undertake spatial and temporal interpolation of PRMS generated recharge and evapotranspiration (unused PET) to the USG-Transport unstructured grid and write the necessary RCH and EVT input files. Both steady-state and transient input files are written, with the former using the long term average recharge and evapotranspiration calculated over the transient calibration period (for the purpose of generating hydrologically sensible initial heads). The EVT input files read external arrays of EVT surface (SURF), EVT extinction depth (EXDP) and EVT nodes (INIEVT). The EXDP array is directly updated by PEST_HP based on the adjustable extinction depth values while the INIEVT array is updated by a custom script using the SURF and updated EXDP arrays. This means the EVT node at each 2D cell location is identified based on the layer within which the EVT extinction depth terminates so that EVT flux is assigned to the correct layer. Note that the units used by the PRMS model are not consistent with those used by the USG-Transport model and unit conversion is undertaken during interpolation to ensure correct RCH and EVT rates written to the USG-Transport input files.
- Extract the lateral flows (runoff and interflow) calculated by the PRMS model for each stream segment and assign these to the corresponding SFR segment as a runoff component, with temporal averaging of flows across the groundwater model stress periods. The steady-state and transient SFR input files are then written using the updated lateral flows and stream bed hydraulic conductivity (the steady-state flows are based on the long term average of the transient flows, as per the RCH and EVT files). The flow rates computed by the PRMS model are converted into the correct unit used by the USG-Transport model during processing.
- Write the steady-state and transient RIV input files based on the specified RIV stage and updated RIV conductance calculated for each RIV cell using the river bed hydraulic conductivity adjusted by PEST_HP and the specified RIV bed thickness and cell area.
- Undertake multiplication of percentage sand grids against multiplier grids adjusted by PEST_HP and write external files of horizontal hydraulic conductivity (read by the LPF package). Similarly, external files of vertical hydraulic conductivity are written by a utility the multiplies the horizontal hydraulic conductivity arrays by vertical hydraulic factors updated by PEST_HP.
- Write the steady-state and transient GHB input files based on the updated conductance values calculated for each GHB cell using the specified cell area (perpendicular to flow direction) and hydraulic conductivity value updated by PEST_HP (read from external hydraulic conductivity files).
- Write the TVM input file using the TVM parameter values updated by PEST_HP. In this case, PEST utility PAR2PAR (Doherty, 2016b) is used to multiply horizontal hydraulic conductivity against the vertical hydraulic conductivity factor to calculate vertical hydraulic conductivity for each of the three TVM zones. The calculated parameter values are then read and processed by a utility that writes the TVM input file.

The post-processing of the USG-Transport model outputs and comparison against their equivalent observation targets are undertaken using PEST utilities and custom scripts. These include:

- PEST utility USGMOD2OBS (Doherty, 2016d) that extracts computed hydraulic heads at the time and location of observations. This is used to compare the observed groundwater levels (head targets) against their modelled equivalent.
- PEST utility SMPDIFF (Doherty, 2016c) that converts the computed hydraulic heads into temporal hydraulic head differences (trends) at the location of observations. This is used to compare the changes in observed groundwater levels over time (head trends) against their modelled equivalent.
- PEST utility SMP2SMP (Doherty, 2016c) that interpolates data in one file to dates and times represented in another file. This is used to extract the modelled stream stage and flow at the time of observation at each stream gauge. A python script has been developed to post-process the modelled stream stage and flow written to the output file of the GAGE package, converting the elapsed (simulation) times into dates so they can be compared against the observed values. In this case, SMP2SMP is required as the length of time series data written by the GAGE package changes for each model run due to different number of time steps generated by the adaptive time stepping algorithm of USG-Transport.
- PEST utility USGBUD2SMP (Doherty, 2016d) that extracts flow rates from cell-by-cell binary budget file and write flow time series files. This utility has been used to extract DRN outflows from the DRN cells used to simulate the aquifer depressurisation effects at the Hazelwood Mine, the flows removed by the WEL cells (representing the actual pumping rates) and stream leakage to and from the SFR cells (used to calculate baseflow contributions). For the Hazelwood DRN outflows, a python script has been developed to convert the flow time series written by USGBUD2SMP into stress period averages so they can be easily compared against the quarterly pumping rates (as applied to the LVRGM). Similarly, the time series of WEL flows are converted into stress period averages (using a similar script) to check against the applied average pumping rates. For the SFR leakage rates, SMP2SMP is used to extract the flows at the times of baseflow observations.
- Custom utility written in fortran that calculates the difference between two USGMOD2OBS output files. This has been used to calculate the difference in the modelled hydraulic heads at the location of nested bores/piezometers, to enable calibration against the measured vertical hydraulic head differences.

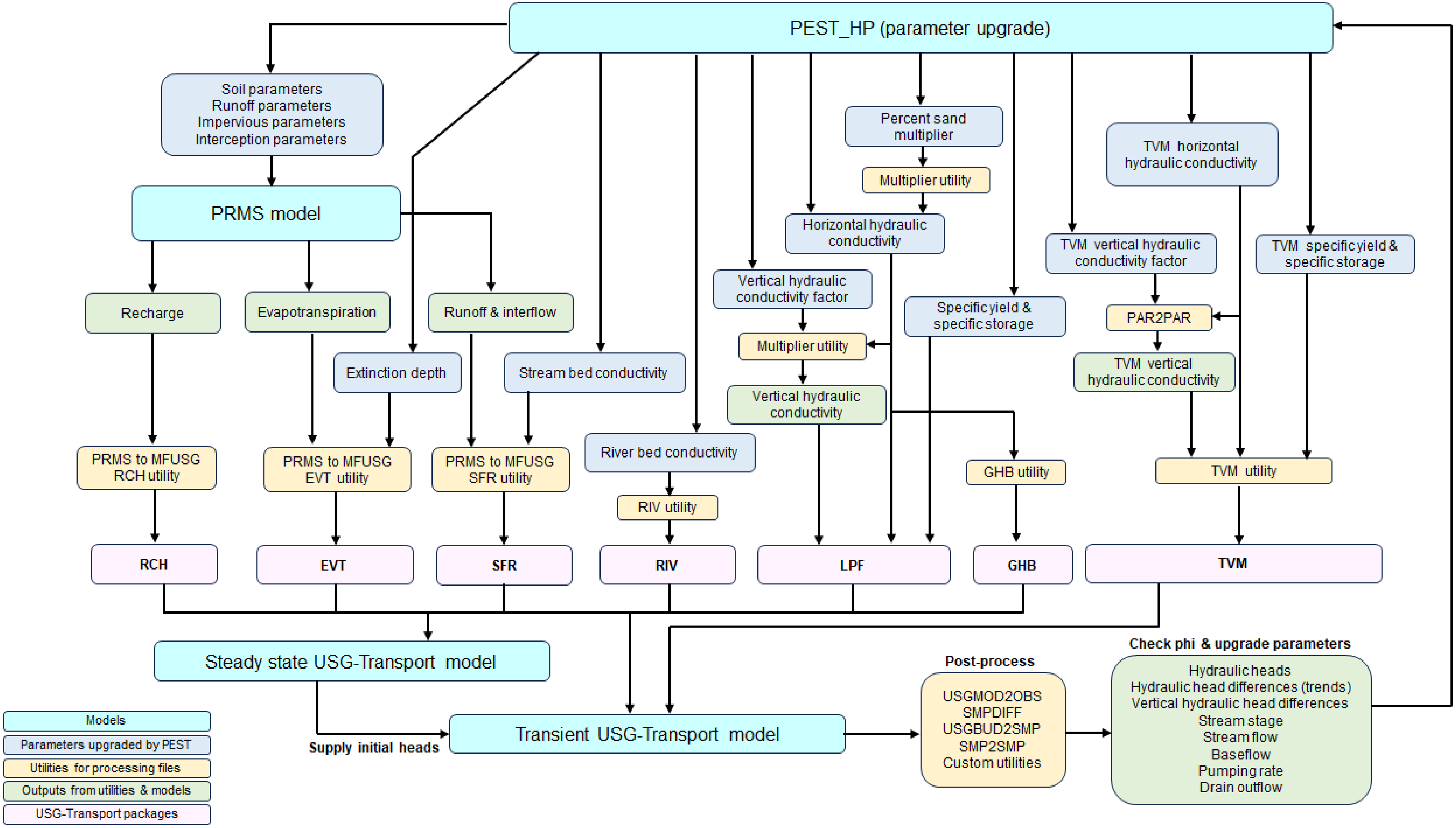

Figure 25 PEST_HP automated calibration workflow

3.2 Calibration results

3.2.1 Calibration performance

3.2.1.1 Groundwater levels and trends

The quality of model calibration with respect to groundwater level observations is described in this section with reference to a series of bore hydrographs and groundwater contour maps generated for the key HSUs. The hydrographs are presented for the entire calibration period, to clearly demonstrate the changes in groundwater levels recorded over time due to the influence of climate, mining and aquifer depressurisation (including the cumulative effects of the significant regional depressurisation of the confined aquifers at the Hazelwood and Loy Yang mines).

Hydrographs of key bores are presented for each HSU, along with a bore location map and groundwater level contours computed at the end of calibration (end of 2021). These are included in Figure 26 to Figure 41, for the purpose of demonstrating the temporal and spatial differences in the observed and simulated groundwater levels in the key HSUs. Additional hydrograph plots are included in Appendix E and hydrographs for all 471 observation bores used in model calibration are included in Appendix F. The groundwater contour maps included in these figures show areas of dry cells, where the simulated hydraulic heads are below the cell bottom, and areas where the aquifers are absent (pinched out or excavated at the mine).

Haunted Hills Formation

Shallow groundwater in the Haunted Hills Formation is locally drained near the mine void, with the groundwater levels fluctuating seasonally in response to recharge and interactions with the surface water systems. Figure 26 and Figure 27 show hydrographs of shallow bores located within the vicinity of the Latrobe River, where the groundwater level is sensitive to the seasonal dynamics of recharge and stream level. There is close agreement between the observed and modelled levels, which has been achieved through detailed modelling of recharge and stream dynamics using the coupled PRMS-USG-Transport modelling approach (with time varying stream flow and stage simulated using Manning's equation). The quality of model calibration achieved in this area of the mine is important for rehabilitation planning, due to the potential for the full pit lake level to locally raise the shallow groundwater level (adjacent to the East Field northern batters) and increase the baseflow to the Latrobe River.

The modelled groundwater levels are slightly elevated compared to the observed values at the upstream end of the Latrobe River and adjacent to the YNOC (bore TE1776_S01, shown on Figure 27, and bores TE1741_S01 and TE1781_S01 shown in Appendix E). This may be related to the local drainage effect of the YNOC, as the observed groundwater levels in some of these bores are similar to or lower than the groundwater levels measured in the bores further downstream. More detailed analysis and modelling of the mine progression and local drainage effect of the YNOC would be necessary to confirm the possible cause of this small discrepancy (and if the calibration could be locally improved by incorporating the drainage effect). This area, however, is located upstream of the mine and on the northern side of the Latrobe River (adjacent to the YNOC), where the hydraulic influence of the future pit lake is expected to be limited compared to the downstream area adjacent to the East Field northern batters (where the quality of calibration is more critical).

The shallow groundwater levels in the Morwell River floodplain are also sensitive to recharge, interactions with the Morwell River and drainage into the mine void. Although the model does not simulate the complex (and short term) flood-induced recharge effects, the modelled groundwater levels and seasonal variation are broadly consistent with those observed (as shown in Figure 28). Additional hydrographs included in Appendix E show that the shallow groundwater levels simulated by the model in other parts of the mine are also reasonable, with groundwater locally flowing towards the mine void where it discharges.

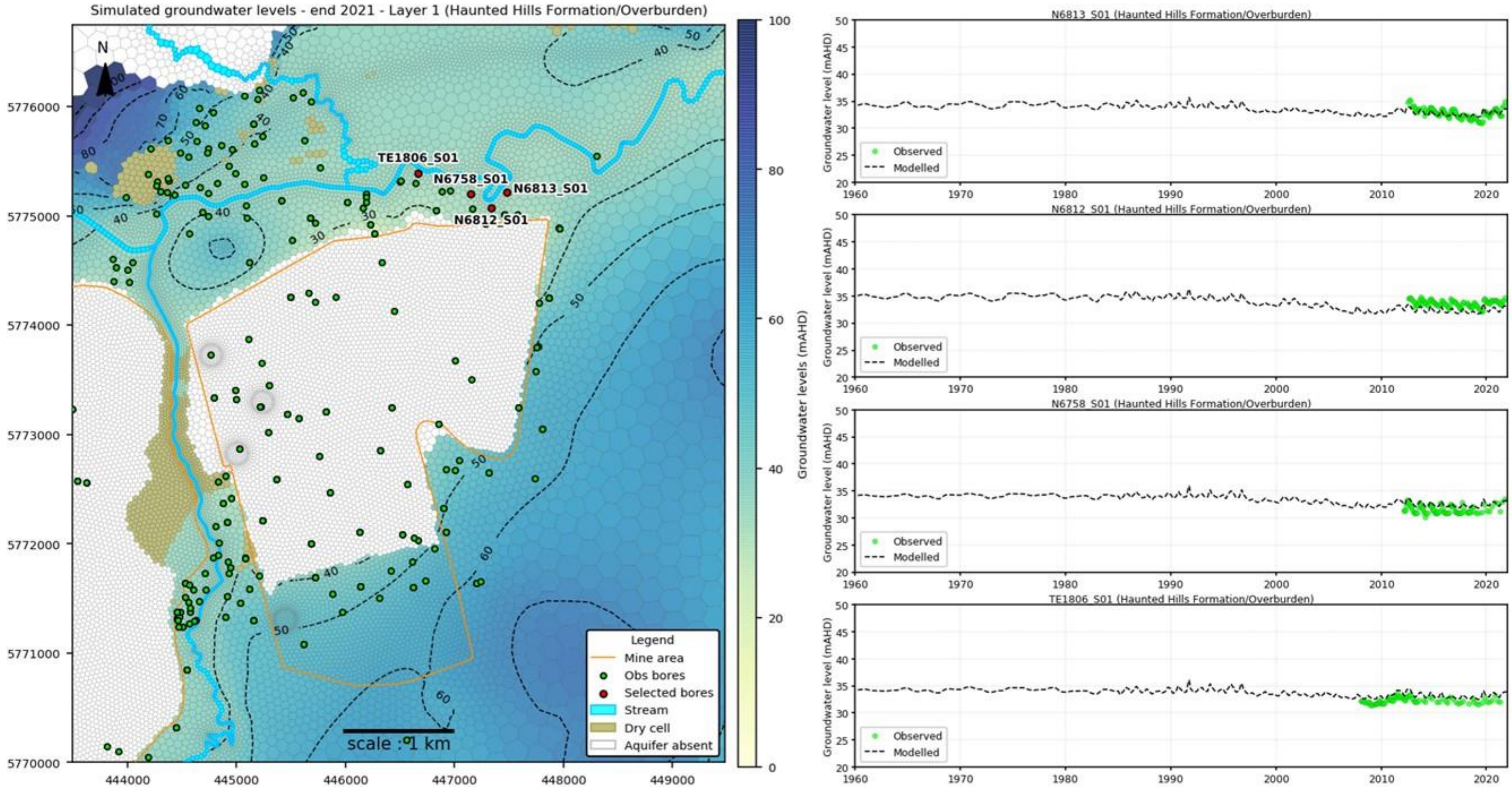

Figure 26 *Haunted Hills Formation – calibration hydrographs – plot 1*

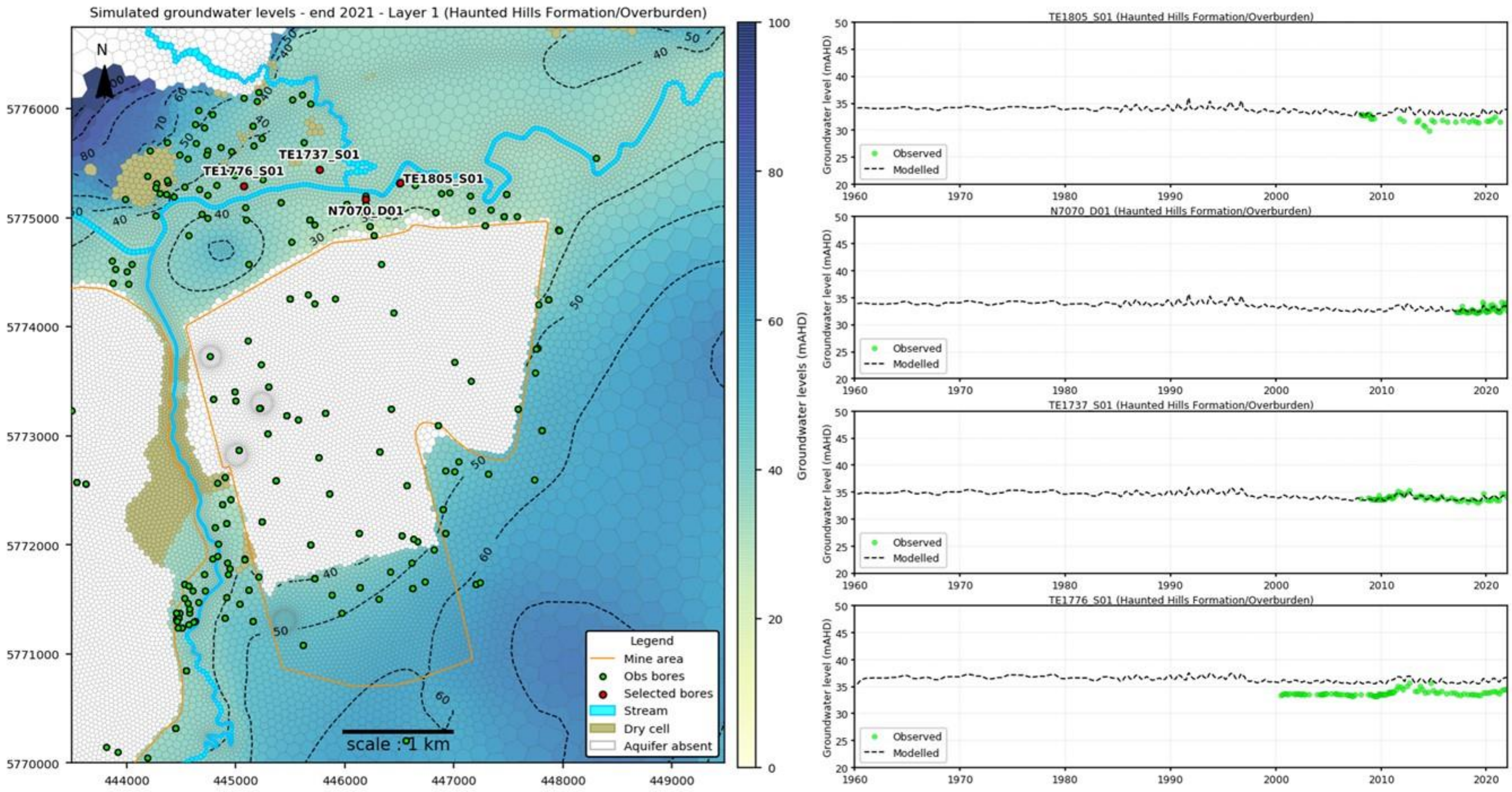

Figure 27 Haunted Hills Formation – calibration hydrographs – plot 2

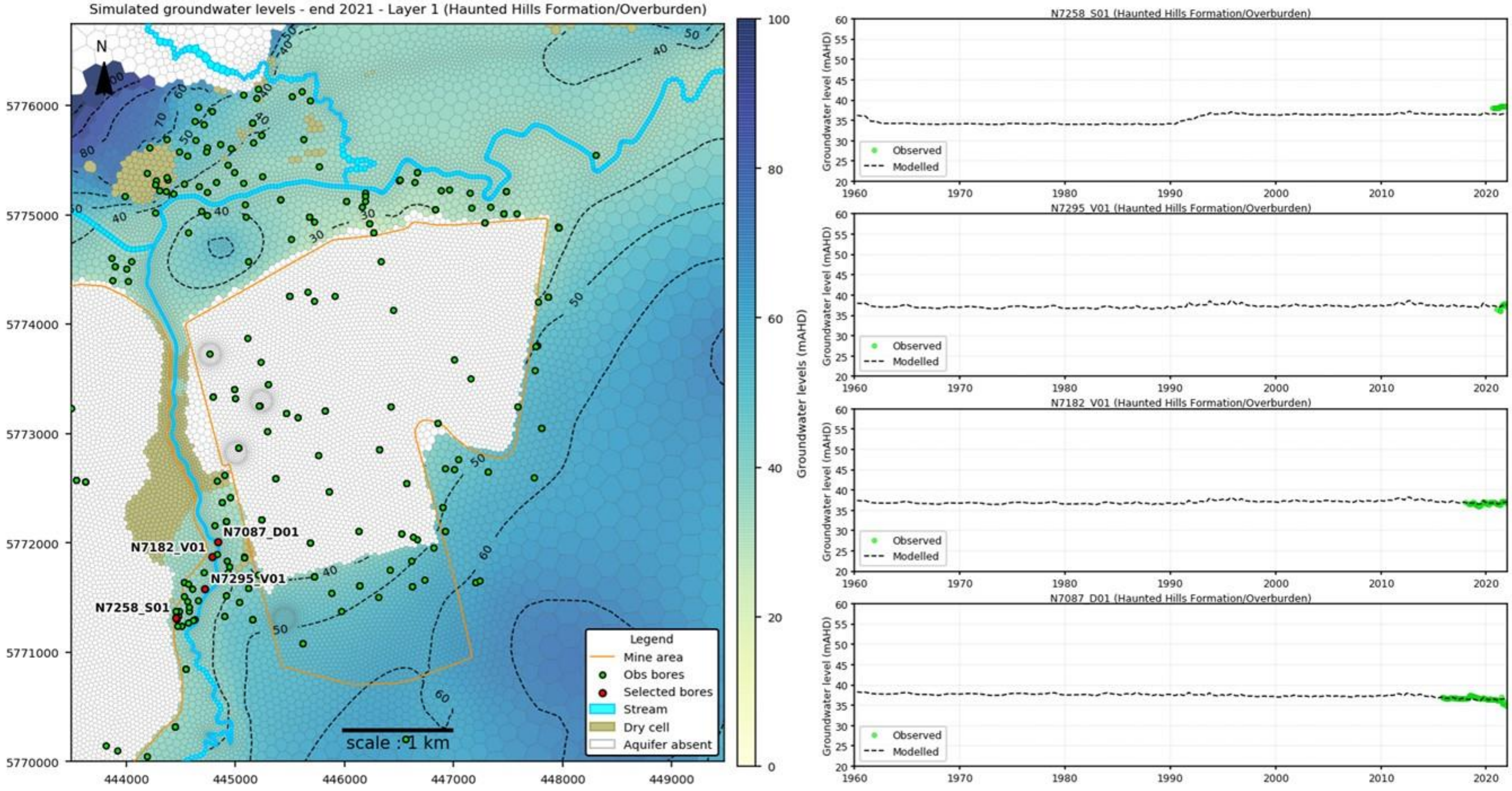

Figure 28 *Haunted Hills Formation – calibration hydrographs – plot 3*

Yallourn Coal/Internal Overburden Dump

The groundwater levels and associated changes observed in the Yallourn Coal and internal overburden (OB) dumps are difficult to replicate accurately due to the complex effect of material property changes experienced over time. For this reason, only selected (representative) observation bores from these units have been included in model calibration (with a low weight assigned to these observations in the PEST_HP calibration). Figure 29 to Figure 31 show selected hydrographs and groundwater contours from model layers 3, 4 and 5 representing the upper, middle and lower Yallourn Coal layers respectively. These layers include the internal OB, which is simulated when the material property changes are applied at the time of the OB placement.

The hydrographs show some abrupt changes in the groundwater level simulated by the model. These are due to the material property changes (coal fracturing and OB dumps) applied to broad areas of the mine over a relatively short time period (linearly interpolated between quarterly stress period boundaries). The changes are temporary and groundwater levels are generally restored quickly albeit with some modifications as the groundwater system adjusts to the changed material properties. Although the groundwater levels in the coal batters are highly variable, the model replicates the overall declining trend (and spatial differences in the magnitude of the decline) broadly consistent with the observed data (at least in some of the key bore locations).

Yallourn Interseam

The groundwater levels in the Yallourn Interseam are sensitive to the depressurisation effect from groundwater extraction in the underlying M1A Interseam, the removal of the overlying Yallourn Coal (pressure relief and material property changes) and the formation of in-pit water features. The groundwater levels and associated trends are therefore complex, resulting in spatially variable calibration quality (the degree of fit between the observed and modelled heads). In general, the model is able to replicate the observed groundwater levels and trends in the area adjacent to the Fire Service Pond (Figure 32) and in Maryvale Field and East Field near the area of the lowest piezometric heads (Figure 33 and Figure 34).

There is a local area beneath the East Field northern batters, where the observed groundwater levels appear to be elevated and difficult for the model to simulate. This mismatch occurs in the area of the historical failure and river realignment fill, potentially reflecting the influence of the changed material properties in the Yallourn Coal that are not well replicated by the model. Packer testing undertaken in this area as part of the Latrobe Valley Brown Coal Mine Batter Stability Research Project suggest that the hydraulic conductivity of the Yallourn Coal in this area could be locally enhanced, potentially facilitating greater vertical flux from the overlying Haunted Hills Formation (resulting in a locally elevated groundwater level in the underlying Yallourn Interseam). The modelled groundwater level at N6344_V02 in the Yallourn Coal (Figure 30) is also higher than the observed value, suggesting the coal/fill may be more drained by the locally higher hydraulic conductivity. More detailed modelling of this area would be necessary to ascertain the cause of the elevated groundwater level in the Yallourn Interseam. It should be noted, however, that the mismatch between the modelled and observed groundwater levels locally within the Yallourn Coal and Interseams does not affect the quality of calibration achieved in the overlying Haunted Hills Formation (with the shallow bores located along the Latrobe River showing some of the closest agreement between the measured and observed values, indicating high model confidence in the shallow groundwater system as demonstrated in Figure 26 and selected hydrographs in Appendix E). Similarly, outside of this localised area, the modelled groundwater levels within the Yallourn Interseam are more consistent with the observed groundwater levels (e.g. bores N6805_V01 and N7066_V01, shown in Figure 35).

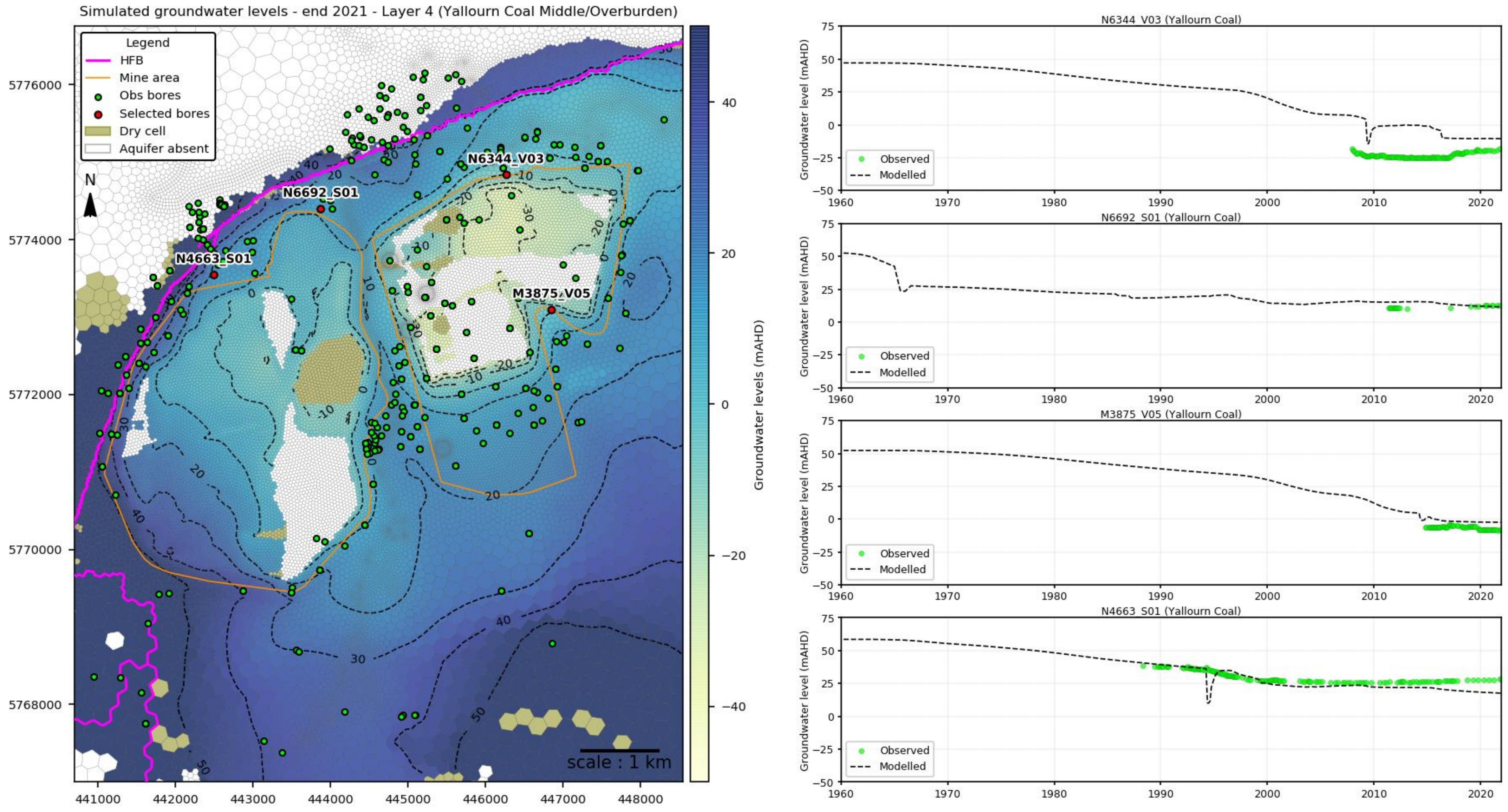

Figure 29 *Yallourn Coal – calibration hydrographs – plot 1*

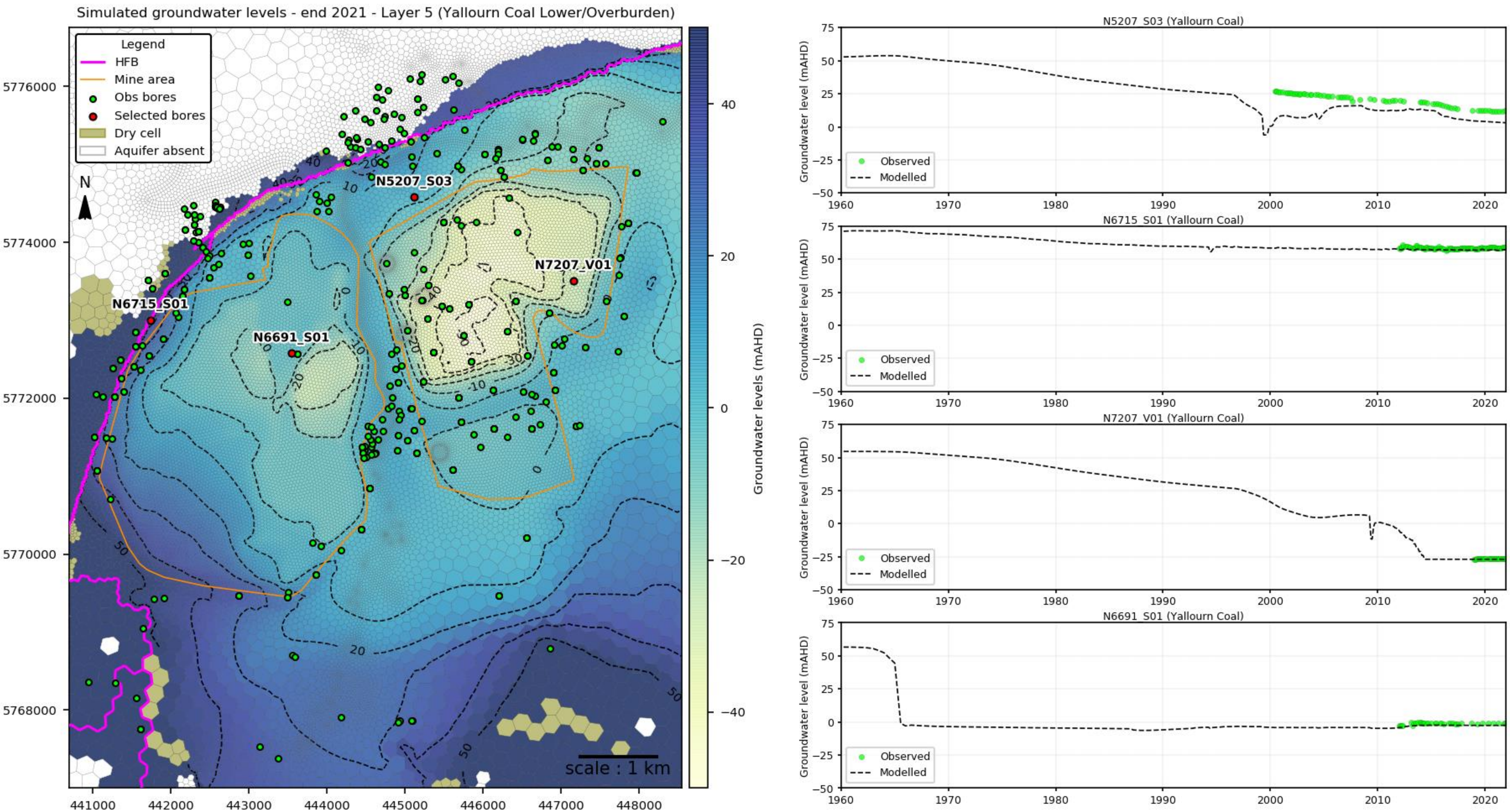

Figure 30 Yallourn Coal – calibration hydrographs – plot 2

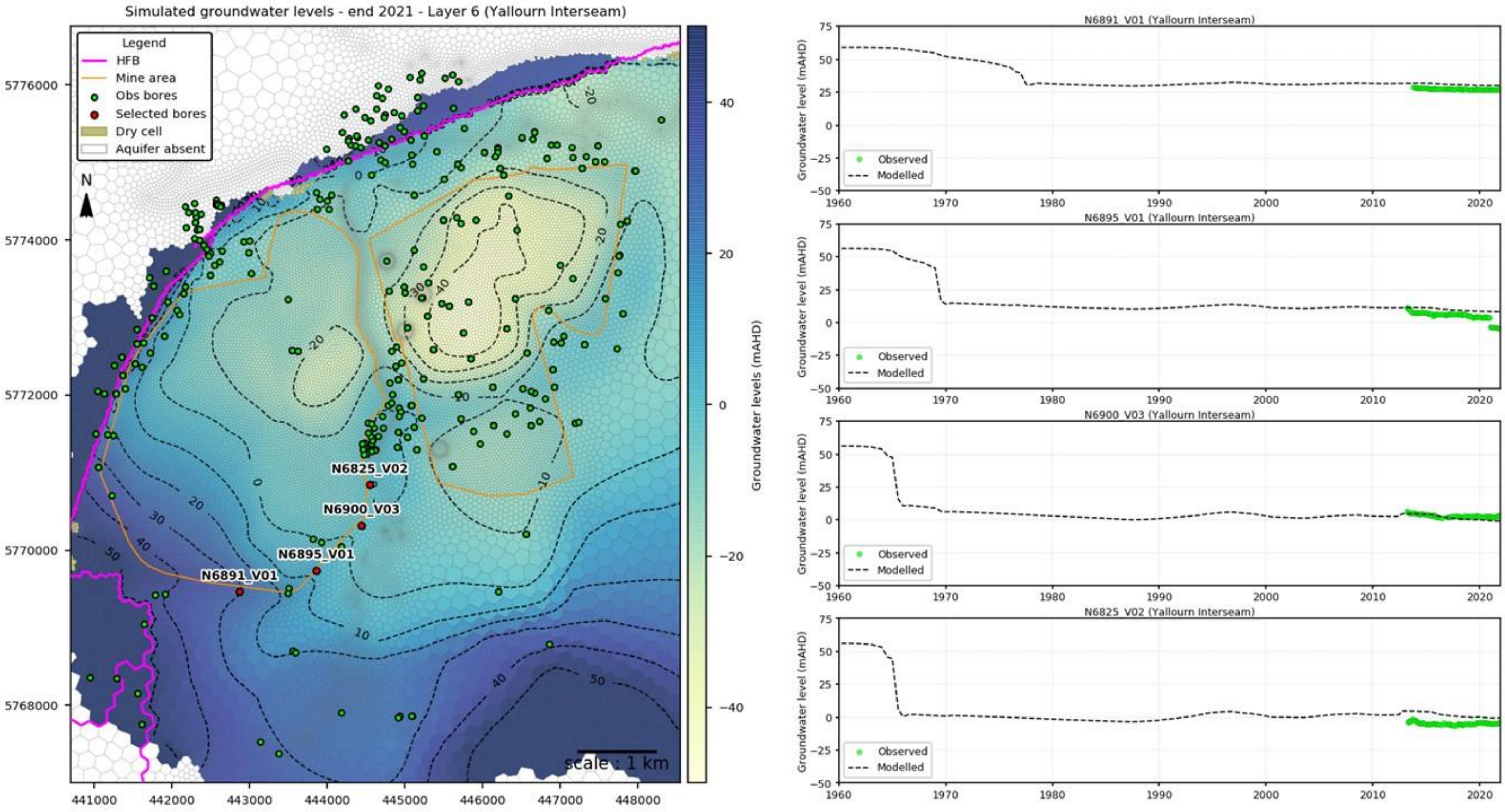

Figure 31 Yallourn Coal – calibration hydrographs – plot 3

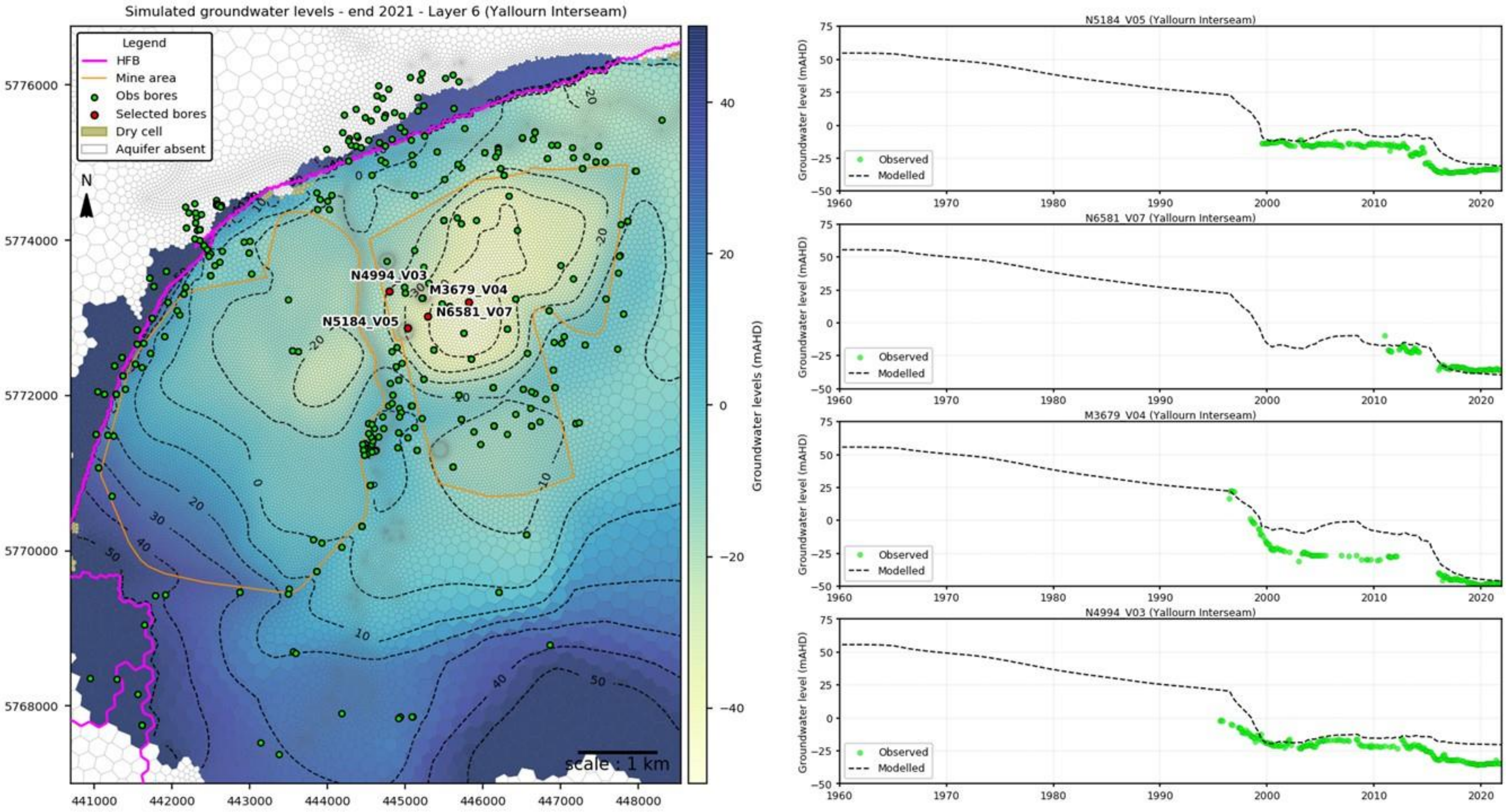

Figure 32 Yallourn Interseam – calibration hydrographs – plot 1

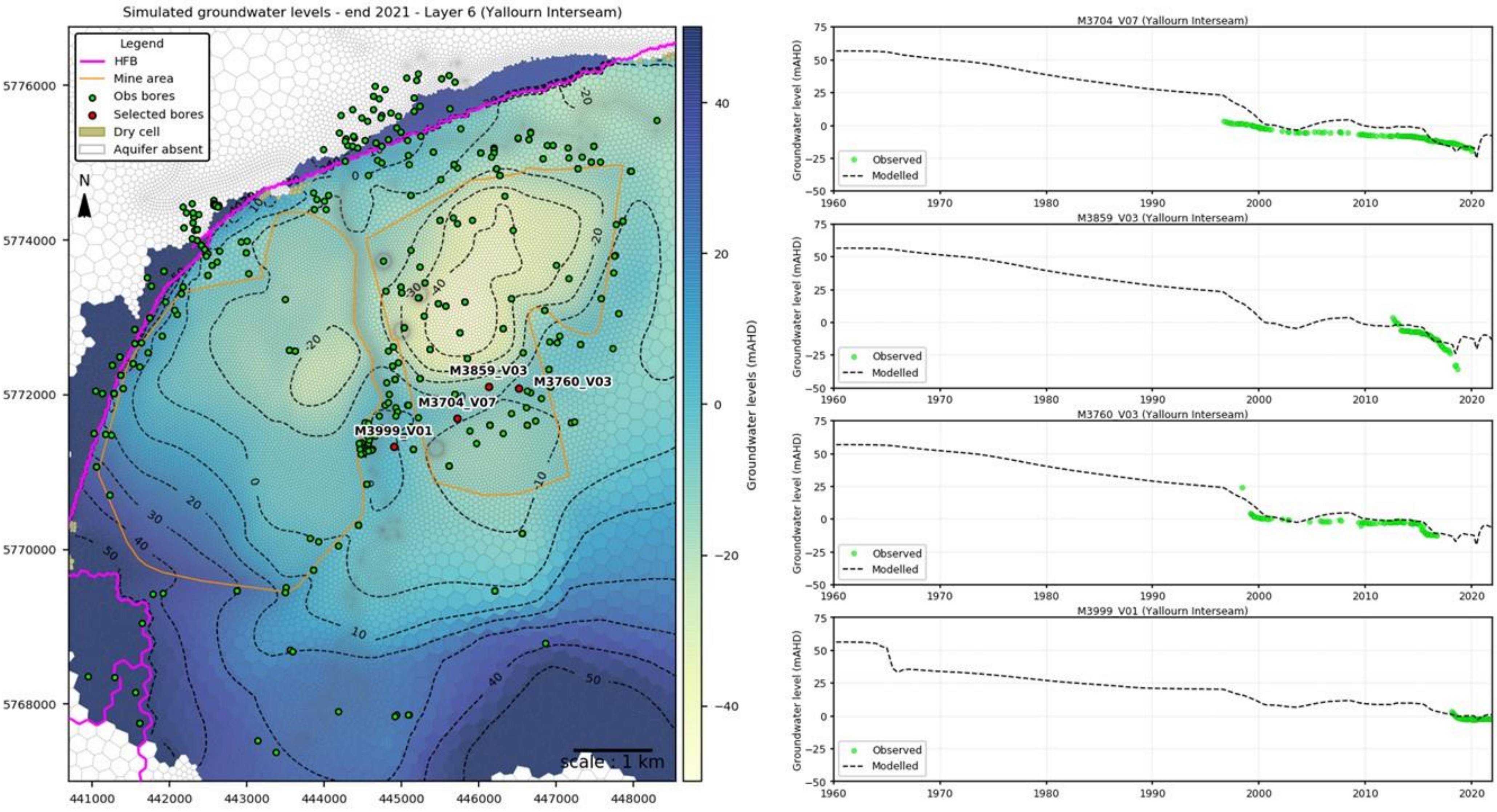

Figure 33 *Yallourn Interseam – calibration hydrographs – plot 2*

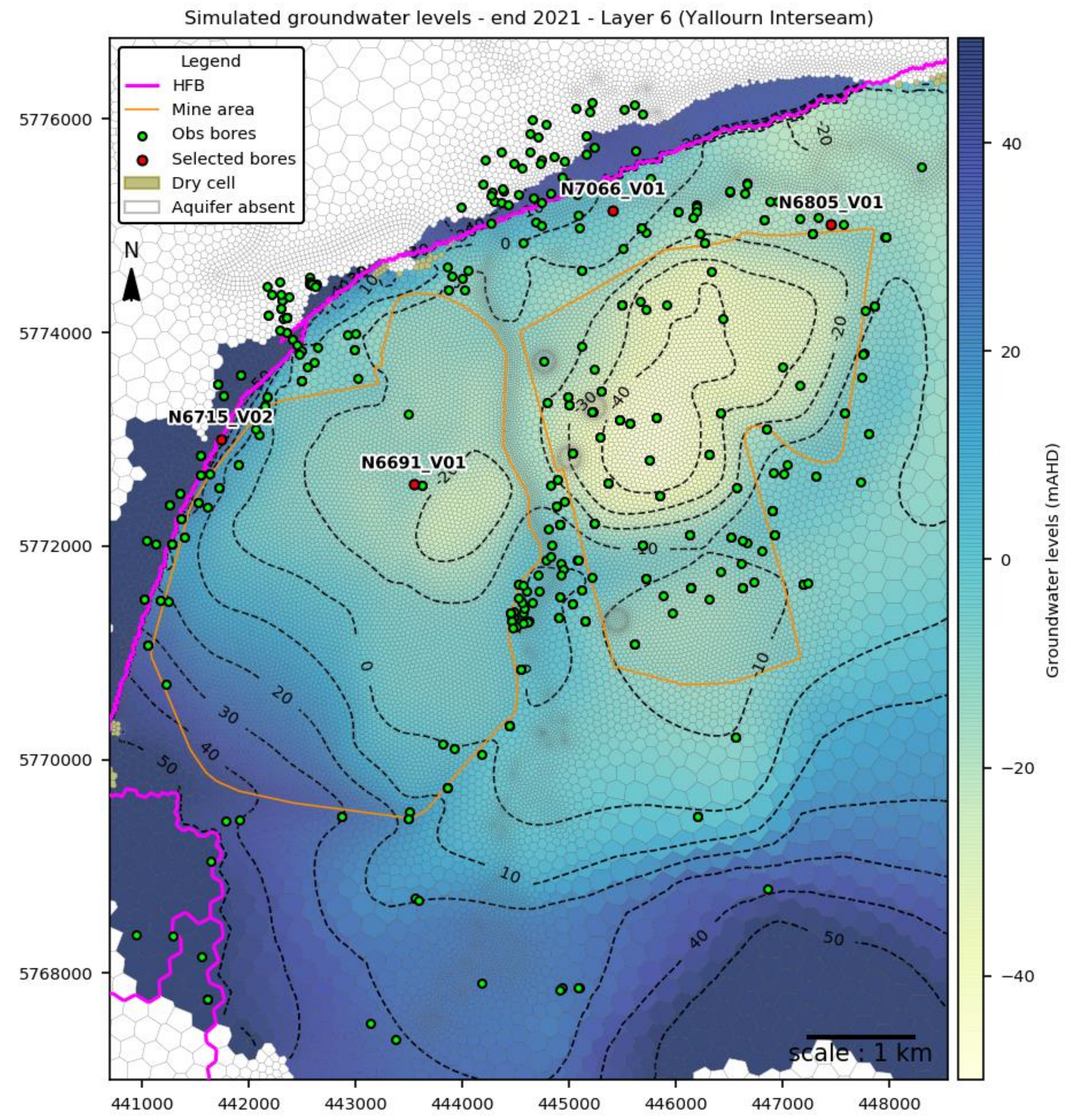

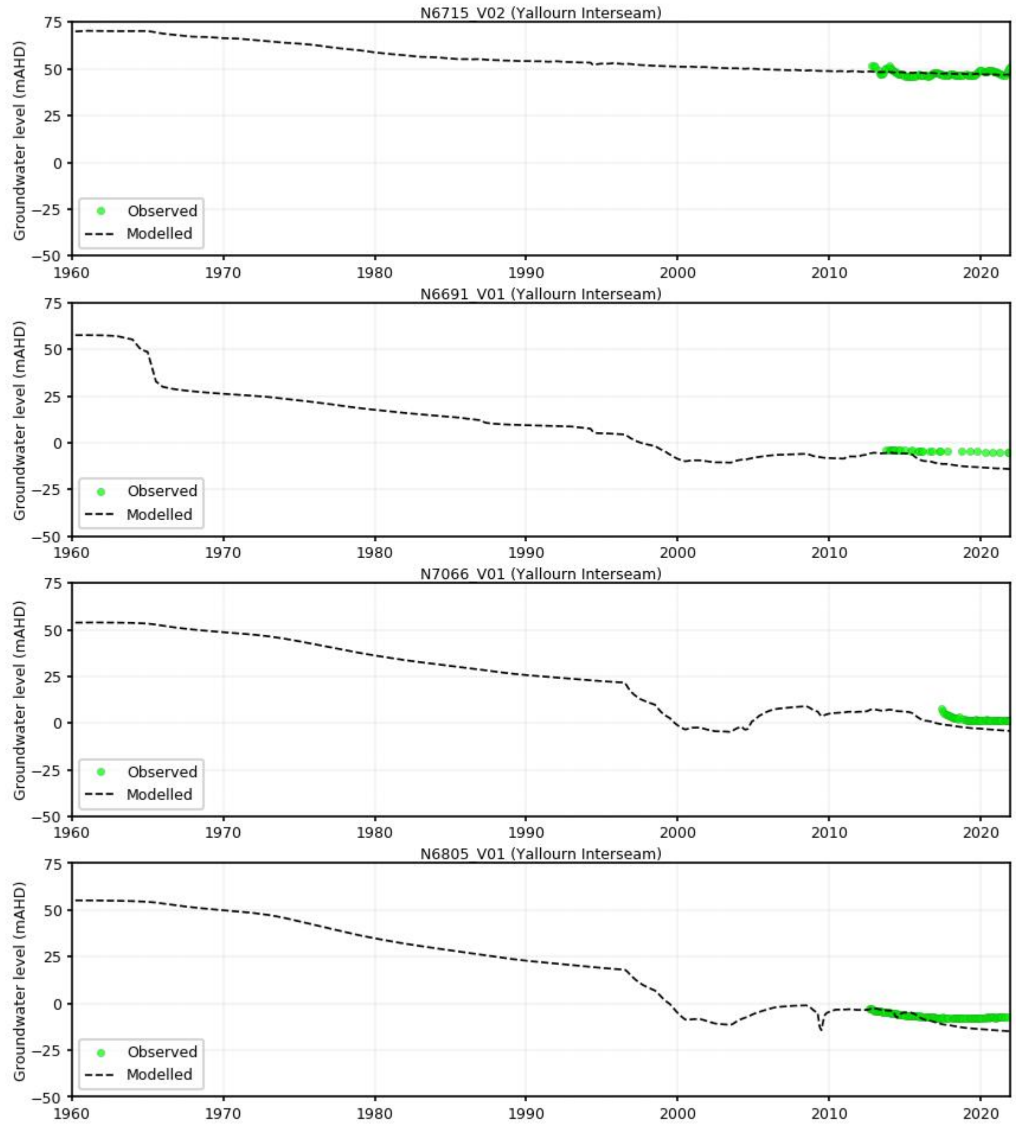

Figure 35 Yallourn Interseam – calibration hydrographs – plot 4

M1A Interseam

The groundwater levels in the M1A Interseam are sensitive to the effect of groundwater extraction, which is generally well replicated by the model as seen in the hydrographs presented in Figure 36 to Figure 39. In some bores close to the pumping bores (e,g. M3679_V02 shown in Figure 38 and N4863_V02 shown in Figure 39), there is a large mismatch between the modelled and observed groundwater levels between 2004 and 2015, when the pumping rate was reduced (particularly between 2004 and 2008, when the annualised pumping rate was as low as around 0.26 ML/d compared to up to around 2.7 ML/d rate in the preceding years). The lack of recovery observed in these bores appears to be inconsistent with the magnitude of reduction in the pumping rate and the typical radial flow behaviour expected in a connected aquifer system. This suggests a possible compartmentalisation effect locally within the M1A Interseam that is not well replicated by the percent sand grids (or alternative parameterisation approaches, such as pilot points, which also failed to replicate the subdued recovery observed in these bores). Another possibility is gaps in the historical pumping record, which may not have captured all of the artesian flows that had discharged from the bores in the MA1 Interseam. This would result in less flows being removed from the model, which would overestimate the temporary recoveries. In general, the model is able to better replicate the groundwater levels and trends observed since around 2015, after the pumping rate had been returned to higher rates (around 3.3 ML/d).

The mode does not have the capability to simulate pore pressure changes due to loading and unloading effects. For example, the model overestimates the declining trend at bore N6581_V06 (Figure 38) towards the end of calibration, which is likely to be due to the stabilisation of pore pressure from the placement of internal overburden dumps.

M2 Interseam

The groundwater levels in the deep M2 Interseam are sensitive to the aquifer depressurisation effects of the Hazelwood Mine and, to a lesser extent, Loy Yang Mine, and the influence of regionally significant geological structures such as the Haunted Hills Fault. Figure 40 shows the contours and hydrographs of bores in the M2 Interseam, showing the magnitude and extent of the regionally significant depressurisation. The model replicates the observed groundwater levels in these regional bores, with the DRN and GHB boundary conditions adequately replicating the aquifer depressurisation effects of the Hazelwood and Loy Yang mines. Figure 41 shows the hydrographs of the M2 Interseam bores located in the Moe Swamp Basin, where the effect of the aquifer depressurisation is minimised by the Haunted Hills Fault acting as a significant flow barrier (supported by the stable groundwater levels observed and simulated at these bores). The sensitivity of the model outputs to the Haunted Hills Fault is discussed further in Section 3.2.3.

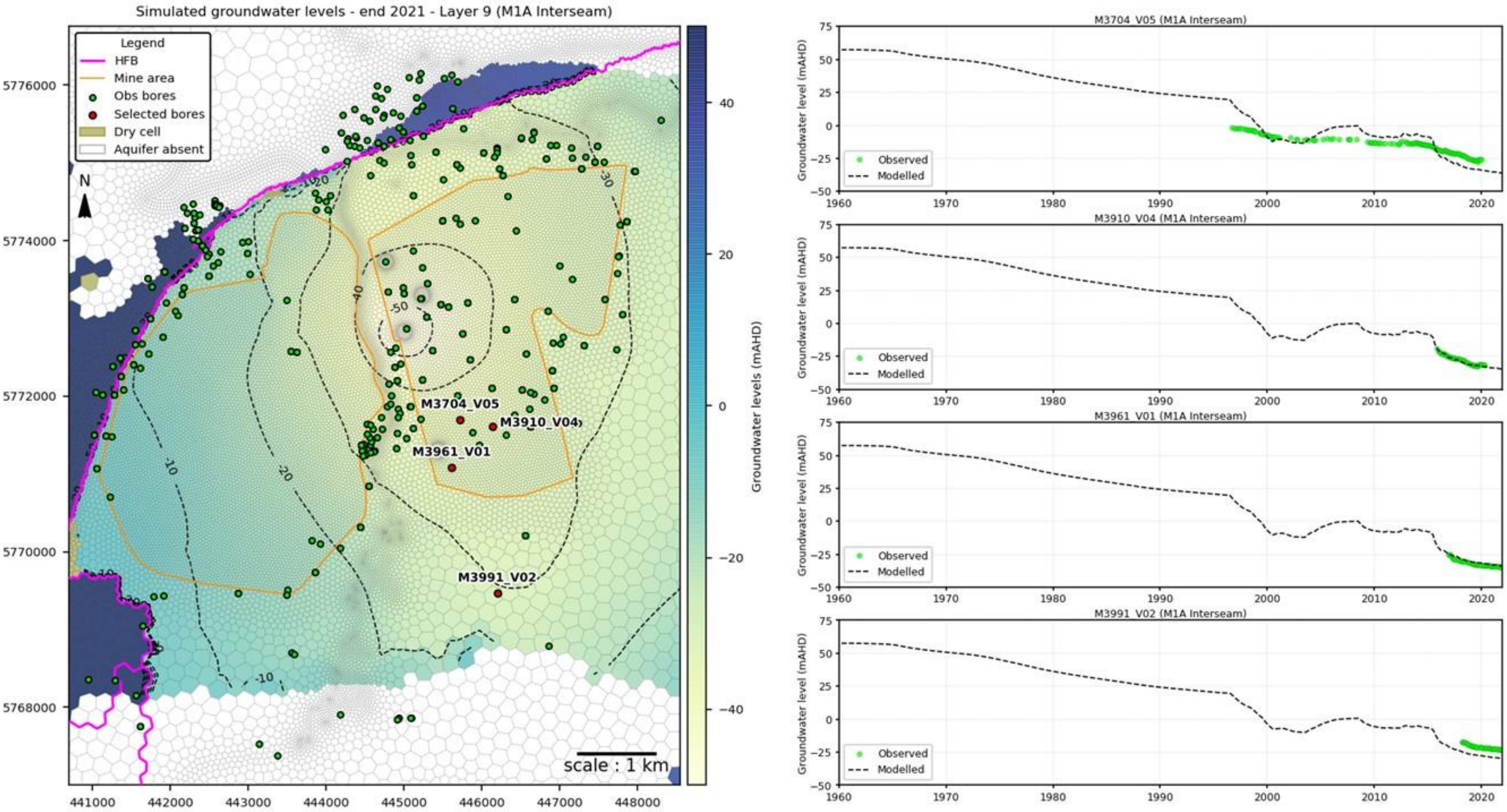

Figure 36 *M1A Interseam – calibration hydrographs – plot 1*

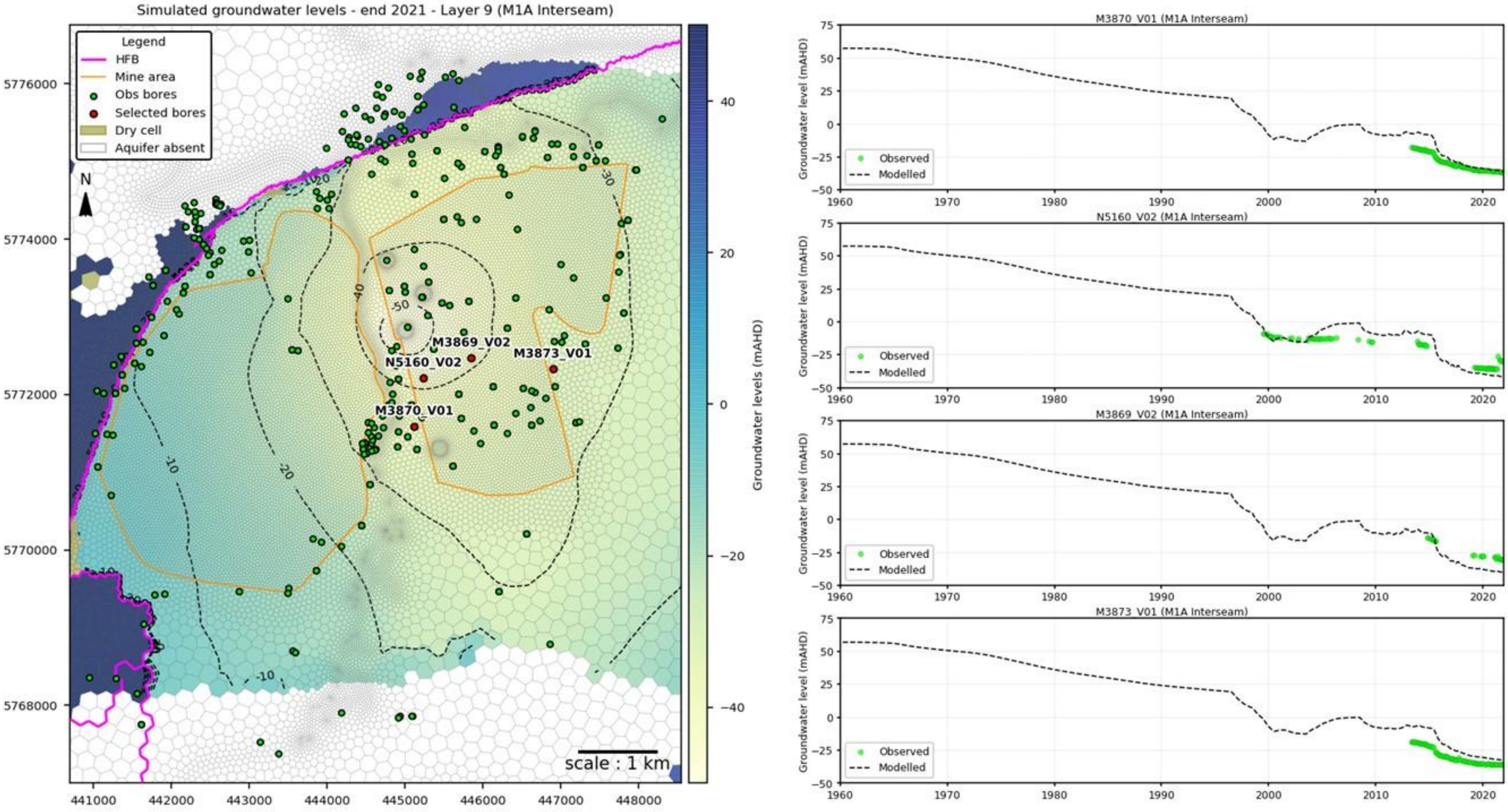

Figure 37 *M1A Interseam – calibration hydrographs – plot 2*

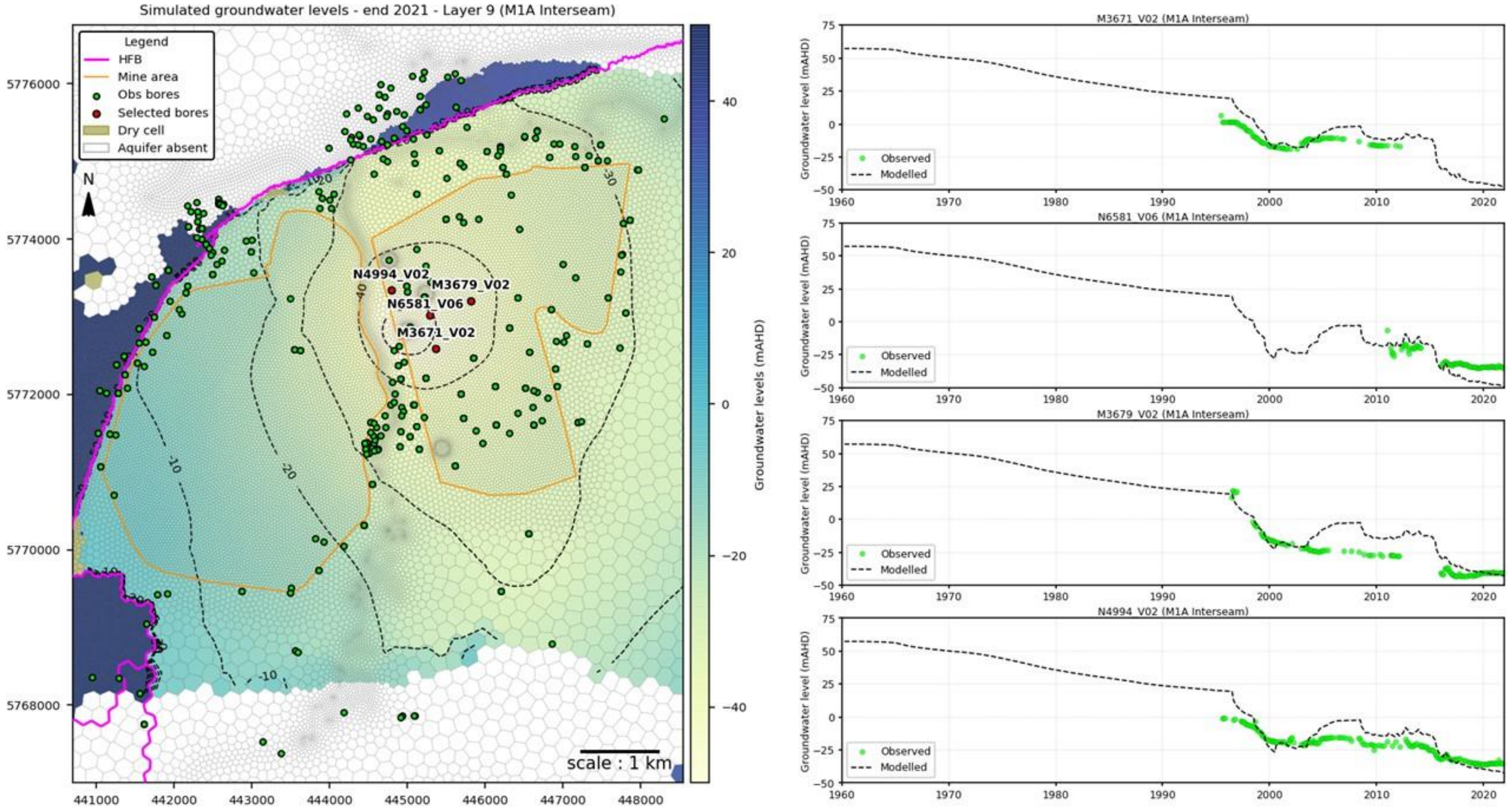

Figure 38 *M1A Interseam – calibration hydrographs – plot 3*

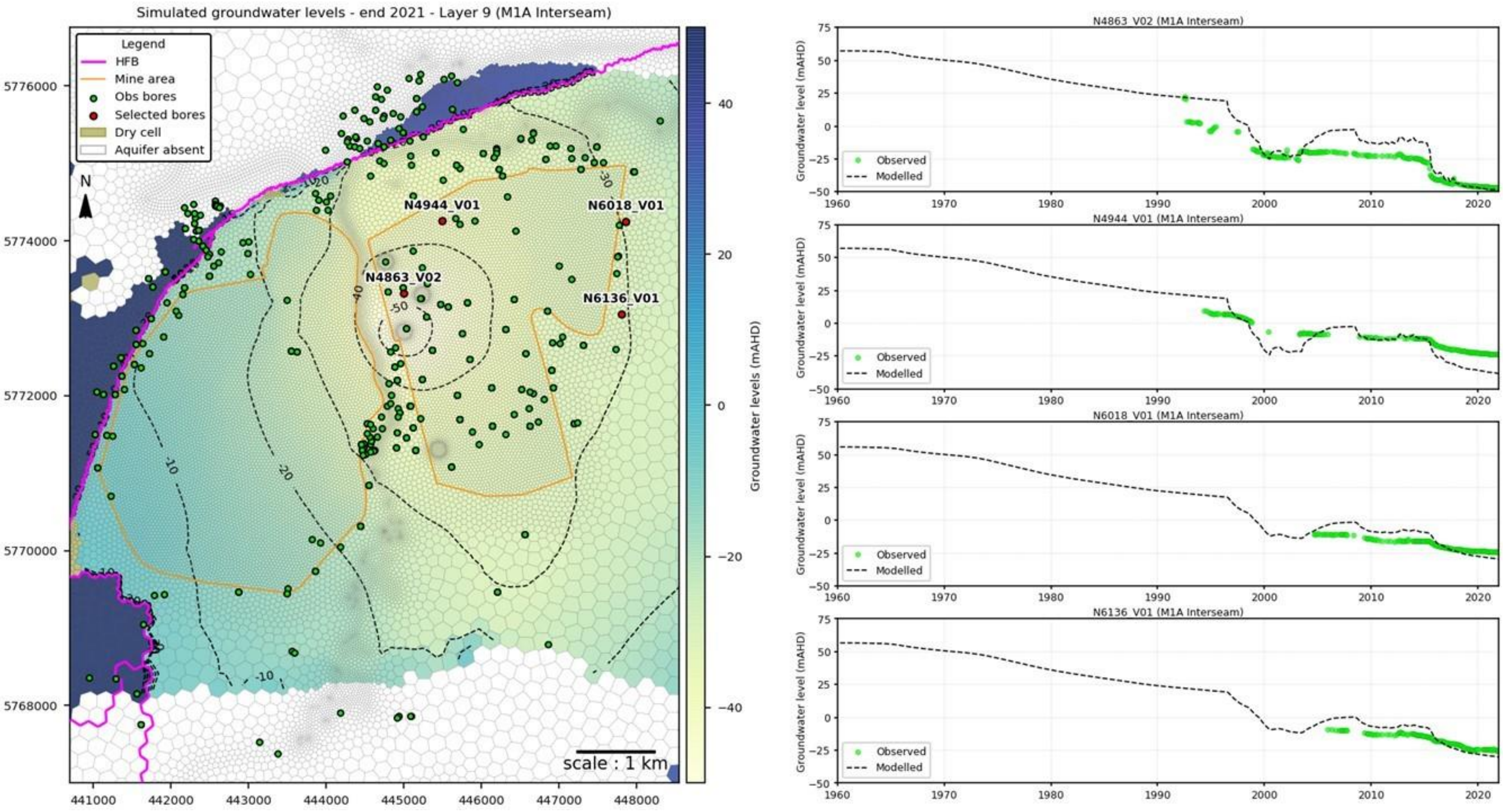

Figure 39 ***M1A Interseam – calibration hydrographs – plot 4***

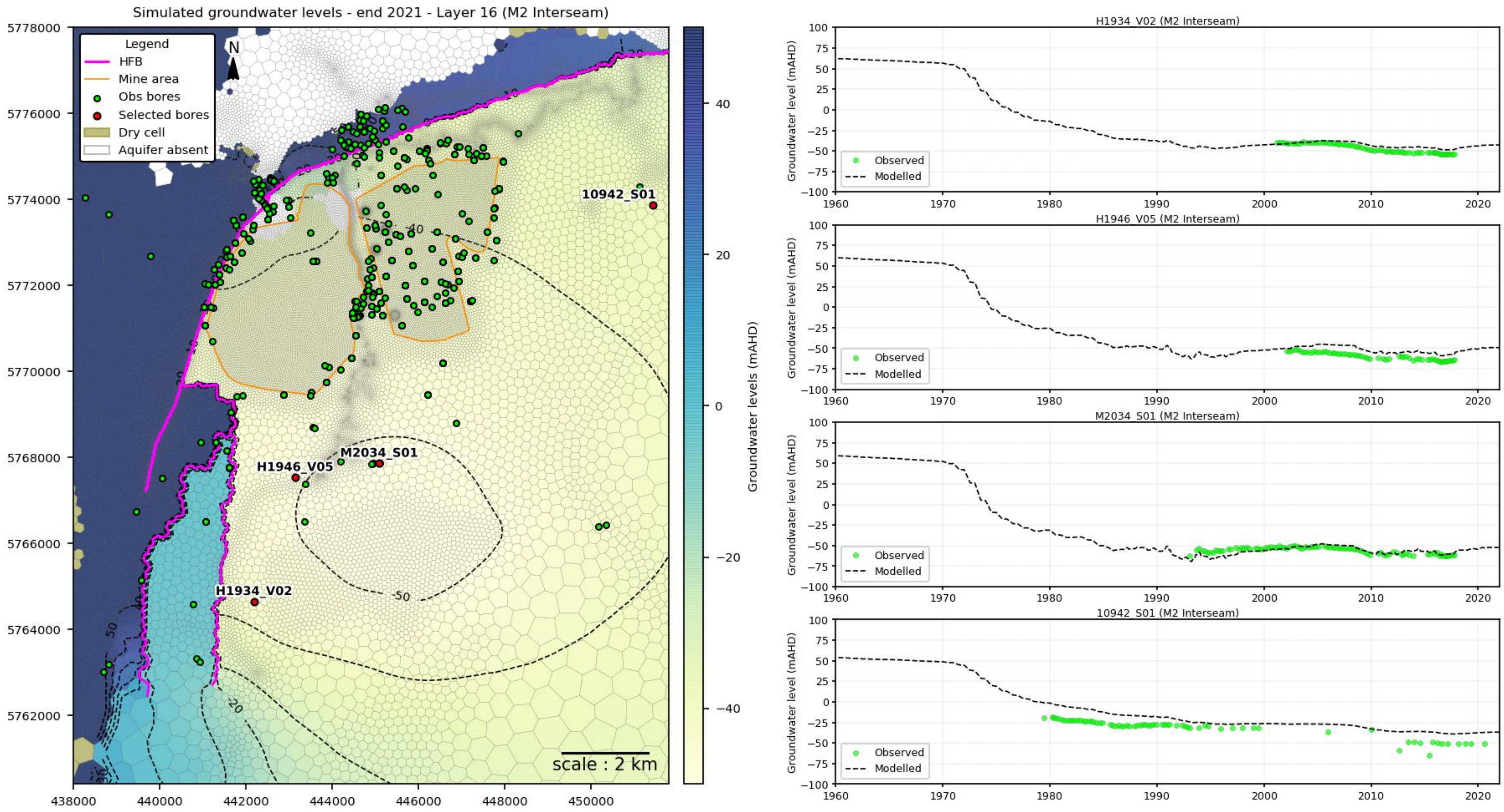

Figure 40 *M2 Interseam – calibration hydrographs – plot 1*

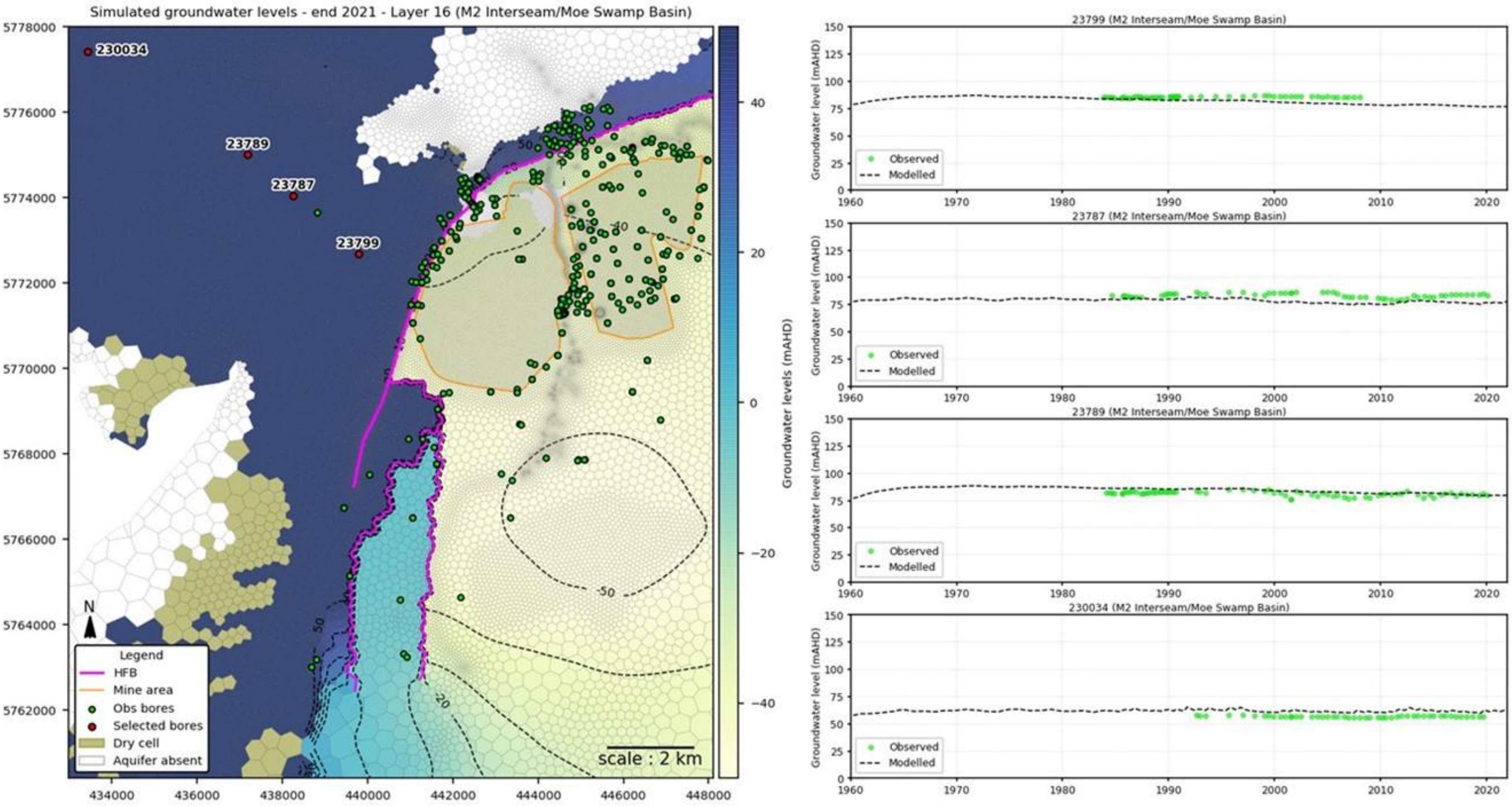

Figure 41 *M2 Interseam – calibration hydrographs – plot 2*

3.2.1.2 Groundwater drawdown

The effect of aquifer depressurisation from mining and groundwater extraction is discussed in this section using contour maps of groundwater drawdown, calculated as the change relative to the initial groundwater levels (the pre-mining groundwater levels computed from the steady-station simulation, taken as the start of 1960 for the purpose modelling as discussed in Section 3.1.1). The contour maps of drawdown are presented for the M1A Interseam (layer 9) and the Yallourn Interseam (layer 6) in Figure 42 and Figure 43 respectively, for the two HSUs (aquifers) where the effects of mining and groundwater extraction are most discernible. The drawdown contours are presented at 10-year increments, to show the changes in the magnitude and spatial extent of drawdown simulated in these aquifers over time.

Prior to pumping at Yallourn (starting in 1995), drawdown in the M1A Interseam is simulated to occur gradually and uniformly across the mine due to downward leakage induced by the significant depressurisation in the underlying M2 Interseam (caused by the groundwater extraction at Hazelwood starting in 1961). The magnitude and rate of drawdown increases as the pumping of the M1A Interseam commences (after 1995), with the cone of depression forming in the aquifer (centred on the pumping bores). Drawdown simulated in 2010 is slightly reduced compared to that simulated in 2000 due to the reduced pumping rate. Drawdown simulated in 2020 is greater than the prior periods due to the higher pumping rates required to enable safe mining in Maryvale Field.

Drawdown simulated in the Yallourn Interseam reflects the mine progression, with the effect of aquifer depressurisation from the underlying M1A Interseam becoming discernible in parts of the mine towards the end of the simulation (via downward vertical leakage, as the cone of depression in the M1A Interseam becomes larger). Drawdown in the Yallourn Interseam is also sensitive to the material property changes assigned to the overlying Yallourn Coal layers. This can be seen in the drawdown contours simulated at the end of 2020, where an area of slightly lower drawdown (around 50 to 60 m) is simulated along the edge of East Field and Maryvale Field where the Yallourn Coal hydraulic conductivity has been increased (encouraging more flow into this area via throughflow and leakage from the Haunted Hills Formation, locally offsetting the drawdown). This effect is further explained in Figure 44, by comparing the modelled hydrographs extracted from locations within and adjacent to the Yallourn Coal fractures zones.

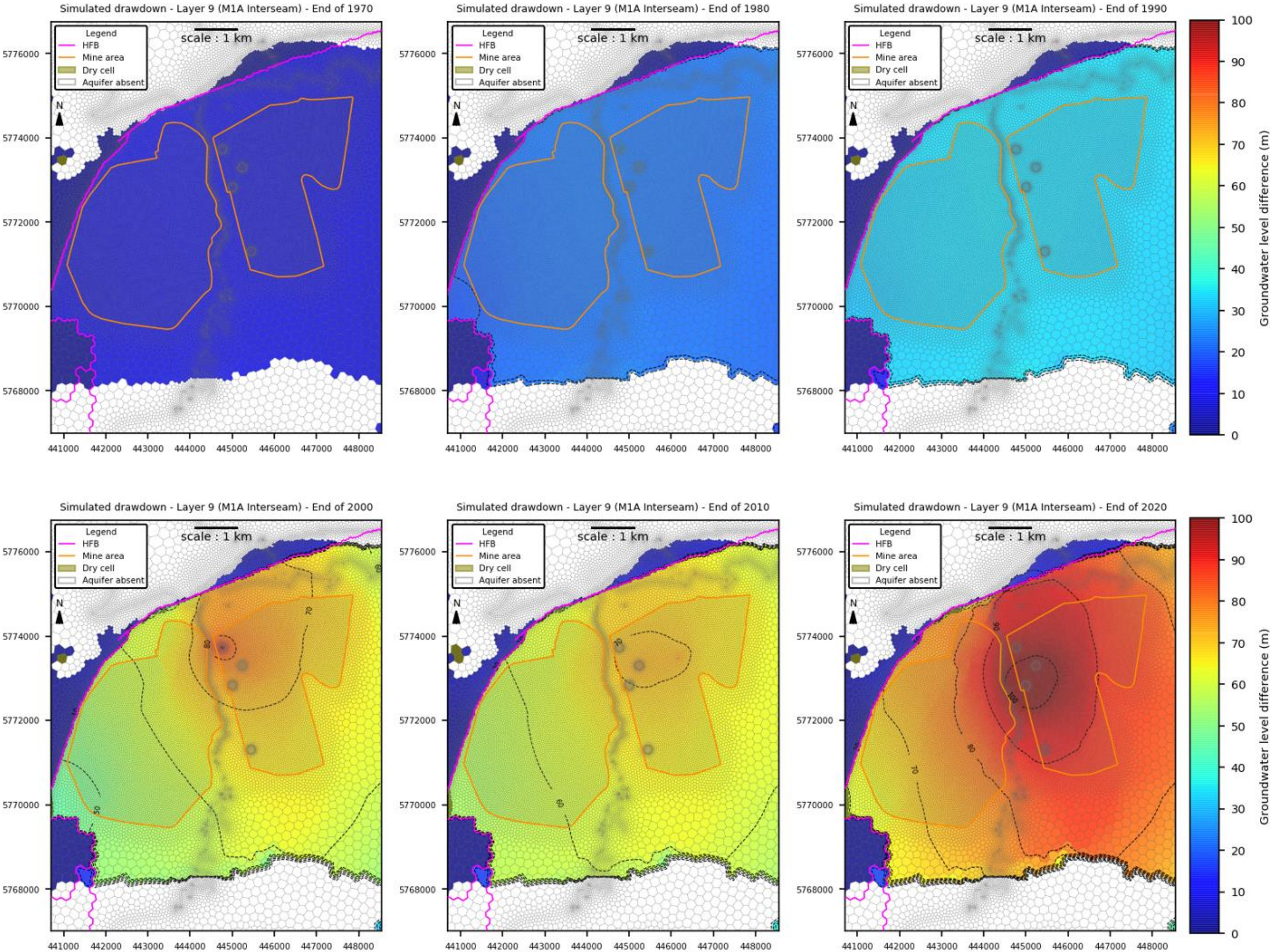

Figure 42 *M1A Interseam drawdown contours*

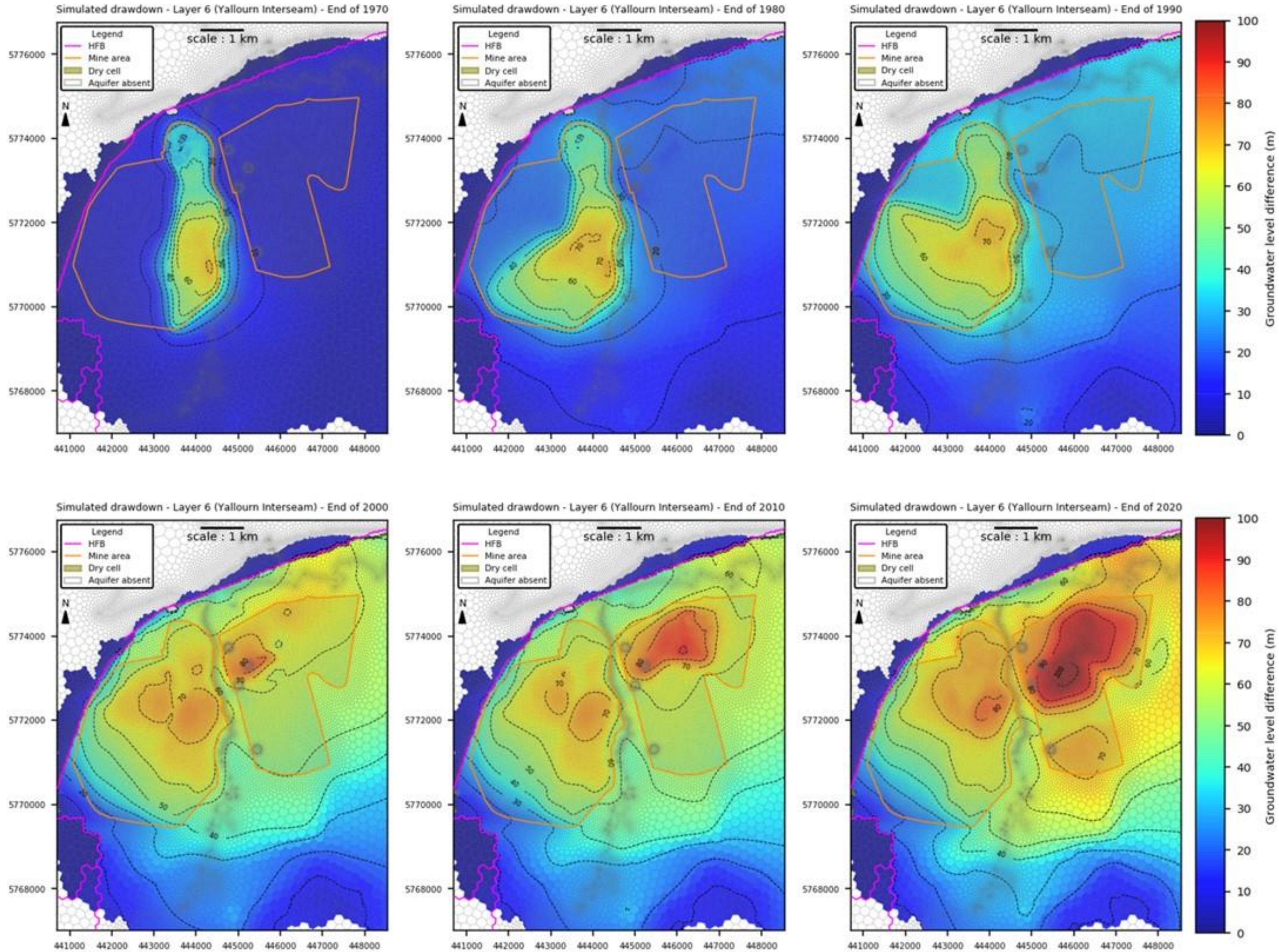

Figure 43 ***Yallourn Interseam drawdown contours***

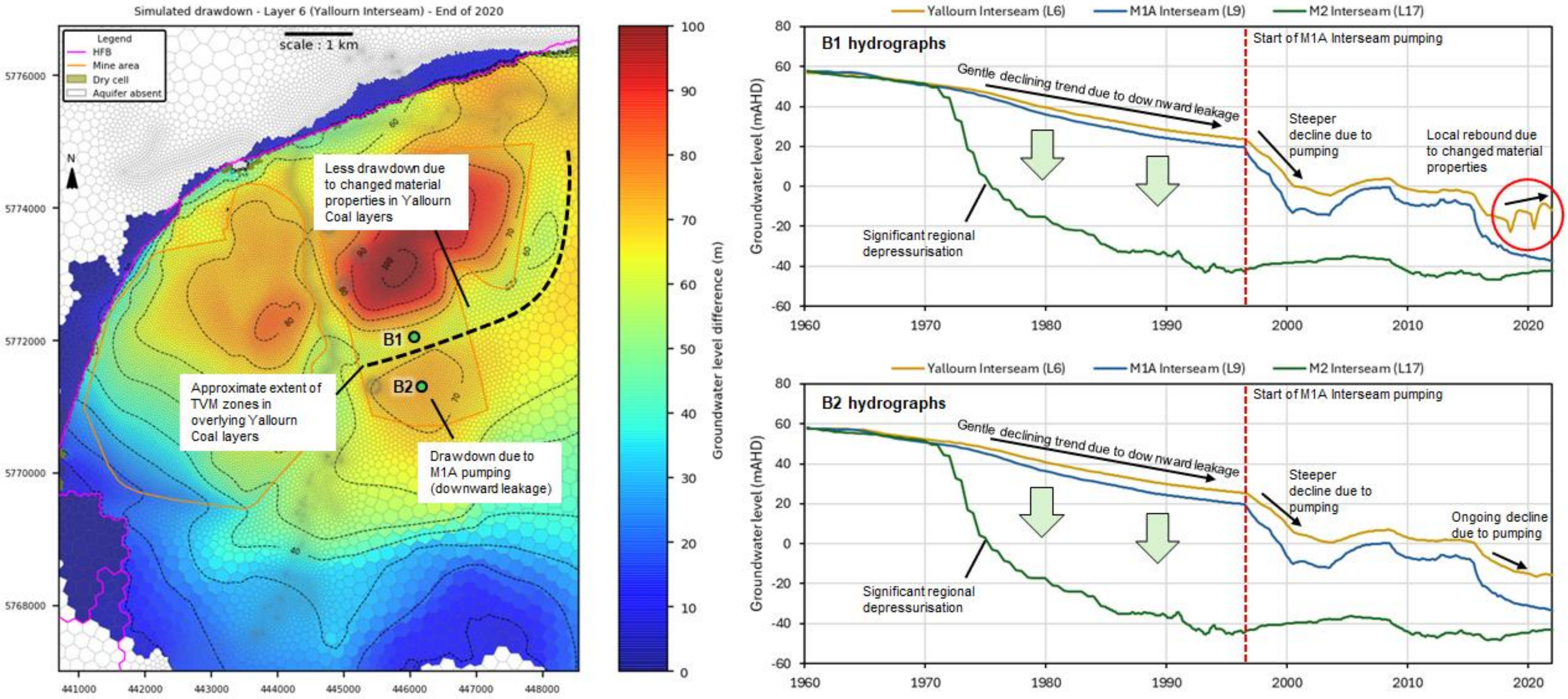

Figure 44 *Yallourn Interseam end 2020 drawdown contours and trends*

3.2.1.3 Groundwater flow

EAY has supplied GHD with estimates of groundwater inflow rates from the horizontal drains constructed within the Yallourn Coal batters. It is understood that these estimates are approximate, with some limitations associated with the accuracy of the flow measurements and different number of horizontal drains measured in different years. For this reason, the estimated seepage rates from the horizontal drains have been aggregated into annualised averages for the purpose of assessing the reasonableness of the modelled seepage rates i.e. whether the model outputs are broadly consistent with the estimated range of flow rates.

The simulated groundwater seepage from the Yallourn Coal has been calculated from the fluxes removed by the drain cells assigned to the Yallourn Coal layers (drain outflow from layers 2,3,4 and 5). Figure 45 compares the annualised drain outflows with the estimated horizontal drain flows. The modelled and estimated fluxes are broadly consistent from 2011 to 2016. The modelled drain outflows are larger than the estimated horizontal drain flows since 2017, noting that the estimated flows could be underestimated due to the significant reduction in the flow rates compared to the periods prior to 2017 (despite the larger mine footprint and wet conditions encountered in 2020 and 2021).

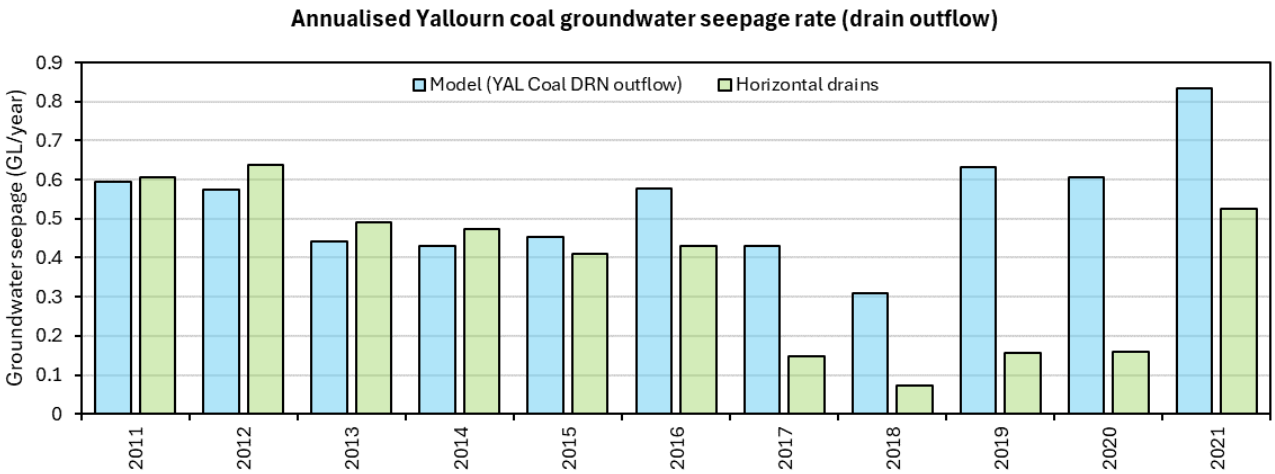

Figure 45 Modelled and estimated Yallourn Coal seepage rates

The modelled drain outflow includes a component of flow derived from recharge that has been assigned directly to the location of drain cells. This recharge has not been adjusted for the condition of the exposed floor of the mine and any excess (rejected) recharge is added to the drain outflow (which would, in reality, be lost as runoff). For this reason, the modelled drain outflows may overestimate the actual groundwater seepage rates from the Yallourn Coal. If the recharge flux is entirely removed from the drain outflow, the modelled seepage rates generally become lower than the estimated horizontal drain flows from 2011 to 2016 (see Figure 46). This suggests that some recharge is occurring over the exposed coal along the mine floor and batters (particularly where the hydraulic conductivity has been enhanced by the ground movement), contributing to the seepage of groundwater at the deeper level in the mine. While estimating the correct recharge rate over the exposed Yallourn Coal is difficult (due to the complex material property changes over time), the modelled drain outflows are broadly consistent with the estimated horizontal drain flows (typically in the range of 0.4 to 0.6 GL/year) and are considered reasonable for the purpose of simulating the mine scale water balance.

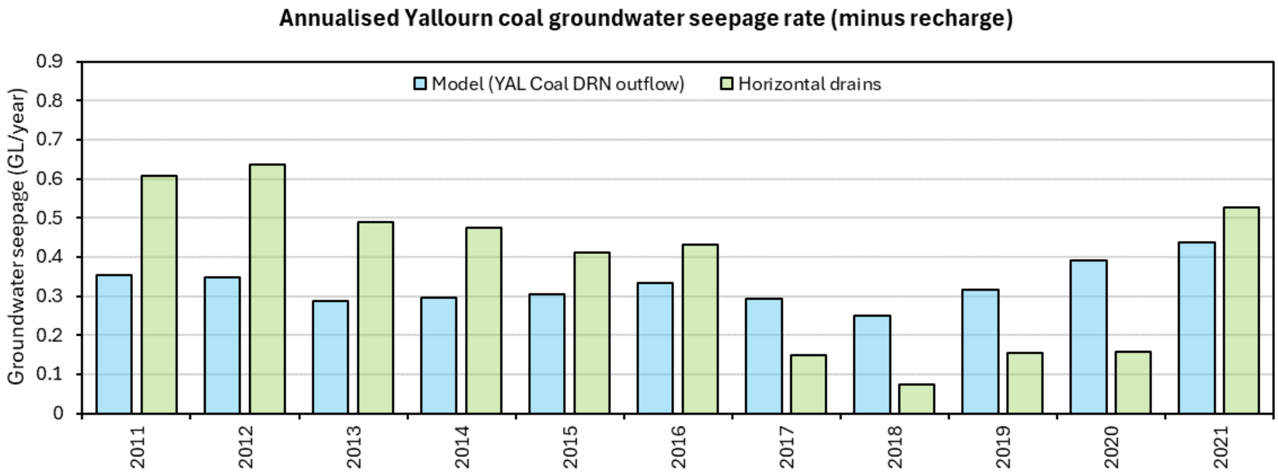

Figure 46 *Modelled and estimated Yallourn Coal seepage rates (minus recharge)*

The total annualised modelled drain outflows at the Yallourn Mine are presented in Figure 47, representing the combined simulated groundwater seepage rate from the Haunted Hills Formation and Yallourn Coal. The modelled annualised total groundwater seepage rate is typically in the range of 2 to 4 GL/year. While an estimate of the total groundwater seepage rate is not available, the site wide water balance (as described in GHD 2023b) can be used to assess if the modelled seepage rates are reasonable. For example, the site wide water balance suggests that up to around 22 GL/year of surface water is typically discharged to the Fire Service Pond (comprising up to around 15 GL/year from the Township Lake and up to 7 GL/year from the East Field dewatering ponds, which includes 1 GL/year of pumped groundwater from the M1A Interseam). From this 22 GL/year, 15 to 21 GL/year is pumped (discharged) to the Morwell River and Witts Gully Reservoir. This means there is up to around 7 GL/year of surplus water (not sourced from the Latrobe River or the M1A Interseam), which could potentially be due to groundwater seepage and runoff. The 2 to 4 GL/year groundwater seepage rate derived from the modelling would account for around half of this surplus water (with the rest originating from ex-pit and in-pit runoffs), which is considered reasonable.

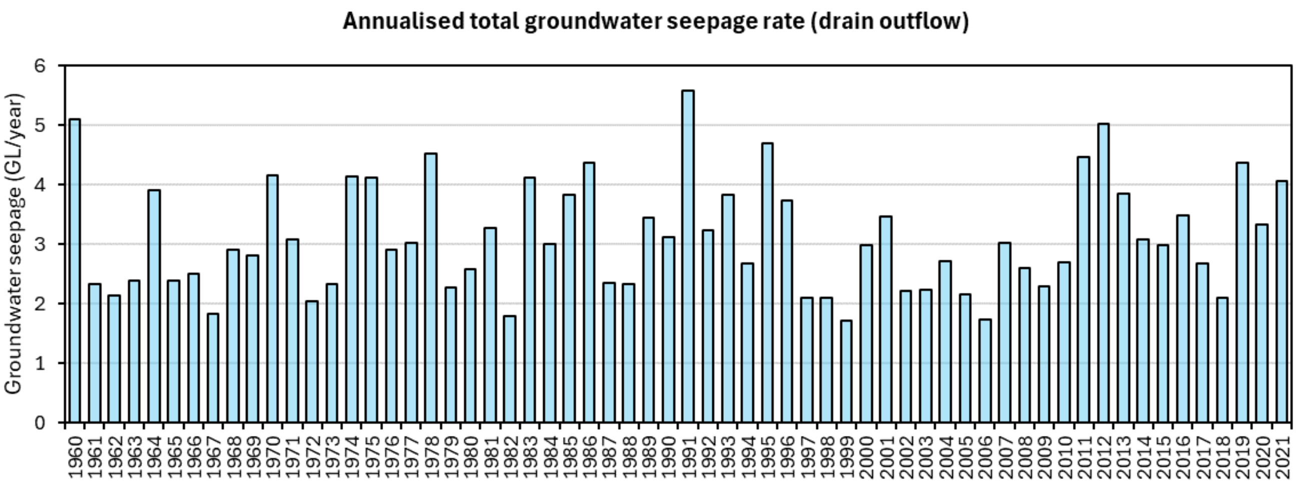

Figure 47 *Annualised modelled total groundwater seepage (drain outflow)*

As detailed in Section 3.1.2.3, the drain outflows from the Hazelwood Mine have been compared against the total groundwater extraction rates at the mine to ensure the volumetric fluxes and prescribed piezometric head changes are consistent. Figure 48 shows the modelled drain outflows and actual pumping rates (as applied to the LVRGM) are similar at the Hazelwood Mine, with the largest discrepancy limited to the early simulation periods (in the 1970s). The modelled drain outflows slightly overestimate the pumping rates from around 2000 and this is partly due to the component of recharge flux applied to the location of drain cells. This effect is minor and the modelled drain outflows are considered appropriate for the purpose of simulating the regional aquifer depressurisation effect at the Hazelwood Mine.

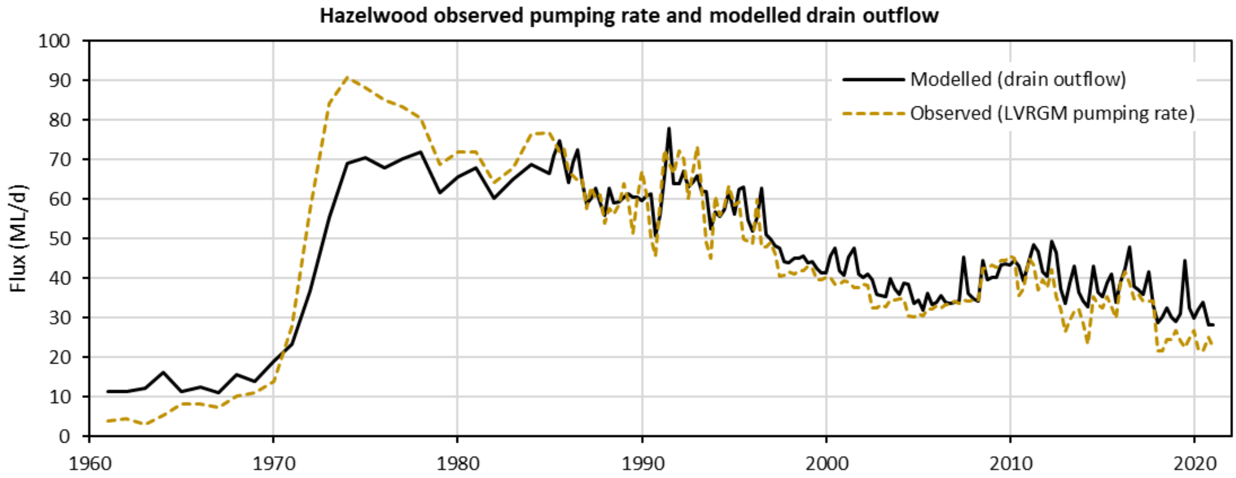

Figure 48 *Hazelwood observed pumping rate and modelled drain outflow*

The model-wide water balance is summarised in Table 3, including the average stress period fluxes and cumulative fluxes for the entire calibration period. Recharge and evapotranspiration represent the largest component of inflow and outflow, respectively. The GHB cells assigned along the perimeter of the model provide throughflow into the model, mostly along the upgradient boundary to mimic regional flow, and out of the model, primarily along the eastern boundary representing connection with the broader Latrobe Valley aquifer system. The river (RIV) boundary condition, representing the water features within and outside of the mine void, provide sources of inflow as well as outflow. The stream (SFR) boundary condition is predominantly acting as a point of outflow, indicating a generally gaining condition (groundwater baseflow) simulated by the model which is consistent with the hydrogeological conceptualisation of the typical stream flow behaviour (GHD, 2023b).

Table 3 *Model water balance summary*

Component	Transient cumulative (ML)		Transient average rate (ML/d)	
	Inflow	Outflow	Inflow	Outflow
Recharge	3,740,785		183	
Evapotranspiration		3,851,534		144
Drain		1,263,257		59
Well		35,035		2
River	531,523	388,153	23	17
Stream	47,845	815,638	2	36
GHB	2,389,777	760,004	99	33
Storage	2,495,600	2,091,934	119	136
Total	**9,205,530**	**9,205,553**	**427**	**427**

The mass balance error is very low, less than 0.01 % for all model time steps as well as cumulatively (well below the 1 % maximum mass balance error recommended by the AGMG).

3.2.1.4 Stream stage and flow

The model calibration performance with respect to stream stage and flow is described by comparing the observed and modelled hydrographs at the location of stream gauges.

Figure 49 includes the observed and modelled hydrographs of stream stage and a map showing the location of stream gauges. The calibration uses stress period average stage (daily stage measurements are included in the hydrographs for context, to show the range of daily variability relative to the stress period averages).

There is generally good agreement between the observed and modelled stage at all four stream gauges used in the calibration. The model slightly underestimates the stage measured at the MRD Southern Crossing gauge (26737) prior to mid-2019, with the model and observed values becoming more closely aligned after mid-2019. At the MRD Northern Crossing gauge (26736), there is close agreement between the modelled and observed stage with a typical difference (residual) of less than 0.05 m since 2014. Single high stream levels recorded at both crossings during the wet (flooding) periods of 2011 and 2012 have been excluded from the hydrographs, as the model is only capable of calculating quarterly (stress period) averages (which would underestimate the peak flood levels). The difference between the modelled and observed stage at gauge 226408 and 226005A is generally less than 0.2 m.

Figure 50 includes the observed and modelled hydrographs of stream flow and a map showing the location of stream gauges used in the flow calibration. As per the stream stage, the stress period average flows are computed by the model and compared against the observed average flows over the same periods. Gauge 226033A is located outside of the model grid and the flow recorded at this gauge has been compared against the flow computed at the last reach of the stream boundary to ensure sensible volumes of stream flow exiting the model. In general, the hydrographs show close agreement between the measured and modelled stress period average stream flows at the three stream gauges used in model calibration.

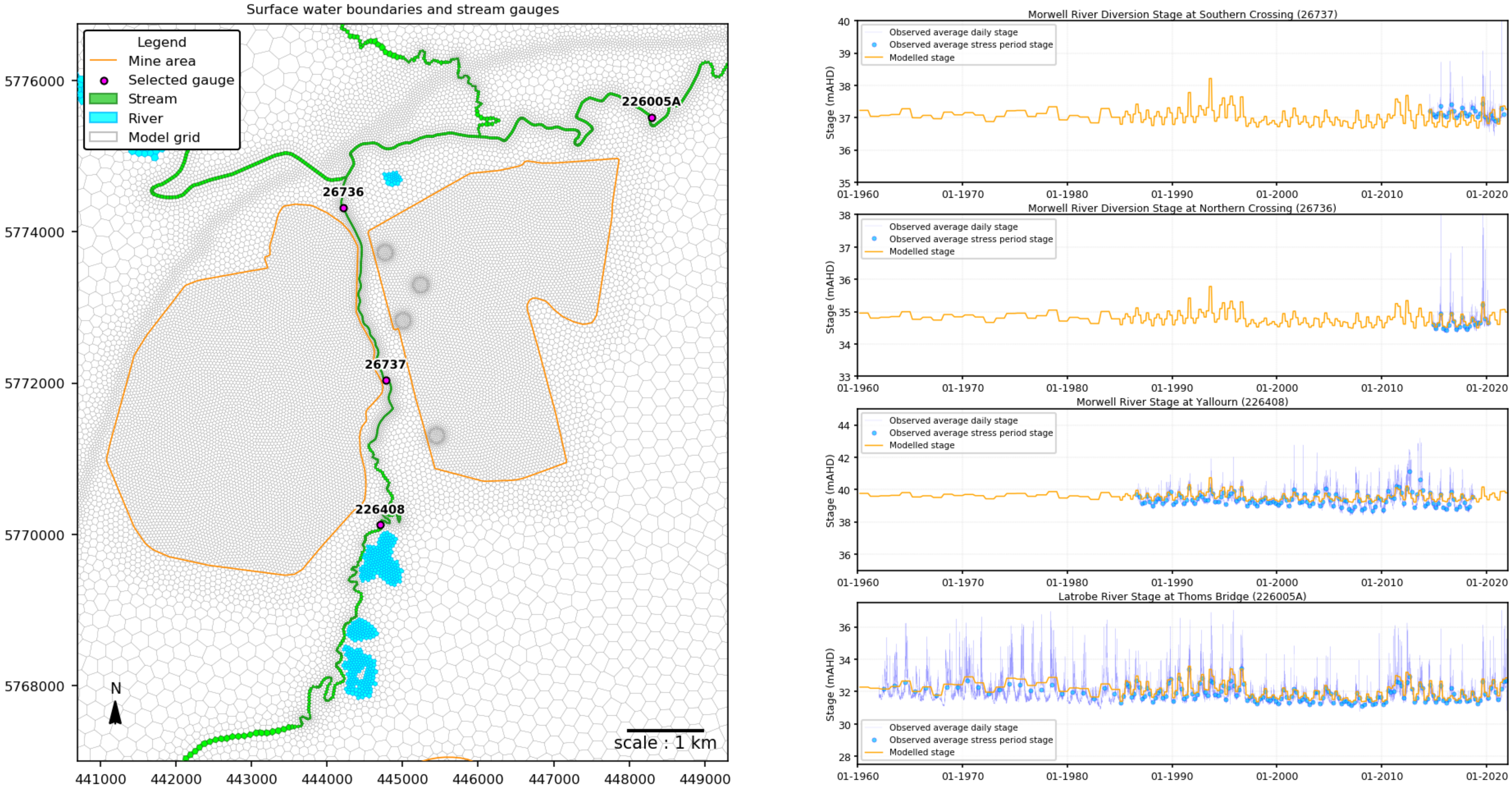

Figure 49 Stream stage calibration hydrographs

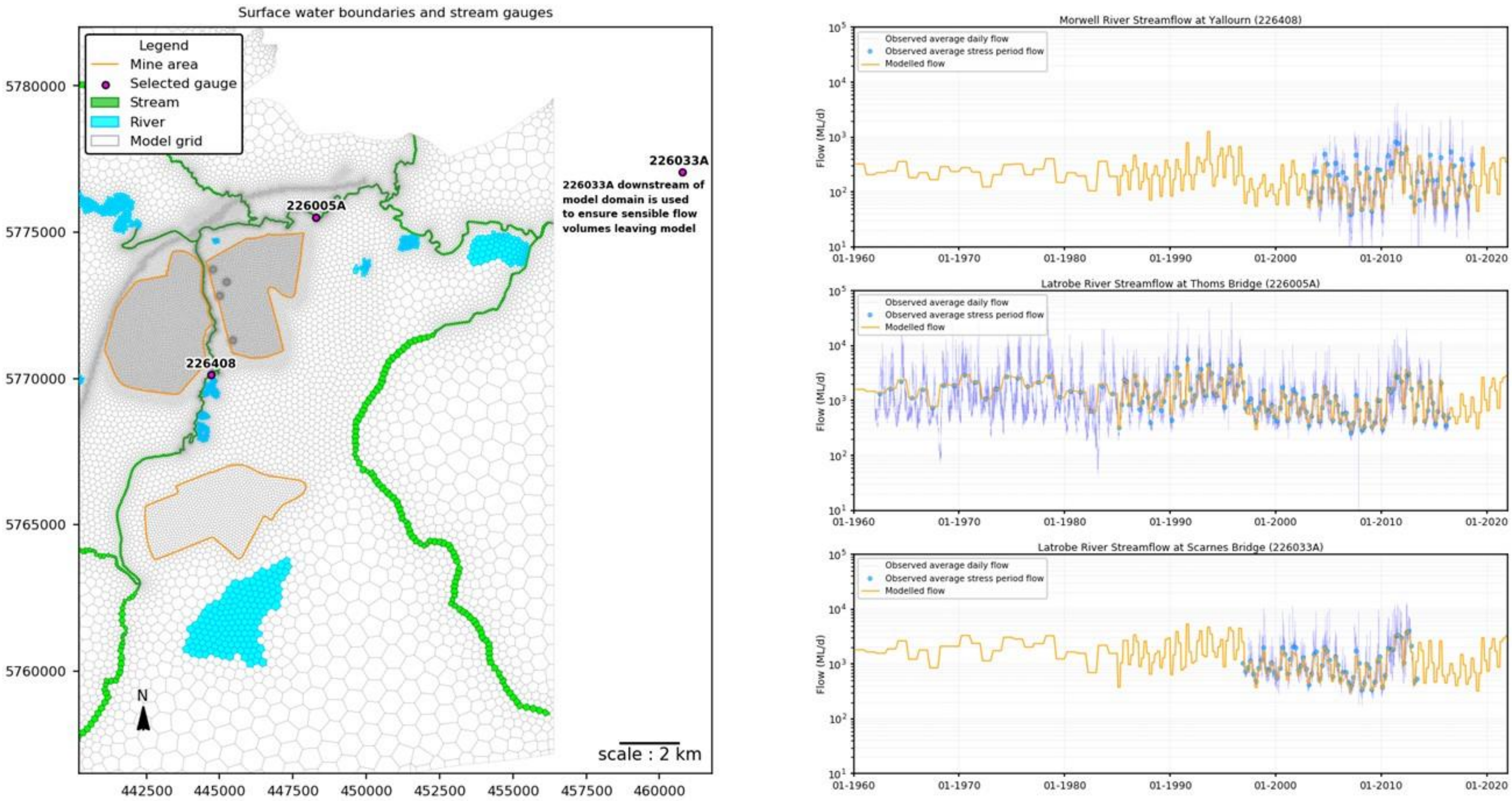

Figure 50 *Stream flow calibration hydrographs*

3.2.1.5 Calibration statistics

Scatter plots of the computed and observed values are presented in this section for groundwater levels, stream stage and stream flow targets. Also included in each plot is the statistical measure of goodness of fit between the computed and observed values including the Scaled Root Mean Squared (SRMS) error, Root Mean Squared (RMS) error and the Mean Sum of Residuals (MSR).

For the groundwater level targets, the SRMS error is 6.61 % and the MSR error is 9.58 m when all 34,778 head targets from 471 bores/piezometers are included in the statistical analysis. The SRMS error is within the 5 to 10 % range that is generally considered acceptable for regional scale modelling, particularly for a model required to simulate complex hydrogeological processes caused by mining and near surface dynamics (where matching the absolute groundwater levels can be challenging). The MSR error of 9.58 m is considered acceptable within the context of large groundwater level changes (of up to 100 m) caused by mining and spatial differences in the groundwater levels observed across 471 bores used to inform the calibration.

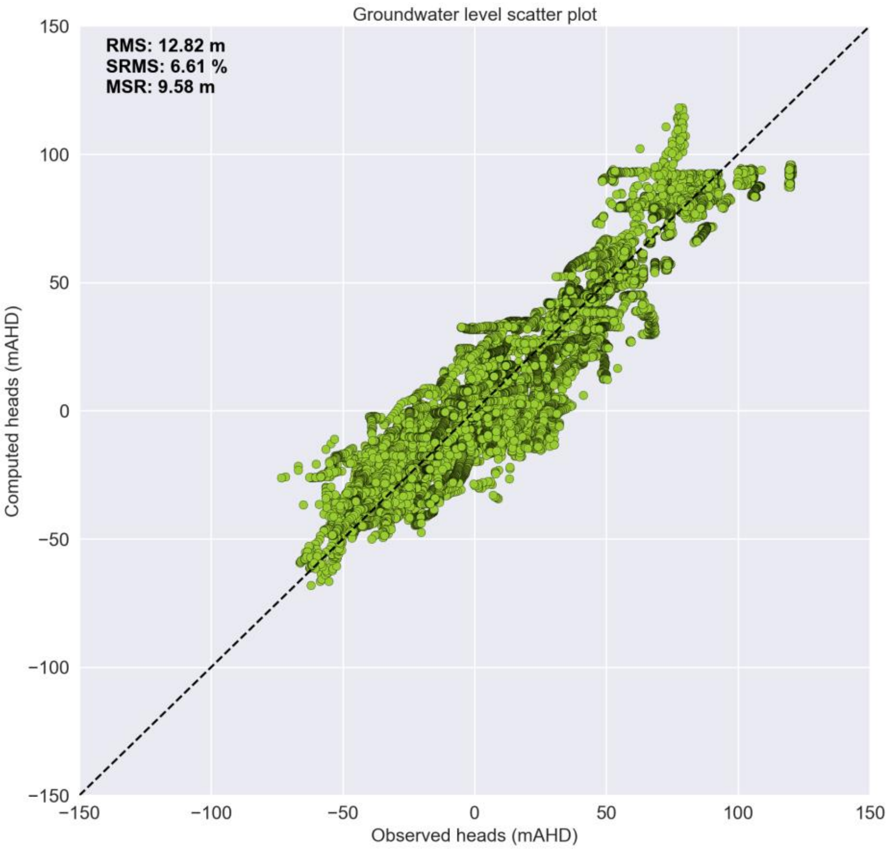

Figure 51 Scatter plot – groundwater levels

For stream stage and flow targets, the SRMS error is 2.54 % and 3.75 % respectively (smaller than the SRMS error for the head calibration albeit with much smaller number of targets). The tightness of fit between the measured and observed stream stage is generally consistent for the full range of values. For the stream flows, there is a greater spread (misfit) at the upper end of the values, potentially due to the way the observed averages are skewed by a small number of very high flow events (whereas the model uses climate and flow inputs that are averaged out over the length of each stress period). The majority of the average flow targets are at the lower end of the range of flow values, where the scatter plot shows a tighter fit between the modelled and observed values.

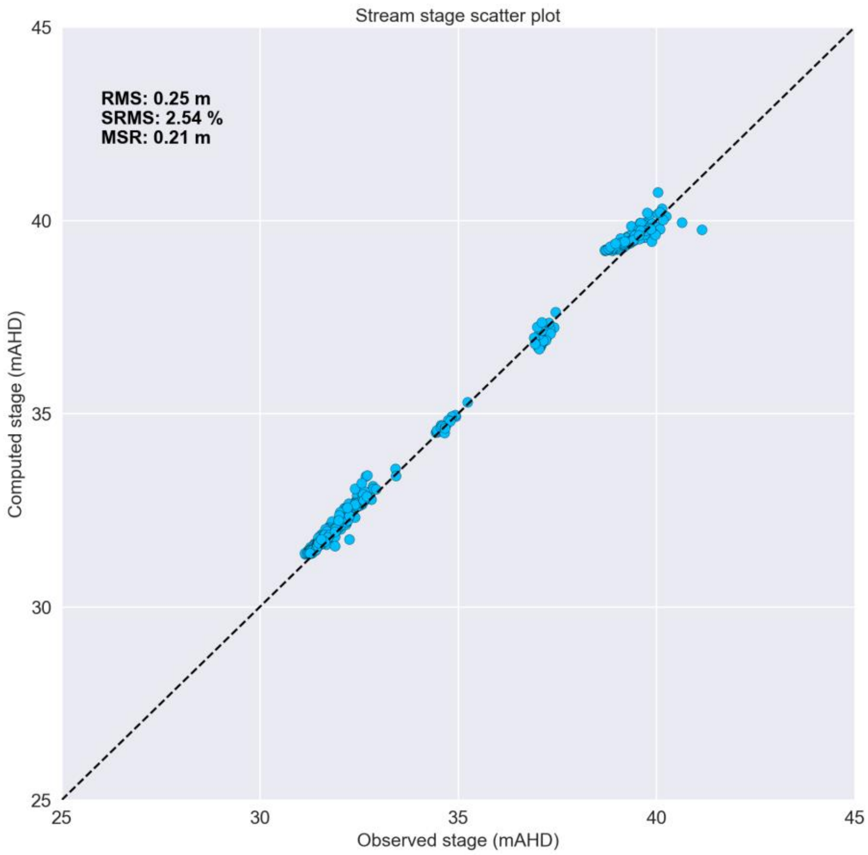

Figure 52 Scatter plot – stream stage

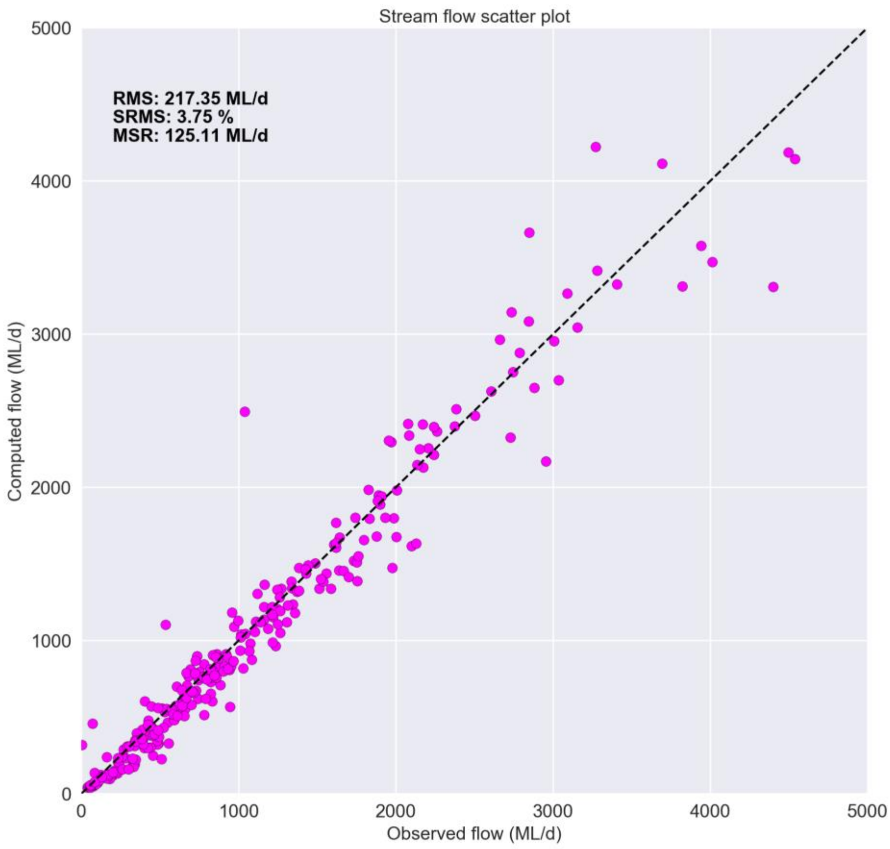

Figure 53 Scatter plot – stream flow

3.2.2 Calibrated model parameters

3.2.2.1 Parameter values

The calibrated model parameter values are summarised in tables and presented graphically in Figure 56 to Figure 60, comparing the calibrated values against the initial estimates and the range of values (upper and lower bound) allowed during calibration.

The calibrated model parameters indicate the following:

- In general, the calibrated parameters of the USG-Transport model show little departure from their initial estimates derived from the LVRGM due to the prior calibration of this regional model (providing sensible initial estimates for the Yallourn model parameters, with little adjustments required during calibration). The largest departures from the initial estimates are seen in some vertical hydraulic conductivity factors, which have been adjusted in response to the more targeted calibration of the model to the data collected from the Yallourn Mine.
- The calibrated PRMS model parameters show much larger departures from their initial values, as this model has not undergone prior calibration. The parameter “soil_moist_max” for most of the soil zones have been increased towards their upper bound estimates, resulting in high soil evapotranspiration and reduced recharge. This is broadly consistent with GHD’s experience with soil water balance modelling, which has the tendency to overestimate diffuse recharge when applied to groundwater models (for example, recharge rates from the PERFECT soil water balance model are scaled down before they are applied to the LVRGM). The PRMS model parameters have been adjusted based on the response simulated in the USG-Transport model, which means the recharge and evapotranspiration rates ultimately applied to the groundwater model are consistent with the groundwater level and flow data used to calibrate the USG-Transport model. the calibrated PRMS parameters are presented graphically in Figure 60 and summarised in a table in Appendix C.
- The calibrated long term average recharge is around 9.8 % of the long term average rainfall and the recharge rates, on a model wide basis, are generally consistent with those of the Victorian Government’s ecoMarkets model. Figure 54 compares the average annualised recharge rates computed by the PRMS model against those from the West Gippsland ecoMarkets model (calculated over the equivalent domain), showing generally close agreement between the two models (with the PRMS model simulating lower recharge during drier periods). There are, however, differences in the spatial distribution of recharge simulated by the two models due to some differences in the underlying assumptions (such as flow cascades incorporated into the PRMS model) and adjustments made to the PRMS model based on the response simulated in the groundwater model during rigorous calibration. Figure 55 shows the long term average recharge and evapotranspiration (EVT) simulated by the PRMS model over the calibration period and the equivalent outputs interpolated to the unstructured grid of the USG-Transport (MFUSG) model. An area of low recharge is simulated to the west of the Hazelwood Mine, where the confined aquifers subcrop and receive recharge. Experience from the LVRGM suggests that the rate of recharge to the confined aquifers in this subcropping zone is low, which is simulated in the LVRGM by scaling the recharge outputs from the PERFECT model. The PRMS modelling has achieved a similar outcome, by reducing recharge in the parameter zones west of the Hazelwood Mine based on the calibration to the groundwater levels and pumping rates (drain outflow, as described in Section 3.1.2.3). The calibrated EVT extinction depth is 0.5 m and 3 m for the grass and tree areas, as per their initial values (Table 6).
- The average calibrated horizontal hydraulic conductivity of the key aquifer units within the Yallourn Mine area is 2.9 m/d for the Haunted Hills Formation (layer 1), 0.014 m/d for the Yallourn Interseam (layer 6) and 0.4 to 1.4 m/d for the M1A Interseam (layers 8,9 and 10). When comparing these (Table 4) against the published range of values (such as those presented in Section 4.4 of GHD, 2023b), it is important to note that aquifer tests have typically targeted discrete sand intervals that yield higher estimates of hydraulic conductivity than the bulk averages for the whole aquifer. For example, the maximum calibrated horizontal hydraulic conductivity for the Haunted Hills Formation is 7 m/d (based on the highest sand percentage), which agrees well with the 4 to 8 m/d range estimated from aquifer testing (refer to Table 3 of GHD, 2023b). Similarly, the maximum calibrated horizontal hydraulic conductivity for the M1A Interseam is 12.7 m/d, which is within the 8 to 15 m/d range derived from pumping tests completed on bores screened across the sand interseams (refer to Table 3 of GHD, 2023b). Figure 56 and Figure 57 show maps of the calibrated hydraulic conductivity of the aquifer layers, focusing on the Yallourn Mine area.

– The calibrated horizontal hydraulic conductivity of the in-situ (undisturbed) Yallourn Coal is 4.3 x 10^{-5} m/d (Table 4), which is within the 3.6 x 10^{-6} to 3.6 x 10^{-4} m/d range estimated for in-tact coal in the Latrobe Valley (Trollope et al, 1965). The calibrated horizontal hydraulic conductivity of the highly fractured zone (TVM zone 1) is 7 x 10^{-3} m/d (Table 6), which is towards the lower end of the range of values derived from packer testing completed in the East Field northern batters but higher than the range of values derived from the laboratory analysis of core samples (up to 3.5 x 10^{-4} m/d) collected from the same location (Baumgartl, 2020, also refer to Section 4.4.2 of GHD, 2023b). This is also similar to the 1.7 x 10^{-3} m/d in-situ permeability estimated for the M1 Coal batters at the Hazelwood Mine (Brown, 1970). The moderately fractured zone (TVM zone 2), representing the transitional zone between the undisturbed and highly fractured zone, has been assigned a calibrated horizontal hydraulic conductivity value of 7 x 10^{-4} m/d, which is approximately an average of the two adjacent zones (between 4.3 x 10^{-5} and 7 x 10^{-3} m/d). The internal overburden dump (TVM zone 3) has been assigned a calibrated horizontal hydraulic conductivity of 1.4 x 10^{-3} m/d.

– The calibrated vertical hydraulic conductivity of the Haunted Hills Formation and interseam layers is 2 to 3 orders of magnitude lower than the horizontal hydraulic conductivity (note the values presented in Table 4 are factors used to convert horizontal hydraulic conductivities into their vertical values). This reflects the interbedded nature of these aquifer layers, leading to much lower hydraulic conductivities in the vertical direction. For example, the Haunted Hills Formation predominantly consists of silty and sandy clays with lenses of sands and gravels that are overlain/separated by clay interbeds e.g. an elongated basal sand and gravel layer that existed prior to the mining of East Field, which was overlain by up to 6.5 m of clay layer and separated by up to 4 m of clay interbeds (Holgate et al, 1979, Geo Eng, 1992). Similarly, the M1A Interseam consists of four discontinuous sand aquifers separated by coal, clay and silt interbeds, including a relatively continuous clay layer of up to 30 m in thickness, which reduces the hydraulic conductivity vertically (see Section 4.3.2.3 and Figure 26 of GHD, 2023b). GHD (2024) also carried out a laboratory permeability analysis on 10 core samples from the Yallourn Interseam (subsequent to the completion of calibration), which generated average and geometric mean vertical hydraulic conductivities of 3.4 x 10^{-5} and 3.0 x 10^{-5} m/d, respectively. These are similar to the calibrated minimum vertical hydraulic conductivity of the Yallourn Interseam (2.2 x 10^{-5} m/d) and around an order of magnitude lower than the calibrated average of 5.3 x 10^{-4} m/d. This is likely to reflect the scale dependent nature of hydraulic conductivities, with the model exhibiting the characteristics of a much larger representative elementary volume than individual core samples.

– The conductance values for the RIV and GHB cells vary spatially based on the calibrated hydraulic conductivities and cell geometry. For the RIV cells representing the in-pit water features, the RIV conductance ranges from 157 to 250 m^2/d while larger values are used for the ex-pit water features (up to 2,273 m^2/d) due to the larger surface areas of the cells further away from the mine. For the GHB cells, conductance varies widely from 0.025 to 780,971 m^2/d (average 30,691 m^2/d) due to the wide range of cell cross-sectional areas (perpendicular to flow), ranging from 83 to 842,898 m^2 (depending on the cell edge length and thickness), and a wide range of calibrated hydraulic conductivity values at the GHB cells (e.g. interseam layers having much higher hydraulic conductivities than the coal layers).

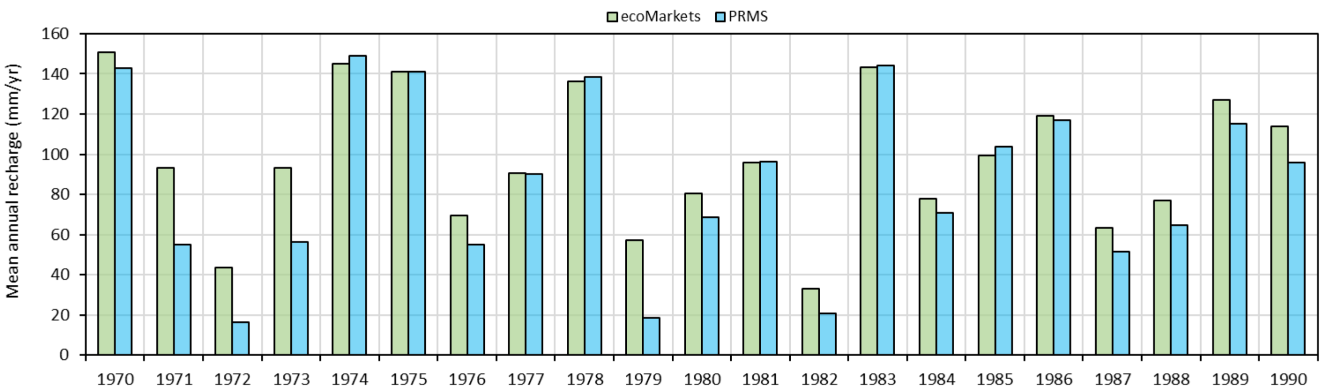

Figure 54 ***Comparison between calibrated PRMS and ecoMarkets recharge rates***

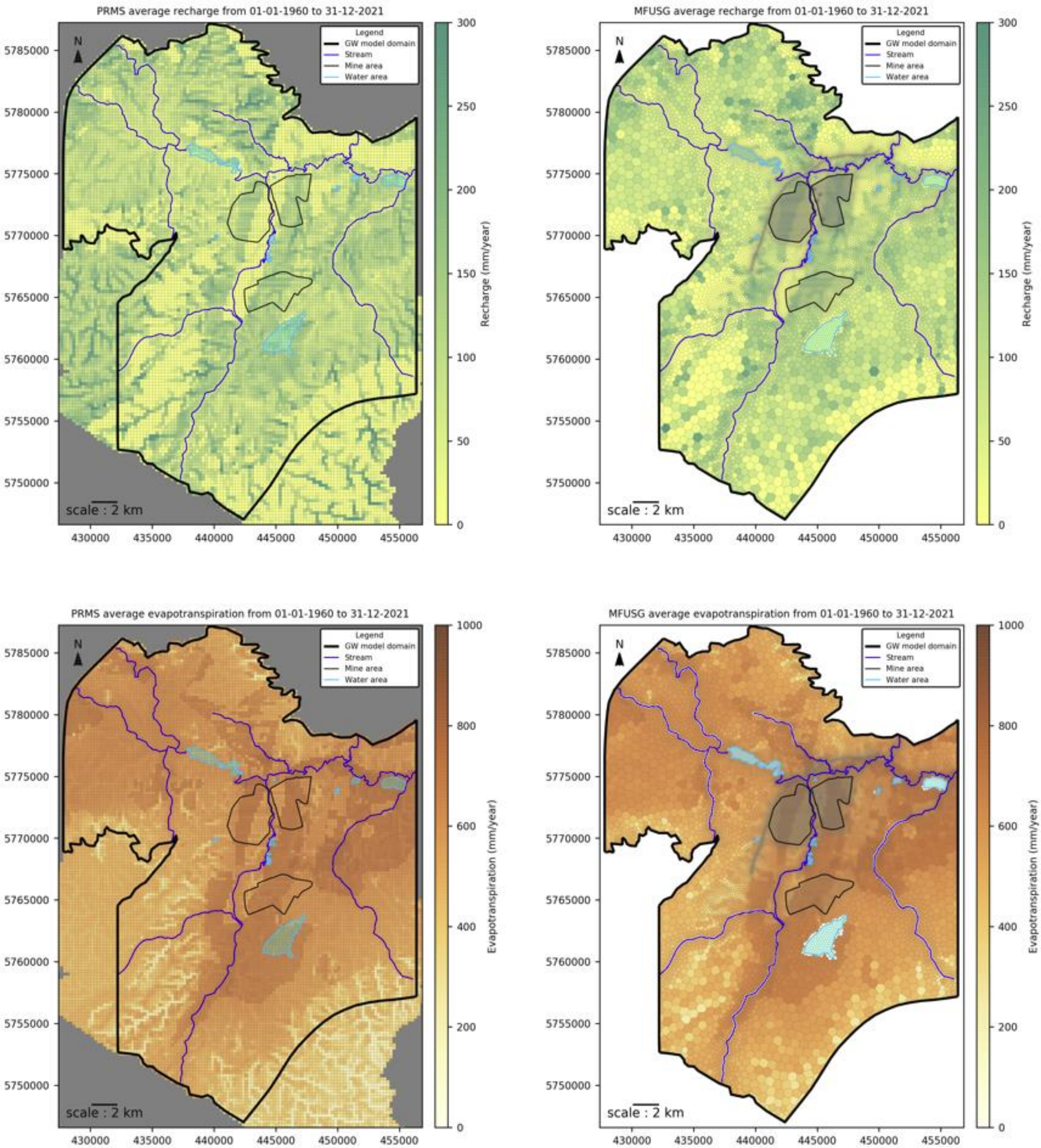

Figure 55 *Average calibrated recharge and evapotranspiration*

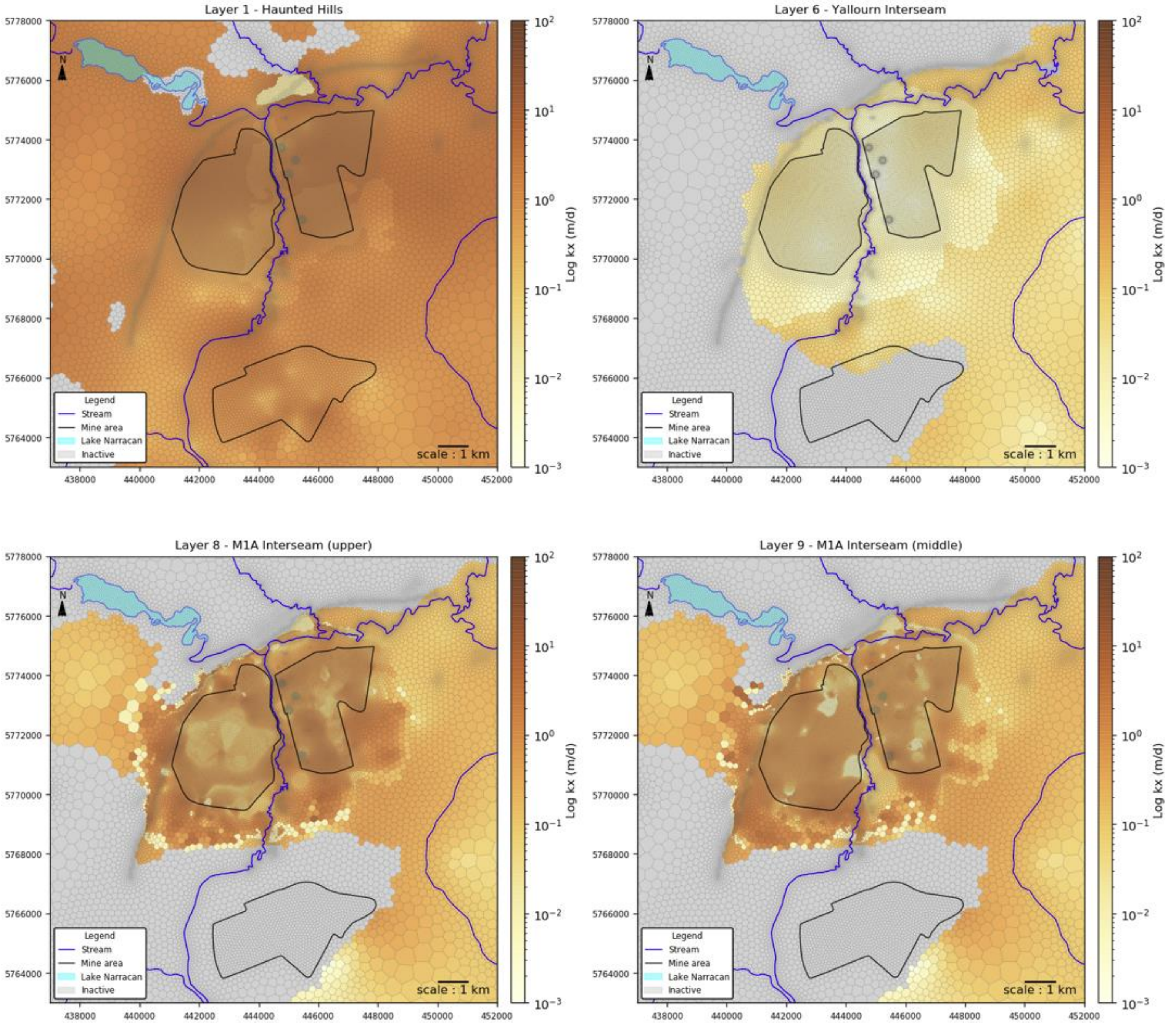

Figure 56 *Calibrated horizontal hydraulic conductivity – layers 1,6,8 and 9*

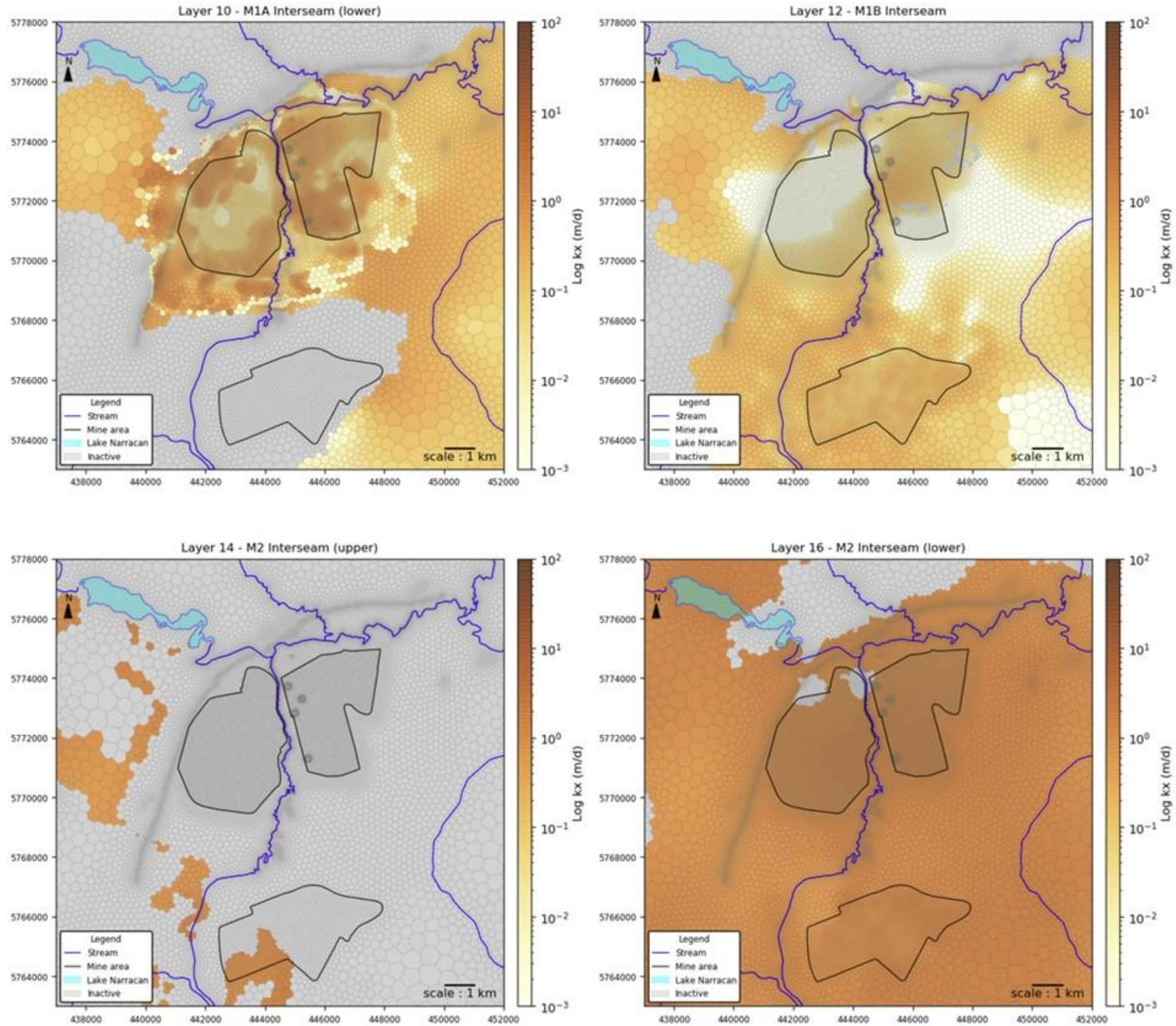

Figure 57 *Calibrated horizontal hydraulic conductivity – layers 10,12,14 and 16*

Table 4 USG-Transport model – calibrated parameters – part1

Model	Parameter	Unit	Initial	Min	Max	Calibrated	Comment
USG	kx2_1	m/d	5.00E-05	4.00E-06	4.00E-04	4.30E-05	Yallourn Coal (undisturbed) horizontal hydraulic conductivity
USG	kx7_1	m/d	4.00E-05	4.00E-06	4.00E-04	4.90E-05	M1A Coal horizontal hydraulic conductivity
USG	kx11_1	m/d	4.00E-04	4.00E-06	4.00E-04	4.00E-04	M1B Coal horizontal hydraulic conductivity
USG	kx13_1	m/d	3.00E-04	4.00E-06	4.00E-04	1.90E-04	M2 Coal horizontal hydraulic conductivity
USG	kx15_1	m/d	0.004	0.00001	0.01	0.0033	Thorpdale Volcanics horizontal hydraulic conductivity
USG	kx17_1	m/d	0.0025	0.00001	0.01	0.0028	Basement horizontal hydraulic conductivity
USG	ynockx	m/d	0.01	0.0001	0.1	0.02	YNOC fill horizontal hydraulic conductivity
USG	pckx1_1	Multiplier	5	0.01	15	4.04	Percent sand to horizontal hydraulic conductivity - Haunted Hills Formation (basal sand)
USG	pckx1_2	Multiplier	5	0.01	15	7.43	Percent sand to horizontal hydraulic conductivity - Haunted Hills Formation
USG	pckx6_1	Multiplier	0.1	0.01	10	0.05	Percent sand to horizontal hydraulic conductivity - Yallourn Interseam (minescape area)
USG	pckx6_2	Multiplier	0.3	0.01	10	0.26	Percent sand to horizontal hydraulic conductivity - Yallourn Interseam (regional)
USG	pckx8_1	Multiplier	10	0.1	20	11.25	Percent sand to horizontal hydraulic conductivity - M1A Interseam upper (minescape area)
USG	pckx9_1	Multiplier	10	0.1	20	9.81	Percent sand to horizontal hydraulic conductivity - M1A Interseam middle (minescape area)
USG	pckx10_1	Multiplier	10	0.1	20	5.08	Percent sand to horizontal hydraulic conductivity - M1A Interseam lower (minescape area)
USG	pckx8_2	Multiplier	0.5	0.1	20	0.9	Percent sand to horizontal hydraulic conductivity - M1A Interseam (regional)
USG	pckx12_1	Multiplier	0.3	0.01	10	0.36	Percent sand to horizontal hydraulic conductivity - M1B Interseam
USG	pckx16_1	Multiplier	2.5	0.01	20	2.77	Percent sand to horizontal hydraulic conductivity - M2 Interseam
USG	kzfac2_1	Multiplier	0.1	0.001	1	0.1	Yallourn Coal (undisturbed) horizontal to vertical hydraulic conductivity factor
USG	kzfac7_1	Multiplier	0.1	0.001	1	0.24	M1A Coal horizontal to vertical hydraulic conductivity factor
USG	kzfac11_1	Multiplier	0.0035	0.001	1	0.02	M1B Coal horizontal to vertical hydraulic conductivity factor
USG	kzfac13_1	Multiplier	0.25	0.001	1	0.08	M2 Coal horizontal to vertical hydraulic conductivity factor
USG	kzfac15_1	Multiplier	0.01	0.001	1	0.01	Thorpdale Volcanics horizontal to vertical hydraulic conductivity factor
USG	kzfac17_1	Multiplier	1	0.001	1	0.44	Basement horizontal to vertical hydraulic conductivity factor
USG	kzfac1_1	Multiplier	0.03	0.001	1	0.017	Haunted Hills Formation (basal sand) horizontal to vertical hydraulic conductivity factor

Model	Parameter	Unit	Initial	Min	Max	Calibrated	Comment
USG	kzfac1_2	Multiplier	0.03	0.001	1	0.0063	Haunted Hills Formation horizontal to vertical hydraulic conductivity factor
USG	kzfac6_1	Multiplier	0.03	0.001	1	0.038	Yallourn Interseam (minescape area) horizontal to vertical hydraulic conductivity factor
USG	kzfac6_2	Multiplier	0.005	0.001	1	0.0027	Yallourn Interseam (regional) horizontal to vertical hydraulic conductivity factor
USG	kzfac8_1	Multiplier	0.0075	0.001	1	0.002	M1A Interseam upper (minescape area) horizontal to vertical hydraulic conductivity factor
USG	kzfac9_1	Multiplier	0.0075	0.001	1	0.0065	M1A Interseam middle (minescape area) horizontal to vertical hydraulic conductivity factor
USG	kzfac10_1	Multiplier	0.0075	0.001	1	0.0037	M1A Interseam lower (minescape area) horizontal to vertical hydraulic conductivity factor
USG	kzfac8_2	Multiplier	0.015	0.001	1	0.014	M1A Interseam (regional) horizontal to vertical hydraulic conductivity factor
USG	kzfac12_1	Multiplier	0.004	0.001	1	0.0022	M1B Interseam horizontal to vertical hydraulic conductivity factor
USG	kzfac16_1	Multiplier	0.5	0.001	1	0.8	M2 Interseam horizontal to vertical hydraulic conductivity factor
USG	kzfynoc	Multiplier	0.1	0.001	1	0.24	YNOC fill horizontal to vertical hydraulic conductivity factor

Table 5 USG-Transport model – calibrated parameters – part2

Model	Parameter	Unit	Initial	Min	Max	Calibrated	Comment
USG	ss2_1	1/m	1.00E-05	1.00E-06	1.30E-05	1.30E-05	Yallourn Coal (undisturbed) specific storage
USG	ss7_1	1/m	5.00E-06	1.00E-06	1.30E-05	2.29E-06	M1A Coal specific storage
USG	ss11_1	1/m	1.30E-06	1.00E-06	1.30E-05	1.19E-06	M1B Coal specific storage
USG	ss13_1	1/m	1.00E-06	1.00E-06	1.30E-05	1.06E-06	M2 Coal specific storage
USG	ss15_1	1/m	1.20E-05	1.00E-06	1.30E-05	1.30E-05	Thorpdale Volcanics specific storage
USG	ss17_1	1/m	1.00E-06	1.00E-06	1.30E-05	1.00E-06	Basement specific storage
USG	ss1_1	1/m	1.00E-05	1.00E-06	1.30E-05	1.00E-05	Haunted Hills Formation (basal sand) specific storage
USG	ss1_2	1/m	1.00E-05	1.00E-06	1.30E-05	1.00E-05	Haunted Hills Formation specific storage
USG	ss6_1	1/m	1.20E-06	1.00E-06	1.30E-05	1.53E-06	Yallourn Interseam (minescape area) specific storage
USG	ss6_2	1/m	1.20E-05	1.00E-06	1.30E-05	1.30E-05	Yallourn Interseam (regional) specific storage
USG	ss8_1	1/m	1.00E-05	1.00E-06	1.30E-05	1.30E-05	M1A Interseam upper (minescape area) specific storage
USG	ss9_1	1/m	1.00E-05	1.00E-06	1.30E-05	1.30E-05	M1A Interseam middle (minescape area) specific storage

Model	Parameter	Unit	Initial	Min	Max	Calibrated	Comment
USG	ss10_1	1/m	1.00E-05	1.00E-06	1.30E-05	1.30E-05	M1A Interseam lower (minescape area) specific storage
USG	ss8_2	1/m	1.00E-05	1.00E-06	1.30E-05	1.17E-05	M1A Interseam (regional) specific storage
USG	ss12_1	1/m	6.40E-06	1.00E-06	1.30E-05	4.08E-06	M1B Interseam specific storage
USG	ss16_1	1/m	1.00E-06	1.00E-06	1.30E-05	1.00E-06	M2 Interseam specific storage
USG	ssynoc	1/m	5.00E-06	1.00E-06	1.30E-05	4.05E-06	YNOC fill specific storage
USG	sy2_1	Fraction	0.045	0.01	0.3	0.045	Yallourn Coal (undisturbed) specific yield
USG	sy7_1	Fraction	0.01	0.01	0.3	0.01	M1A Coal specific yield
USG	sy11_1	Fraction	0.01	0.01	0.3	0.015	M1B Coal specific yield
USG	sy13_1	Fraction	0.01	0.01	0.3	0.01	M2 Coal specific yield
USG	sy15_1	Fraction	0.02	0.01	0.3	0.034	Thorpdale Volcanics specific yield
USG	sy17_1	Fraction	0.01	0.01	0.3	0.01	Basement specific yield
USG	sy1_1	Fraction	0.01	0.01	0.3	0.018	Haunted Hills Formation (basal sand) specific yield
USG	sy1_2	Fraction	0.01	0.01	0.3	0.025	Haunted Hills Formation specific yield
USG	sy6_1	Fraction	0.015	0.01	0.3	0.055	Yallourn Interseam (minescape area) specific yield
USG	sy6_2	Fraction	0.07	0.01	0.3	0.043	Yallourn Interseam (regional) specific yield
USG	sy8_1	Fraction	0.2	0.01	0.3	0.3	M1A Interseam upper (minescape area) specific yield
USG	sy9_1	Fraction	0.2	0.01	0.3	0.3	M1A Interseam middle (minescape area) specific yield
USG	sy10_1	Fraction	0.2	0.01	0.3	0.253	M1A Interseam lower (minescape area) specific yield
USG	sy8_2	Fraction	0.02	0.01	0.3	0.048	M1A Interseam (regional) specific yield
USG	sy12_1	Fraction	0.2	0.01	0.3	0.093	M1B Interseam specific yield
USG	sy16_1	Fraction	0.1	0.01	0.3	0.088	M2 Interseam specific yield
USG	syynoc	Fraction	0.1	0.01	0.3	0.288	YNOC fill specific yield

Table 6 USG-Transport model – calibrated parameters – part3

Model	Parameter	Unit	Initial	Min	Max	Calibrated	Comment
USG	tvm_kx1	m/d	0.005	0.004	0.4	0.007	TVM horizontal hydraulic conductivity - Yallourn coal highly fractured zone
USG	tvm_kx2	m/d	0.0005	0.0004	0.004	0.0007	TVM horizontal hydraulic conductivity - Yallourn coal moderately fractured zone
USG	tvm_kx3	m/d	0.001	0.0001	0.1	0.0014	TVM horizontal hydraulic conductivity - Internal overburden dump

Model	Parameter	Unit	Initial	Min	Max	Calibrated	Comment
USG	tvm_kzf1	m/d	0.1	0.001	1	0.025	TVM horizontal to vertical hydraulic conductivity factor - Yallourn coal highly fractured zone
USG	tvm_kzf2	m/d	0.1	0.001	1	0.089	TVM horizontal to vertical hydraulic conductivity factor - Yallourn coal moderately fractured zone
USG	tvm_kzf3	m/d	0.1	0.001	1	0.1	TVM horizontal to vertical hydraulic conductivity factor - Internal overburden dump
USG	tvm_ss1	m/d	5.00E-06	1.00E-06	1.30E-05	5.00E-06	TVM specific storage - Yallourn coal highly fractured zone
USG	tvm_ss2	m/d	5.00E-06	1.00E-06	1.30E-05	5.00E-06	TVM specific storage - Yallourn coal moderately fractured zone
USG	tvm_ss3	m/d	5.00E-06	1.00E-06	1.30E-05	5.00E-06	TVM specific storage - Internal overburden dump
USG	tvm_sy1	m/d	0.045	0.01	0.3	0.046	TVM specific yield - Yallourn coal highly fractured zone
USG	tvm_sy2	m/d	0.045	0.01	0.3	0.046	TVM specific yield - Yallourn coal moderately fractured zone
USG	tvm_sy3	m/d	0.1	0.01	0.3	0.049	TVM specific yield - Internal overburden dump
USG	sfrk1	m/d	0.01	0.001	1	0.01	SFR bed hydraulic conductivity - Morwell River (natural)
USG	sfrk2	m/d	1.00E-05	1.00E-06	1.00E-04	1.15E-05	SFR bed hydraulic conductivity - Morwell River (MRD) clay lined
USG	sfrk3	m/d	5.00E-07	1.00E-07	1.00E-06	4.80E-07	SFR bed hydraulic conductivity - Morwell River (MRD) geosynthetic lined
USG	sfrk4	m/d	0.01	0.001	1	0.0095	SFR bed hydraulic conductivity - Latrobe River
USG	sfrk5	m/d	0.01	0.001	1	0.0109	SFR bed hydraulic conductivity - Others
USG	rivk_mine	m/d	0.01	0.0001	1	0.0107	RIV bed hydraulic conductivity - water features within mine
USG	rivk_blue	m/d	0.01	0.0001	1	0.01	RIV bed hydraulic conductivity - Blue lagoon
USG	rivk_narra	m/d	0.01	0.0001	1	0.0093	RIV bed hydraulic conductivity - Lake Narracan
USG	rivk_morwet	m/d	0.01	0.0001	1	0.0103	RIV bed hydraulic conductivity - Morwell wetlands
USG	rivk_wig	m/d	0.01	0.0001	1	0.0112	RIV bed hydraulic conductivity - Witts Gully reservoir
USG	rivk_pine	m/d	0.01	0.0001	1	0.0099	RIV bed hydraulic conductivity - Pine Gully reservoir
USG	rivk_apm	m/d	0.0008	0.0001	1	0.0008	RIV bed hydraulic conductivity - APM lagoons
USG	rivk_hcp	m/d	0.001	0.0001	1	0.0012	RIV bed hydraulic conductivity - Hazelwood Cooling Pond
USG	exdp1	m/d	0.5	0.2	2	0.502	Evapotranspiration extinction depth - grass
USG	exdp2	m/d	3	2	6	3.019	Evapotranspiration extinction depth - trees

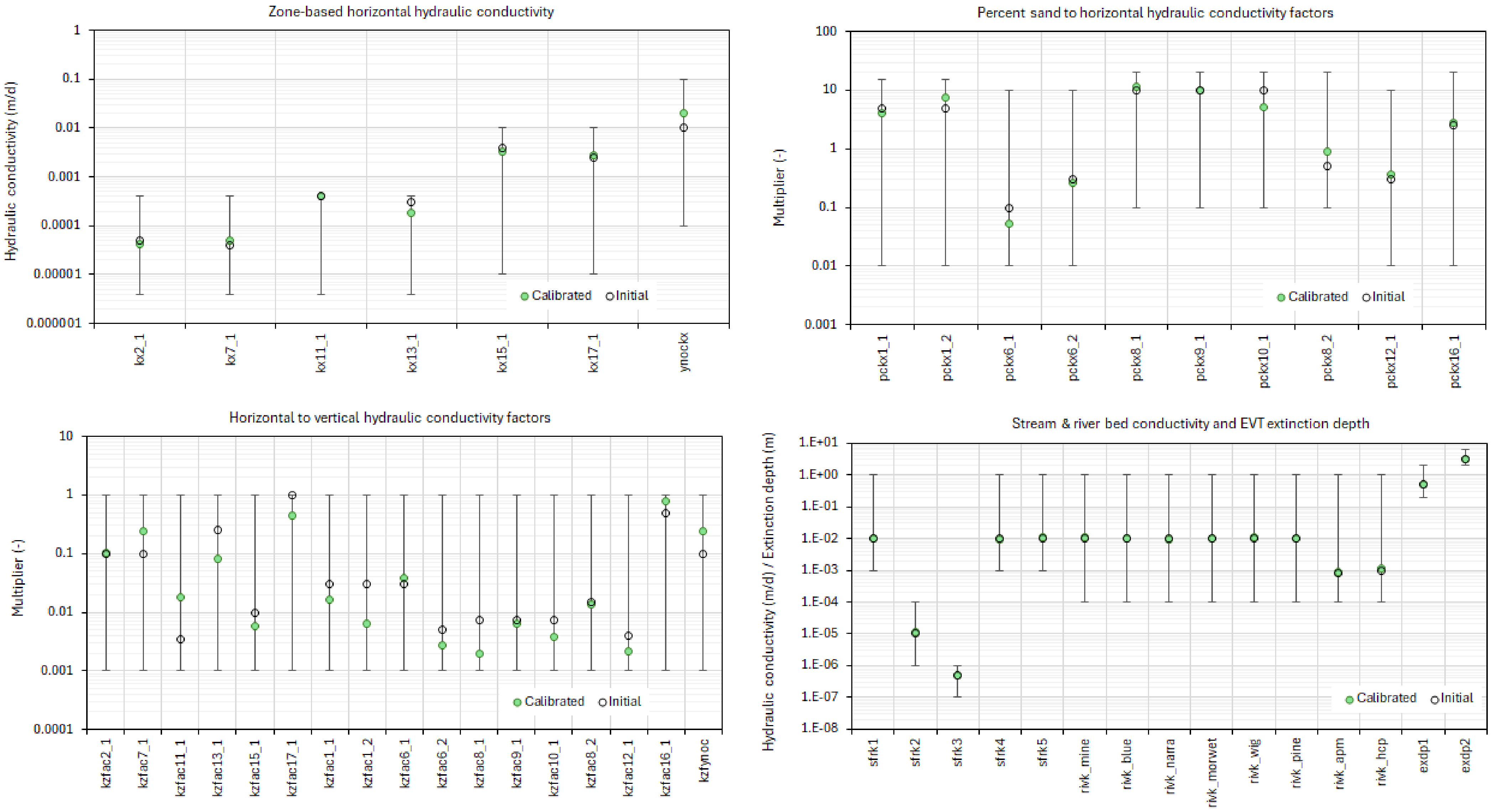

Figure 58 *USG-Transport calibrated model parameters – graphical summary - part 1*

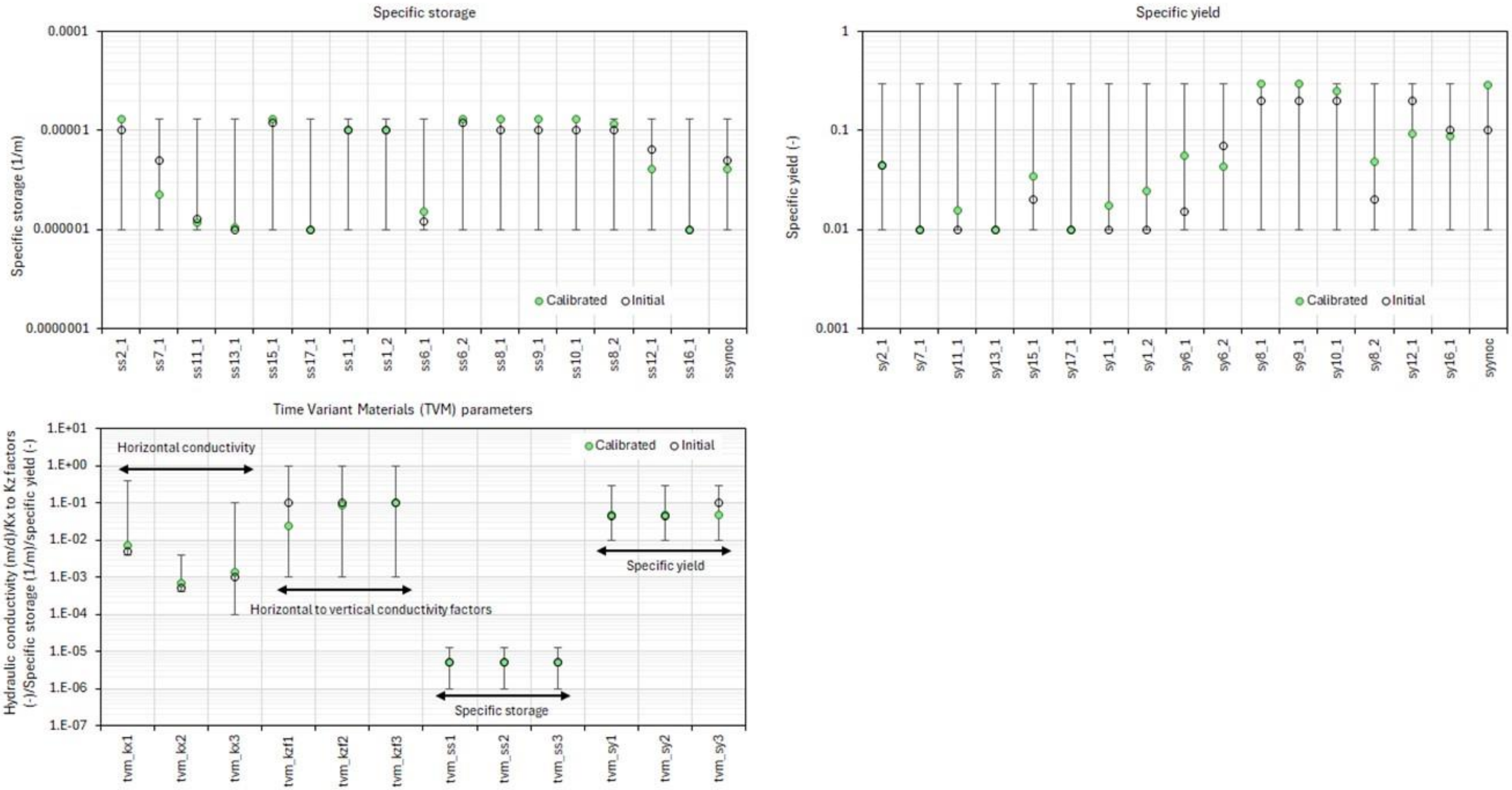

Figure 59 USG-Transport calibrated model parameters – graphical summary - part 2

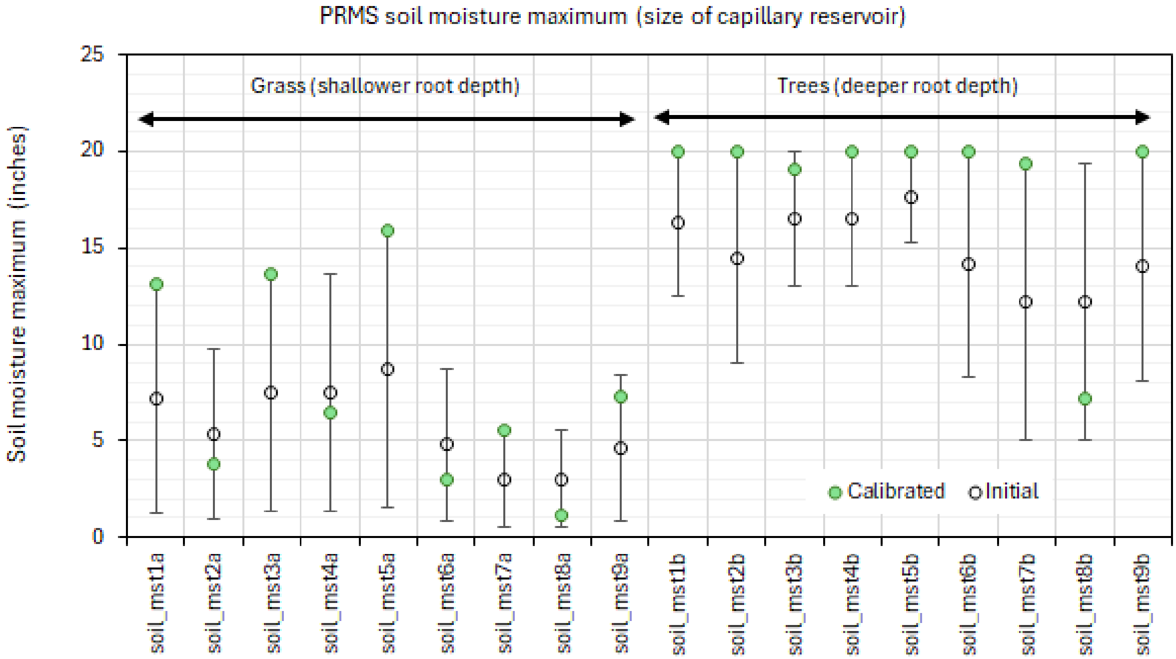

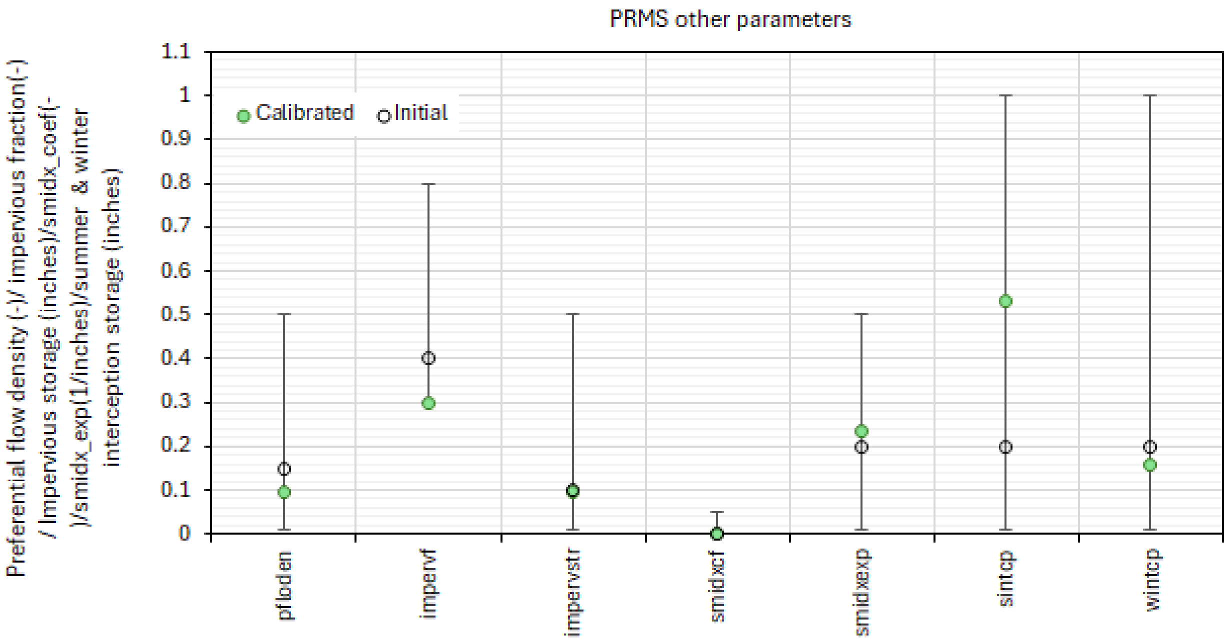

Figure 60 ***PRMS calibrated model parameters – graphical summary***

3.2.2.2 Parameter sensitivity

During model calibration, PEST_HP calculates a figure known as composite parameter sensitivity which provides a useful measure of the relative sensitivity of model parameters to the observation data used to inform the model calibration.

Figure 61 shows the composite parameter sensitivities of the most sensitive parameters, calculated by PEST_HP using the final (calibrated) set of model parameter values. The figure indicates the model is particularly sensitive to the specific yield of the Yallourn Coal, both for the undisturbed ("sy2_1") and fractured ("tvm_sy1" and "tvm_sy2") zones. This appears to be due to large changes in hydraulic heads that can arise in response to sudden changes in aquifer storage, when the components of flow budget are unchanged i.e. the same applied recharge flux (or inter-aquifer fluxes derived from recharge). The model is particularly sensitive when the specific yield of the fractured zone is reduced, resulting in large spikes in hydraulic heads in response to the same applied recharge (resulting in large mismatch between the modelled and observed heads). The effect is far less extreme when the specific yield is increased, as higher storage dampens the effect of recharge and does not lead to anomalously large head changes. Due to this high sensitivity, the calibration exercise has resulted in effectively identical specific yield values for both the undisturbed and fractured Yallourn Coal (to minimise large changes in heads).

Conceptually, the fracturing of the coal and opening of joints would be expected to result in higher specific yield. Given the lower sensitivity to increased storage, a better parameterisation approach may have been to adjust the specific yield of the fractured zone as a multiplier of the specific yield of the undisturbed coal (with a minimum value of 1, such that the fractured zone specific yield cannot be greater than that of the undisturbed coal). However, there is no guarantee that this would have yielded better calibration results as PEST_HP was provided with the flexibility to adjust the specific yield values independently and this did not result in higher specific yield for the fractured zone. It should also be noted that joints can open and close over time, which means permanently higher specific yield of may not be representative in some places.

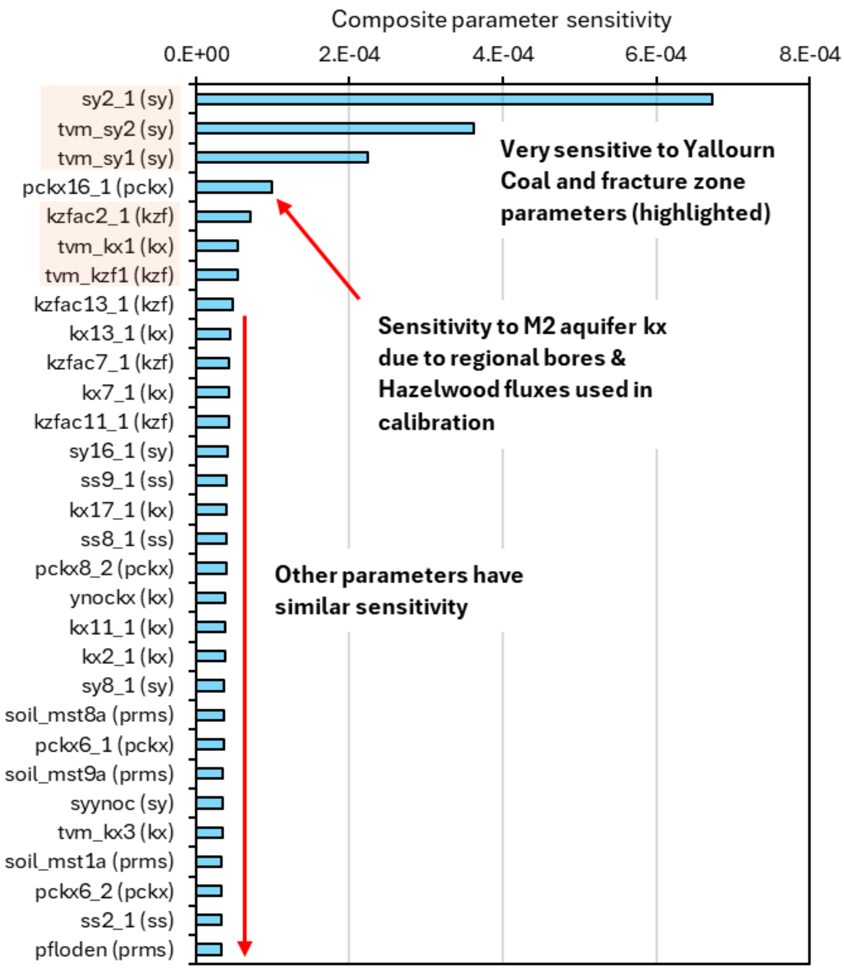

Figure 61 Composite parameter sensitivity

Figure 62 shows the composite parameter sensitivities of the USG-Transport model parameters, grouped by the parameter types. When comparing the parameter sensitivities, it is important to note that some parameters represent model-wide values that can influence the model response over much wider areas than other parameters assigned to discrete zones. For example, the model outputs are sensitive to parameter “pckx16_1”, which represents the horizontal hydraulic conductivity of the M2 Interseam across its full extent i.e. the M2 Interseam horizontal hydraulic conductivity is represented by this single parameter. This parameter has a strong influence on the drain fluxes at the Hazelwood Mine, which are calibrated against the pumping rates, and regional aquifer depressurisation effects that are calibrated against the groundwater levels measured in regional bores. The regionally significant aquifer depressurisation effect also influences the rate of downward vertical leakage (inter-aquifer fluxes) and hydraulic heads simulated within the overlying M1A Interseam and Yallourn Interseam (and calibration with respect to the head observations within these aquifers). In contrast, the model outputs show less sensitivity to the horizontal hydraulic conductivity of the M1A Interseam because this is parameterised using several different parameters to provide more flexibility during model calibration. For example, parameters “pckx8_1”, ‘pckx9_1” and “pckx10_1” are assigned over the footprint of the Yallourn Mine and to each of the three model layers representing the M1A Interseam, resulting in lower sensitivity individually (the combined sensitivity of all these parameters, representing the net effect of the M1A Interseam horizontal hydraulic conductivity, would be greater).

The vertical hydraulic conductivity parameters with high sensitivities belong to the coal layers. The flow through the low hydraulic conductivity coal layers is primarily vertical, with the vertical hydraulic conductivity controlling the rate of inter-aquifer fluxes exchanged between the adjacent aquifer (interseam) layers. The model is most sensitive to the vertical hydraulic conductivity of the Yallourn Coal layers, which influences the rate of vertical leakage into the underlying Yallourn Interseam (as well as leakage from the overlying Haunted Hills Formation). The model is also sensitive to the vertical hydraulic conductivities of the M1A Coal, M1B Coal and M2 Coal, which provide the resistance flow against the aquifer depressurisation effects from the underlying M2 Interseam (ultimately controlling the rate of vertical leakage out from the M1A Interseam).

The specific storage parameters with high sensitivities belong to the confined aquifer layers below the Yallourn Mine, specifically the M1 Interseam (“ss91_” and “ss8_1”), Yallourn Coal (“ss2_1”) and Yallourn Interseam (“ss6_1”). Specific storage influences the rate of change of hydraulic heads and high model sensitivity to the confined aquifer storage parameters is consistent with the calibration to pumping and other mining-induced groundwater level trends.

The parameter sensitivities, such as those calculated by PEST, can be used in conjunction with the measure of uncertainty in these parameters (defined by their plausible range of values, as summarised in Table 4 to Table 6) to quantify uncertainty associated with model outputs, particularly those associated with model predictions. The uncertainty quantification techniques range in complexity from a simple deterministic analysis to more sophisticated probabilistic analyses (such as linear and non-linear/ensemble analyses, as detailed in Peeters and Middlemis, 2023). Uncertainty can be reduced where the parameters are easily identifiable from the calibration dataset, leading to a narrow range of plausible values. It is also possible for the model outputs from the calibration and prediction periods to exhibit different levels of parameter sensitivity, with some parameters that are poorly constrained by the calibration dataset becoming more important when the model is used to make predictions (due to different hydrogeological regimes of the past and future). While a detailed uncertainty analysis is a scope for the future modelling work, the PEST based automated calibration workflow described in this report can be readily extended to enable quantifications of model uncertainty using published methods and a suite of PEST utilities.

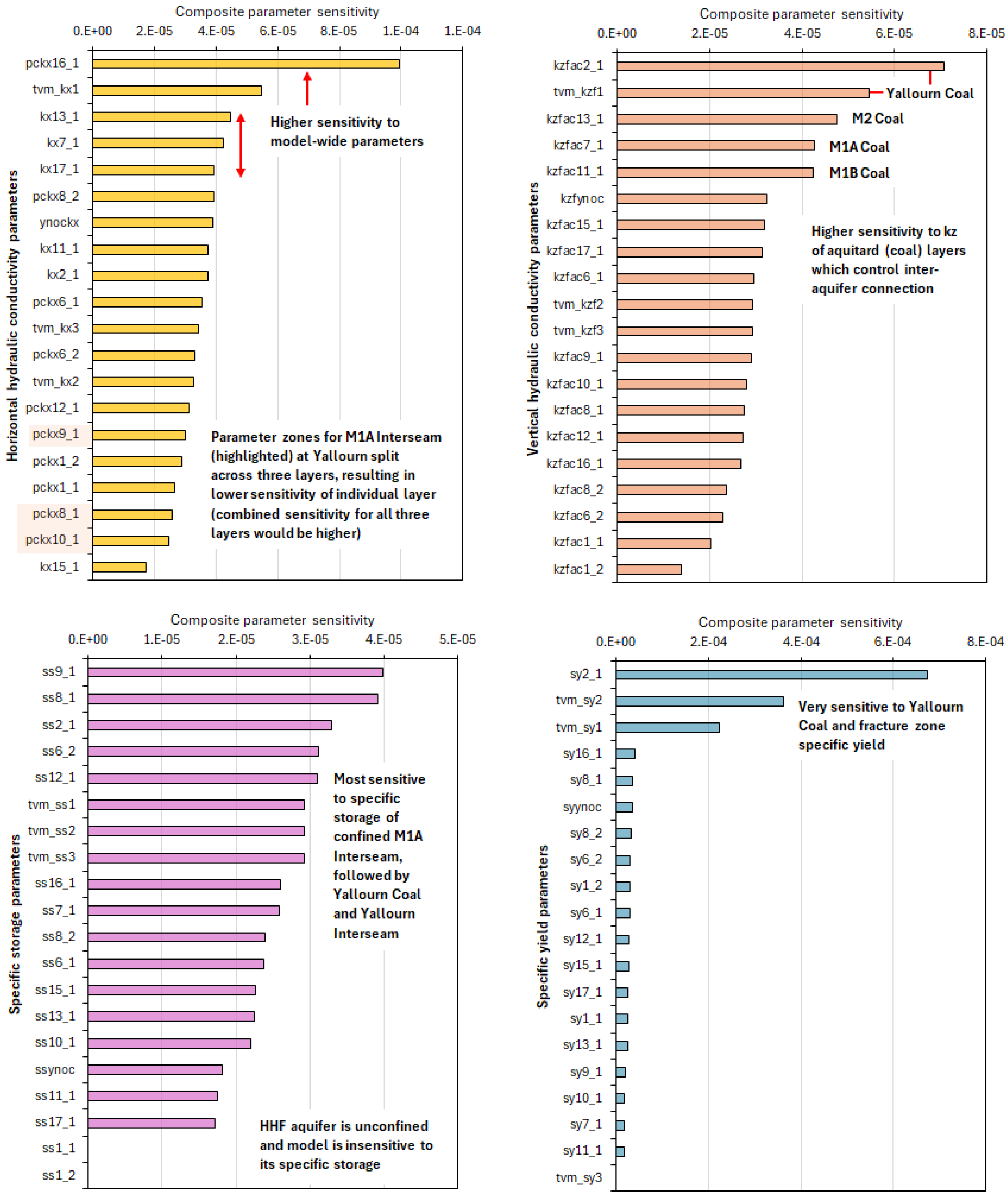

Figure 62 Composite parameter sensitivity by parameter groups

3.2.3 Effects of geological structure

The effects of geological structures such as monoclines, synclines and anticlines are simulated in the model by adjusting the elevation, thickness and extent of the model layers (including pinch out of layers, simulated using inactive cells and vertical pass-through cells). The regionally significant Haunted Hills Fault/Yallourn Monocline is represented by the steep elevation changes of model layers and the termination (pinch out) of model layers where they are truncated by the fault (see cross-sections 2 and 3 in Figure 9 and Figure 10). Although the reduced layer thickness and elevation changes restrict the flow of groundwater, the continuity of model layers across the fault in some places (e.g. where the confined aquifers appear in the YNOC) results in excess drainage and depressurisation of the aquifers to the north of the fault. To simulate the compartmentalisation effect of the fault more accurately, horizontal flow barriers (HFBs) have been incorporated into model layers 2 to 16 (from below the Haunted Hills Formation to the top of the Basement) as vertically continuous features.

The effect of the HFBs is demonstrated in this section by comparing the hydrographs of bores located to the north of the fault and in the Moe Swamp Basin, when the HFBs are included and removed. Figure 63 shows that a large area of the YNOC is drained when the HFBs are excluded (indicated by dry cells), with the hydrographs showing excess lowering of the groundwater levels. When the HFBs are incorporated, the flow barrier effect of the fault is more accurately simulated and the modelled groundwater levels are maintained higher, consistent with the observed groundwater levels. Similarly, Figure 64 shows the aquifer depressurisation effect extending into the Moe Swamp Basin when the HFBs are removed, causing the modelled groundwater level to decline at the regional bores constructed within the deeper M2 Interseam.

The Haunted Hills Fault has been conceptualised in the literature as an effective flow barrier (Brumley and Holgate, 1983), consistent with the expectation that faults in the Gippsland Basin generally act as flow barriers (Schaeffer, 2008; Underschultz et al, 2006). The model calibration to the long term monitoring data, both near the Yallourn Mine and regionally in the Moe Swamp Basin, supports this conceptualisation, with the explicit representation of the flow barrier necessary to adequately simulate the hydrogeological effect of this major fault.

As presented in Figure 20, the fault line interpreted by EAY deviates from the fault line delineated by GHD as part of a preliminary seismicity assessment (GHD, 2023c). The location of the HFBs assigned to the model follows the fault line of EAY more closely and is based on the simulated barrier effects on the groundwater levels (compared against the observed values). Figure 65 focuses on the area north of Township Field where the two interpreted fault lines deviate. The modelled hydrographs show the barrier effect is necessary at the location of the HFBs to maintain the groundwater levels elevated at the selected bores (close to their observed values), which is not possible when the HFBs are removed or pushed further to the north. Given the complexity of faulting, it is possible that the different interpretations of fault line reflect the compartmentalised nature of the fault zone where there may be more than one fault/displacement. The HFBs are a practical means of simulating the hydrogeological effects of such complex zones, by introducing resistance to flow based on the observed groundwater levels.

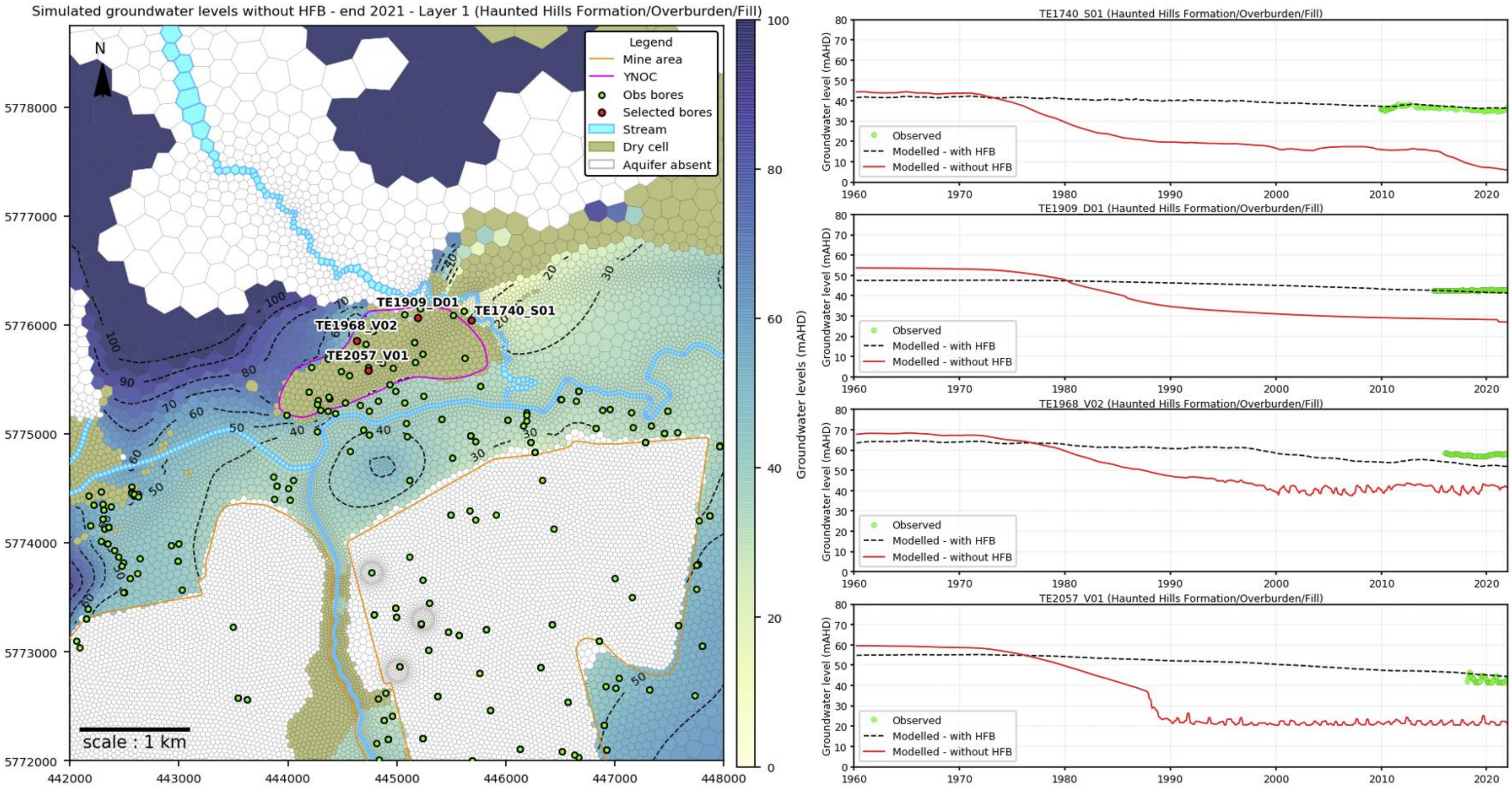

Figure 63 *Horizontal flow barrier effect - YNOC*

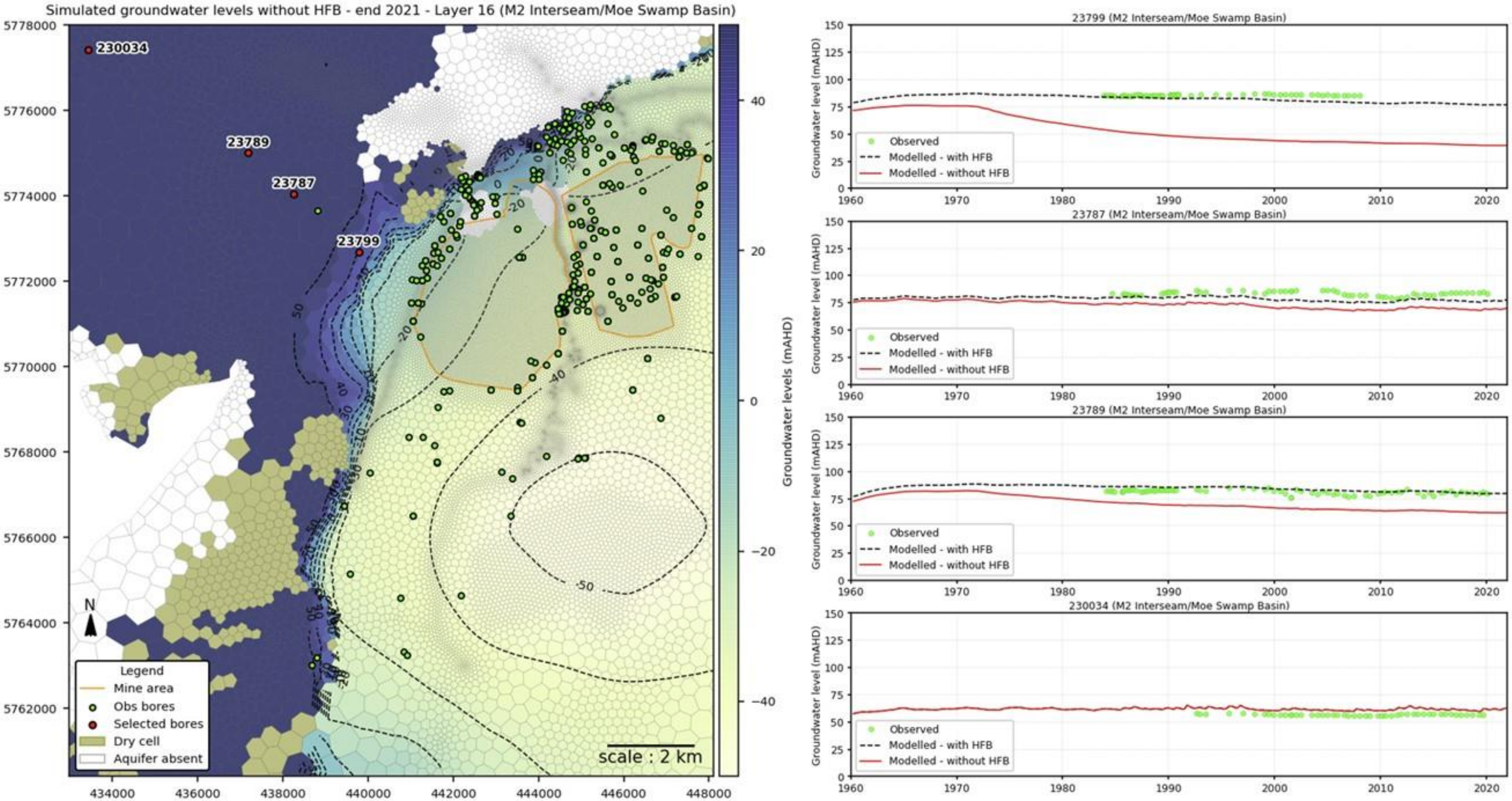

Figure 64 *Horizontal flow barrier effect – Moe Swamp Basin*

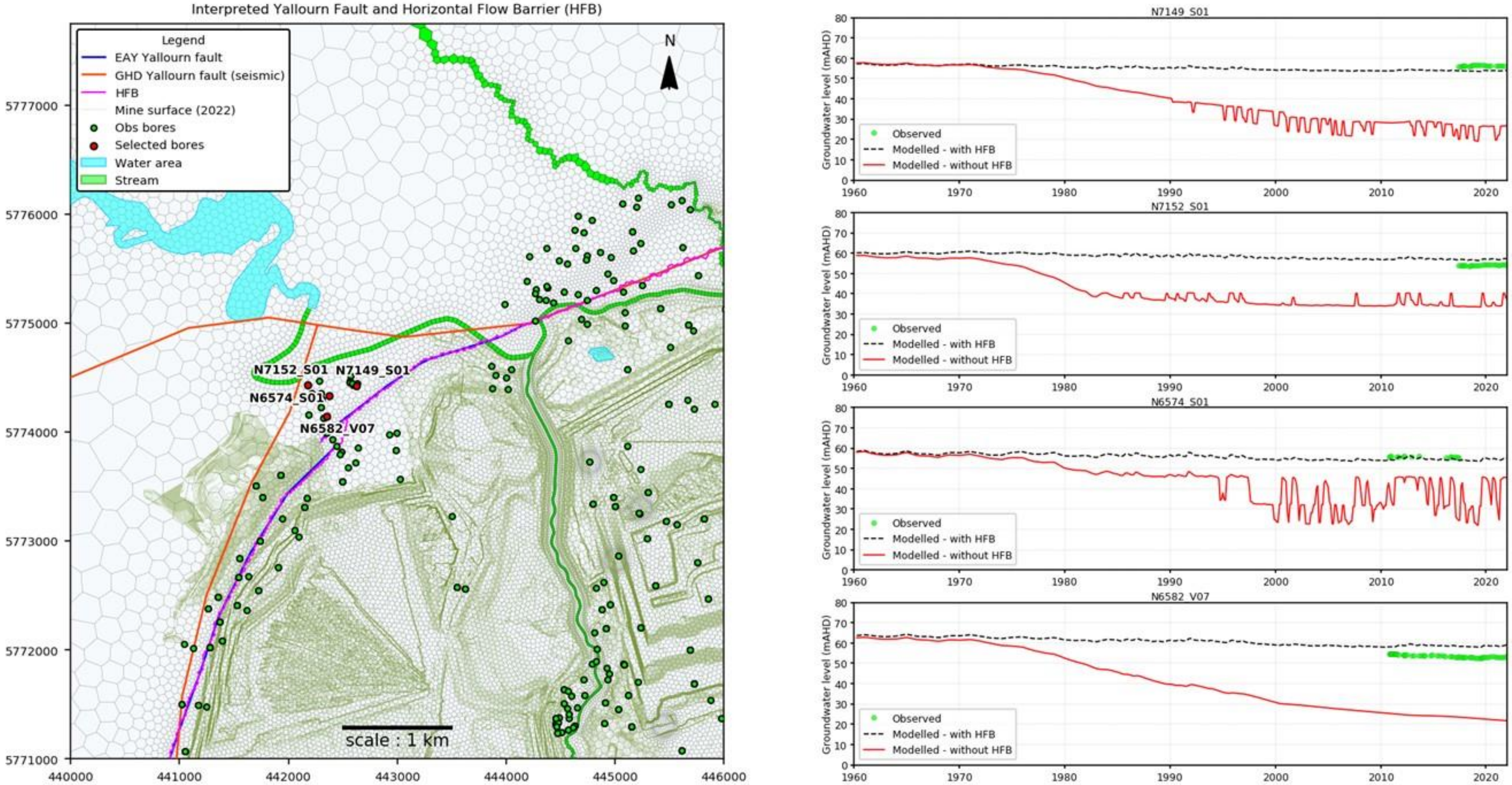

Figure 65 *Horizontal flow barrier effect – interpreted fault lines and modelled HFB*

4. Model verification

4.1 Verification approach

The AGMG describes verification as a process of comparing the predictions of the calibrated model to a set of measurements that were not used to calibrate the model, so the model's use as a predictive tool can be verified. The AGMG recognises that verification should only be attempted where a large quantity of calibration data is available and it is possible to set aside a number of observations for later verification (without compromising the quality of calibration by not making full use of all available data for calibration).

The groundwater model for the Yallourn Mine has been calibrated to the end of 2021. By the time the calibration was completed, an additional two years of groundwater level monitoring data had been collected (from 2022 to end of 2023). This enabled short term verification of the calibrated model to be undertaken, by extending the model simulation for additional two years using the climate, mining and pumping data from 2022 to end 2023 and comparing the modelled groundwater levels against those measured in selected monitoring bores where additional data are available.

Verification, as described in this section, applies only within the context of historical conditions and observations used to calibrate the model i.e. the capability of the model to predict ongoing effects of mining and climate, similar to the hydrogeological stresses that have occurred in the past. Given the ultimate purpose of the model is to make predictions of the mine rehabilitation effects, a true verification of model's capability to meet this objective would not be possible until the mine rehabilitation commences and relevant hydrogeological data become available.

4.2 Verification results

A scatter plot of the computed and observed groundwater levels (heads) for the two-year verification period is shown below, based on 6,061 head observations from 341 bores. The calibration statistics are similar to those of the calibration period, with a slight reduction in the key statistical measures e.g. the SRMS error for the verification period, based on a much smaller number of observations, is 6.17 %, compared to the 6.61 % SRMS error from the calibration period. The similarity in the quality of calibration is further demonstrated by comparing the modelled and observed hydrographs from selected key bores in each aquifer unit   The observed groundwater levels from the verification period are shown in red.

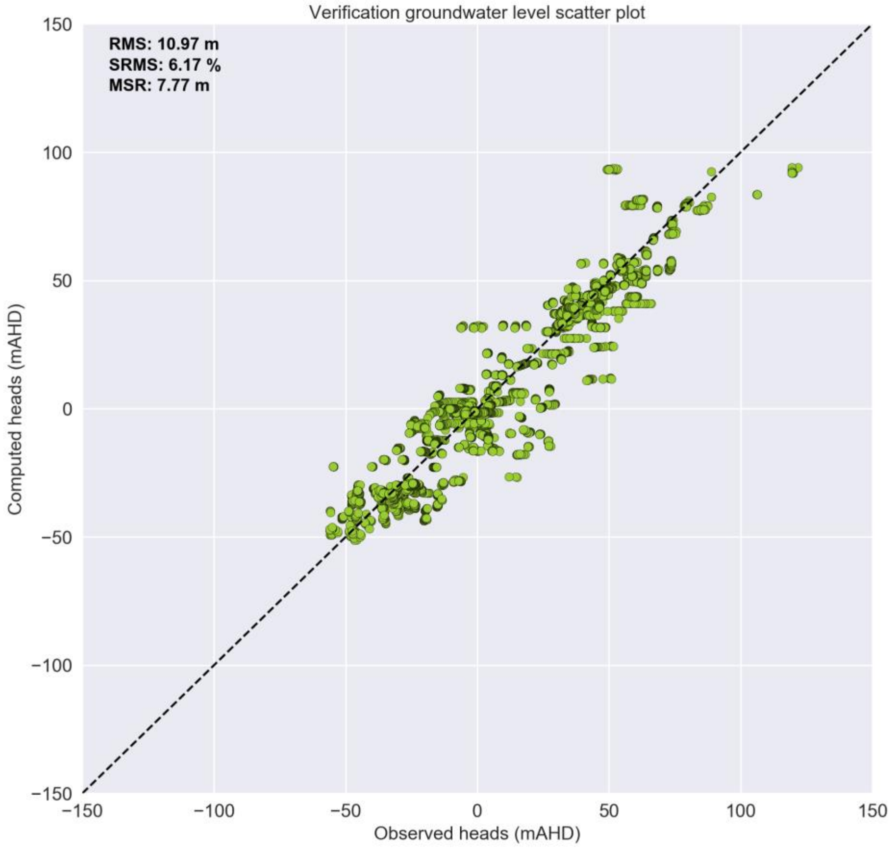

Figure 66 ***Scatter plot (verification) – groundwater levels***

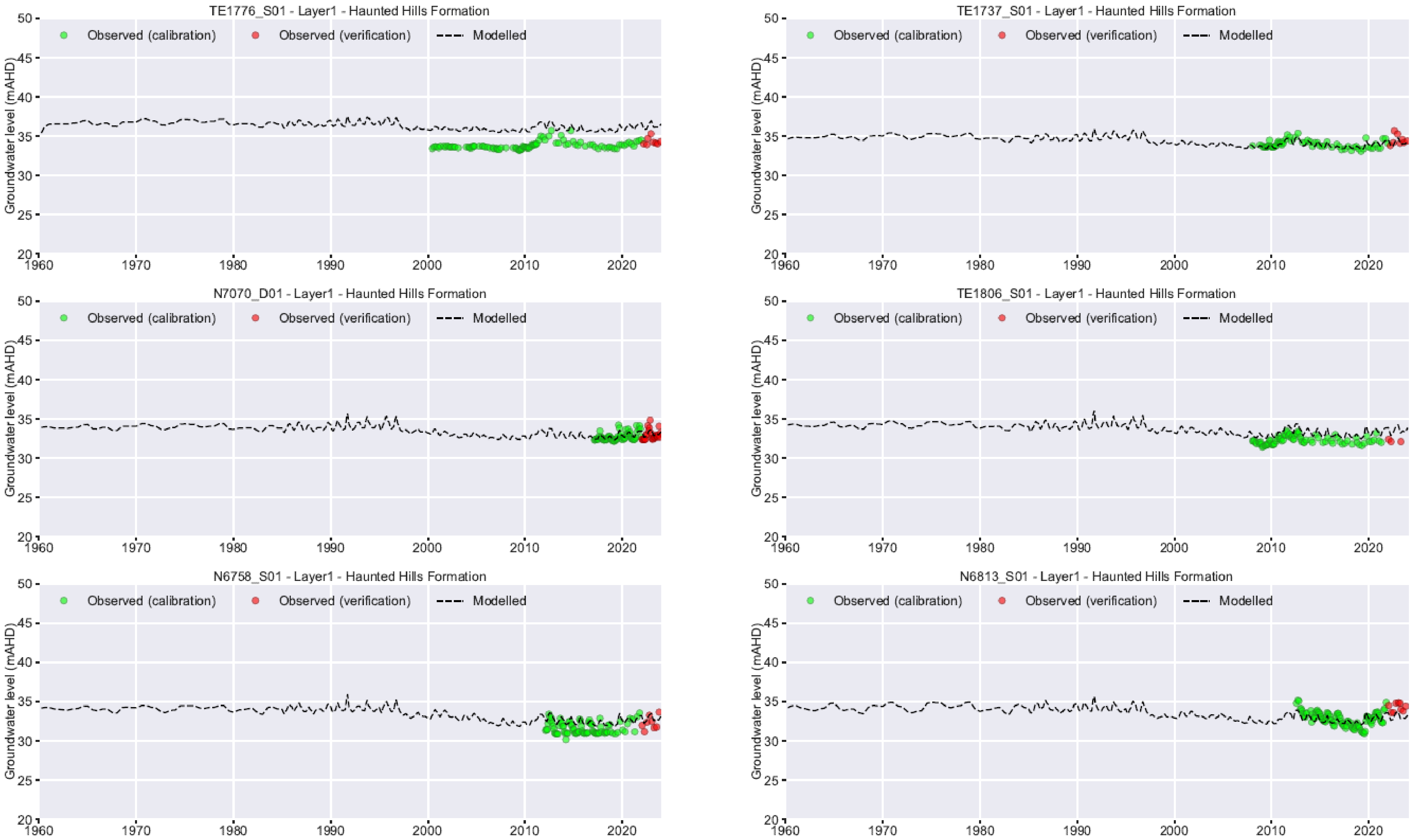

Figure 67 Verification hydrographs – Haunted Hills Formation (adjacent to Latrobe River)

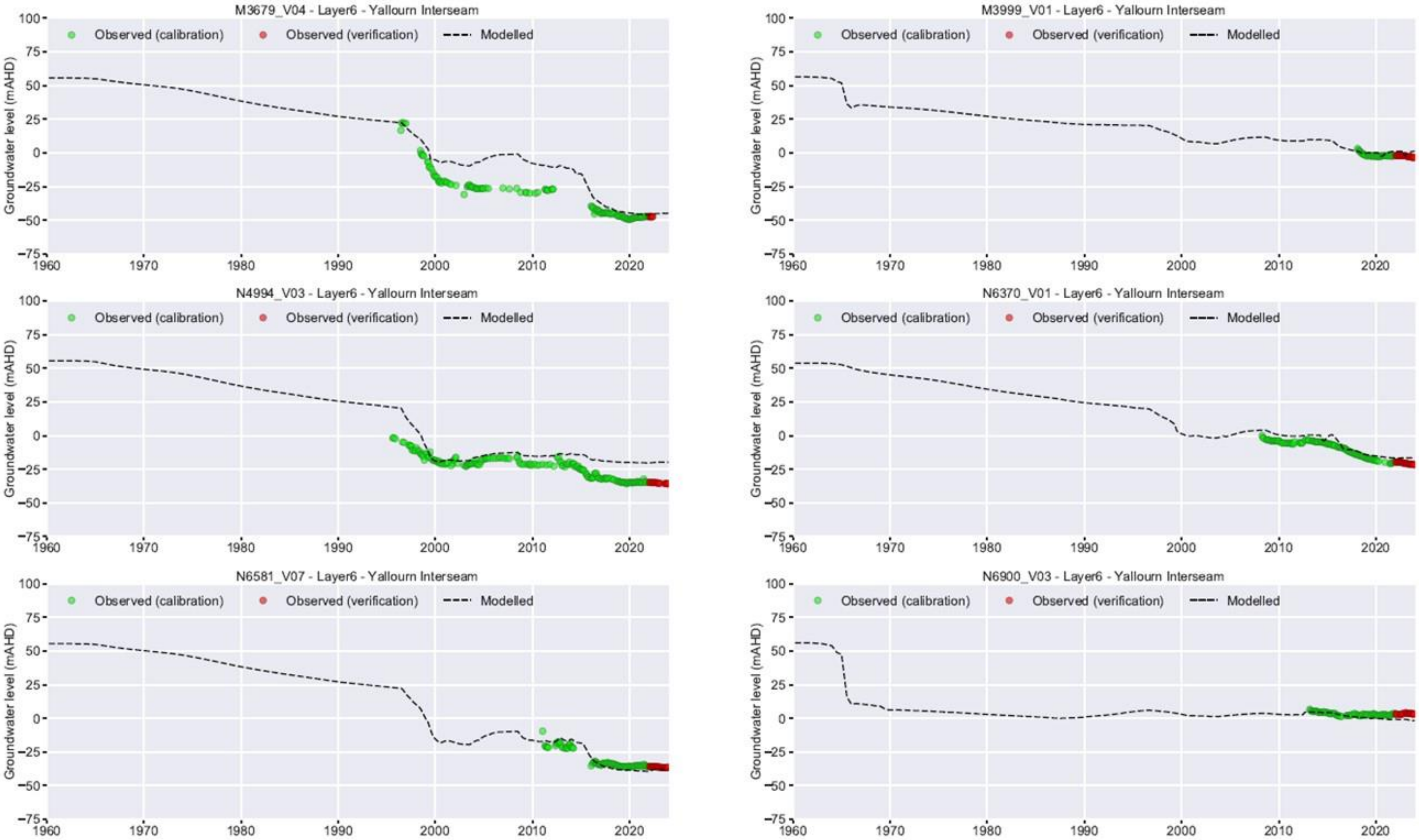

Figure 68 *Verification hydrographs – Yallourn Interseam*

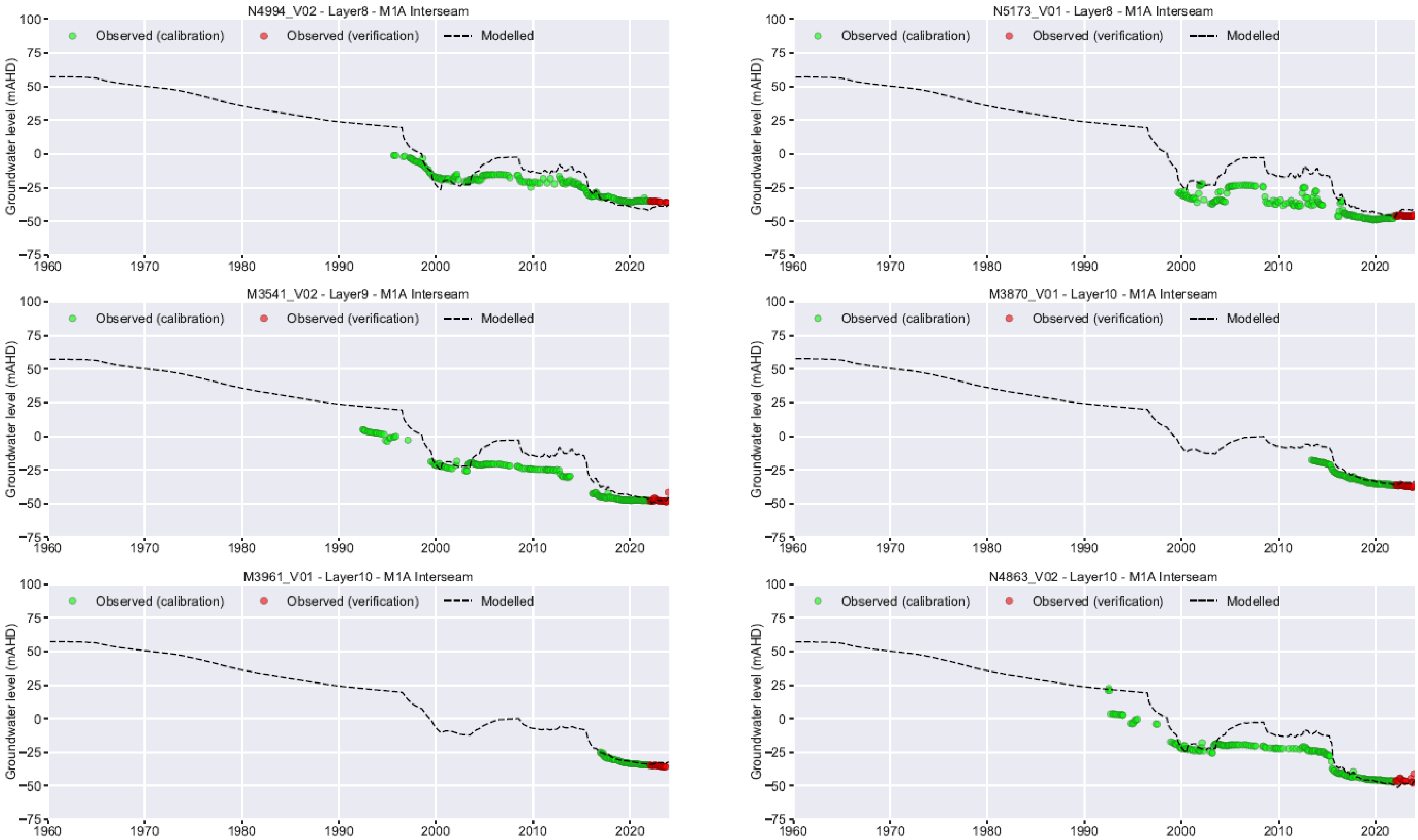

Figure 69 Verification hydrographs – M1A Interseam

5. Conclusions

5.1 Summary of key outcomes

The key outcomes of the design, construction and calibration of the numerical groundwater model developed for the Yallourn Mine rehabilitation project are summarised as follows:

– The groundwater modelling for the rehabilitation planning and subsequent implementation is required to simulate mine-scale processes (e.g. formation of a future pit lake) as well as regional scale processes (e.g. the cumulative effect of aquifer depressurisation within the Latrobe Valley), necessitating a model domain that covers a large spatial extent with a locally refined grid that provides accuracy in areas of interest. The level of refinement introduced into the model grid must be balanced by the need to maintain a sensible model size (and ultimately model run times to meet the needs of run intensive procedures such as calibration and uncertainty analysis). This has been achieved by harnessing the unstructured gridding capability of the USG-Transport code and making use of the outputs from the existing Latrobe Valley Regional Groundwater Model (LVRGM) to simulate the aquifer depressurisation effects from the neighbouring Hazelwood and Loy Yang mines in an efficient manner. The model domain covers an area of 774.4 km^2 and the total number of cells within a 2d unstructured grid is 38,981.

– In order to accurately simulate the complex hydrostratigraphy, a Leapfrog geological model has been developed for the entire model domain. The process of developing the surfaces of the Leapfrog model has been highly iterative and technically challenging, requiring the geological contacts from different data sources, resolution and accuracy to be integrated and verified against representative borehole logs. This required matching and merging the surfaces from the detailed mine scale models of the Yallourn and Hazelwood mines (as represented in the LVRGM) across model boundaries and extrapolating these across the broader area of the model using the surfaces from the Latrobe Valley Coal Model and ultimately the Victorian Aquifer Framework. The Haunted Hills Fault/Yallourn Monocline has been simulated by incorporating steep elevation changes across the fault and the Thorpdale Volcanics has been simulated as an intrusive feature that cuts across geological surfaces.

– The surfaces of the hydrostratigraphic units from the Leapfrog model have been used to define the extent and elevation of the USG-Transport model layers. The Yallourn Coal and M1A Interseam have been split into multiple model layers to improve numerical accuracy in the vertical direction, resulting in a model with a total of 17 layers and 662,677 cells. A vertical pass-through approach is used to by-pass inactive cells (to simulate pinch out of model layers) and improve numerical accuracy, resulting in a total of 457,973 active cells.

– The model boundary conditions used to simulate the effects of mining and hydrological processes include the drains (mine progression), wells (pumping), general heads (aquifer though-flow), rivers (water features) and streams (major rivers and creeks). The aquifer depressurisation effects associated with the Hazelwood and Loy Yang mines have been simulated by extracting the modelled heads from the LVRGM and incorporating these into the USG-Transport model as head-dependent flux boundary conditions (drain and general head boundaries). This enabled the regionally significant aquifer depressurisation effect to be simulated efficiently without having to explicitly model the complex excavation and pumping regimes of these mines, allowing the modelling effort to be directed at the processes critical for the Yallourn Mine.

– Precipitation Runoff Modelling System (PRMS) is used to derive hydrologically sensible recharge and evapotranspiration, which are interpolated to the unstructured grid of the USG-Transport model. The PRMS model also computes runoff, which is apportioned to the stream segments of the USG-Transport model to enable total stream flow and variable stream stage to be simulated by the stream boundary condition (allowing realistic interactions between the surface water and groundwater systems). The PRMS and USG-Transport models have been coupled and successfully incorporated into the automated calibration workflow, enabling recharge, evapotranspiration and runoff to be calibrated based on the response simulated in the groundwater model.

- The aquifer layers (interseams) in the model have been parameterised using the percentage sand grids, consistent with the LVRGM. This approach allows spatial variability in hydraulic conductivity to be incorporated in an efficient manner, consistent with the geological data. Testing during calibration indicated that alternative parameterisation approaches, using pilot points, did not materially improve the model calibration compared to the more efficient approach using the percentage sand grids. The material properties of the Yallourn Coal layers have been modified using the Time-Variant Materials package of the USG-Trasport code to simulate the effect of fracturing due to ground movement and the placement of internal overburden dumps as mining progressed. This is simulated over time using discrete zones, resulting in the model simulating abrupt changes to groundwater levels when the material property changes are activated. This effect is temporary and the modelled groundwater levels are generally restored as the groundwater system adjusts to the changed material properties.
- The model calibration has been undertaken using a combination of manual and automated methods. The rigorous automated calibration procedure has been completed using PEST_HP, a highly parallelised version of the parameter estimation code PEST. The USG-Transport groundwater model has been calibrated to 34,778 absolute head targets from 471 bores/piezometers and other head targets derived from these, such as head difference/change (34,872) and vertical head difference (1,858) targets. The targets used to constrain the surface water-groundwater interactions included 356 stream stage targets at four stream gauges and 279 flow targets at three gauges. Additionally, outflows from the drain cells assigned to the Hazelwood Mine have been calibrated against the net pumping rates to ensure the drain outflow and adopted material properties are consistent with the measured pumping rates.
- The USG-Transport model is generally well calibrated to shallow groundwater levels measured at bores in the Haunted Hills Formation, both spatially and over time. The hydrographs of the modelled and observed groundwater levels near the Latrobe River show close agreement, enabled by the accurate simulation of the river stage and shallow groundwater dynamics using the coupled PRMS and USG-Transport modelling approach. This occurs to the north of the East Field northern batters, which is an area of focus for the rehabilitation planning due to the potential for the future pit lake to locally increase the shallow groundwater level and discharge of groundwater (baseflow) to the river.
- The USG-Transport model is also able to adequately replicate the aquifer depressurisation effect observed in the confined M1A Interseam, although the model overestimates the temporary aquifer pressure rebound that was observed during a period of reduced pumping rate (particularly between 2004 and 2008). The limited rebound observed in the monitoring data is somewhat inconsistent with a typical radial flow behaviour expected towards pumping bores and may reflect a local compartmentalisation effect within the M1A Interseam aquifer (material property variability not reflected in the percentage sand grids) or gaps in the pumping record (such as incomplete artesian flow record, leading to underestimate of the actual pumping rates).
- The groundwater levels observed in the Yallourn Interseam and Yallourn Coal are variable due to the effects of pressure relief from the mining of coal and depressurisation of the M1A Interseam from below, as well as material property changes such as coal fracturing and overburden placement. The USG-Transport model is generally capable of simulating the observed trends and matches the absolute groundwater levels well in some locations (e.g. adjacent to the Fire Service Pond and near the pumping bores). The model underestimates the Yallourn Interseam groundwater levels measured in the area of the historical failure and river realignment fill (in the East Field northern batters), which could be due to the localised influence of the changed material properties in the Yallourn Coal that are difficult to accurately simulate. Further work is required to ascertain the cause of the locally elevated groundwater levels and material property changes required by the model to simulate the observed groundwater levels. This limitation does not affect the model's ability to match the shallow groundwater levels in the overlying Haunted Hills Formation, where some of the best calibration has been achieved along the Latrobe River.
- The groundwater levels measured in regional bores constructed within the deep M2 Interseam are sensitive to the regionally extensive aquifer depressurisation effects from the Hazelwood and Loy Yang mines. These are well replicated by the USG-Transport model based on the head-dependent flux boundary conditions used to efficiently simulate the regional aquifer pressure changes. Horizontal Flow Barriers (HFBs) have been assigned along the Haunted Hills Fault/Yallourn Monocline to simulate the flow barrier effect of the fault, based on the groundwater levels observed in the bores located to the north of the fault (in the YNOC and into the Moe Swamp Basin).

- There is generally good agreement between the observed and modelled stream targets (flow and stage) at key stream gauges. The typical difference between the observed and modelled stream stage is around 0.25 m, with the difference reducing to less than 0.05 m at the MRD Northern Crossing gauge (since 2014). The Scaled Root Mean Squared (SRMS) error for the stream stage and flow targets is 2.54 % and 3.75 % respectively. For the groundwater level targets, the SRMS error is 6.61 % (albeit based on a much larger dataset than the stream flow and stage targets).
- The simulated groundwater seepage from the Yallourn Coal is broadly consistent with the estimated horizontal drain flows from 2011 to 2016, typically in the range of 0.4 to 0.6 giga litres (GL) per year. The total simulated groundwater seepage rate is typically in the range of 2 to 4 GL/year, which would account for around half of the surplus water generated at the mine (based on the mine water balance). This is considered reasonable, with the remaining half of the surplus mine water likely to be derived from the ex-pit and in-pit runoff.
- The calibrated recharge rates, on a model wide basis, are generally consistent with the Victorian Government's ecoMarkets recharge rates (equating to about 9.8 % of rainfall on average), albeit with some differences in their spatial distributions. An area of low recharge has been simulated to the west of the Hazelwood Mine in the subcropping zone of the confined aquifers, consistent with the prior modelling experience with the LVRGM.
- The average calibrated horizontal hydraulic conductivity of the key aquifer units within the Yallourn Mine area is 2.9 m/d for the Haunted Hills Formation (layer 1), 0.014 m/d for the Yallourn Interseam (layer 6) and 0.4 to 1.4 m/d for the M1A Interseam (layers 8,9 and 10). The maximum calibrated horizontal hydraulic conductivity is 7 m/d for the Haunted Hills Formation and 12.7 m/d for the M1A Interseam, which are similar to the estimates derived from aquifer testing of the sand intervals (4 to 8 m/d for the Haunted Hills Formation and 8 to 15 m/d for the M1A Interseam). The calibrated horizontal hydraulic conductivity of the in-situ (undisturbed) Yallourn Coal is 4.3 x 10^{-5} m/d, which is within the range of literature derived values for intact coal. For the highly fractured zone in the coal batters and along the floor of the mine, the calibrated value is 7 x 10^{-3} m/d (around two orders of the magnitude higher). This is towards the lower end of the range of values derived from packer testing but higher than the range of values derived from the laboratory analysis of core samples (from the East Field northern batters). The moderately fractured zone has been assigned a calibrated horizontal hydraulic conductivity value of 7 x 10^{-4} m/d (average of the two adjacent zones). The calibrated vertical hydraulic conductivity of the Haunted Hills Formation and interseam layers is 2 to 3 orders of magnitude lower than the horizontal hydraulic conductivity, reflecting the influence of clay, silt and coal interbeds that reduce the hydraulic conductivities in the vertical direction. For the Yallourn Interseam, the vertical hydraulic conductivities derived from laboratory analysis of core samples are towards the lower end of the calibrated range of hydraulic conductivity.
- A short-term verification of the calibrated USG-Transport model has been undertaken using 6,061 groundwater level observations from 341 bores collected in 2022 and 2023. The SRMS error for the verification period is 6.17 %, similar to the 6.61 % SRMS error from the long term calibration period.

5.2 Confidence level classification

The proposed rehabilitation of the Yallourn Mine involves turning the mine void into a full pit lake, within ongoing pumping required during filling to maintain a safe rehabilitation condition. The magnitude of future hydrological stresses is therefore expected to be similar to that of the historical stresses, with the predictive modelling of the future rehabilitation scenarios required over a period of time similar to the period of historical observations (length of calibration). This, combined with an acceptable level of calibration with respect to a range of observations and very low mass balance errors, suggests that the model developed of the Yallourn Mine satisfies some of the key attributes of the Class 3 (the highest) confidence level classification of the AGMG. It should be noted, however, that there are some recognised limitations with the model and model predictions will carry an element of uncertainty particularly with respect to the formation of a full pit lake, given the interaction between the groundwater and future lake systems (above the water levels of the existing in-pit water features) can only be estimated by the model based on the available historical dataset used in calibration. In this context, a confidence level classification of 2 with some attributes of 3, indicating moderate to high confidence level, is considered appropriate as per the target confidence level discussed in Section 1.3.2.

The uncertainty analysis guideline recently updated by the IESC suggests the confidence level classification of the AGMG should be replaced by more effective uncertainty analysis techniques (Peeters and Middlemis, 2023). A detailed uncertainty analysis is part of the future modelling scope, where the model parameter uncertainty will be explored in the context of the proposed rehabilitation strategy.

6. References

Barnett, B, Townley, LR, Post ,V, Evans, RE, Hunt, RJ, Peeters, L., Richardson, S, Werner, AD, Knapton, A, and Boronkay, A., 2012. Australian Groundwater Modelling Guidelines, National Water Commission, Waterlines Report Series No. 82 June 2012 ISBN: 978-1-921853-91-3 (online)

Baumgartl T, 2020. Batter Stability Project Report, CRICOS Provider No. 00103D | RTO Code 4909

Brown A., 1970. Insitu Permeability Test Morwell Open Cut, SEC Report DD12, July 1970

Brumley, JC and Holdgate, GR., 1983. An Assessment of the Confined Groundwater Resources of the Moe Swamp Basin Victoria, Australia. Paper International Conference on Groundwater and Man, Sydney, 1983

Department of Environment, Land, Water and Planning (DELWP), 2012. VicMap Regional Land Use and Statewide DEM, VicMaps GIS Datasets

Department of Environment, Land, Water and Planning (DELWP), 2017. Victorian Aquifer Framework (VAF) Secure Allocation Future Entitlements (SAFE) project data

Doherty, J., 2016a. PEST. Model-Independent Parameterisation. User Manual Part I: PEST, SENSAN and Global Optimisers. Brisbane : Watermark Numerical Computing, 2016

Doherty, J., 2016b. PEST. Model-Independent Parameterisation. User Manual Part II: PEST Utility Support Software. Brisbane : Watermark Numerical Computing., 2016

Doherty, J., 2016c. Groundwater Data Utilities. Part B: Program Descriptions. Brisbane : Watermark Numerical Computing., 2016

Doherty, J., 2016d. Groundwater Data Utilities. Part C: Programs Written for Unstructured Grid Models. Brisbane : Watermark Numerical Computing., 2016

Doherty, J., 2017. PEST_HP. PEST for Highly Parallelized Computing Environments. Watermark Numerical Computing, 2017

Geo Eng, 1992. Overburden dewatering (eastern area). Results of investigations and proposed dewatering strategy. Report to Yallourn East Field. June 1992

GHD, 2010b. West Gippsland CMA Groundwater Model. Transient model development report. Report for the Dept. of Sustainability and Environment, Victoria

GHD, 2013a, Baseflow Estimation Method Pilot Trial: Characterising Groundwater Contribution to Baseflow Dependent Waterways. prepared for Department of Sustainability and Environment.

GHD, 2013b, Groundwater Assessment – Baseflow Dependent Rivers: Characterising Baseflow Contribution to Baseflow Dependent Waterways. Prepared for Department of Environment and Primary Industries

GHD, 2023a. Numerical Groundwater Model: Design Basis Memorandum. Prepared for EnergyAustralia Yallourn, 28 July 2023

GHD, 2023b. Yallourn Rehabilitation Hydrogeological modelling: Hydrogeological Conceptual Model. Prepared for EnergyAustralia Yallourn

GHD, 2023c. Yallourn Rehabilitation: Mine Pit Lake Triggered Seismicity Preliminary Assessment. Prepared for EnergyAustralia Yallourn. Draft

GHD, 2024. Core permeability test results. A letter to EnergyAustralia Yallourn. December 2024

Henson, W.R., Medina, R.L., Mayers, C.J., Niswonger, R.G., and Regan. R.S., 2013. CRT—Cascade Routing Tool to Define and Visualize Flow Paths for Grid-Based Watershed Models. U.S. Geological Survey Techniques and Methods 6-D2, 28 p.

Holgate, G., Barton, C., and Galiberti, A., 1979. Notes on aspects of the overburden geology and hydrogeology over the Yallourn East Field. Exploration and Geology Division, Fuel Department. March 1979

HydroAlgorithmics, 2020. AlgoMesh 2 User Guide de Kretser,D., Matthews,B., and Williams,M., 2002. CFD program helps improve water velocity in wastewater lagoon. In: WaterWorld. https://www.waterworld.com/wastewater-treatment/article/16201415/cfd-program-helps-improve-water-velocity-in-wastewater-lagoon

Langevin, C.D., Hughes, J.D., Provost, A.M., Banta, E.R., Niswonger, R.G., and Panday, S., 2017. Documentation for the MODFLOW 6 Groundwater Flow (GWF) Model: U.S. Geological Survey Techniques and Methods, book 6, chap. A55, 197 p., accessed August 4, 2017

Littleboy, M., Silburn, D.M., Freebairn, D.M., Woodruff, D.R. and Hammer, G.L.,1989. PERFECT: A simulation model of Productivity, Erosion, Runoff Functions to Evaluate Conservation Techniques. Queensland Department of Primary Industries, Bulletin QB89005,135pp.

Markstrom, S.L., Regan, R.S., Hay, L.E., Viger, R.J., Webb, R.M.T., Payn, R.A., and LaFontaine, J.H., 2015. PRMS-IV, the precipitation-runoff modeling system, version 4: U.S. Geological Survey Techniques and Methods, book 6, chap. B7, 158 p.

McKenzie, N.J., Jacquier, D.W., Ashton, L.J., and Cresswell, H.P., 2000. Estimation of Soil Properties Using the Atlas of Australian Soil. CSIRO Land and Water, Technical Report 11/00, February 2000

Niswonger, R.G., Panday, S., and Ibaraki, M., 2011. MODFLOW-NWT, A Newton formulation for MODFLOW-2005: U.S. Geological Survey Techniques and Methods 6–A37, 44 p.

Panday, S., Langevin, C.D., Niswonger, R.G., Ibaraki, M., and Hughes, J., 2013. MODFLOW–USG Version 1: An Unstructured Grid Version of MODFLOW for Simulating Groundwater Flow and Tightly Coupled Processes Using a Control Volume Finite-Difference Formulation. Chapter 45 of Section A, Groundwater Book 6, Modeling Techniques. Techniques and Methods 6–A45.

Panday, S., 2023. USG-Transport Version 2.2.0: Transport and Other Enhancements to MODFLOW-USG, GSI Environmental, August 2023

Parsons Brinckerhoff (PB), 2014. Australian Paper Maryvale Groundwater Audit CARMS #60649-6. 216254B-RPT-001 RevB. June 2014

Peeters LJM and Middlemis, H, 2023. Information Guidelines Explanatory Note: Uncertainty Analysis for Groundwater Modelling. A report prepared for the Independent Expert Scientific Committee on Coal Seam Gas and Large Coal Mining Development through the Department of Climate Change, Energy, the Environment and Water, Commonwealth of Australia, 2023

Rau, G.C., Acworth, T.I., Halloran, L.J.S., Timms, W.A., and Cuthbert, M.O., 2018. Quantifying Compressible Groundwater Storage by Combining Cross-hole Seismic Surveys and Head Response to Atmospheric Tides. Journal of Geophysical Research: Earth Surface 123(8),1910-1930

Schaeffer, J., 2008. Scaling point based aquifer data for developing regional groundwater models: application to the Gippsland groundwater system. PhD thesis, Engineering, Civil and Environmental Engineering, The University of Melbourne

Trollope, D.H., Rosengren, K., and Brown E.T., 1965. The Mechanics of Brown Coal. Geotechnique Vol 15 page 363-86

Underschultz, J.B., W, Freij-Ayoub, Otto, C., 2006. Wealth from Oceans. Falling Water Levels in the Latrobe aquifer, Gippsland Basin. Offshore Aquifer Update, Onshore Fault Seal Analysis, and Preliminary Numerical Simulation of Coastal Subsidence Risk. CSIRO National Research Flagships Report

Appendices

Appendix A

Leapfrog model data extent and thicknesses

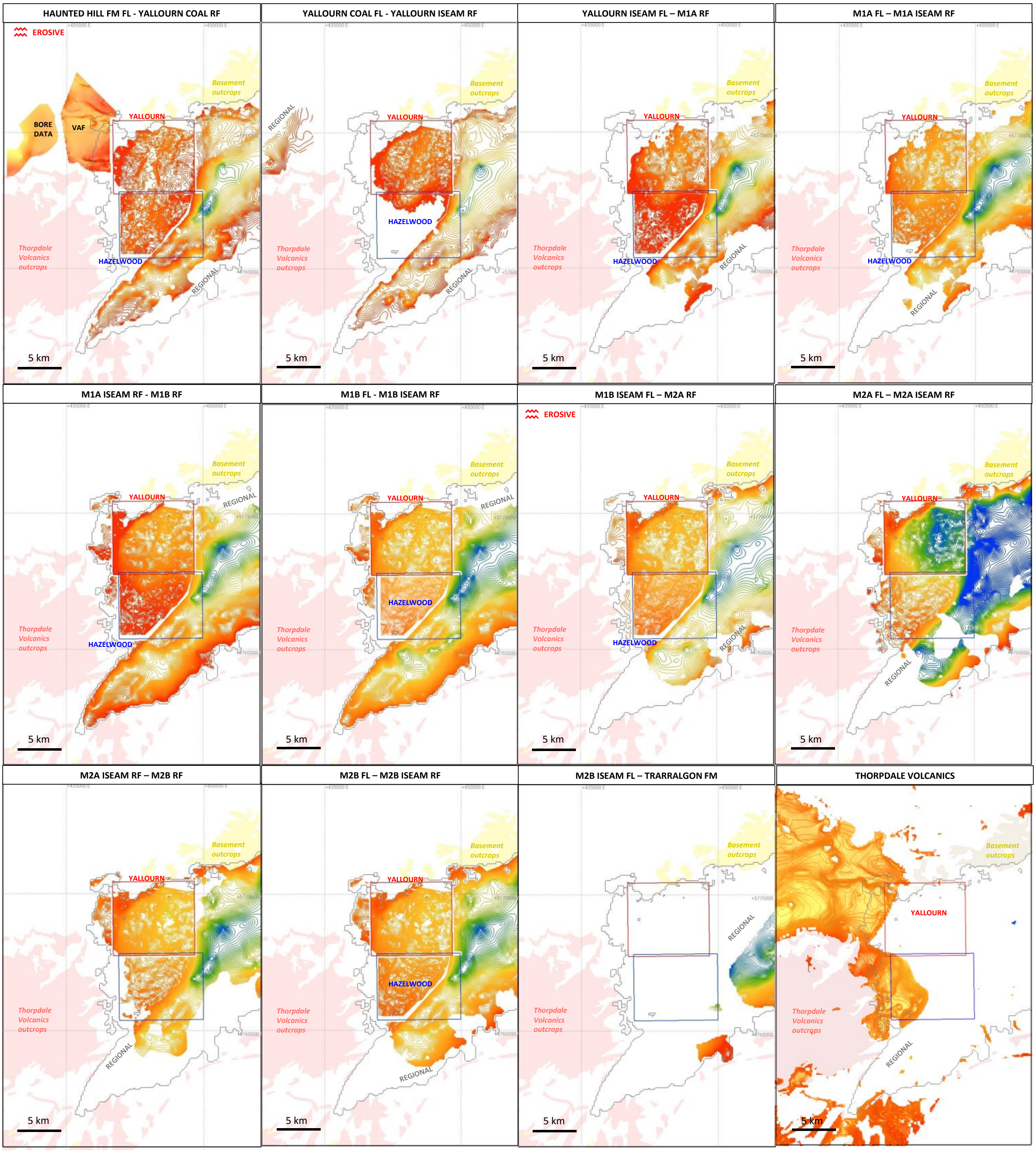

Extent of coverage for each surface modelled

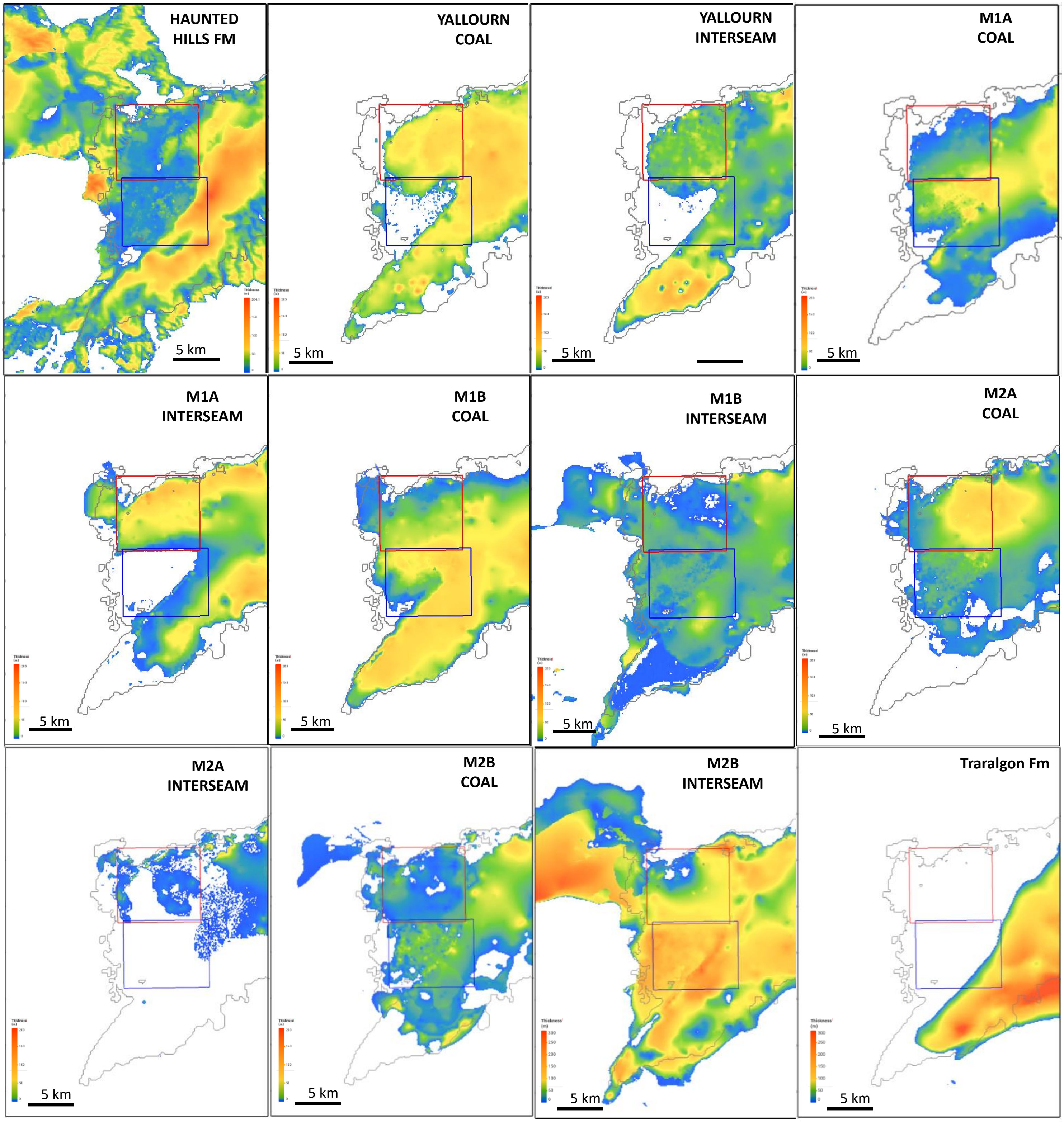

Thickness map of each Leapfrog model layer

Appendix B

Groundwater model layer elevation

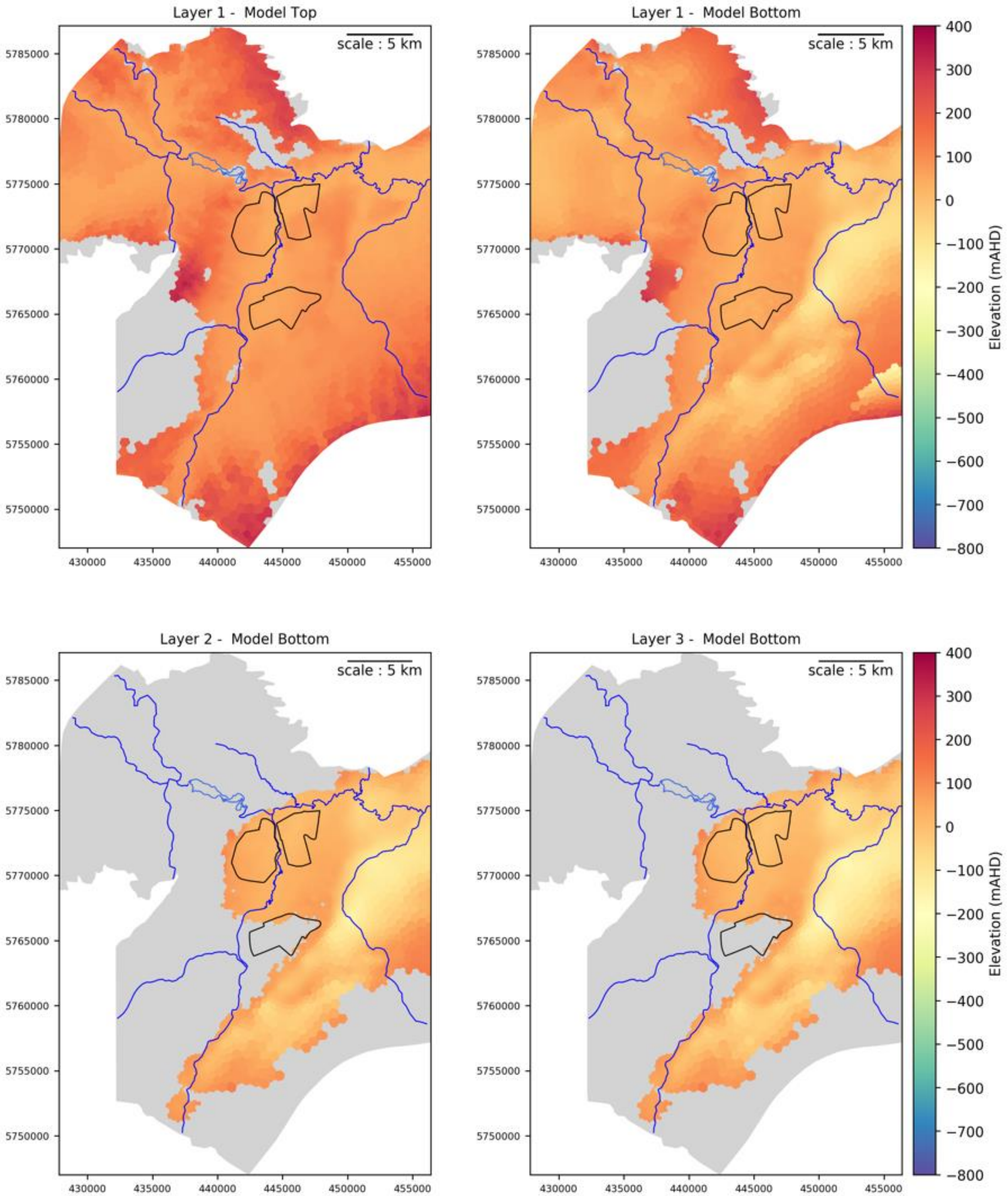
Layer 1 - Model Top
Layer 1 - Model Bottom
Layer 2 - Model Bottom
Layer 3 - Model Bottom
scale : 5 km
5785000
5780000
5775000
5770000
5765000
5760000
5755000
5750000
430000
435000
440000
445000
450000
455000
400
300
200
100
0
−100
−200
−300
−400
−500
−600
−700
−800
Elevation (mAHD)

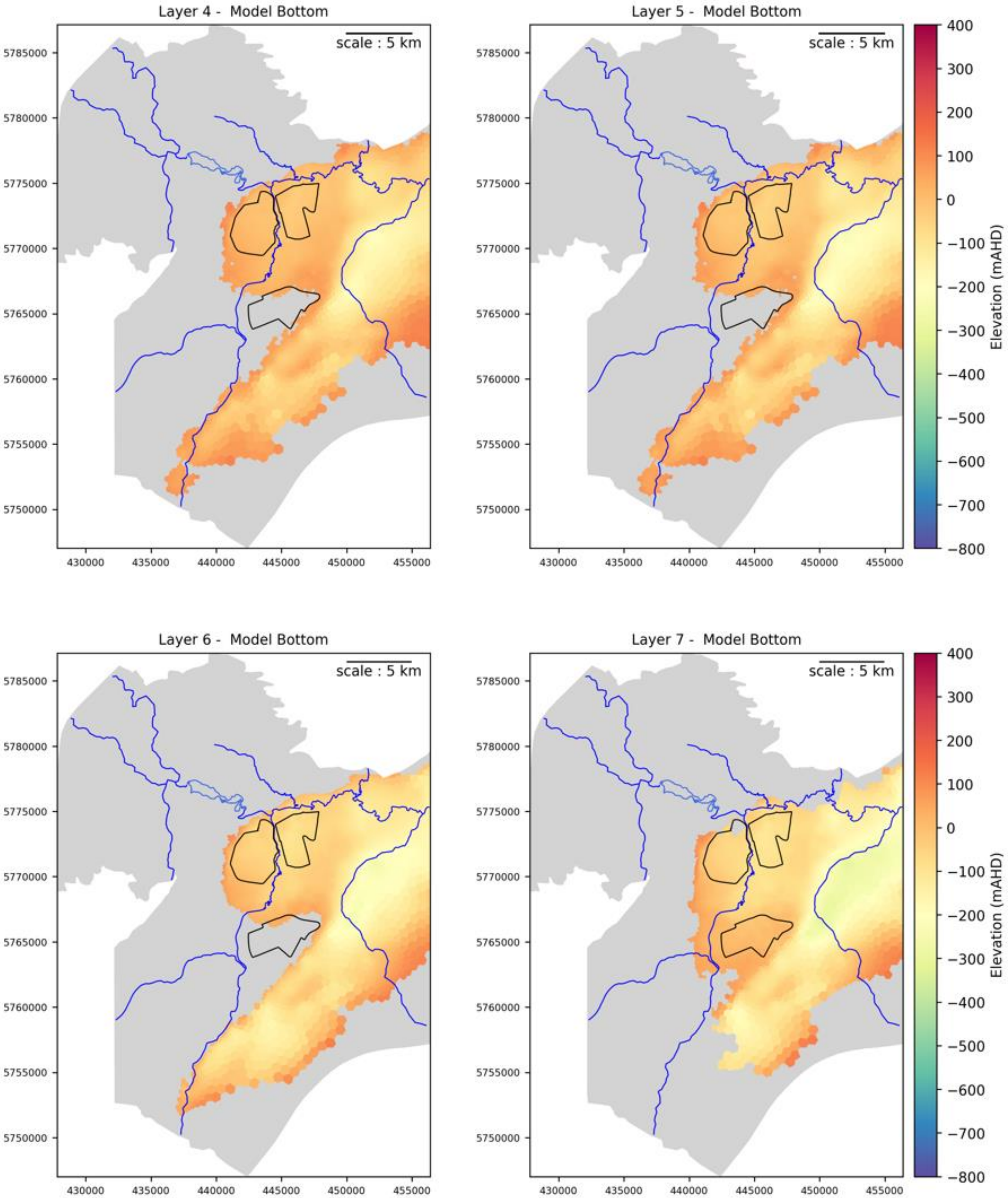
Layer 4 - Model Bottom
Layer 5 - Model Bottom
Layer 6 - Model Bottom
Layer 7 - Model Bottom
scale : 5 km
5785000
5780000
5775000
5770000
5765000
5760000
5755000
5750000
430000
435000
440000
445000
450000
455000
400
300
200
100
0
−100
−200
−300
−400
−500
−600
−700
−800
Elevation (mAHD)

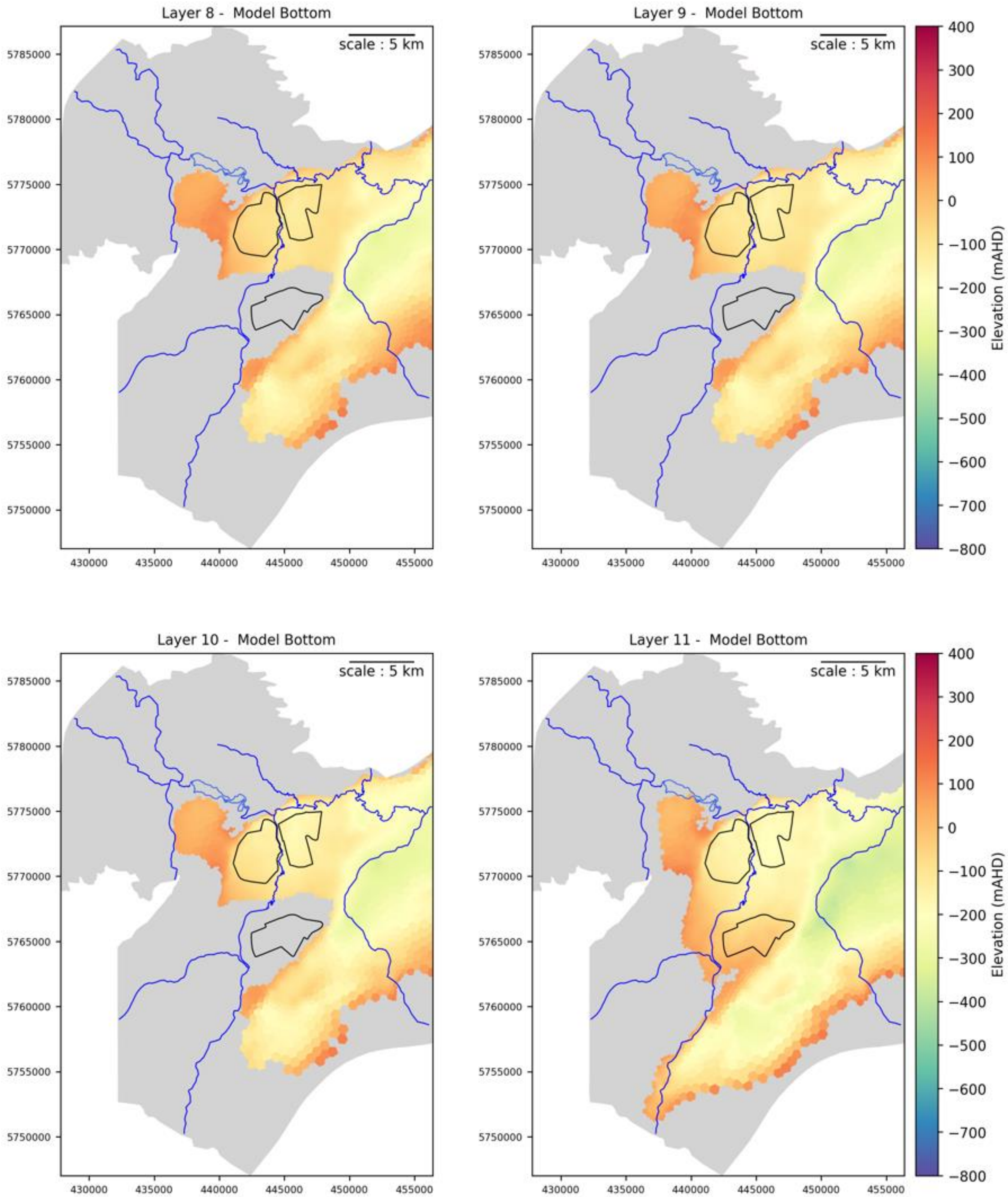
Layer 8 - Model Bottom
Layer 9 - Model Bottom
Layer 10 - Model Bottom
Layer 11 - Model Bottom
scale : 5 km
5785000
5780000
5775000
5770000
5765000
5760000
5755000
5750000
430000
435000
440000
445000
450000
455000
400
300
200
100
0
−100
−200
−300
−400
−500
−600
−700
−800
Elevation (mAHD)

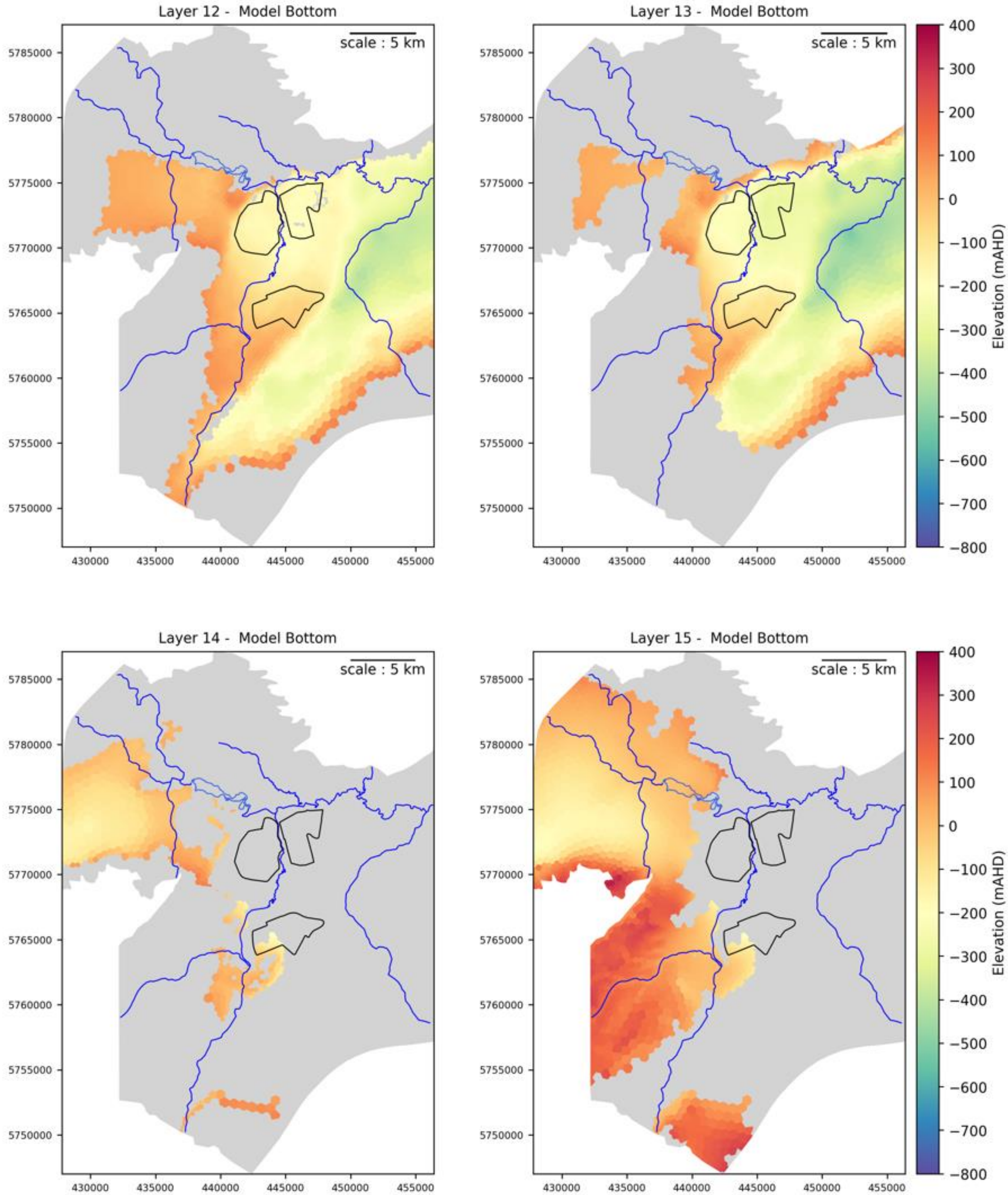

Layer 12 - Model Bottom
scale : 5 km
Layer 13 - Model Bottom
scale : 5 km
Layer 14 - Model Bottom
scale : 5 km
Layer 15 - Model Bottom
scale : 5 km
5785000
5780000
5775000
5770000
5765000
5760000
5755000
5750000
430000
435000
440000
445000
450000
455000
400
300
200
100
0
−100
−200
−300
−400
−500
−600
−700
−800
Elevation (mAHD)

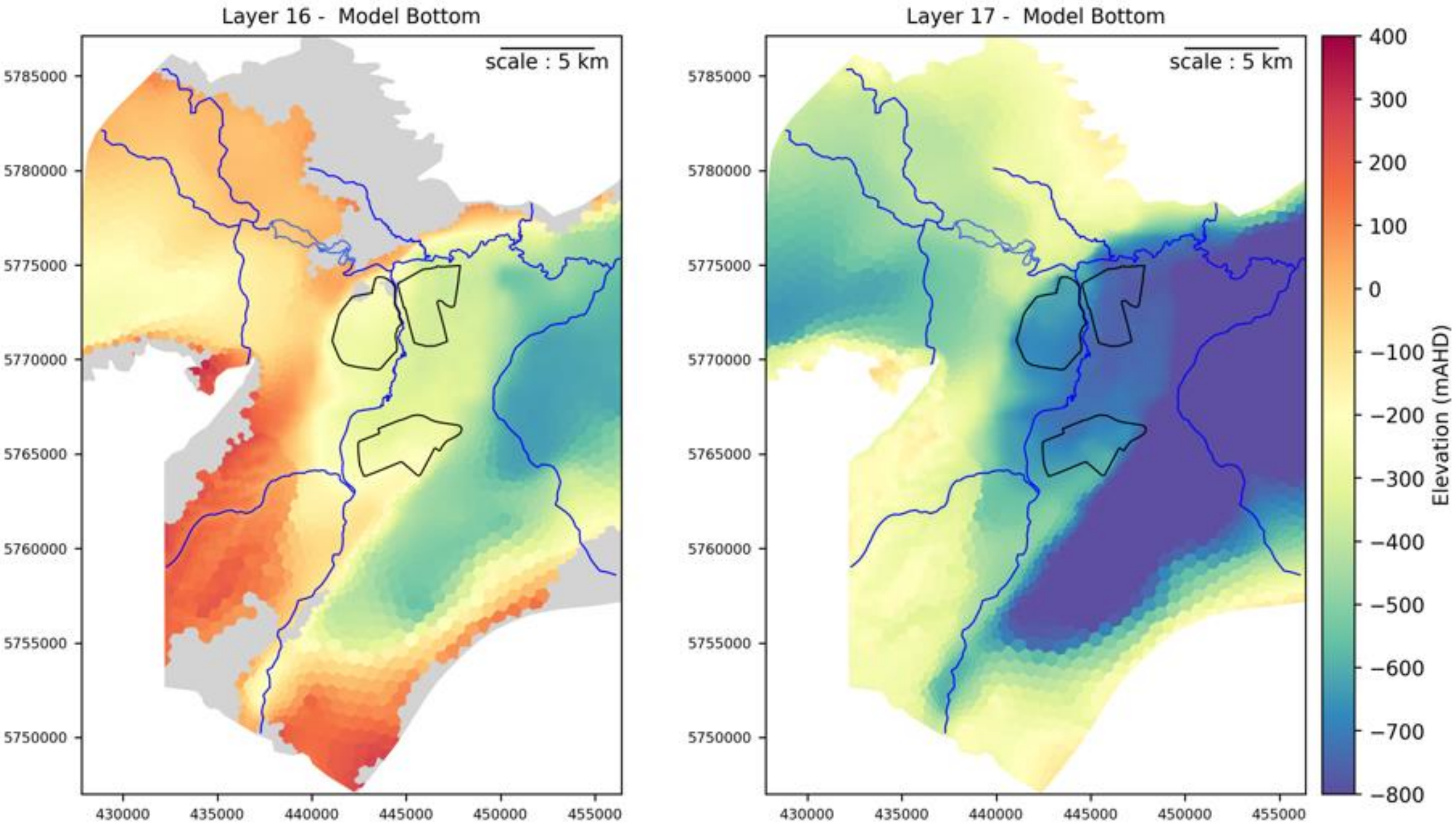

Layer 16 - Model Bottom
scale : 5 km
Layer 17 - Model Bottom
scale : 5 km
5785000
5780000
5775000
5770000
5765000
5760000
5755000
5750000
430000
435000
440000
445000
450000
455000
400
300
200
100
0
−100
−200
−300
−400
−500
−600
−700
−800
Elevation (mAHD)

Appendix C

PRMS model data

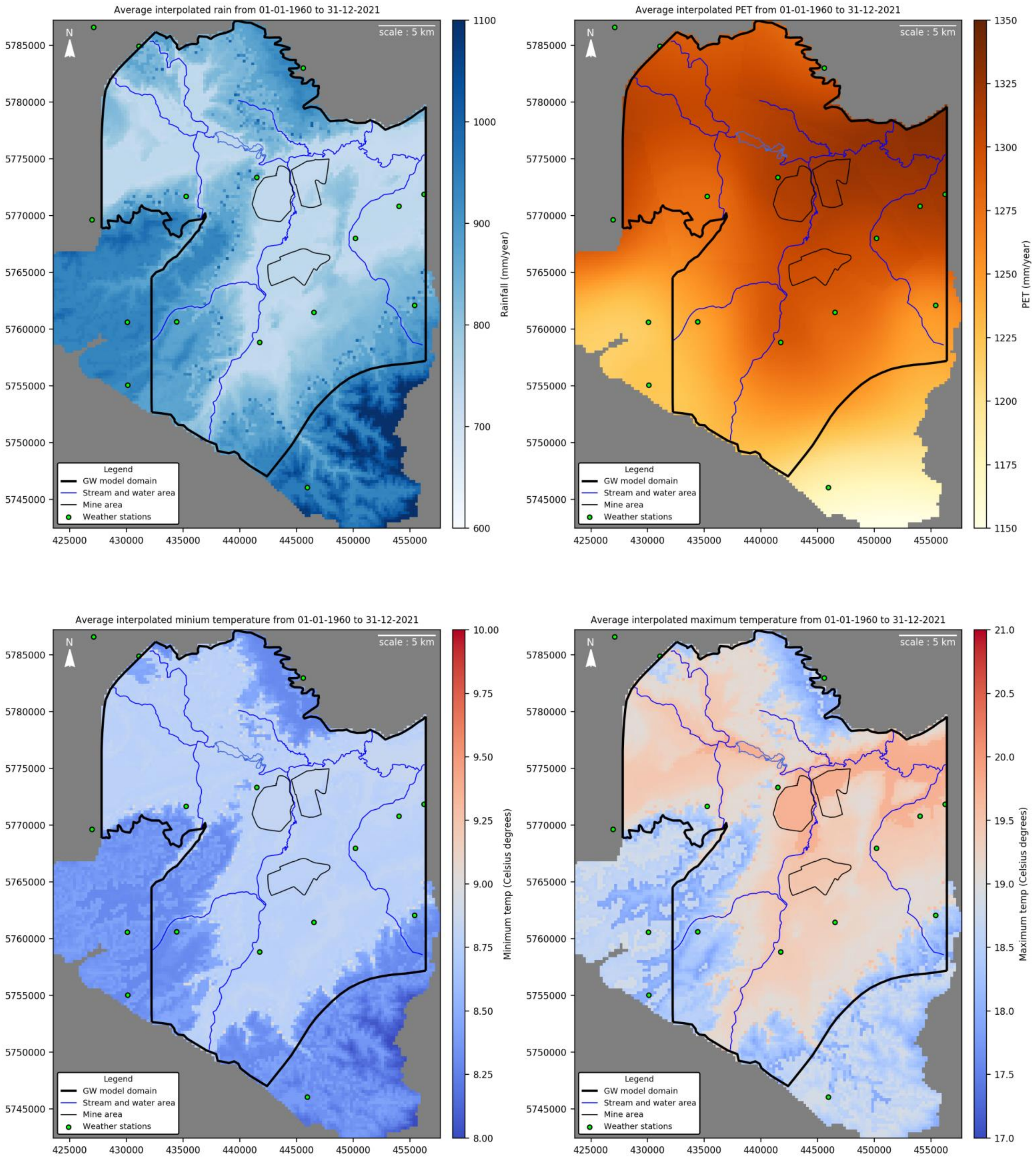

PRMS model long term average climate

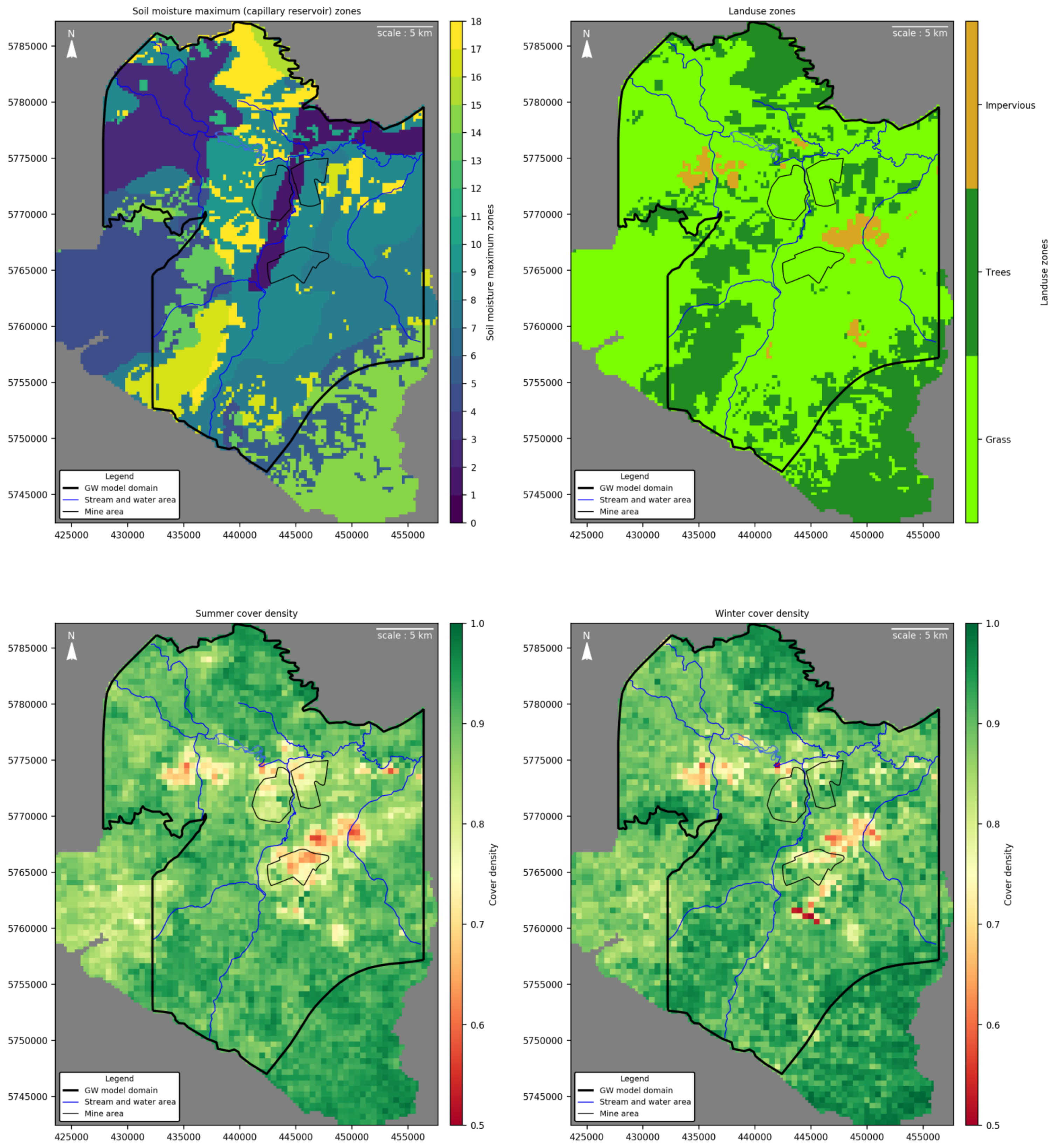

PRMS model parameters

PRMS model – calibrated parameters

Model	Parameter	Unit	Initial	Min	Max	Calibrated	Comment
PRMS	soil_mst1a	Inches	7.17	1.26	13.08	13.08	Soil moisture maximum (size of capillary reservoir) in areas of predominantly grass cover (shallow effective depth of soil moisture evapotranspiration)
PRMS	soil_mst2a	Inches	5.33	0.9	9.77	3.81	
PRMS	soil_mst3a	Inches	7.46	1.31	13.62	13.62	
PRMS	soil_mst4a	Inches	7.46	1.31	13.62	6.5	
PRMS	soil_mst5a	Inches	8.73	1.53	15.92	15.92	
PRMS	soil_mst6a	Inches	4.8	0.83	8.77	2.98	
PRMS	soil_mst7a	Inches	3.02	0.51	5.54	5.54	
PRMS	soil_mst8a	Inches	3.02	0.51	5.54	1.18	
PRMS	soil_mst9a	Inches	4.63	0.81	8.44	7.24	
PRMS	soil_mst1b	Inches	16.28	12.56	20	20	Soil moisture maximum (size of capillary reservoir) in areas of predominantly tree cover (deep effective depth of soil moisture evapotranspiration). 20 inches is the physical limit permitted in PRMS
PRMS	soil_mst2b	Inches	14.5	9	20	20	
PRMS	soil_mst3b	Inches	16.54	13.07	20	19.05	
PRMS	soil_mst4b	Inches	16.54	13.07	20	20	
PRMS	soil_mst5b	Inches	17.65	15.3	20	20	
PRMS	soil_mst6b	Inches	14.15	8.29	20	20	
PRMS	soil_mst7b	Inches	12.23	5.06	19.39	19.39	
PRMS	soil_mst8b	Inches	12.23	5.06	19.39	7.18	
PRMS	soil_mst9b	Inches	14.06	8.12	20	20	
PRMS	pfloden	Decimal fraction	0.15	0.01	0.5	0.094	Preferential flow density
PRMS	impervf	Decimal fraction	0.4	0.3	0.8	0.3	Fraction of each HRU area that is impervious
PRMS	impervstr	Inches	0.1	0.01	0.5	0.094	Maximum impervious area retention storage for each HRU
PRMS	smidxcf	Decimal fraction	0.001	0.0001	0.05	0.001	Coefficient in non-linear contributing area algorithm for each HRU
PRMS	smidxexp	1/inch	0.2	0.01	0.5	0.234	Exponent in non-linear contributing area algorithm for each HRU
PRMS	sintcp	Inches	0.2	0.01	1	0.531	Summer rain interception storage capacity for major vegetation type in each HRU
PRMS	wintcp	Inches	0.2	0.01	1	0.161	Winter rain interception storage capacity for major vegetation type in each HRU

Appendix D

Sand fraction maps

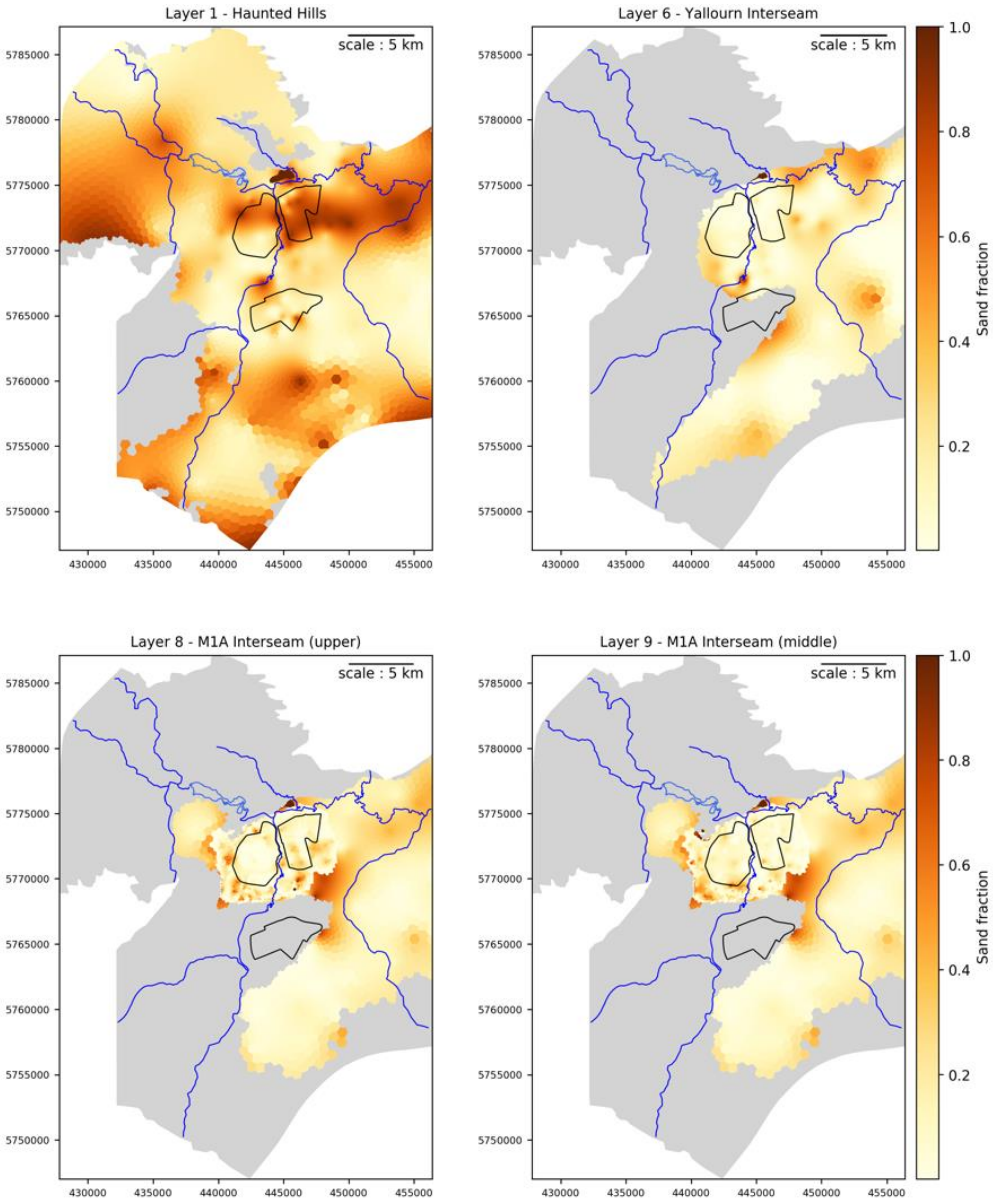
Layer 1 - Haunted Hills
Layer 6 - Yallourn Interseam
Layer 8 - M1A Interseam (upper)
Layer 9 - M1A Interseam (middle)
scale : 5 km
5785000
5780000
5775000
5770000
5765000
5760000
5755000
5750000
430000
435000
440000
445000
450000
455000
1.0
0.8
0.6
0.4
0.2
Sand fraction

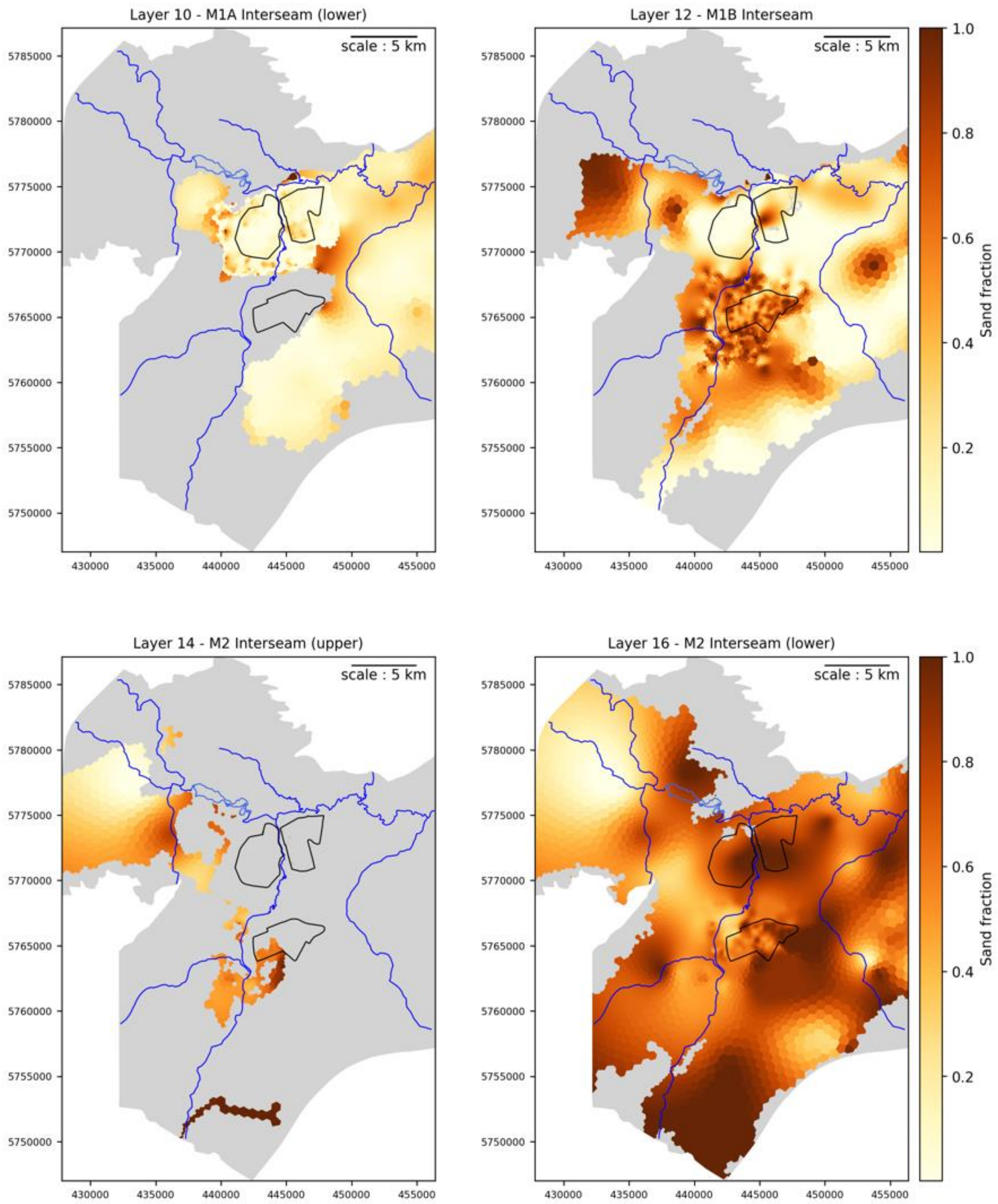
Layer 10 - M1A Interseam (lower)
Layer 12 - M1B Interseam
Layer 14 - M2 Interseam (upper)
Layer 16 - M2 Interseam (lower)
scale : 5 km
5785000
5780000
5775000
5770000
5765000
5760000
5755000
5750000
430000
435000
440000
445000
450000
455000
Sand fraction
1.0
0.8
0.6
0.4
0.2

Appendix E

Additional hydrograph plots

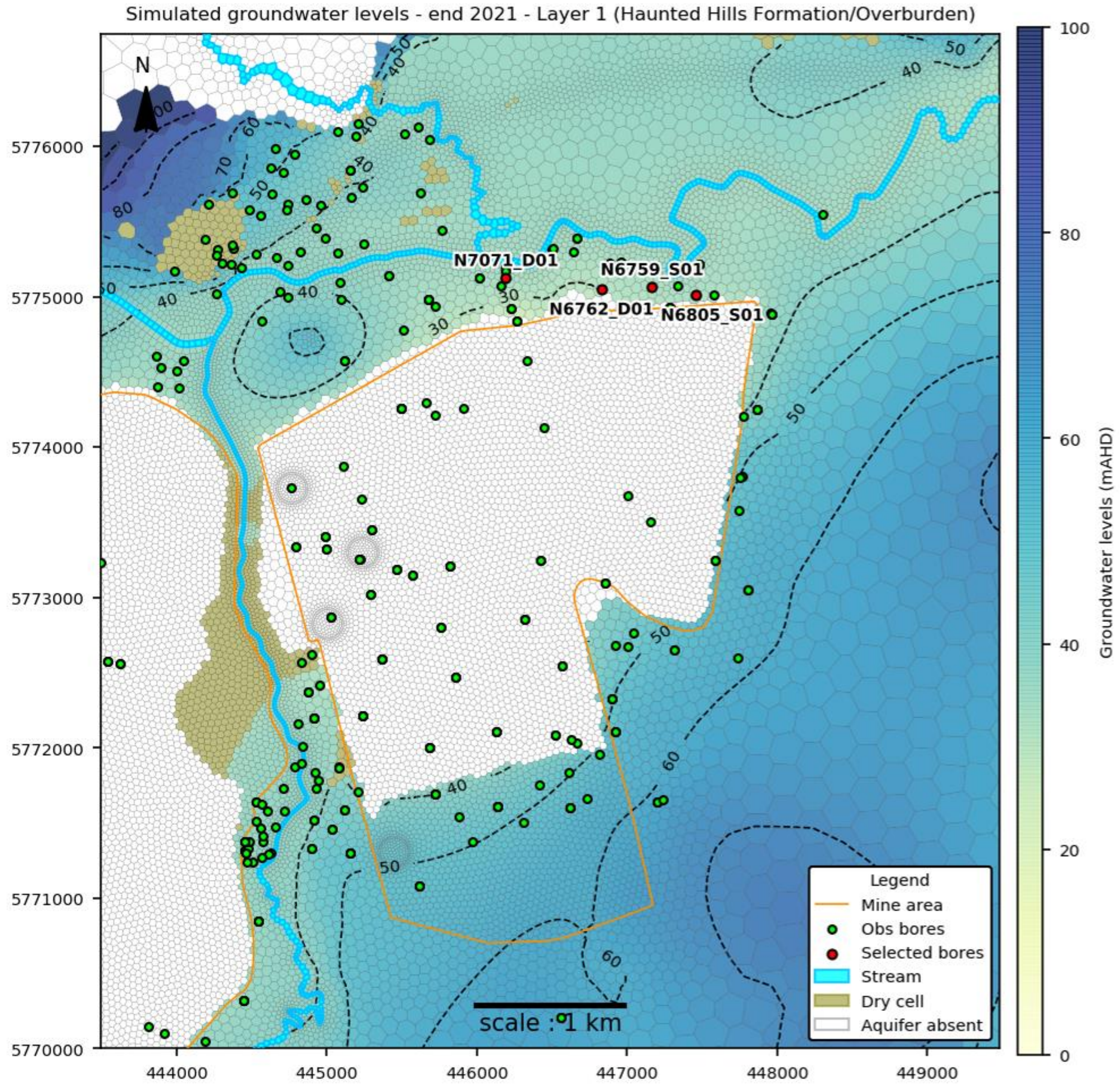

Simulated groundwater levels - end 2021 - Layer 1 (Haunted Hills Formation/Overburden)
N
N7071_D01
N6759_S01
N6762_D01
N6805_S01
Groundwater levels (mAHD)
Legend
Mine area
Obs bores
Selected bores
Stream
Dry cell
Aquifer absent
scale : 1 km

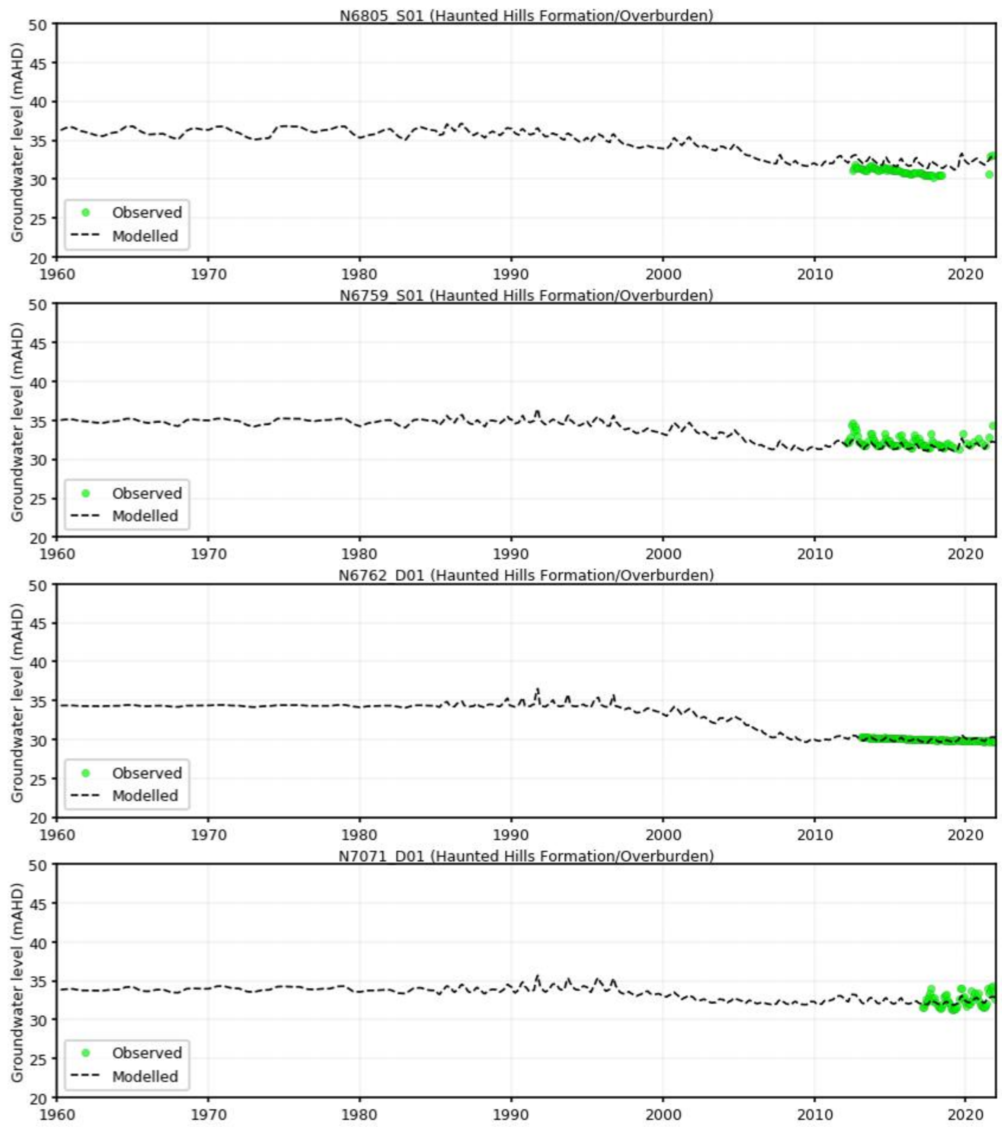

N6805_S01 (Haunted Hills Formation/Overburden)
N6759_S01 (Haunted Hills Formation/Overburden)
N6762_D01 (Haunted Hills Formation/Overburden)
N7071_D01 (Haunted Hills Formation/Overburden)
Groundwater level (mAHD)
Observed
Modelled

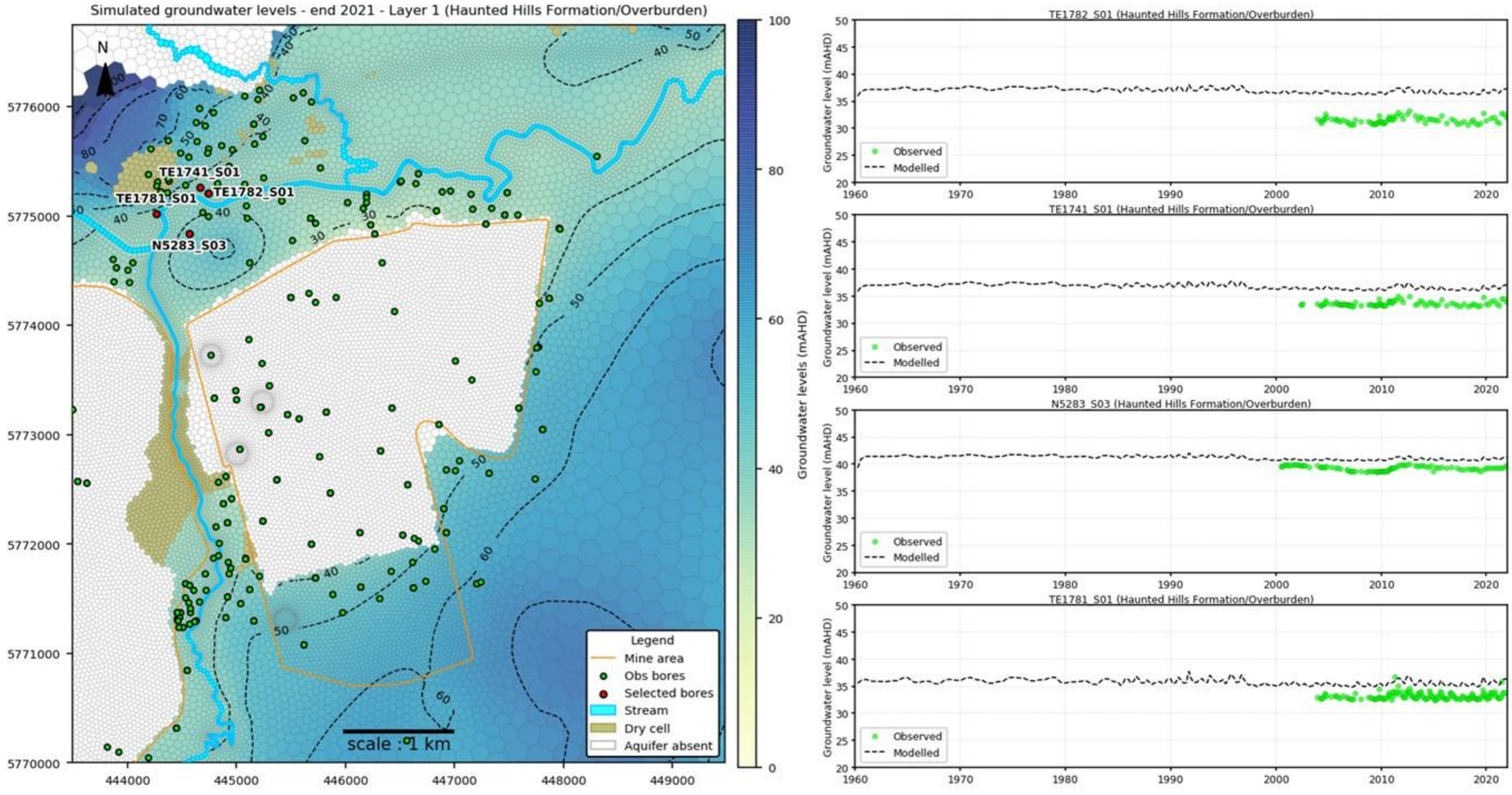
Simulated groundwater levels - end 2021 - Layer 1 (Haunted Hills Formation/Overburden)
N
TE1741_S01
TE1782_S01
TE1781_S01
N5283_S03
scale : 1 km
Legend
Mine area
Obs bores
Selected bores
Stream
Dry cell
Aquifer absent
Groundwater levels (mAHD)
TE1782_S01 (Haunted Hills Formation/Overburden)
TE1741_S01 (Haunted Hills Formation/Overburden)
N5283_S03 (Haunted Hills Formation/Overburden)
TE1781_S01 (Haunted Hills Formation/Overburden)
Groundwater level (mAHD)
Observed
Modelled

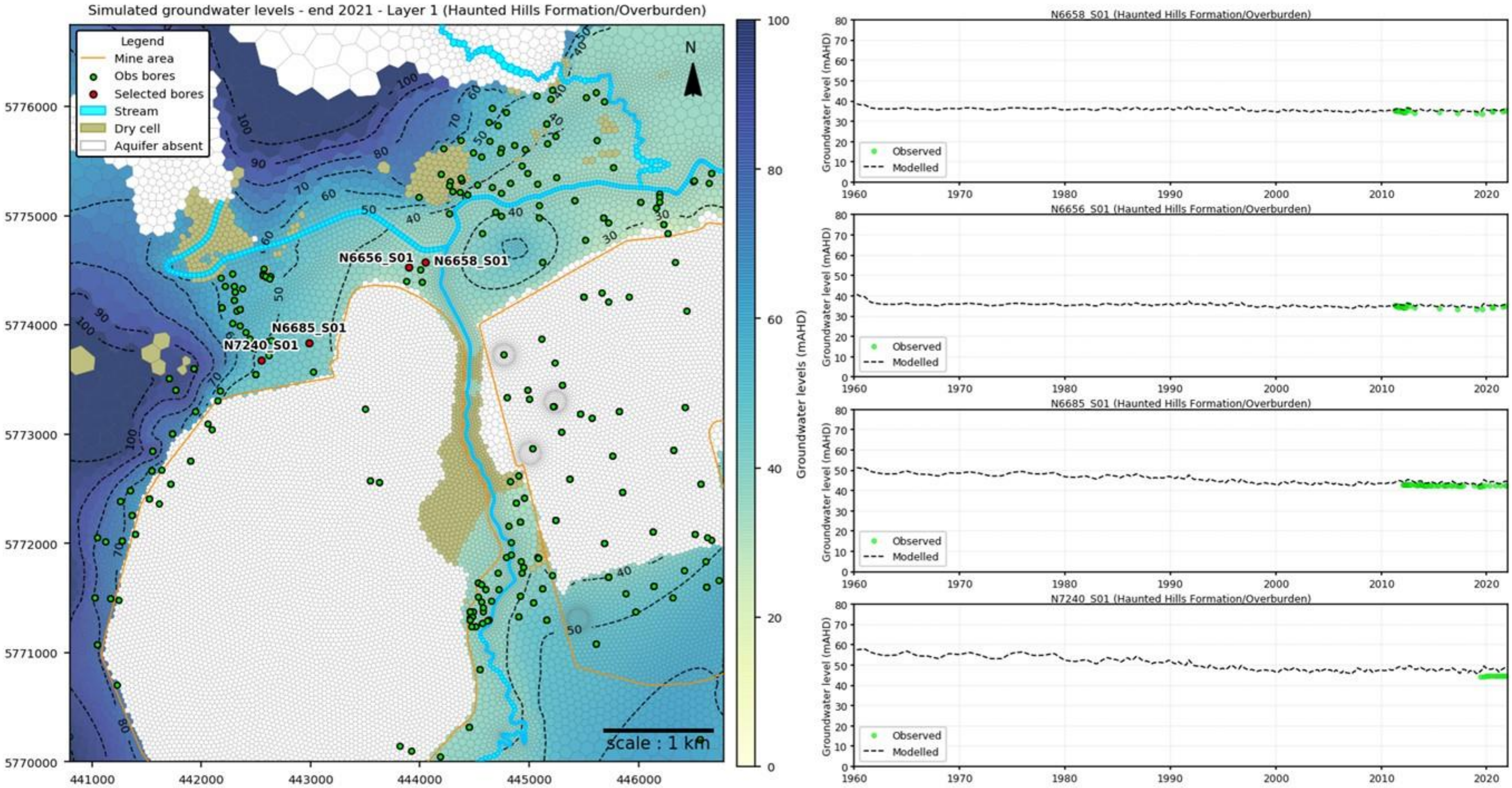
Simulated groundwater levels - end 2021 - Layer 1 (Haunted Hills Formation/Overburden)
Legend
Mine area
Obs bores
Selected bores
Stream
Dry cell
Aquifer absent
N
N6656_S01
N6658_S01
N6685_S01
N7240_S01
scale : 1 km
Groundwater levels (mAHD)
N6658_S01 (Haunted Hills Formation/Overburden)
N6656_S01 (Haunted Hills Formation/Overburden)
N6685_S01 (Haunted Hills Formation/Overburden)
N7240_S01 (Haunted Hills Formation/Overburden)
Groundwater level (mAHD)
Observed
Modelled

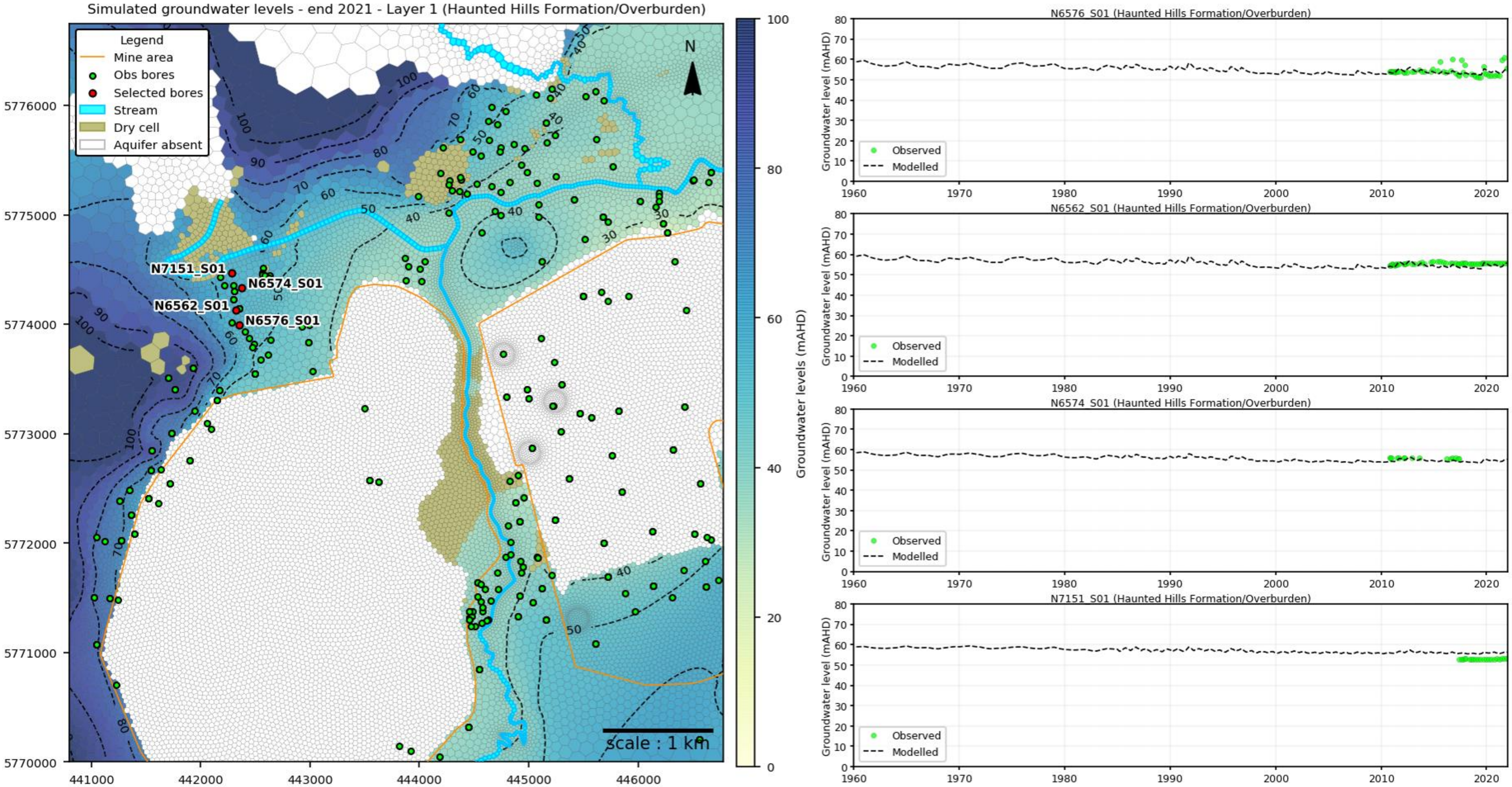
Simulated groundwater levels - end 2021 - Layer 1 (Haunted Hills Formation/Overburden)
Legend
Mine area
Obs bores
Selected bores
Stream
Dry cell
Aquifer absent
N
N7151_S01
N6574_S01
N6562_S01
N6576_S01
scale : 1 km
Groundwater levels (mAHD)
N6576_S01 (Haunted Hills Formation/Overburden)
N6562_S01 (Haunted Hills Formation/Overburden)
N6574_S01 (Haunted Hills Formation/Overburden)
N7151_S01 (Haunted Hills Formation/Overburden)
Groundwater level (mAHD)
Observed
Modelled

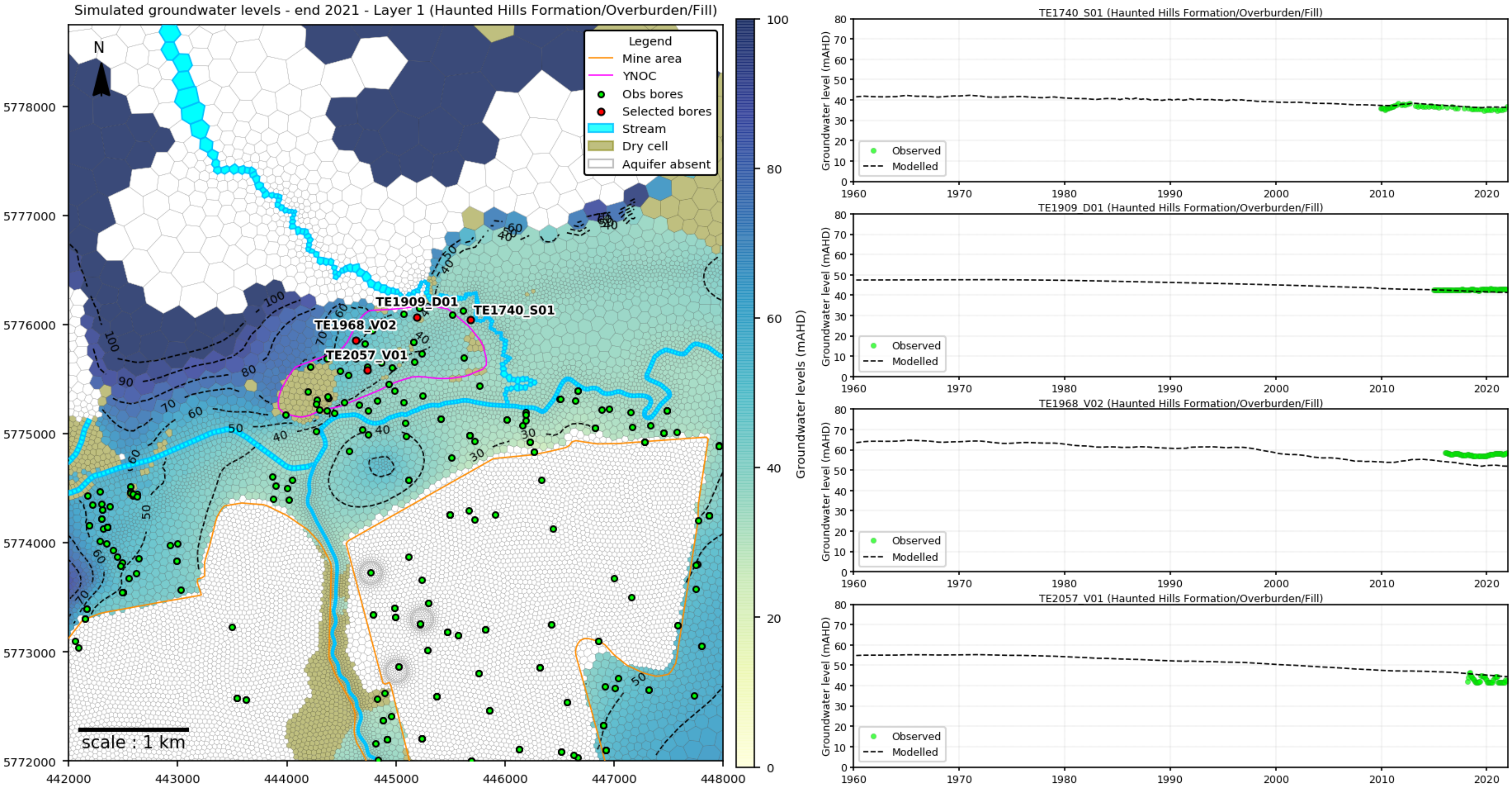
Simulated groundwater levels - end 2021 - Layer 1 (Haunted Hills Formation/Overburden/Fill)
Legend
Mine area
YNOC
Obs bores
Selected bores
Stream
Dry cell
Aquifer absent
TE1909_D01
TE1740_S01
TE1968_V02
TE2057_V01
scale : 1 km
N
Groundwater levels (mAHD)
TE1740_S01 (Haunted Hills Formation/Overburden/Fill)
TE1909_D01 (Haunted Hills Formation/Overburden/Fill)
TE1968_V02 (Haunted Hills Formation/Overburden/Fill)
TE2057_V01 (Haunted Hills Formation/Overburden/Fill)
Groundwater level (mAHD)
Observed
Modelled

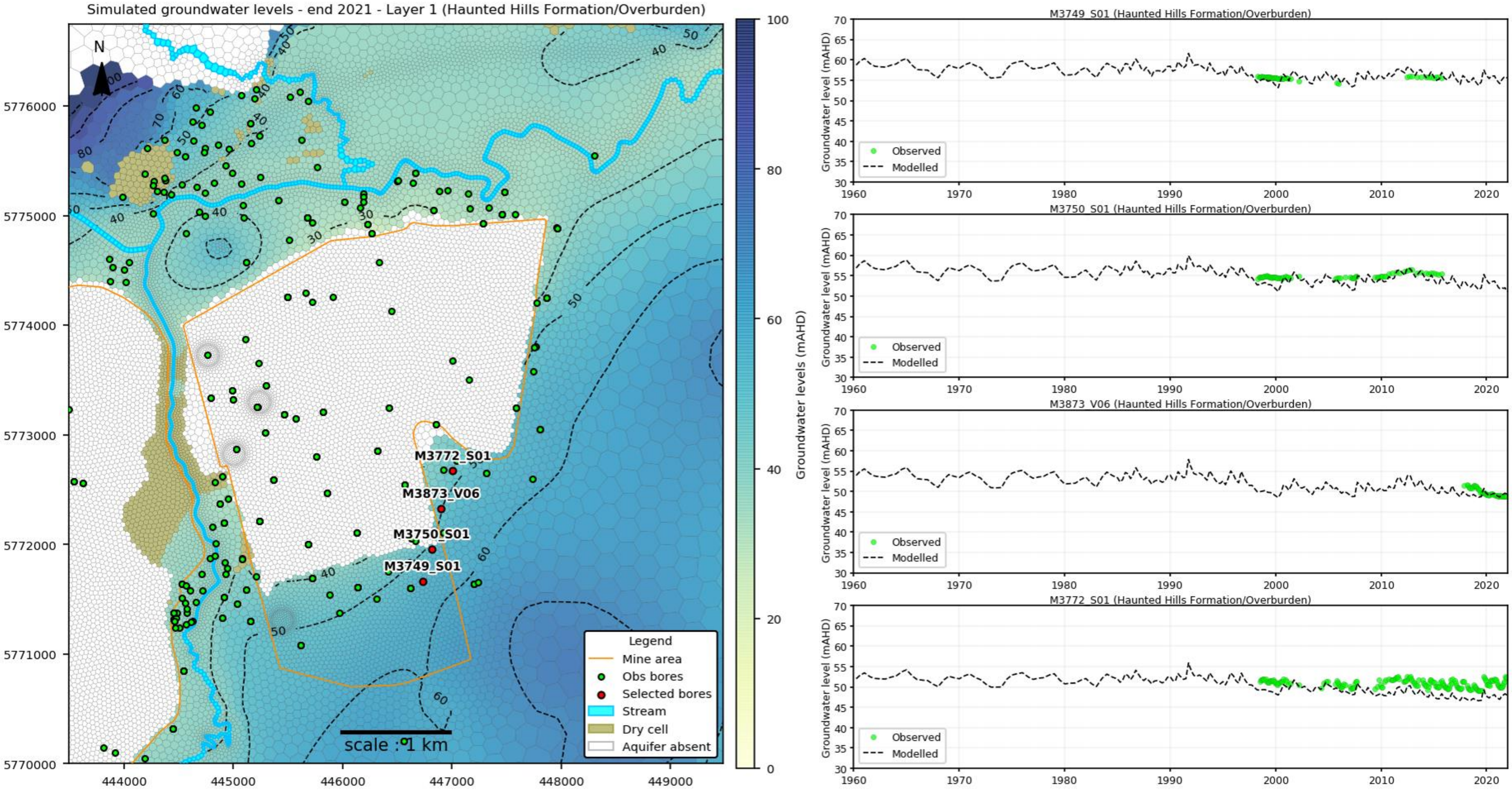

Simulated groundwater levels - end 2021 - Layer 1 (Haunted Hills Formation/Overburden)
N
M3772_S01
M3873_V06
M3750_S01
M3749_S01
scale : 1 km
Legend
Mine area
Obs bores
Selected bores
Stream
Dry cell
Aquifer absent
Groundwater levels (mAHD)
M3749_S01 (Haunted Hills Formation/Overburden)
M3750_S01 (Haunted Hills Formation/Overburden)
M3873_V06 (Haunted Hills Formation/Overburden)
M3772_S01 (Haunted Hills Formation/Overburden)
Groundwater level (mAHD)
Observed
Modelled

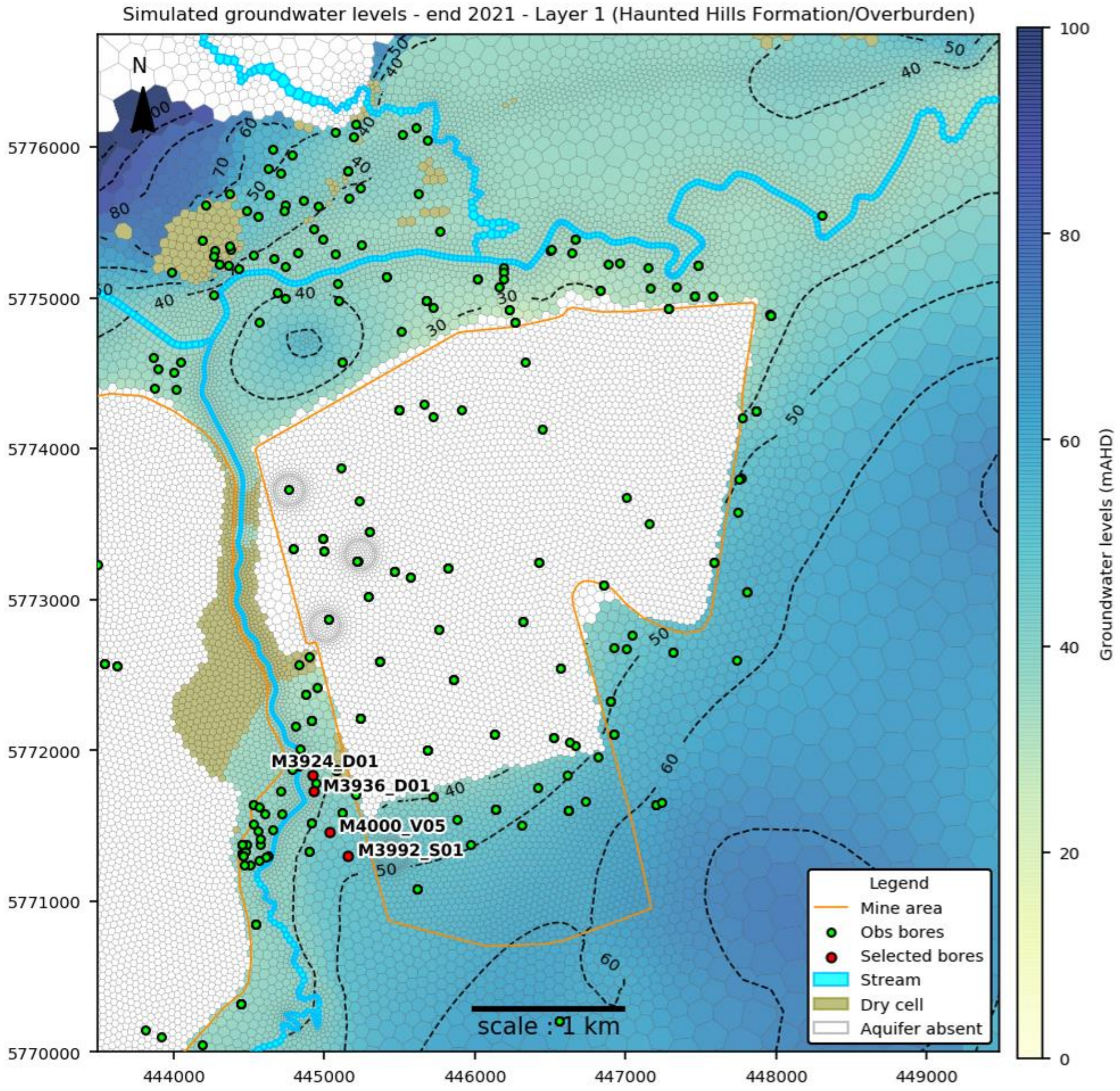
Simulated groundwater levels - end 2021 - Layer 1 (Haunted Hills Formation/Overburden)
N
M3924_D01
M3936_D01
M4000_V05
M3992_S01
scale : 1 km
Legend
Mine area
Obs bores
Selected bores
Stream
Dry cell
Aquifer absent
Groundwater levels (mAHD)

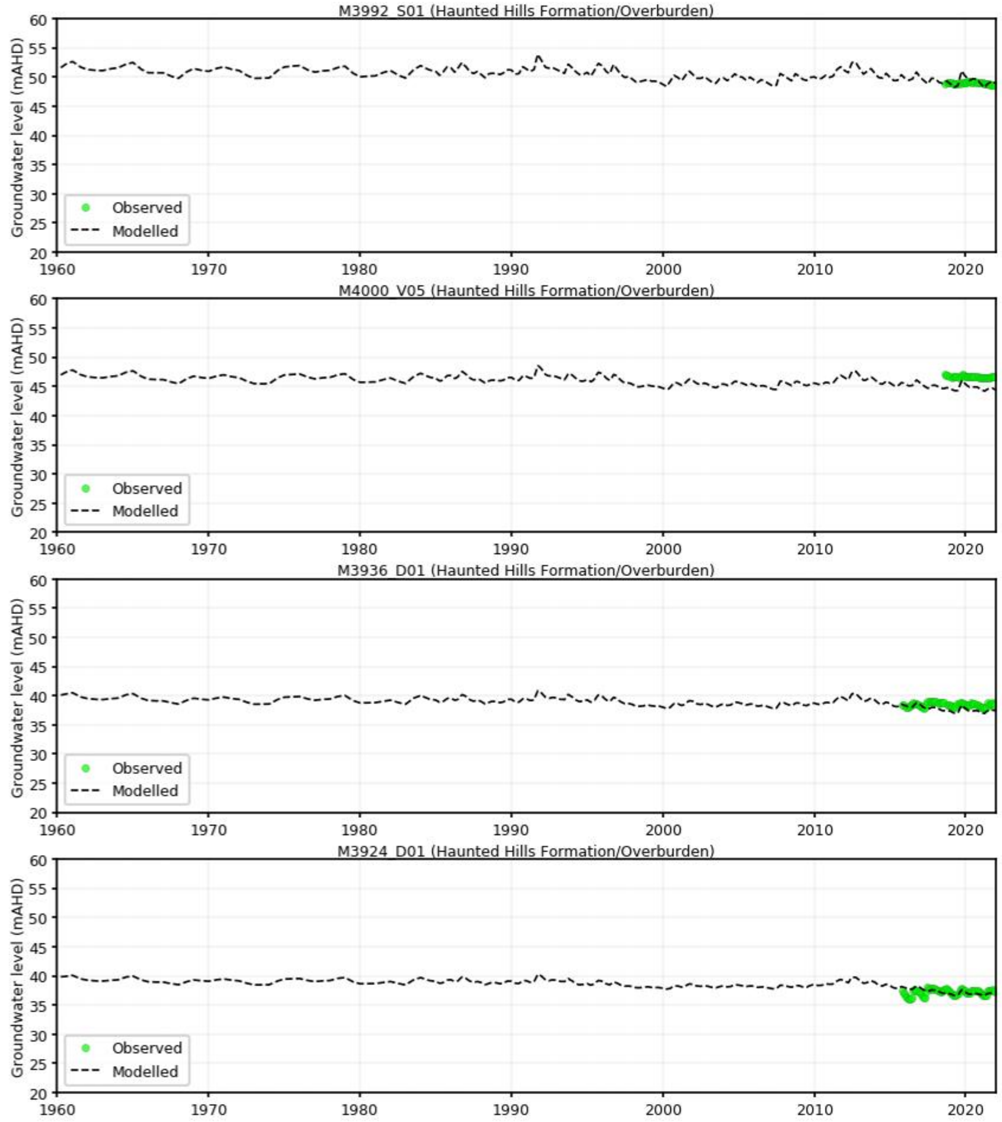
M3992_S01 (Haunted Hills Formation/Overburden)
M4000_V05 (Haunted Hills Formation/Overburden)
M3936_D01 (Haunted Hills Formation/Overburden)
M3924_D01 (Haunted Hills Formation/Overburden)
Groundwater level (mAHD)
Observed
Modelled

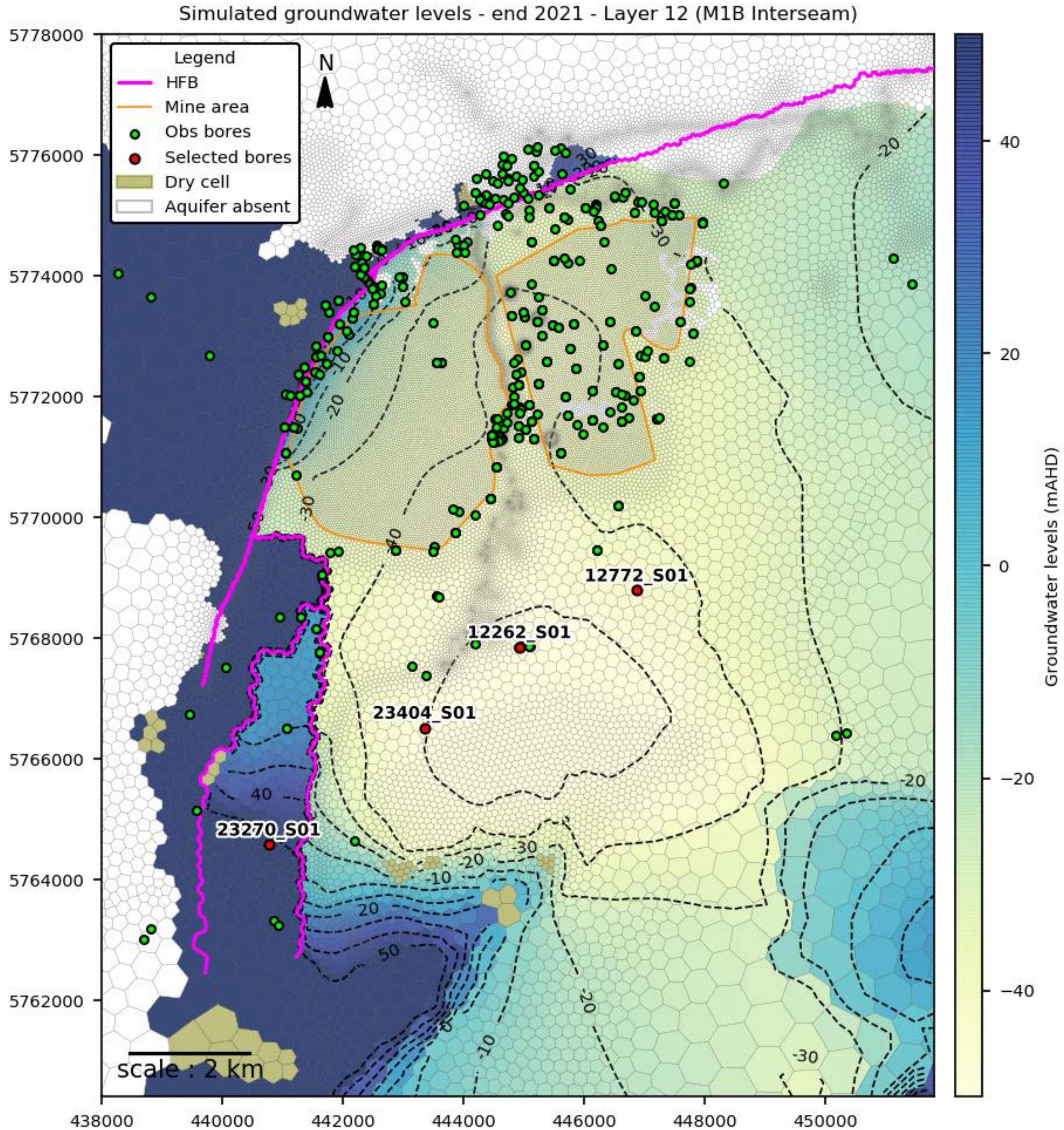
Simulated groundwater levels - end 2021 - Layer 12 (M1B Interseam)
Legend
HFB
Mine area
Obs bores
Selected bores
Dry cell
Aquifer absent
N
12772_S01
12262_S01
23404_S01
23270_S01
scale : 2 km
Groundwater levels (mAHD)

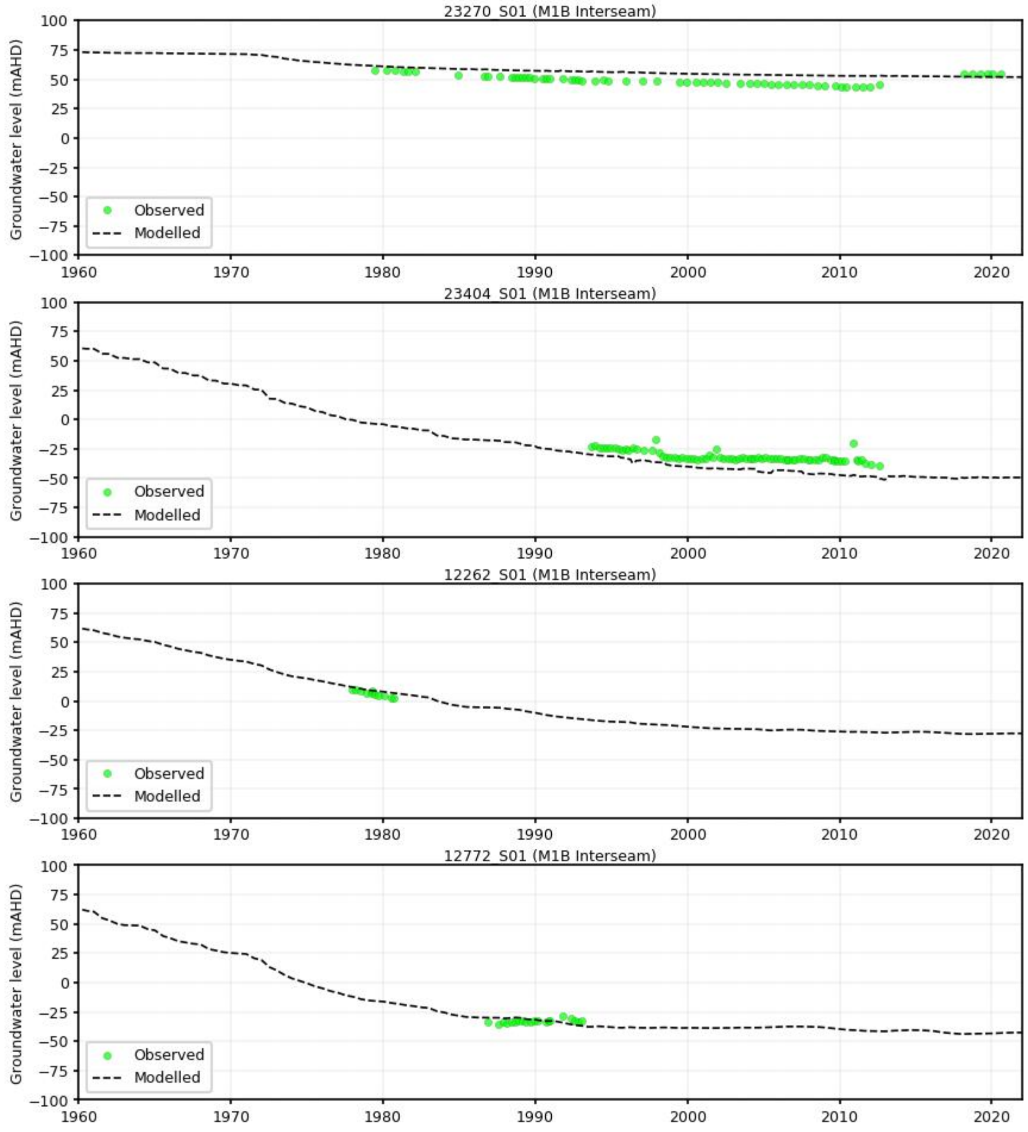
23270_S01 (M1B Interseam)
23404_S01 (M1B Interseam)
12262_S01 (M1B Interseam)
12772_S01 (M1B Interseam)
Groundwater level (mAHD)
Observed
Modelled

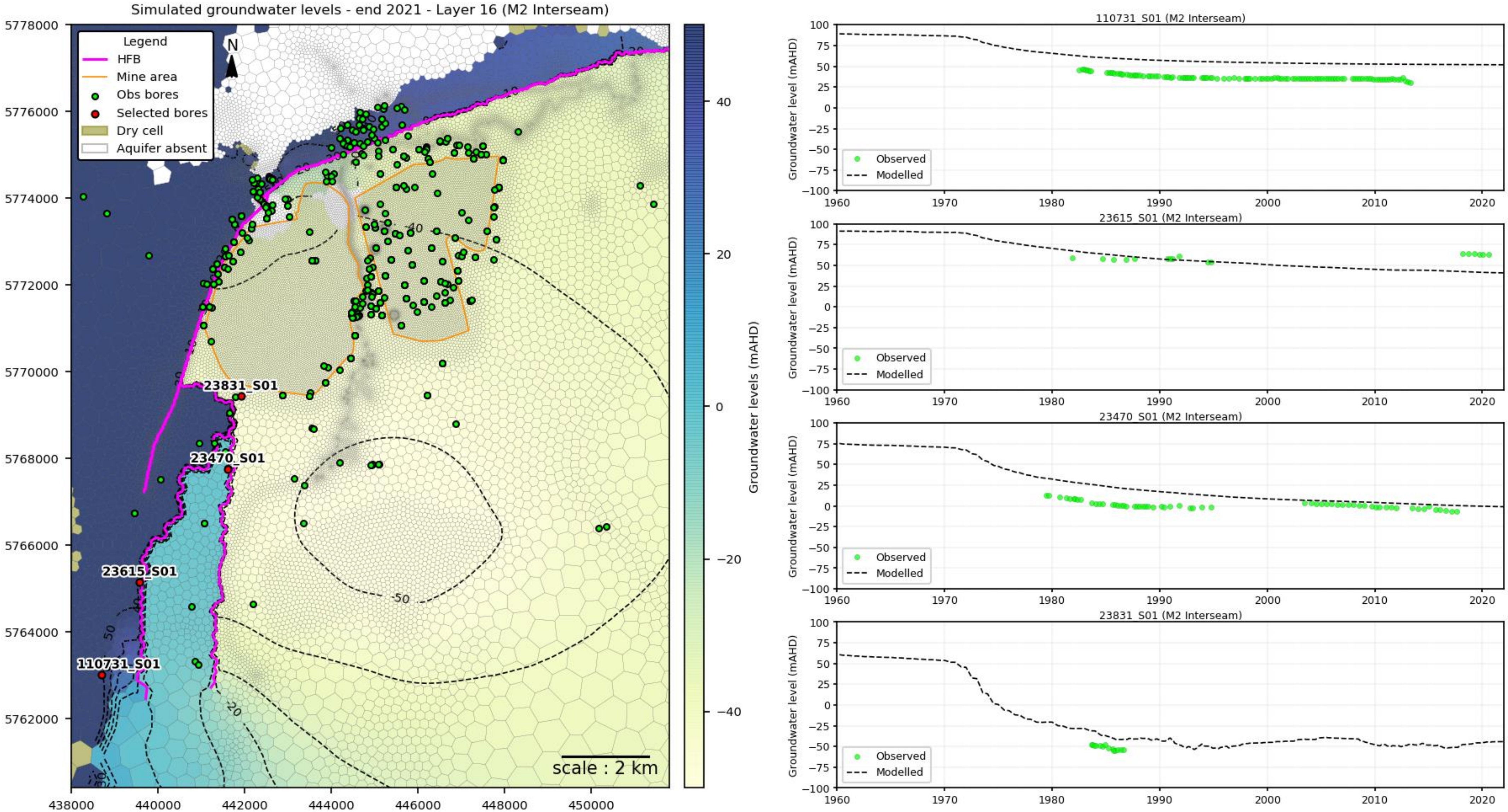

Simulated groundwater levels - end 2021 - Layer 16 (M2 Interseam)
Legend
HFB
Mine area
Obs bores
Selected bores
Dry cell
Aquifer absent
N
23831_S01
23470_S01
23615_S01
110731_S01
scale : 2 km
Groundwater levels (mAHD)
110731_S01 (M2 Interseam)
23615_S01 (M2 Interseam)
23470_S01 (M2 Interseam)
23831_S01 (M2 Interseam)
Groundwater level (mAHD)
Observed
Modelled

Appendix F

All observation bore hydrographs

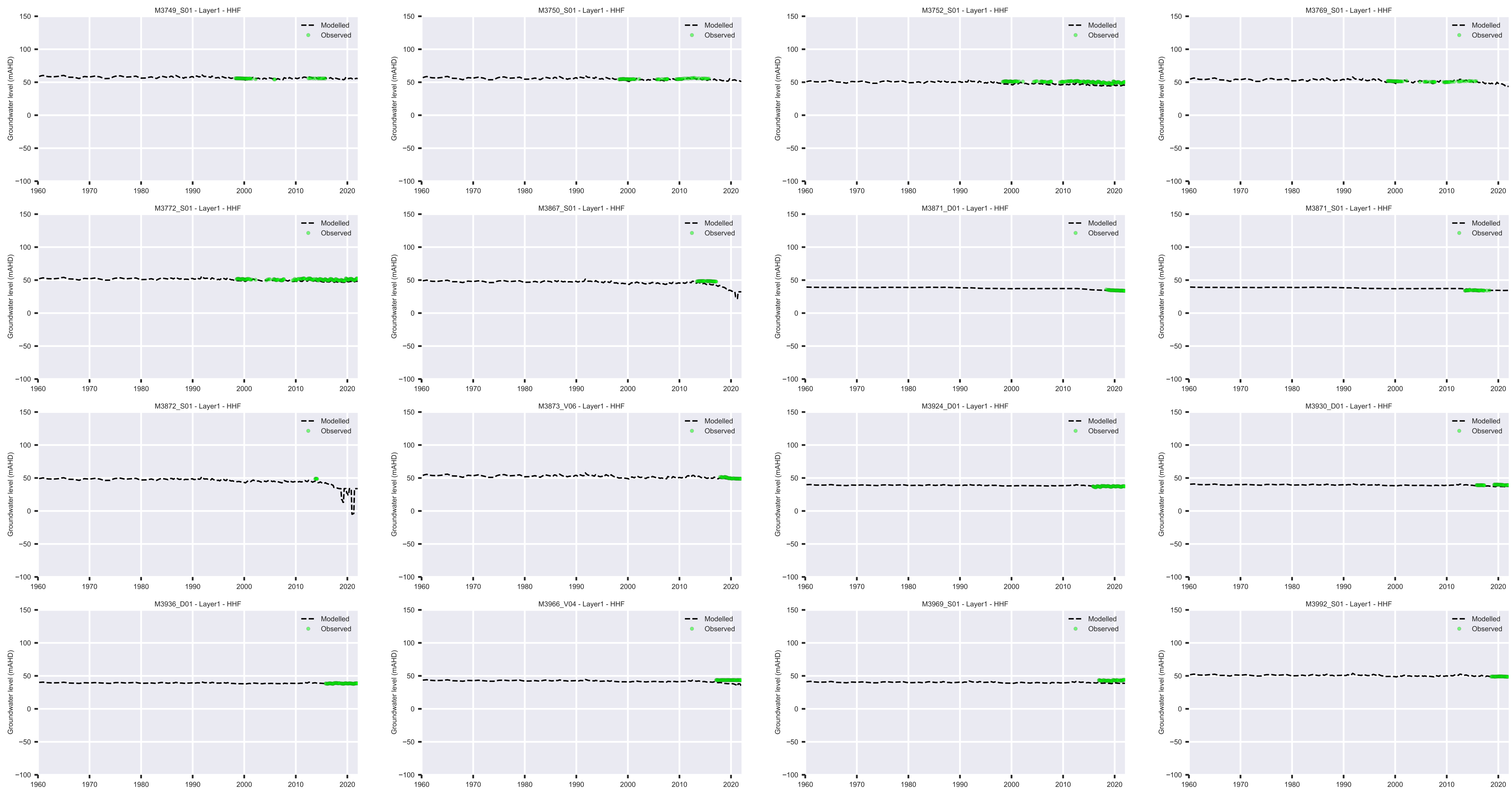
M3749_S01 - Layer1 - HHF
M3750_S01 - Layer1 - HHF
M3752_S01 - Layer1 - HHF
M3769_S01 - Layer1 - HHF
M3772_S01 - Layer1 - HHF
M3867_S01 - Layer1 - HHF
M3871_D01 - Layer1 - HHF
M3871_S01 - Layer1 - HHF
M3872_S01 - Layer1 - HHF
M3873_V06 - Layer1 - HHF
M3924_D01 - Layer1 - HHF
M3930_D01 - Layer1 - HHF
M3936_D01 - Layer1 - HHF
M3966_V04 - Layer1 - HHF
M3969_S01 - Layer1 - HHF
M3992_S01 - Layer1 - HHF
Modelled
Observed
Groundwater level (mAHD)
150
100
50
0
−50
−100
1960
1970
1980
1990
2000
2010
2020

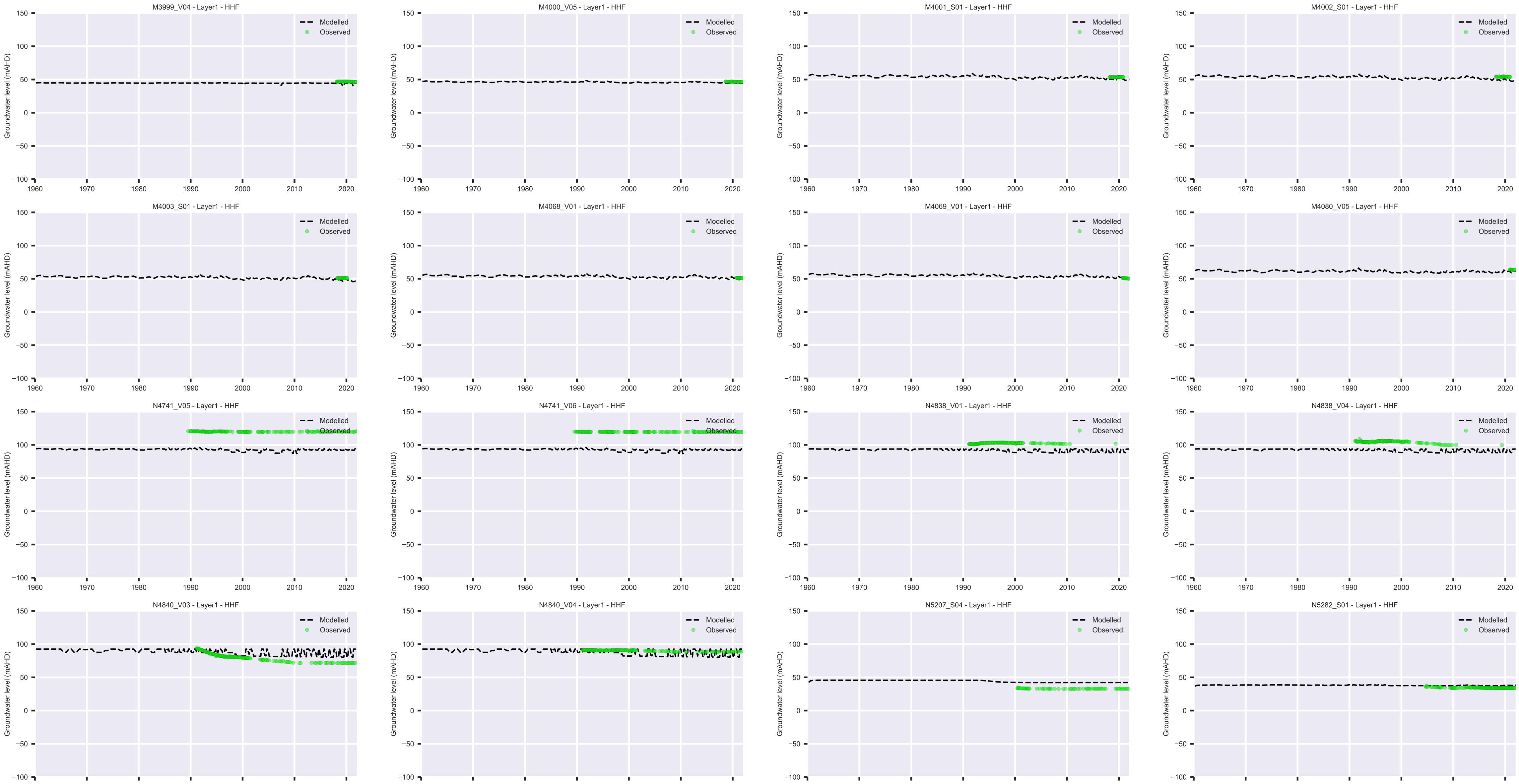
M3999_V04 - Layer1 - HHF
M4000_V05 - Layer1 - HHF
M4001_S01 - Layer1 - HHF
M4002_S01 - Layer1 - HHF
M4003_S01 - Layer1 - HHF
M4068_V01 - Layer1 - HHF
M4069_V01 - Layer1 - HHF
M4080_V05 - Layer1 - HHF
N4741_V05 - Layer1 - HHF
N4741_V06 - Layer1 - HHF
N4838_V01 - Layer1 - HHF
N4838_V04 - Layer1 - HHF
N4840_V03 - Layer1 - HHF
N4840_V04 - Layer1 - HHF
N5207_S04 - Layer1 - HHF
N5282_S01 - Layer1 - HHF
Modelled
Observed
Groundwater level (mAHD)
150
100
50
0
−50
−100
1960
1970
1980
1990
2000
2010
2020

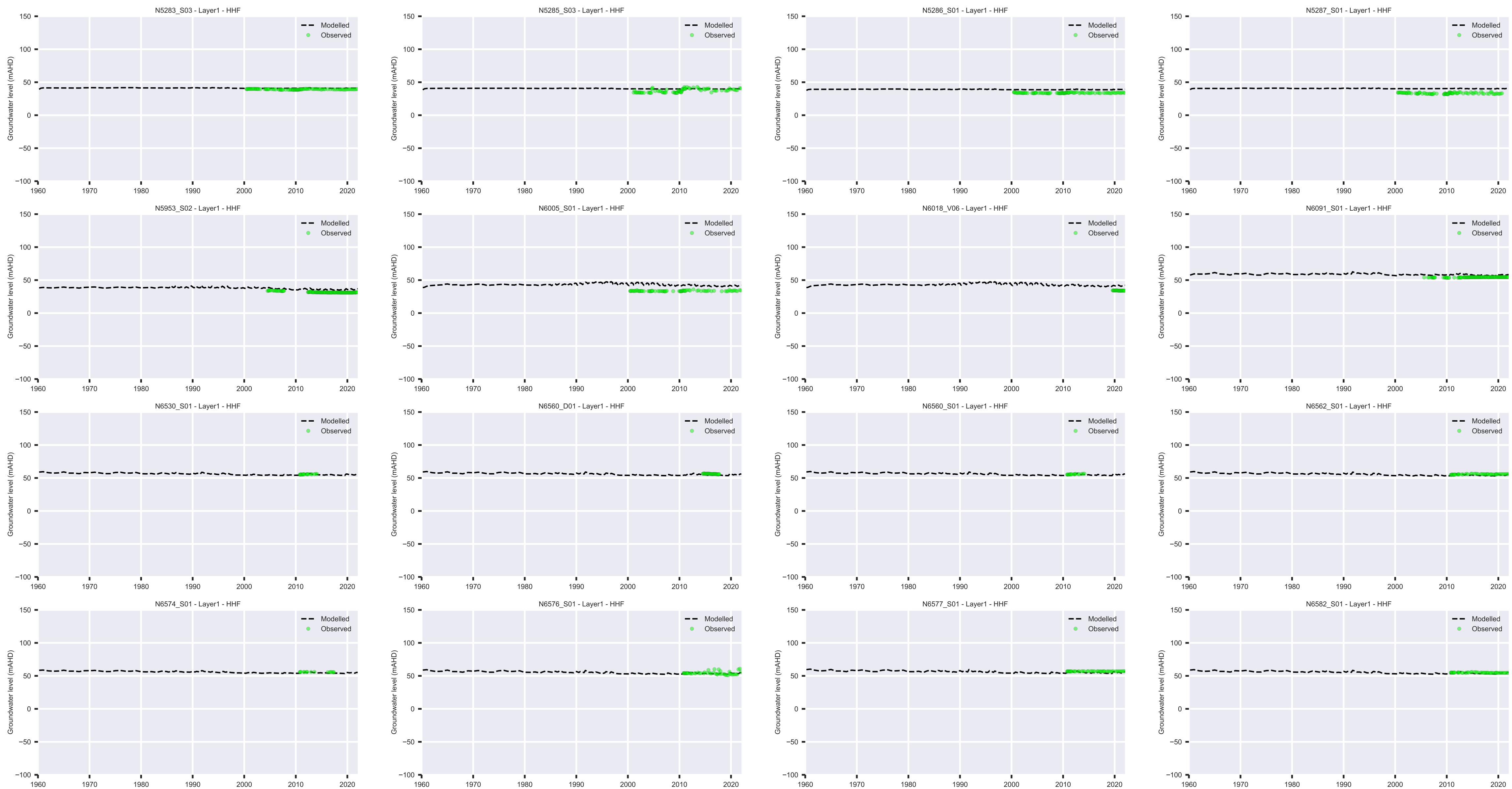
N5283_S03 - Layer1 - HHF
N5285_S03 - Layer1 - HHF
N5286_S01 - Layer1 - HHF
N5287_S01 - Layer1 - HHF
N5953_S02 - Layer1 - HHF
N6005_S01 - Layer1 - HHF
N6018_V06 - Layer1 - HHF
N6091_S01 - Layer1 - HHF
N6530_S01 - Layer1 - HHF
N6560_D01 - Layer1 - HHF
N6560_S01 - Layer1 - HHF
N6562_S01 - Layer1 - HHF
N6574_S01 - Layer1 - HHF
N6576_S01 - Layer1 - HHF
N6577_S01 - Layer1 - HHF
N6582_S01 - Layer1 - HHF
Modelled
Observed
Groundwater level (mAHD)
150
100
50
0
−50
−100
1960
1970
1980
1990
2000
2010
2020

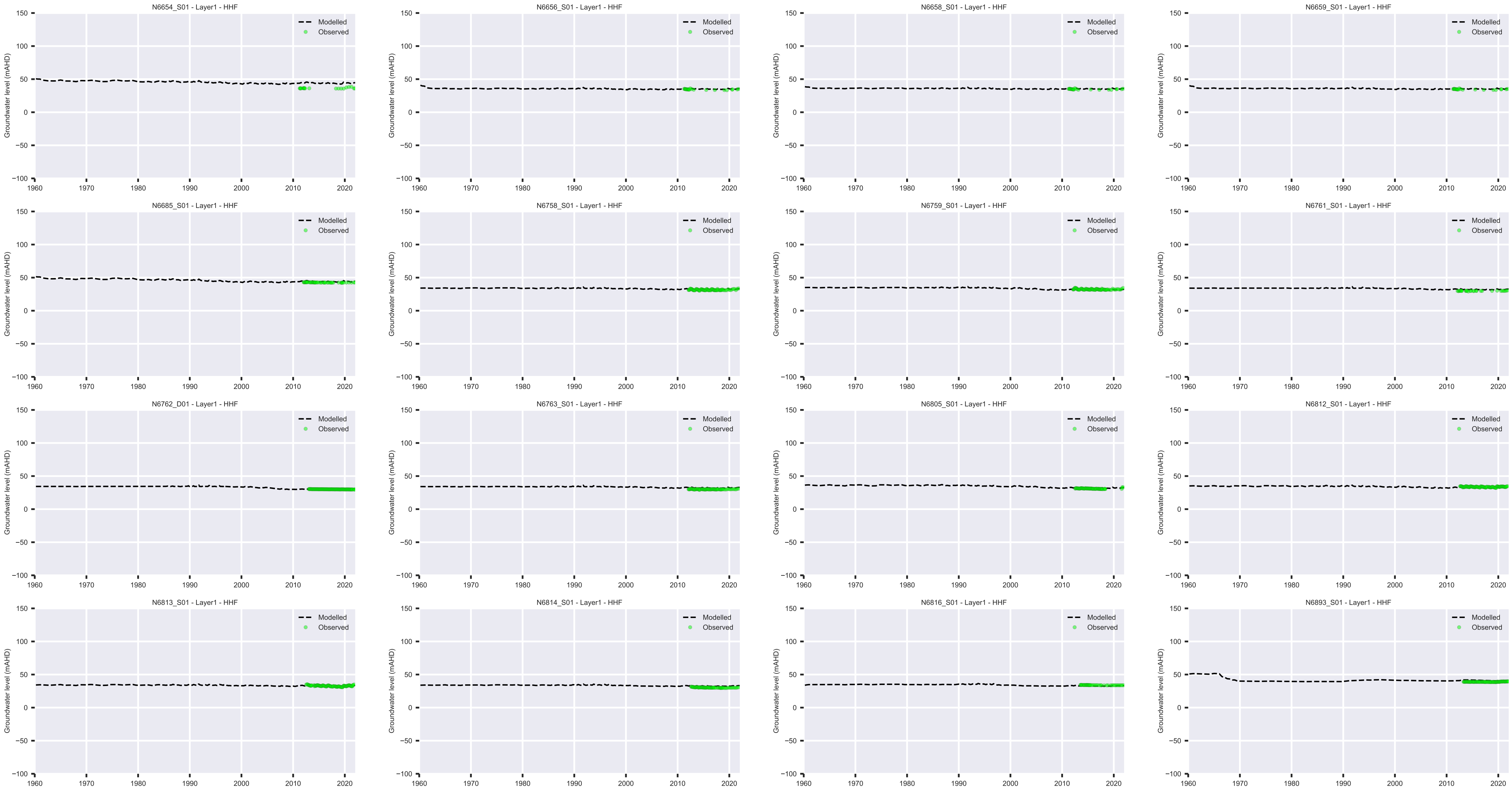
N6654_S01 - Layer1 - HHF
N6656_S01 - Layer1 - HHF
N6658_S01 - Layer1 - HHF
N6659_S01 - Layer1 - HHF
N6685_S01 - Layer1 - HHF
N6758_S01 - Layer1 - HHF
N6759_S01 - Layer1 - HHF
N6761_S01 - Layer1 - HHF
N6762_D01 - Layer1 - HHF
N6763_S01 - Layer1 - HHF
N6805_S01 - Layer1 - HHF
N6812_S01 - Layer1 - HHF
N6813_S01 - Layer1 - HHF
N6814_S01 - Layer1 - HHF
N6816_S01 - Layer1 - HHF
N6893_S01 - Layer1 - HHF
Modelled
Observed
Groundwater level (mAHD)
150
100
50
0
−50
−100
1960
1970
1980
1990
2000
2010
2020

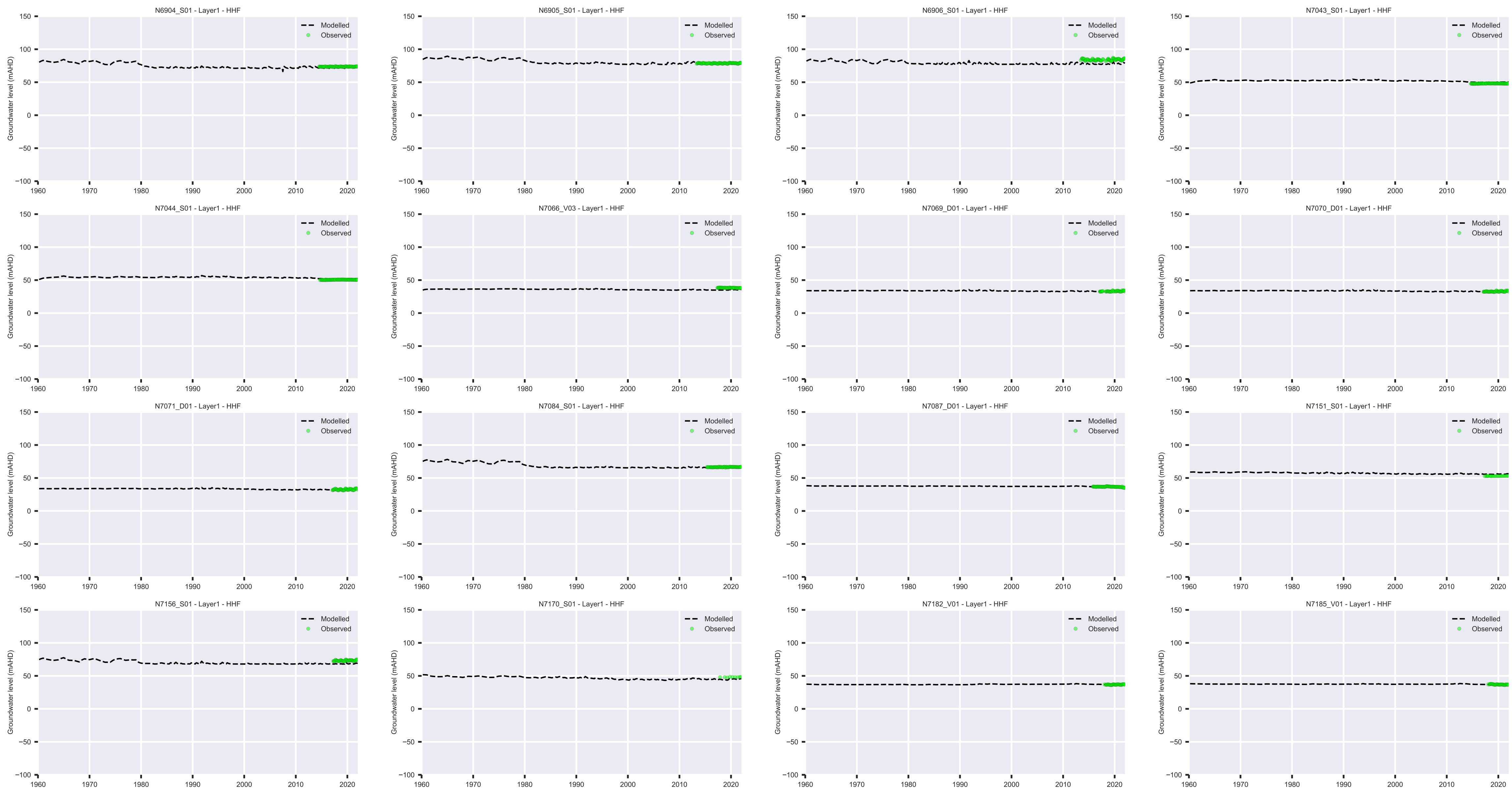
N6904_S01 - Layer1 - HHF
N6905_S01 - Layer1 - HHF
N6906_S01 - Layer1 - HHF
N7043_S01 - Layer1 - HHF
N7044_S01 - Layer1 - HHF
N7066_V03 - Layer1 - HHF
N7069_D01 - Layer1 - HHF
N7070_D01 - Layer1 - HHF
N7071_D01 - Layer1 - HHF
N7084_S01 - Layer1 - HHF
N7087_D01 - Layer1 - HHF
N7151_S01 - Layer1 - HHF
N7156_S01 - Layer1 - HHF
N7170_S01 - Layer1 - HHF
N7182_V01 - Layer1 - HHF
N7185_V01 - Layer1 - HHF
Modelled
Observed
Groundwater level (mAHD)
150
100
50
0
−50
−100
1960
1970
1980
1990
2000
2010
2020

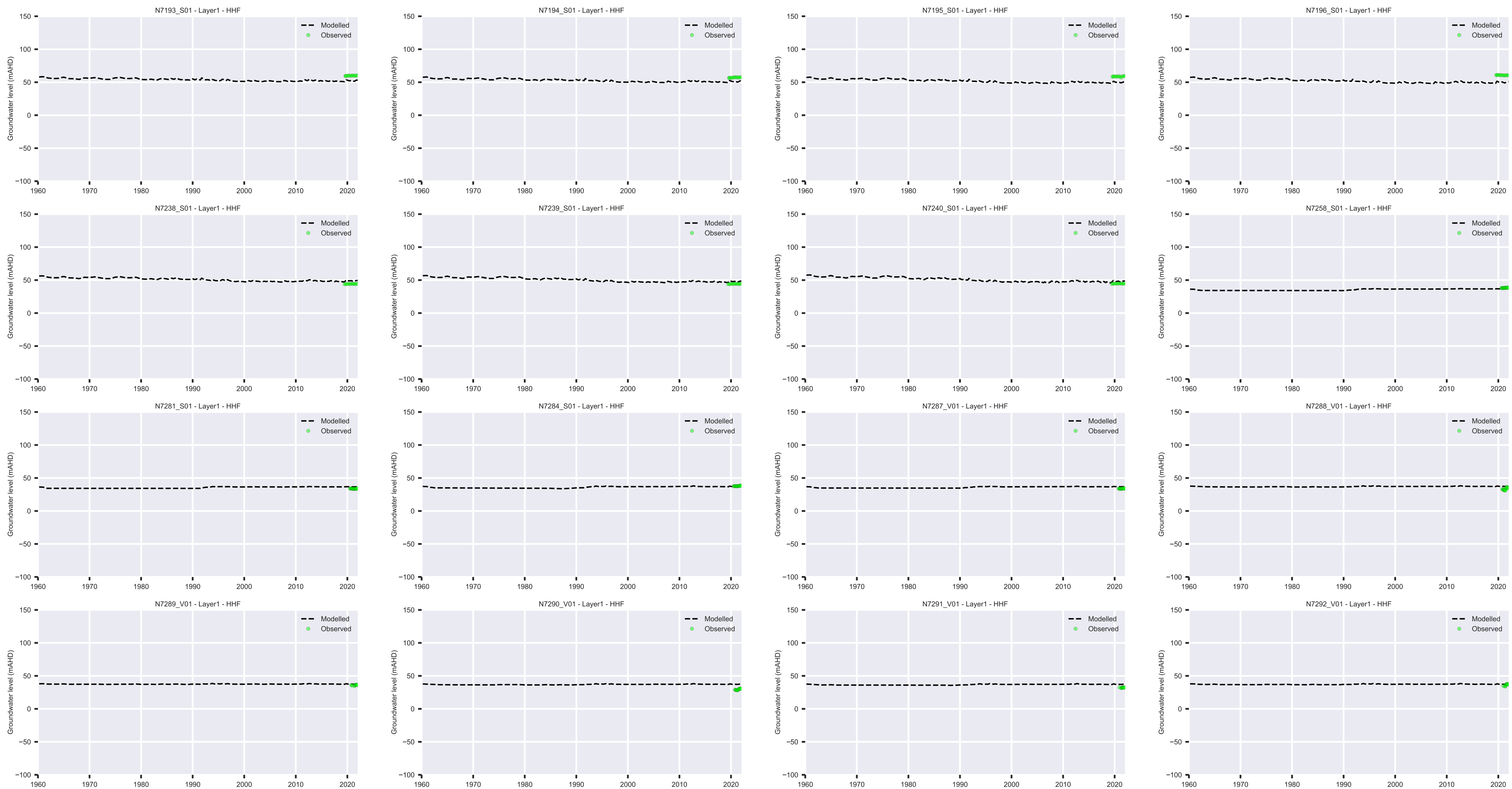
N7193_S01 - Layer1 - HHF
N7194_S01 - Layer1 - HHF
N7195_S01 - Layer1 - HHF
N7196_S01 - Layer1 - HHF
N7238_S01 - Layer1 - HHF
N7239_S01 - Layer1 - HHF
N7240_S01 - Layer1 - HHF
N7258_S01 - Layer1 - HHF
N7281_S01 - Layer1 - HHF
N7284_S01 - Layer1 - HHF
N7287_V01 - Layer1 - HHF
N7288_V01 - Layer1 - HHF
N7289_V01 - Layer1 - HHF
N7290_V01 - Layer1 - HHF
N7291_V01 - Layer1 - HHF
N7292_V01 - Layer1 - HHF
Modelled
Observed
Groundwater level (mAHD)
150
100
50
0
−50
−100
1960
1970
1980
1990
2000
2010
2020

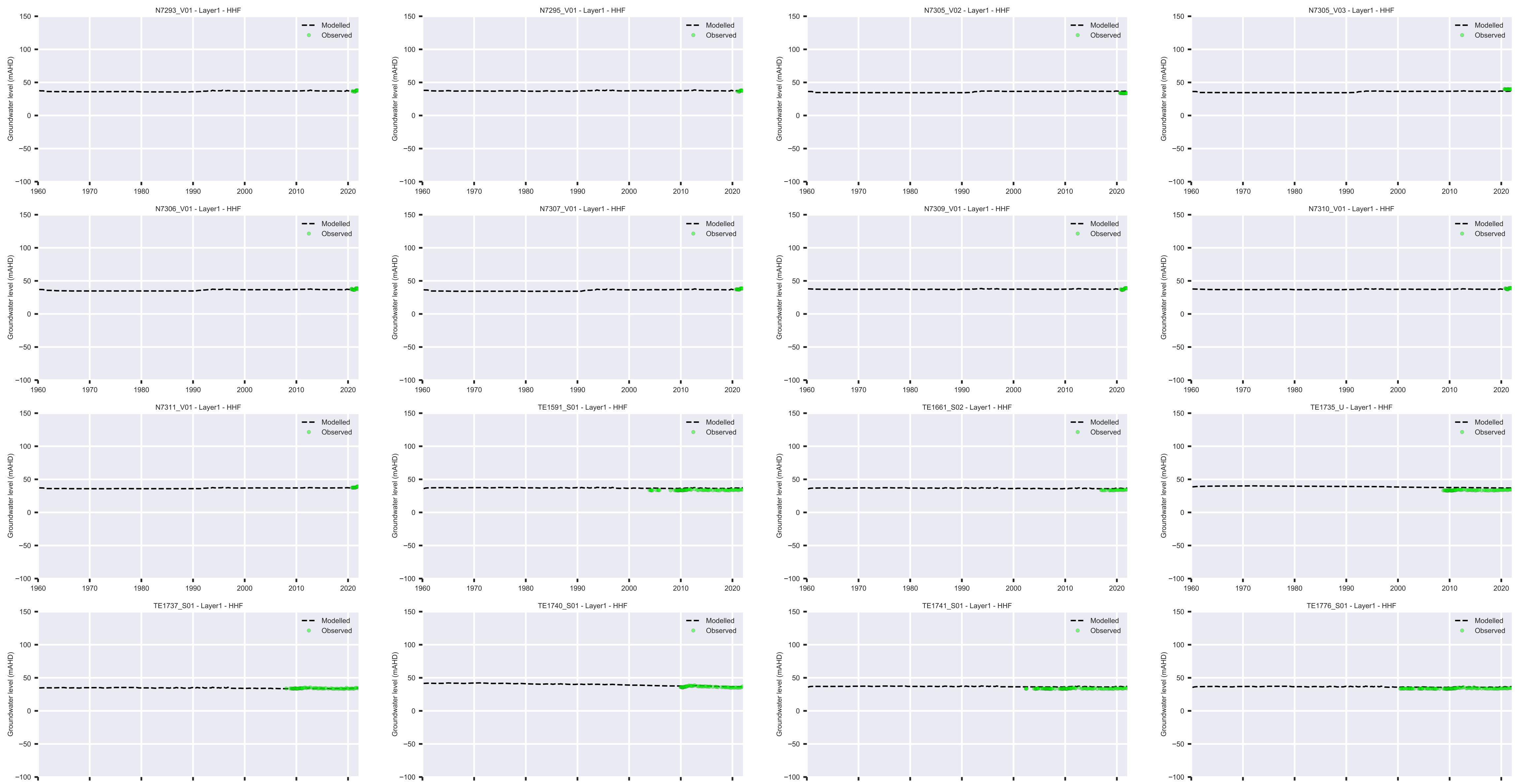
N7293_V01 - Layer1 - HHF
N7295_V01 - Layer1 - HHF
N7305_V02 - Layer1 - HHF
N7305_V03 - Layer1 - HHF
N7306_V01 - Layer1 - HHF
N7307_V01 - Layer1 - HHF
N7309_V01 - Layer1 - HHF
N7310_V01 - Layer1 - HHF
N7311_V01 - Layer1 - HHF
TE1591_S01 - Layer1 - HHF
TE1661_S02 - Layer1 - HHF
TE1735_U - Layer1 - HHF
TE1737_S01 - Layer1 - HHF
TE1740_S01 - Layer1 - HHF
TE1741_S01 - Layer1 - HHF
TE1776_S01 - Layer1 - HHF
Modelled
Observed
Groundwater level (mAHD)
150
100
50
0
−50
−100
1960
1970
1980
1990
2000
2010
2020

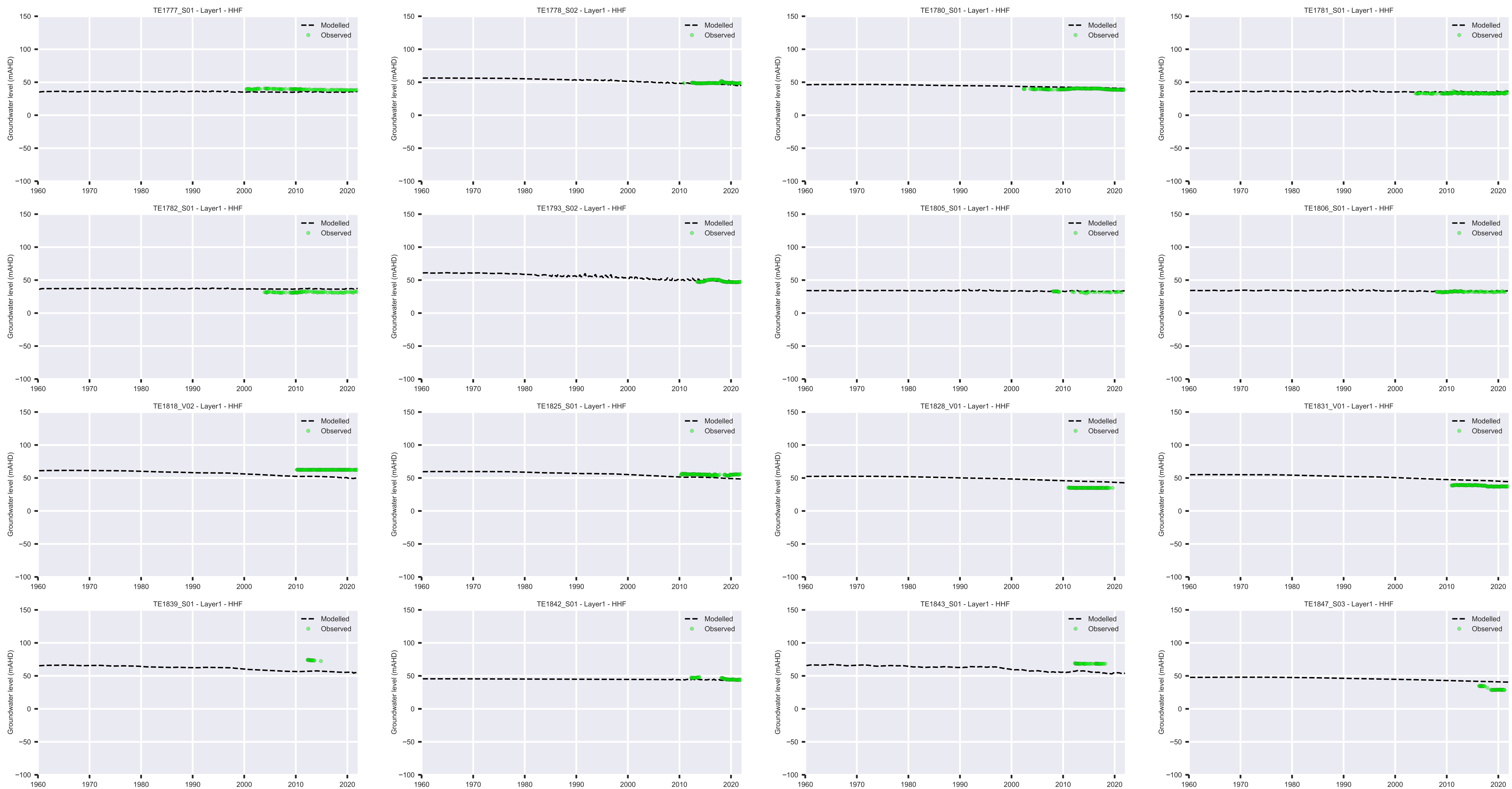
TE1777_S01 - Layer1 - HHF
TE1778_S02 - Layer1 - HHF
TE1780_S01 - Layer1 - HHF
TE1781_S01 - Layer1 - HHF
TE1782_S01 - Layer1 - HHF
TE1793_S02 - Layer1 - HHF
TE1805_S01 - Layer1 - HHF
TE1806_S01 - Layer1 - HHF
TE1818_V02 - Layer1 - HHF
TE1825_S01 - Layer1 - HHF
TE1828_V01 - Layer1 - HHF
TE1831_V01 - Layer1 - HHF
TE1839_S01 - Layer1 - HHF
TE1842_S01 - Layer1 - HHF
TE1843_S01 - Layer1 - HHF
TE1847_S03 - Layer1 - HHF
Modelled
Observed
Groundwater level (mAHD)
150
100
50
0
−50
−100
1960
1970
1980
1990
2000
2010
2020

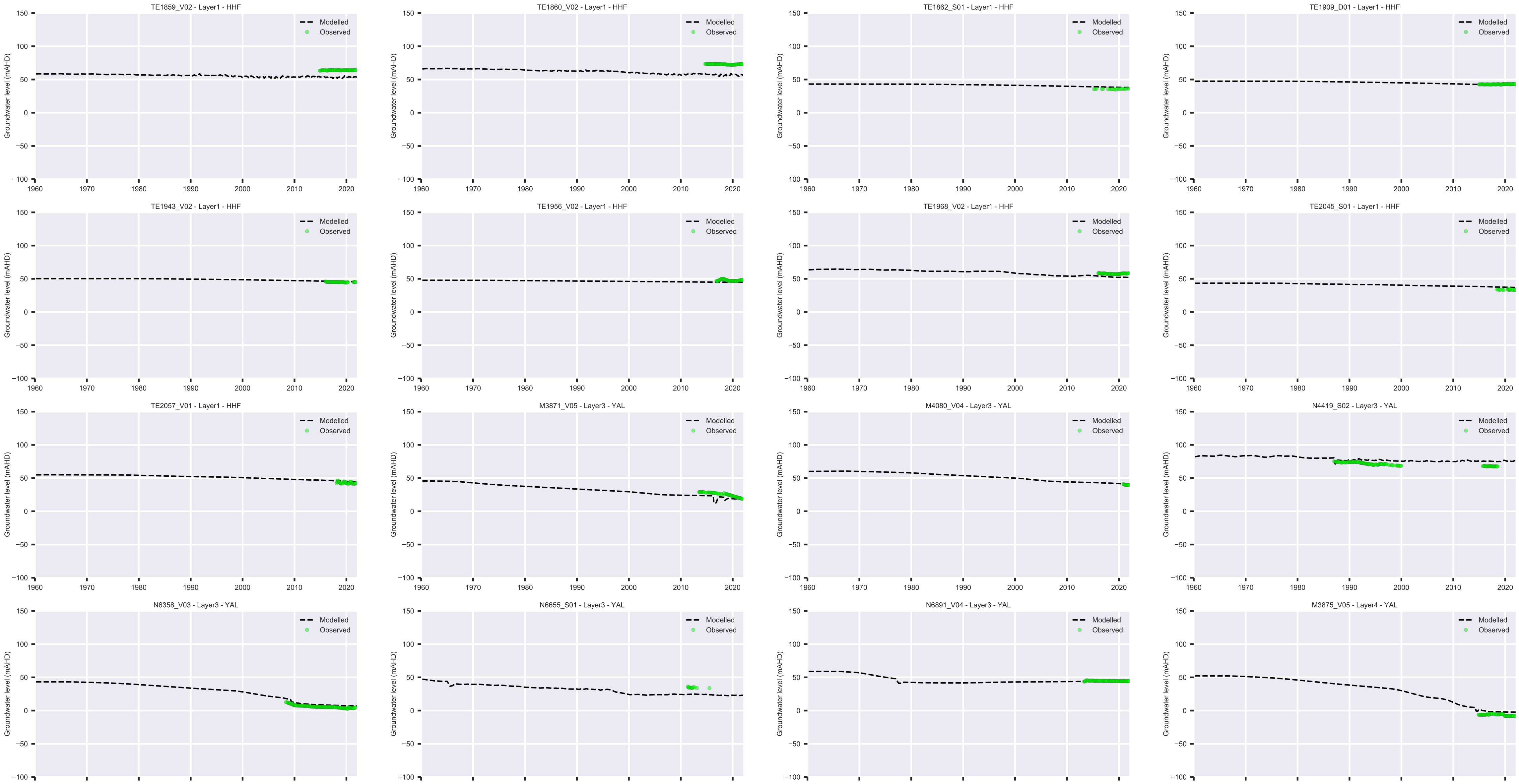
TE1859_V02 - Layer1 - HHF
TE1860_V02 - Layer1 - HHF
TE1862_S01 - Layer1 - HHF
TE1909_D01 - Layer1 - HHF
TE1943_V02 - Layer1 - HHF
TE1956_V02 - Layer1 - HHF
TE1968_V02 - Layer1 - HHF
TE2045_S01 - Layer1 - HHF
TE2057_V01 - Layer1 - HHF
M3871_V05 - Layer3 - YAL
M4080_V04 - Layer3 - YAL
N4419_S02 - Layer3 - YAL
N6358_V03 - Layer3 - YAL
N6655_S01 - Layer3 - YAL
N6891_V04 - Layer3 - YAL
M3875_V05 - Layer4 - YAL
Modelled
Observed
Groundwater level (mAHD)

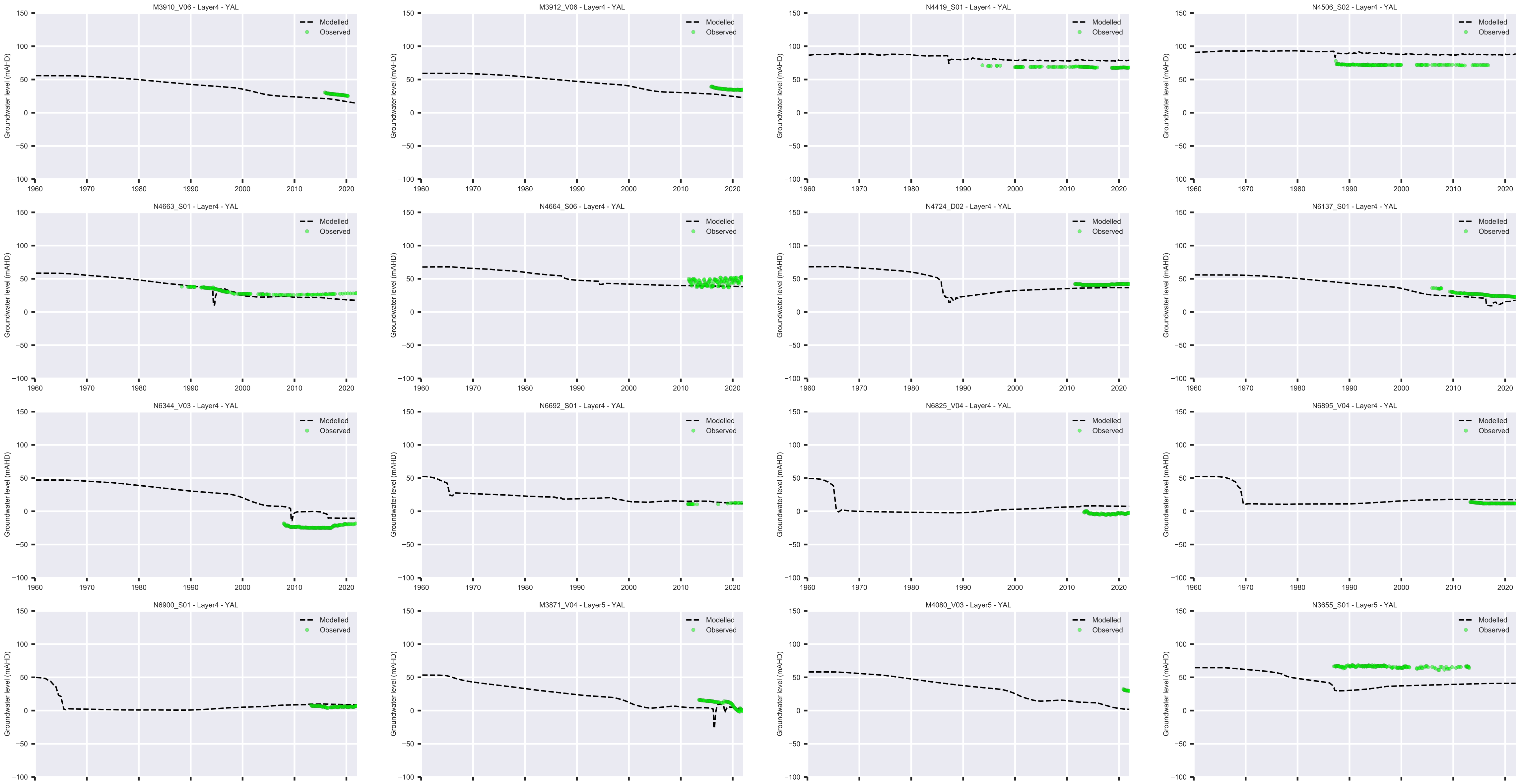
M3910_V06 - Layer4 - YAL
M3912_V06 - Layer4 - YAL
N4419_S01 - Layer4 - YAL
N4506_S02 - Layer4 - YAL
N4663_S01 - Layer4 - YAL
N4664_S06 - Layer4 - YAL
N4724_D02 - Layer4 - YAL
N6137_S01 - Layer4 - YAL
N6344_V03 - Layer4 - YAL
N6692_S01 - Layer4 - YAL
N6825_V04 - Layer4 - YAL
N6895_V04 - Layer4 - YAL
N6900_S01 - Layer4 - YAL
M3871_V04 - Layer5 - YAL
M4080_V03 - Layer5 - YAL
N3655_S01 - Layer5 - YAL
Modelled
Observed
Groundwater level (mAHD)

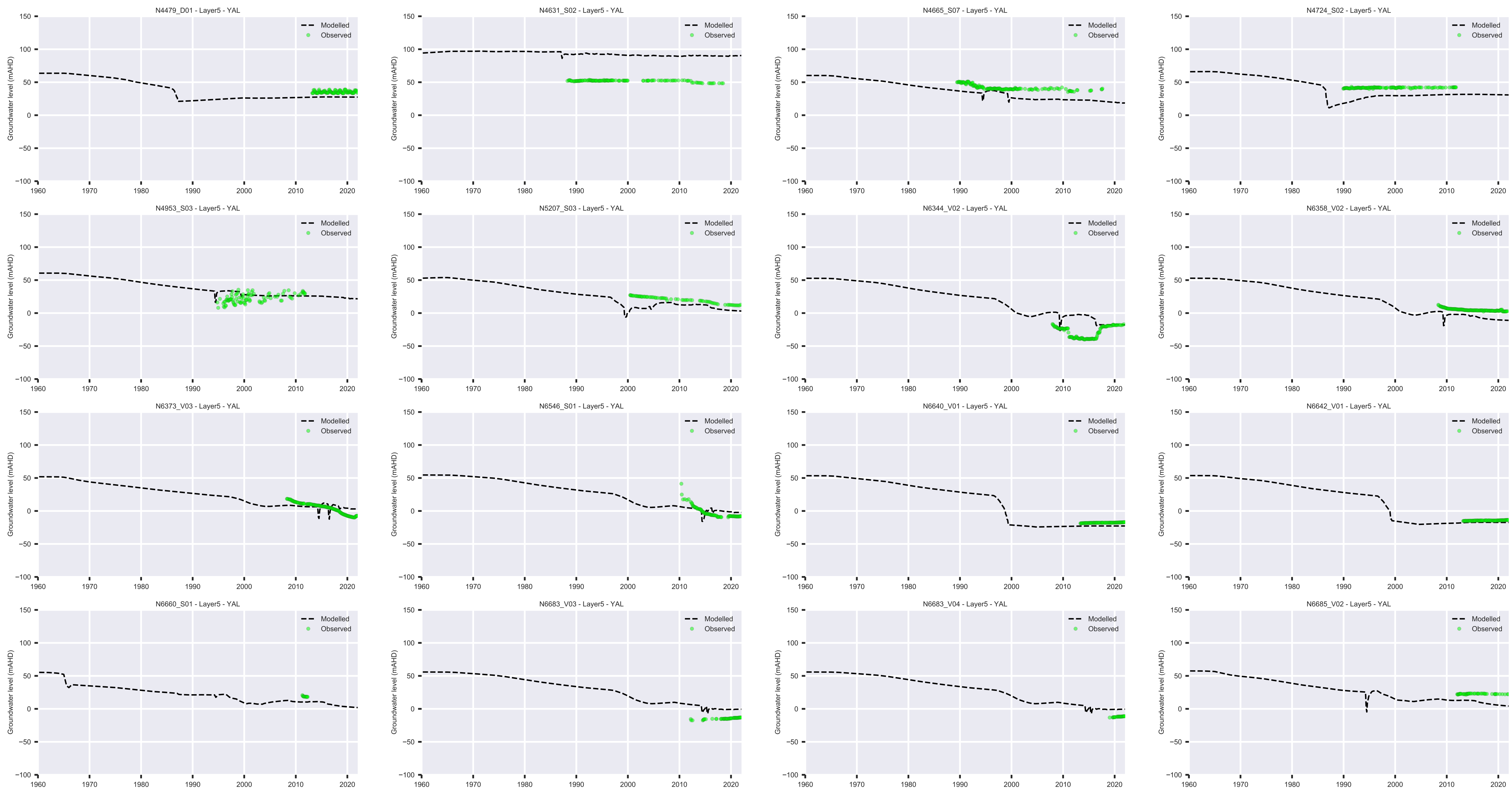
N4479_D01 - Layer5 - YAL
N4631_S02 - Layer5 - YAL
N4665_S07 - Layer5 - YAL
N4724_S02 - Layer5 - YAL
N4953_S03 - Layer5 - YAL
N5207_S03 - Layer5 - YAL
N6344_V02 - Layer5 - YAL
N6358_V02 - Layer5 - YAL
N6373_V03 - Layer5 - YAL
N6546_S01 - Layer5 - YAL
N6640_V01 - Layer5 - YAL
N6642_V01 - Layer5 - YAL
N6660_S01 - Layer5 - YAL
N6683_V03 - Layer5 - YAL
N6683_V04 - Layer5 - YAL
N6685_V02 - Layer5 - YAL
Modelled
Observed
Groundwater level (mAHD)
150
100
50
0
−50
−100
1960
1970
1980
1990
2000
2010
2020

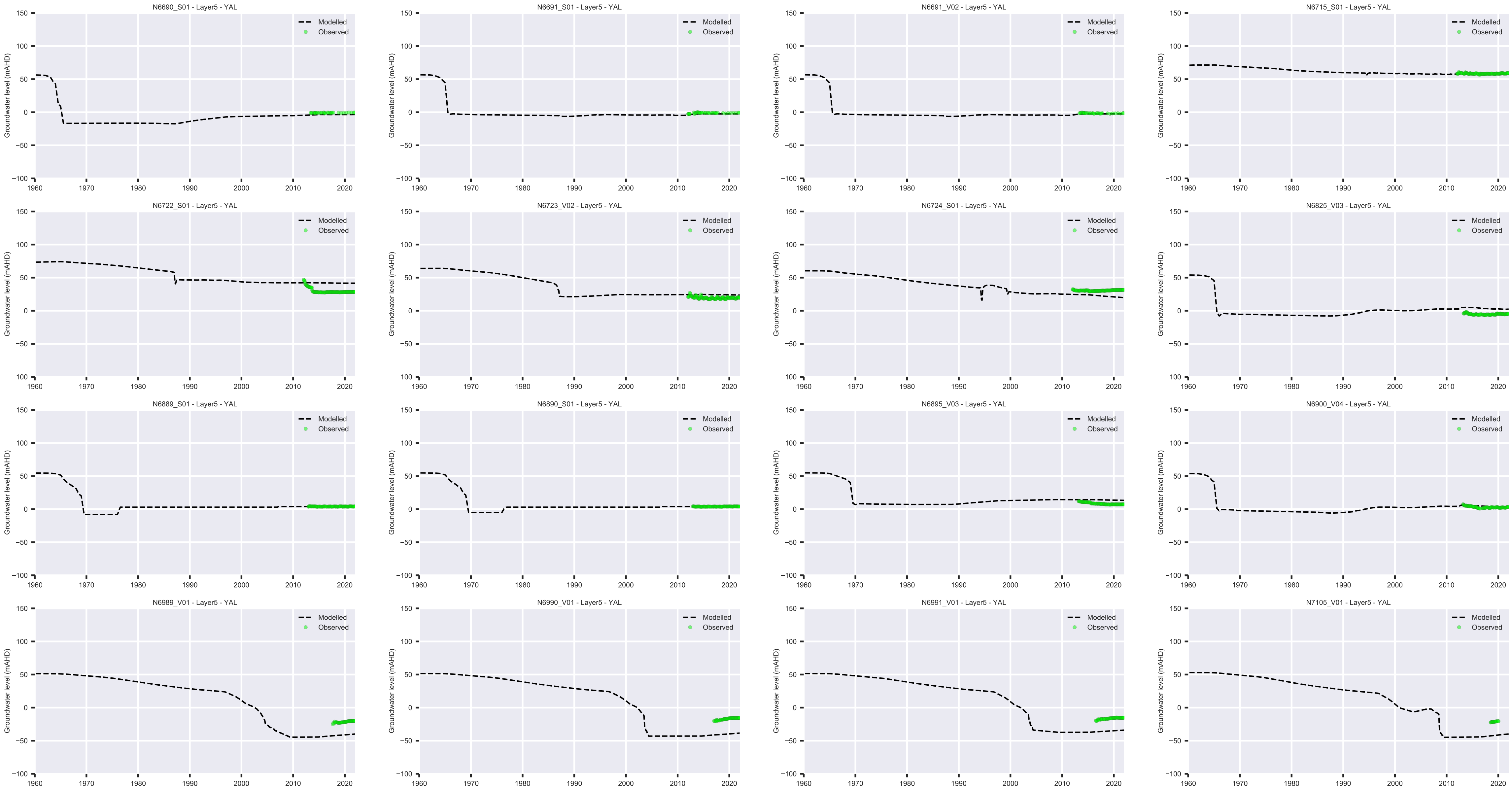
N6690_S01 - Layer5 - YAL
N6691_S01 - Layer5 - YAL
N6691_V02 - Layer5 - YAL
N6715_S01 - Layer5 - YAL
N6722_S01 - Layer5 - YAL
N6723_V02 - Layer5 - YAL
N6724_S01 - Layer5 - YAL
N6825_V03 - Layer5 - YAL
N6889_S01 - Layer5 - YAL
N6890_S01 - Layer5 - YAL
N6895_V03 - Layer5 - YAL
N6900_V04 - Layer5 - YAL
N6989_V01 - Layer5 - YAL
N6990_V01 - Layer5 - YAL
N6991_V01 - Layer5 - YAL
N7105_V01 - Layer5 - YAL
Modelled
Observed
Groundwater level (mAHD)
150
100
50
0
−50
−100
1960
1970
1980
1990
2000
2010
2020

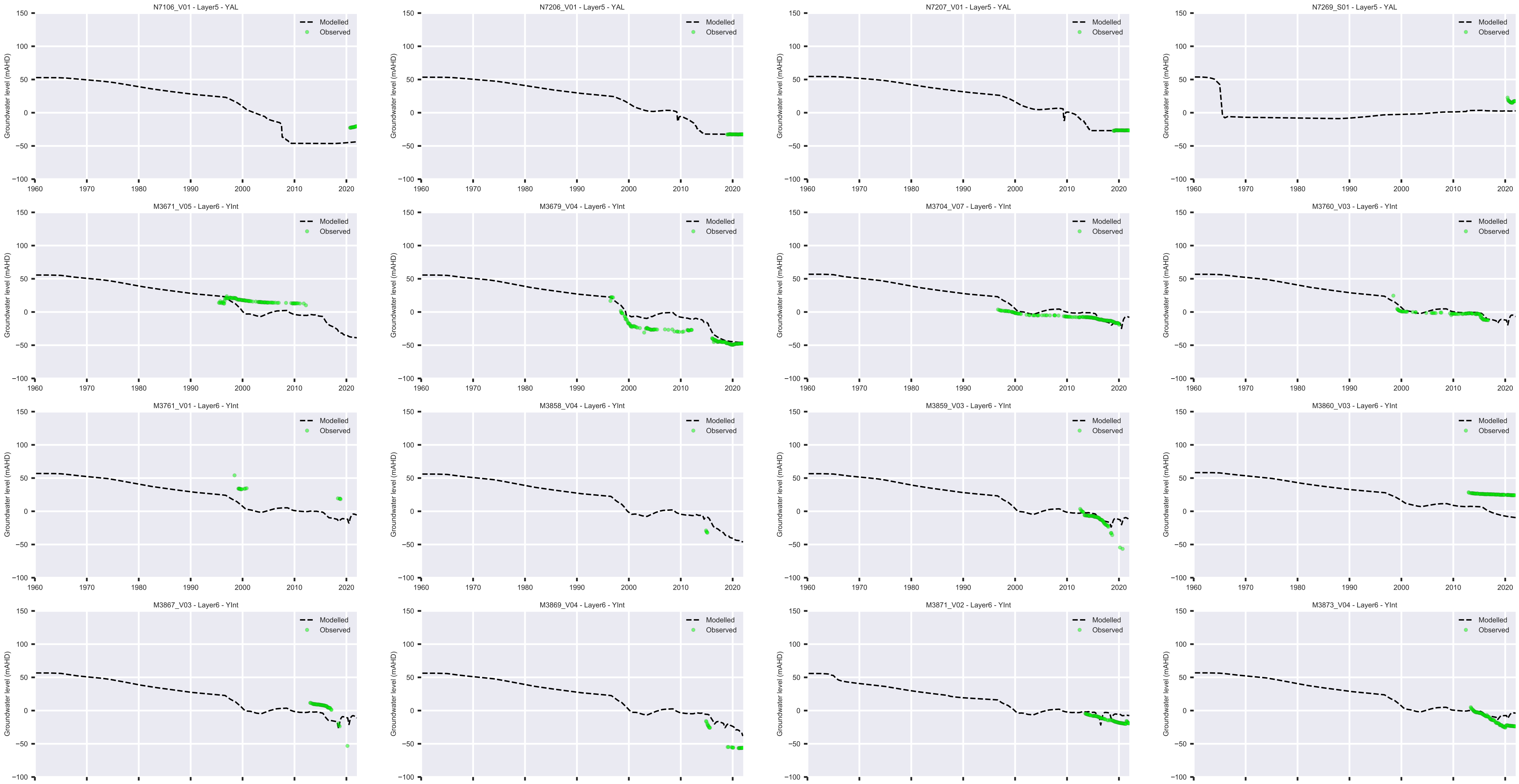
N7106_V01 - Layer5 - YAL
N7206_V01 - Layer5 - YAL
N7207_V01 - Layer5 - YAL
N7269_S01 - Layer5 - YAL
M3671_V05 - Layer6 - YInt
M3679_V04 - Layer6 - YInt
M3704_V07 - Layer6 - YInt
M3760_V03 - Layer6 - YInt
M3761_V01 - Layer6 - YInt
M3858_V04 - Layer6 - YInt
M3859_V03 - Layer6 - YInt
M3860_V03 - Layer6 - YInt
M3867_V03 - Layer6 - YInt
M3869_V04 - Layer6 - YInt
M3871_V02 - Layer6 - YInt
M3873_V04 - Layer6 - YInt
Modelled
Observed
Groundwater level (mAHD)
150
100
50
0
−50
−100
1960
1970
1980
1990
2000
2010
2020

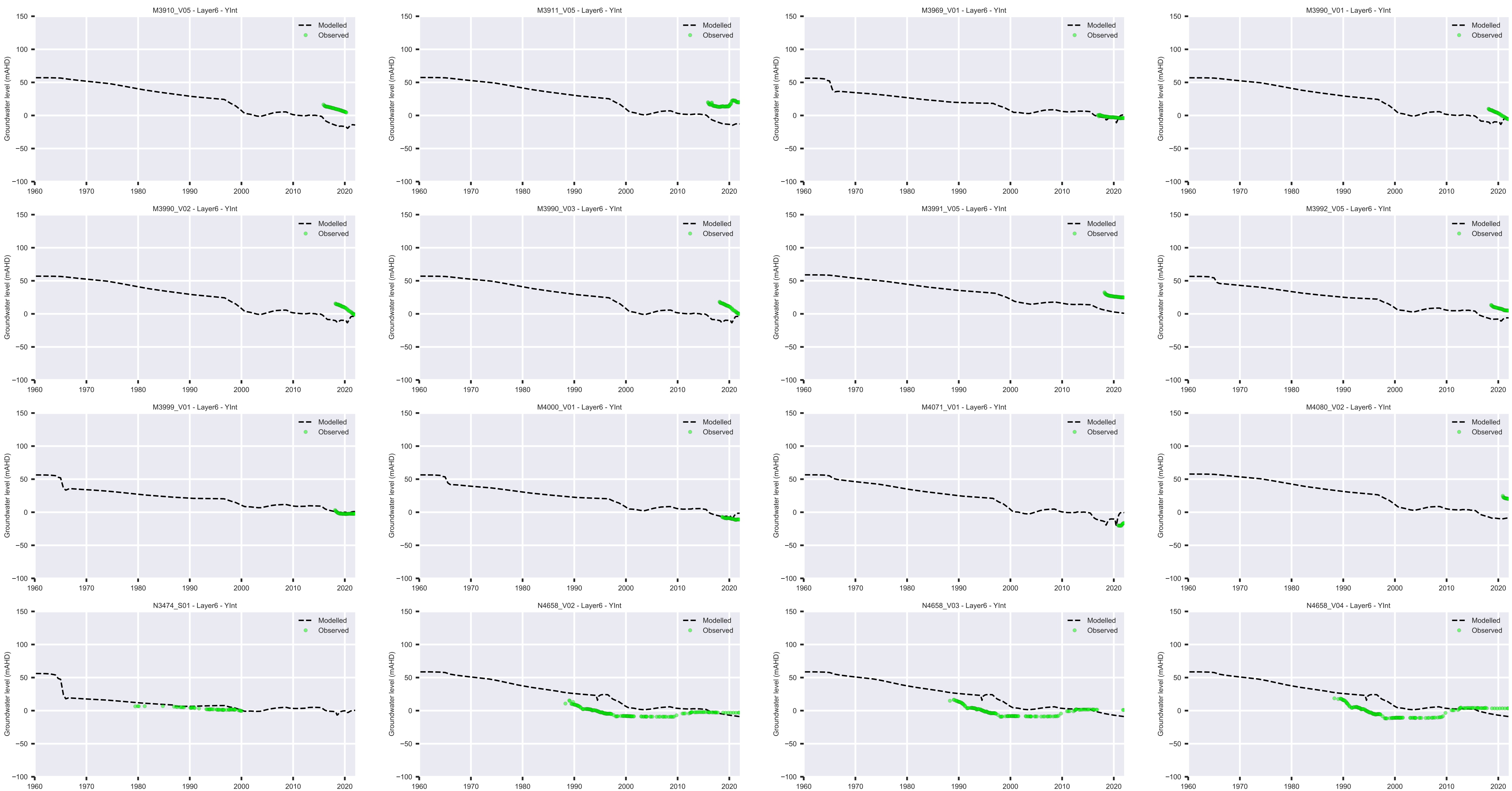
M3910_V05 - Layer6 - YInt
M3911_V05 - Layer6 - YInt
M3969_V01 - Layer6 - YInt
M3990_V01 - Layer6 - YInt
M3990_V02 - Layer6 - YInt
M3990_V03 - Layer6 - YInt
M3991_V05 - Layer6 - YInt
M3992_V05 - Layer6 - YInt
M3999_V01 - Layer6 - YInt
M4000_V01 - Layer6 - YInt
M4071_V01 - Layer6 - YInt
M4080_V02 - Layer6 - YInt
N3474_S01 - Layer6 - YInt
N4658_V02 - Layer6 - YInt
N4658_V03 - Layer6 - YInt
N4658_V04 - Layer6 - YInt
Modelled
Observed
Groundwater level (mAHD)
150
100
50
0
−50
−100
1960
1970
1980
1990
2000
2010
2020

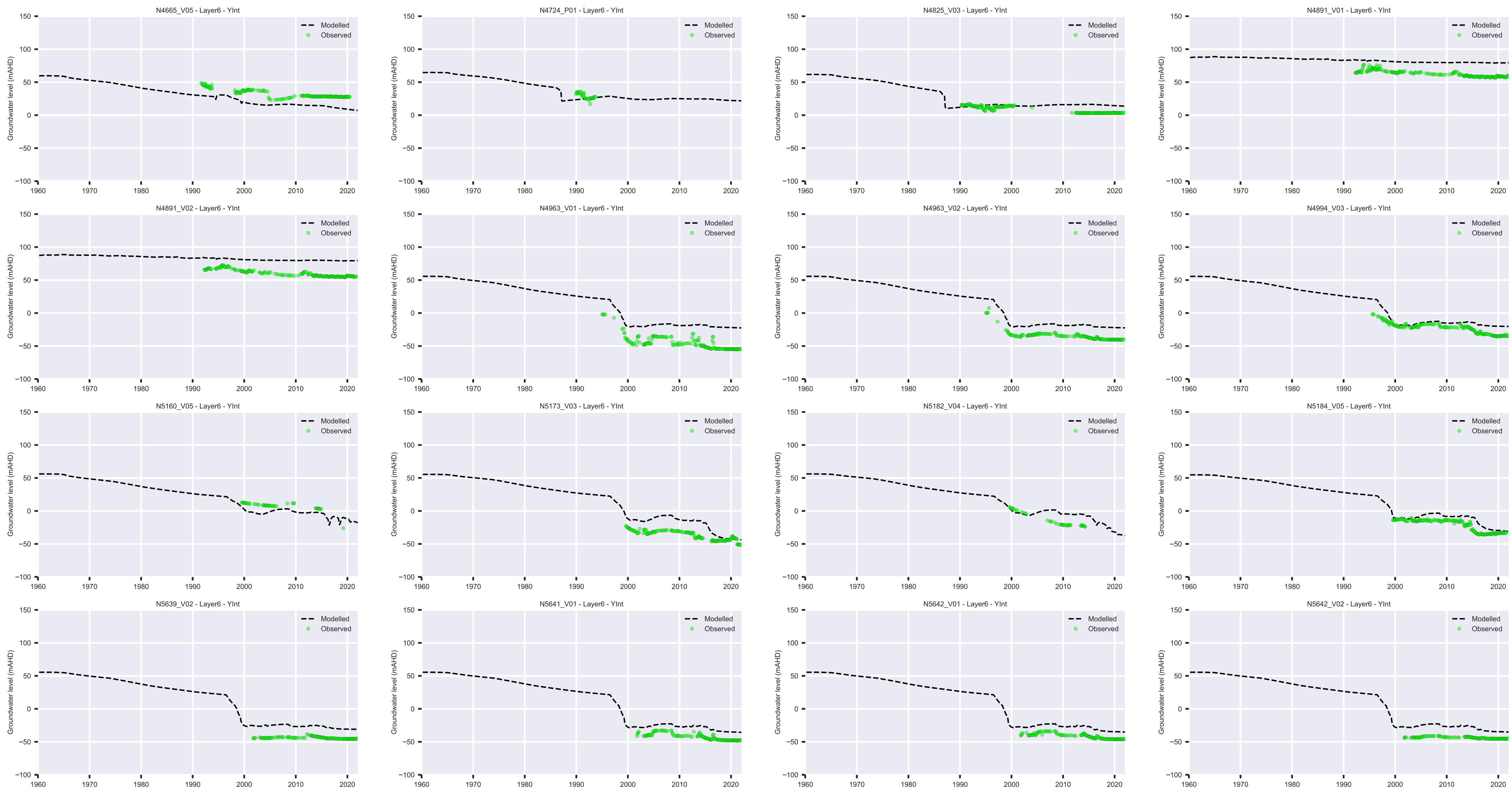
N4665_V05 - Layer6 - YInt
N4724_P01 - Layer6 - YInt
N4825_V03 - Layer6 - YInt
N4891_V01 - Layer6 - YInt
N4891_V02 - Layer6 - YInt
N4963_V01 - Layer6 - YInt
N4963_V02 - Layer6 - YInt
N4994_V03 - Layer6 - YInt
N5160_V05 - Layer6 - YInt
N5173_V03 - Layer6 - YInt
N5182_V04 - Layer6 - YInt
N5184_V05 - Layer6 - YInt
N5639_V02 - Layer6 - YInt
N5641_V01 - Layer6 - YInt
N5642_V01 - Layer6 - YInt
N5642_V02 - Layer6 - YInt
Modelled
Observed
Groundwater level (mAHD)

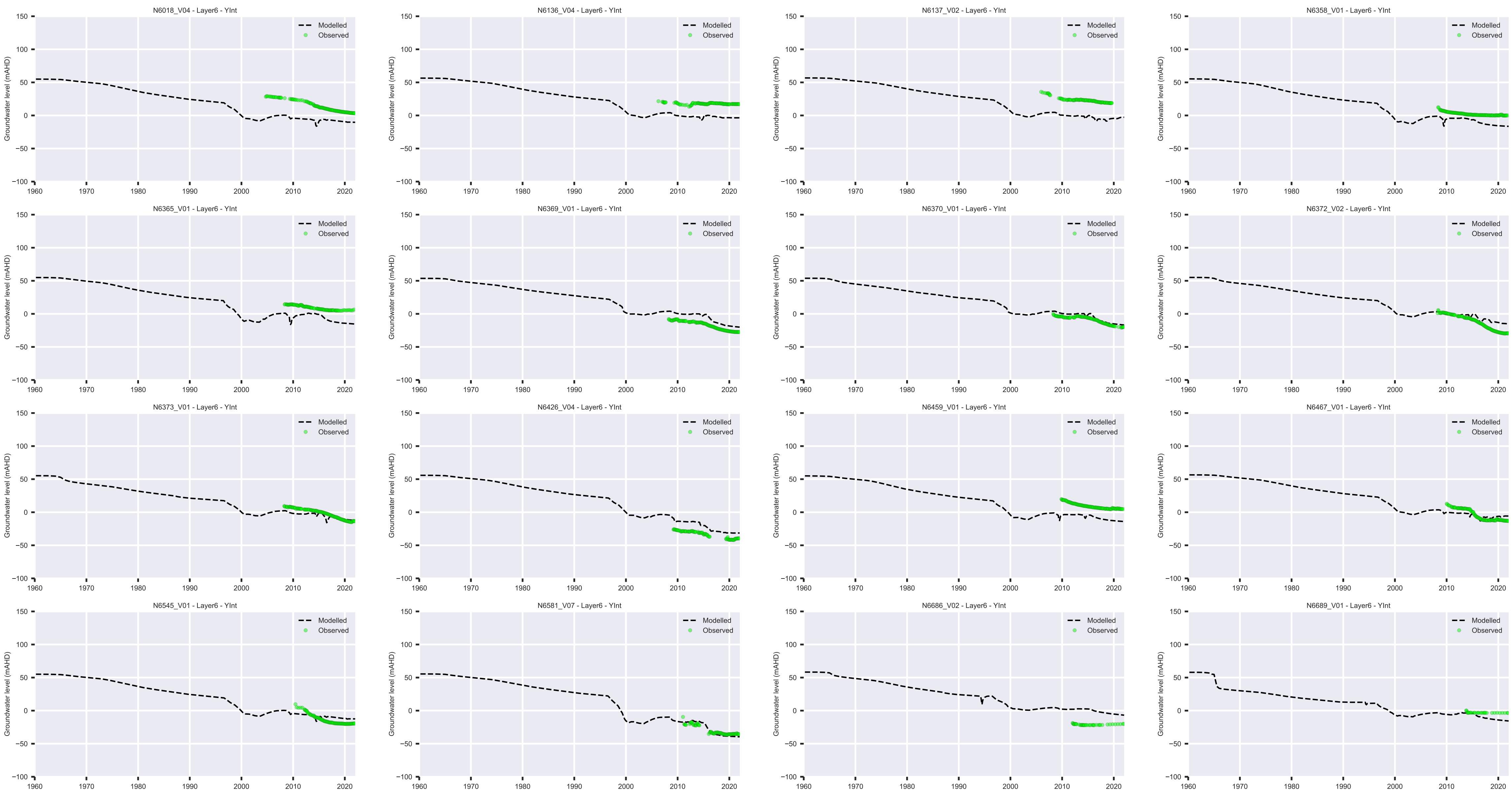

N6018_V04 - Layer6 - YInt
N6136_V04 - Layer6 - YInt
N6137_V02 - Layer6 - YInt
N6358_V01 - Layer6 - YInt
N6365_V01 - Layer6 - YInt
N6369_V01 - Layer6 - YInt
N6370_V01 - Layer6 - YInt
N6372_V02 - Layer6 - YInt
N6373_V01 - Layer6 - YInt
N6426_V04 - Layer6 - YInt
N6459_V01 - Layer6 - YInt
N6467_V01 - Layer6 - YInt
N6545_V01 - Layer6 - YInt
N6581_V07 - Layer6 - YInt
N6686_V02 - Layer6 - YInt
N6689_V01 - Layer6 - YInt
Groundwater level (mAHD)
Modelled
Observed

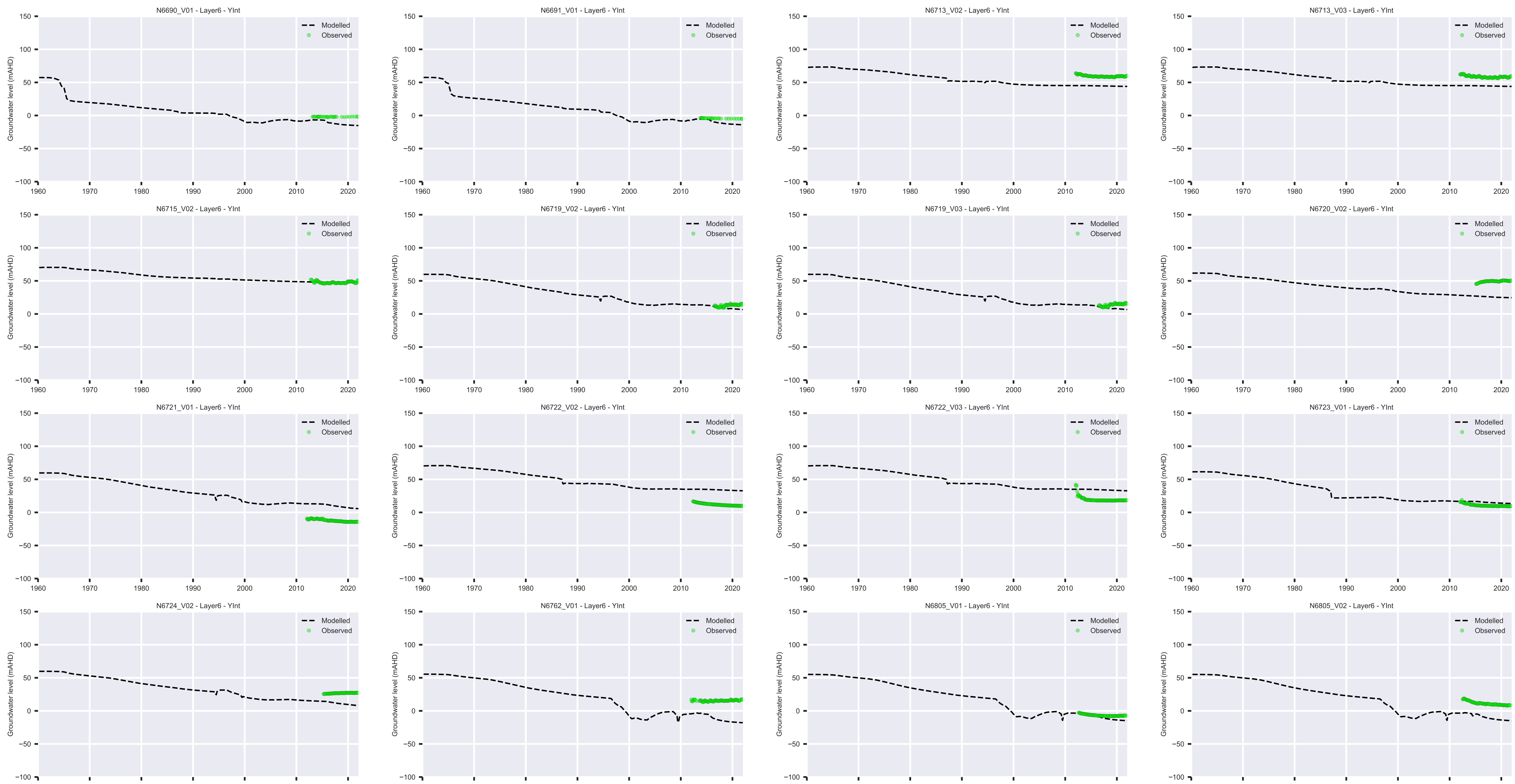
N6690_V01 - Layer6 - YInt
N6691_V01 - Layer6 - YInt
N6713_V02 - Layer6 - YInt
N6713_V03 - Layer6 - YInt
N6715_V02 - Layer6 - YInt
N6719_V02 - Layer6 - YInt
N6719_V03 - Layer6 - YInt
N6720_V02 - Layer6 - YInt
N6721_V01 - Layer6 - YInt
N6722_V02 - Layer6 - YInt
N6722_V03 - Layer6 - YInt
N6723_V01 - Layer6 - YInt
N6724_V02 - Layer6 - YInt
N6762_V01 - Layer6 - YInt
N6805_V01 - Layer6 - YInt
N6805_V02 - Layer6 - YInt
Modelled
Observed
Groundwater level (mAHD)
150
100
50
0
−50
−100
1960
1970
1980
1990
2000
2010
2020

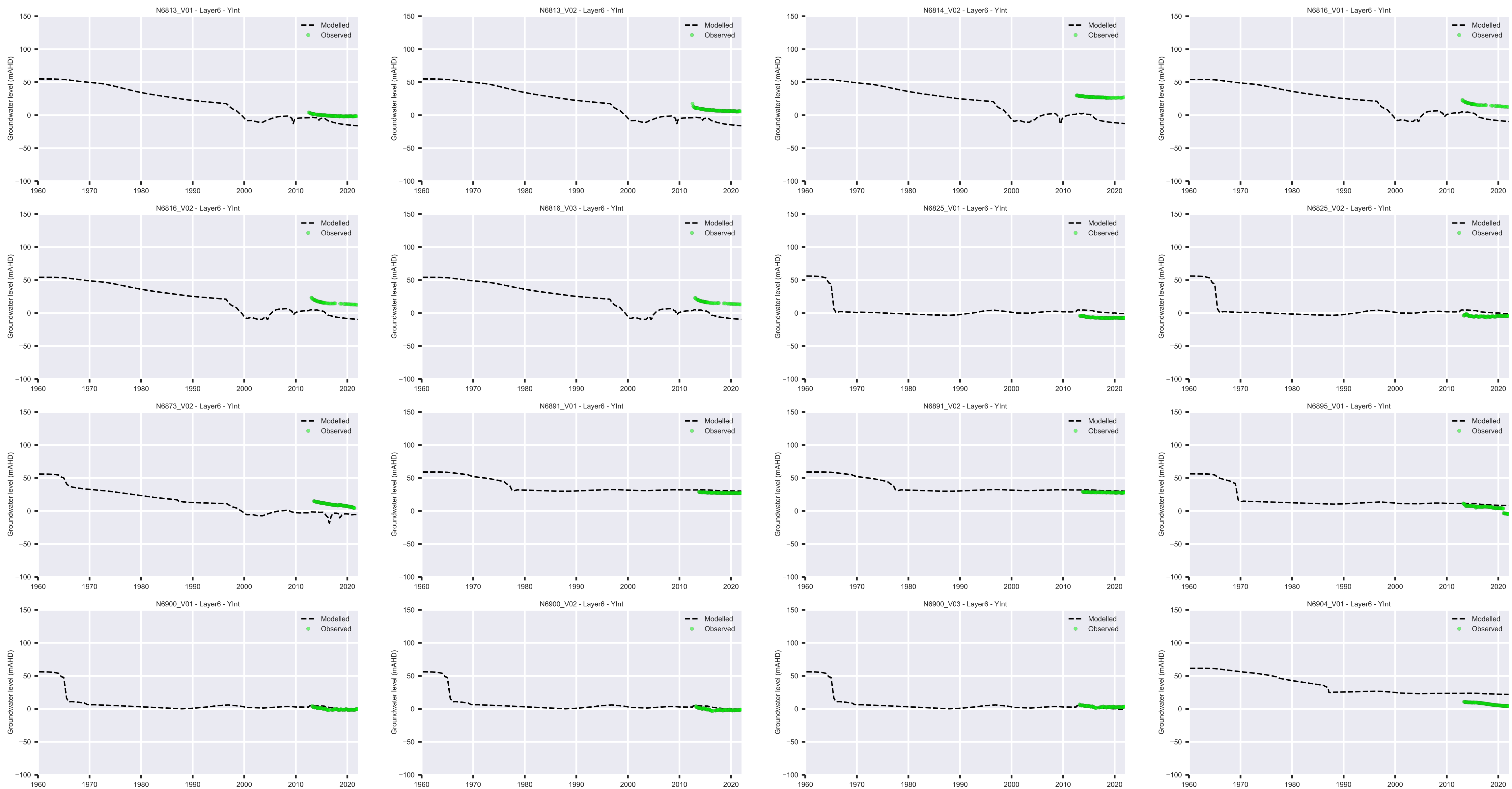

N6813_V01 - Layer6 - YInt
N6813_V02 - Layer6 - YInt
N6814_V02 - Layer6 - YInt
N6816_V01 - Layer6 - YInt
N6816_V02 - Layer6 - YInt
N6816_V03 - Layer6 - YInt
N6825_V01 - Layer6 - YInt
N6825_V02 - Layer6 - YInt
N6873_V02 - Layer6 - YInt
N6891_V01 - Layer6 - YInt
N6891_V02 - Layer6 - YInt
N6895_V01 - Layer6 - YInt
N6900_V01 - Layer6 - YInt
N6900_V02 - Layer6 - YInt
N6900_V03 - Layer6 - YInt
N6904_V01 - Layer6 - YInt
Modelled
Observed
Groundwater level (mAHD)
150
100
50
0
−50
−100
1960
1970
1980
1990
2000
2010
2020

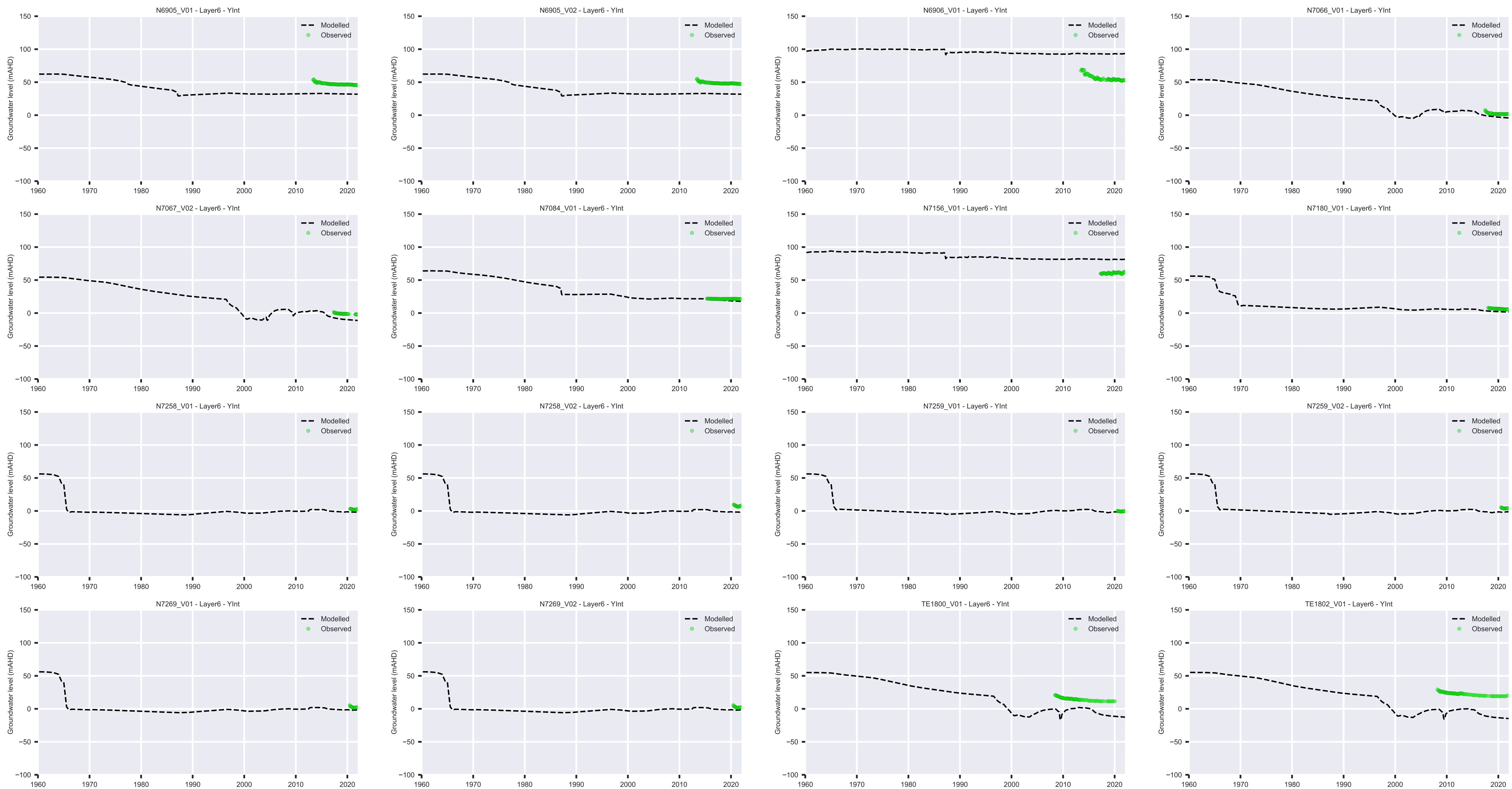
N6905_V01 - Layer6 - YInt
N6905_V02 - Layer6 - YInt
N6906_V01 - Layer6 - YInt
N7066_V01 - Layer6 - YInt
N7067_V02 - Layer6 - YInt
N7084_V01 - Layer6 - YInt
N7156_V01 - Layer6 - YInt
N7180_V01 - Layer6 - YInt
N7258_V01 - Layer6 - YInt
N7258_V02 - Layer6 - YInt
N7259_V01 - Layer6 - YInt
N7259_V02 - Layer6 - YInt
N7269_V01 - Layer6 - YInt
N7269_V02 - Layer6 - YInt
TE1800_V01 - Layer6 - YInt
TE1802_V01 - Layer6 - YInt
Modelled
Observed
Groundwater level (mAHD)
150
100
50
0
−50
−100
1960
1970
1980
1990
2000
2010
2020

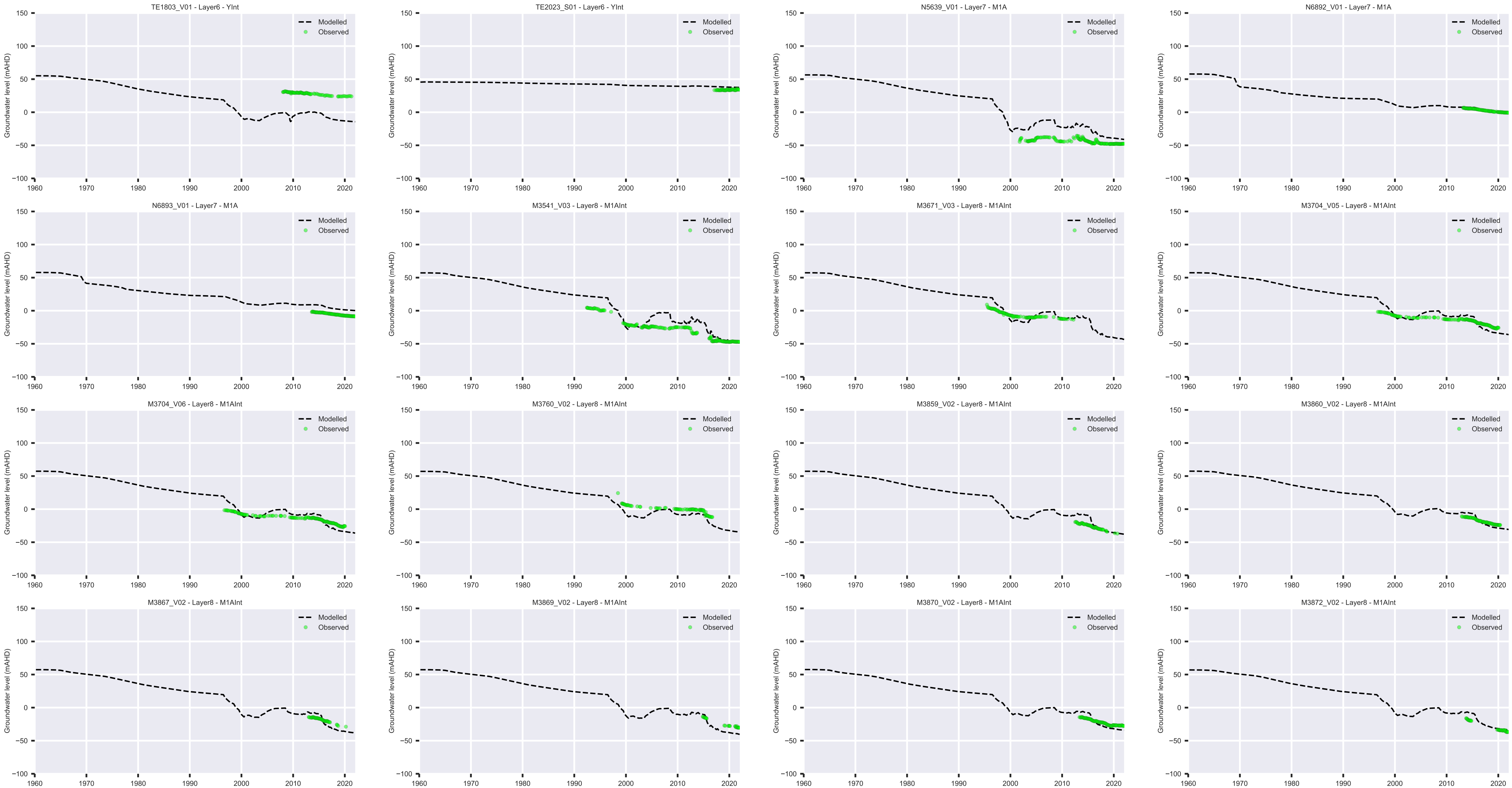
TE1803_V01 - Layer6 - YInt
TE2023_S01 - Layer6 - YInt
N5639_V01 - Layer7 - M1A
N6892_V01 - Layer7 - M1A
N6893_V01 - Layer7 - M1A
M3541_V03 - Layer8 - M1AInt
M3671_V03 - Layer8 - M1AInt
M3704_V05 - Layer8 - M1AInt
M3704_V06 - Layer8 - M1AInt
M3760_V02 - Layer8 - M1AInt
M3859_V02 - Layer8 - M1AInt
M3860_V02 - Layer8 - M1AInt
M3867_V02 - Layer8 - M1AInt
M3869_V02 - Layer8 - M1AInt
M3870_V02 - Layer8 - M1AInt
M3872_V02 - Layer8 - M1AInt
Modelled
Observed
Groundwater level (mAHD)

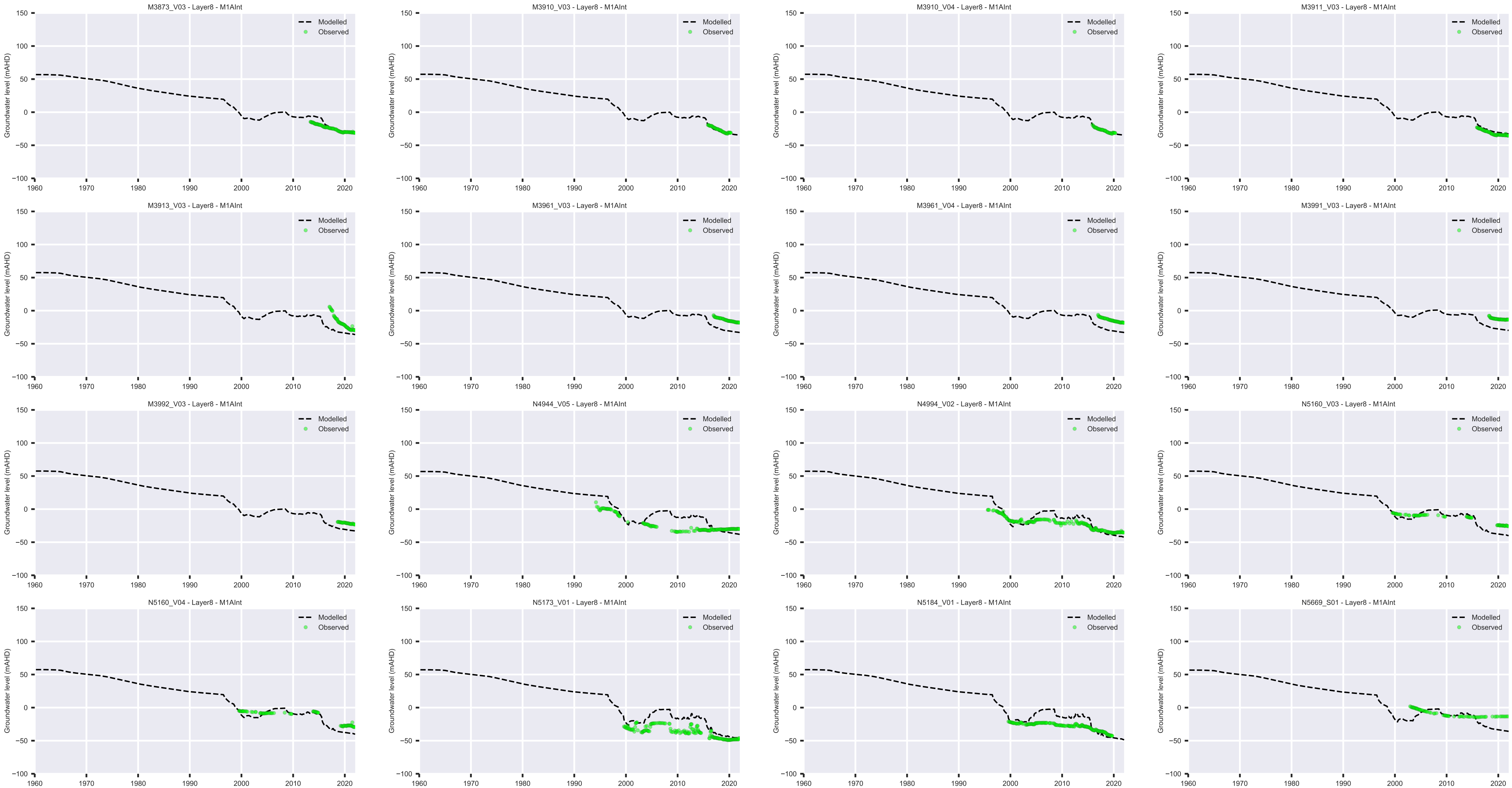
M3873_V03 - Layer8 - M1AInt
M3910_V03 - Layer8 - M1AInt
M3910_V04 - Layer8 - M1AInt
M3911_V03 - Layer8 - M1AInt
M3913_V03 - Layer8 - M1AInt
M3961_V03 - Layer8 - M1AInt
M3961_V04 - Layer8 - M1AInt
M3991_V03 - Layer8 - M1AInt
M3992_V03 - Layer8 - M1AInt
N4944_V05 - Layer8 - M1AInt
N4994_V02 - Layer8 - M1AInt
N5160_V03 - Layer8 - M1AInt
N5160_V04 - Layer8 - M1AInt
N5173_V01 - Layer8 - M1AInt
N5184_V01 - Layer8 - M1AInt
N5669_S01 - Layer8 - M1AInt
Modelled
Observed
Groundwater level (mAHD)
150
100
50
0
−50
−100
1960
1970
1980
1990
2000
2010
2020

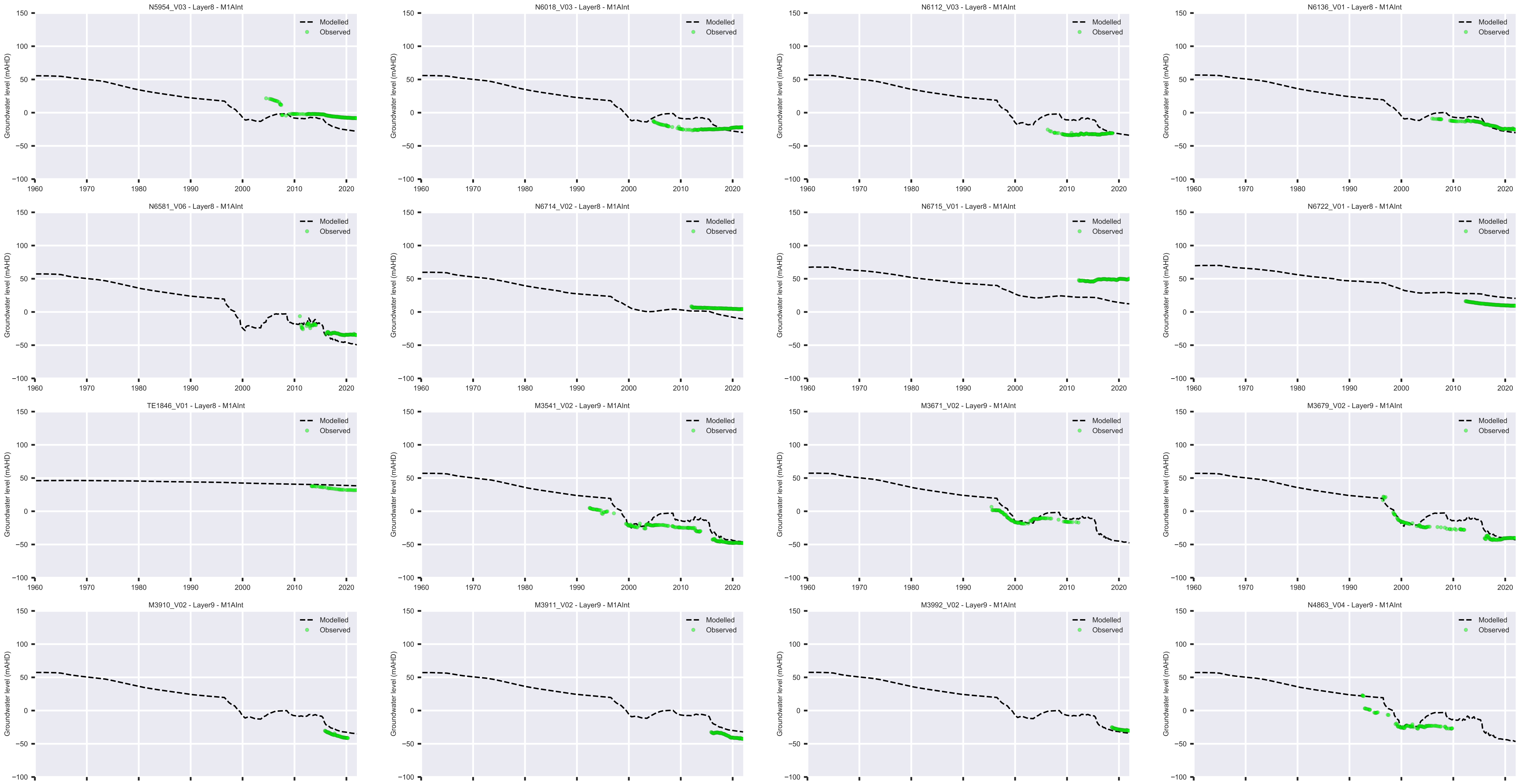
N5954_V03 - Layer8 - M1AInt
N6018_V03 - Layer8 - M1AInt
N6112_V03 - Layer8 - M1AInt
N6136_V01 - Layer8 - M1AInt
N6581_V06 - Layer8 - M1AInt
N6714_V02 - Layer8 - M1AInt
N6715_V01 - Layer8 - M1AInt
N6722_V01 - Layer8 - M1AInt
TE1846_V01 - Layer8 - M1AInt
M3541_V02 - Layer9 - M1AInt
M3671_V02 - Layer9 - M1AInt
M3679_V02 - Layer9 - M1AInt
M3910_V02 - Layer9 - M1AInt
M3911_V02 - Layer9 - M1AInt
M3992_V02 - Layer9 - M1AInt
N4863_V04 - Layer9 - M1AInt
Modelled
Observed
Groundwater level (mAHD)
150
100
50
0
−50
−100
1960
1970
1980
1990
2000
2010
2020

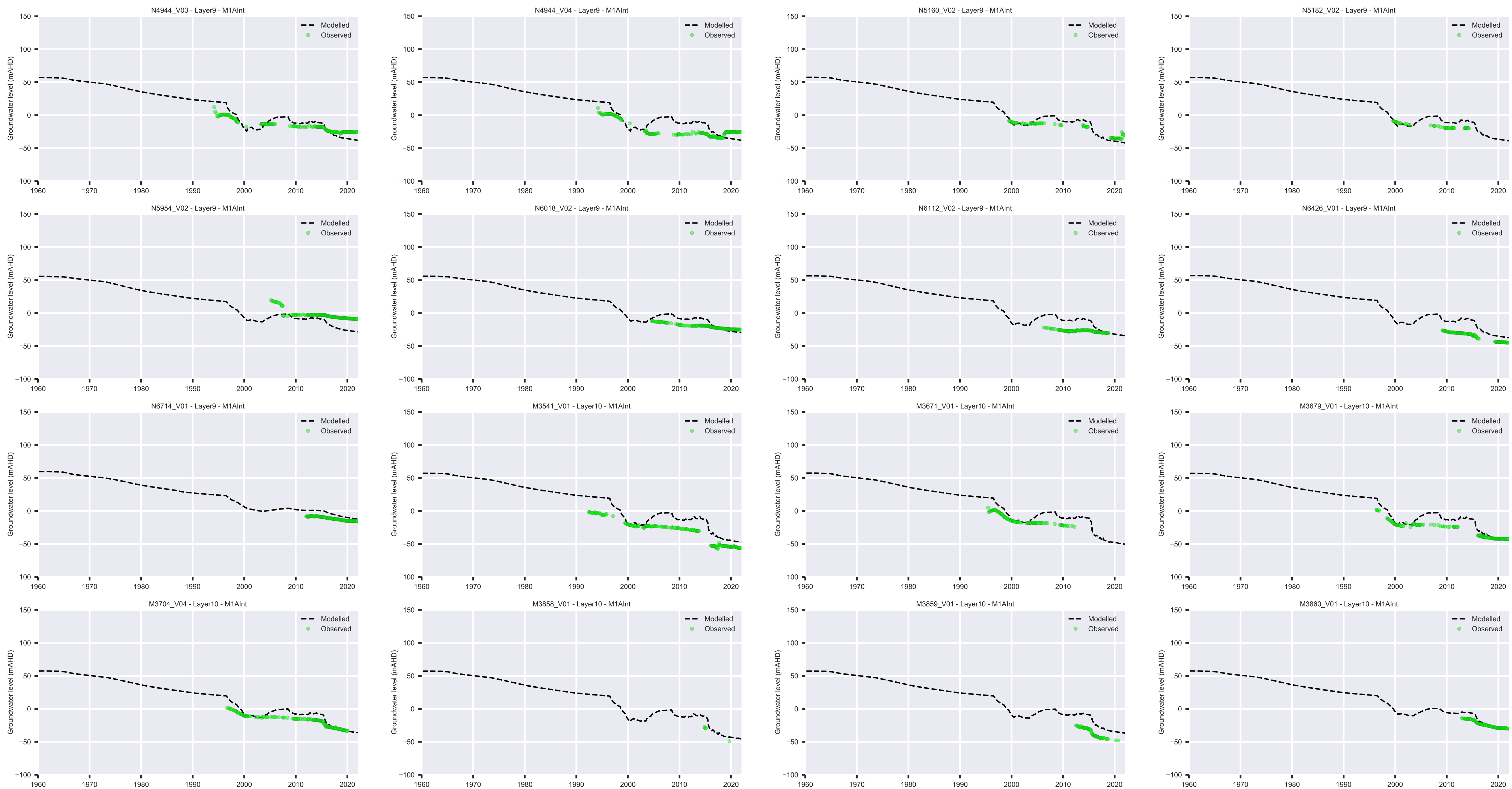

N4944_V03 - Layer9 - M1AInt
N4944_V04 - Layer9 - M1AInt
N5160_V02 - Layer9 - M1AInt
N5182_V02 - Layer9 - M1AInt
N5954_V02 - Layer9 - M1AInt
N6018_V02 - Layer9 - M1AInt
N6112_V02 - Layer9 - M1AInt
N6426_V01 - Layer9 - M1AInt
N6714_V01 - Layer9 - M1AInt
M3541_V01 - Layer10 - M1AInt
M3671_V01 - Layer10 - M1AInt
M3679_V01 - Layer10 - M1AInt
M3704_V04 - Layer10 - M1AInt
M3858_V01 - Layer10 - M1AInt
M3859_V01 - Layer10 - M1AInt
M3860_V01 - Layer10 - M1AInt
Modelled
Observed
Groundwater level (mAHD)
150
100
50
0
−50
−100
1960
1970
1980
1990
2000
2010
2020

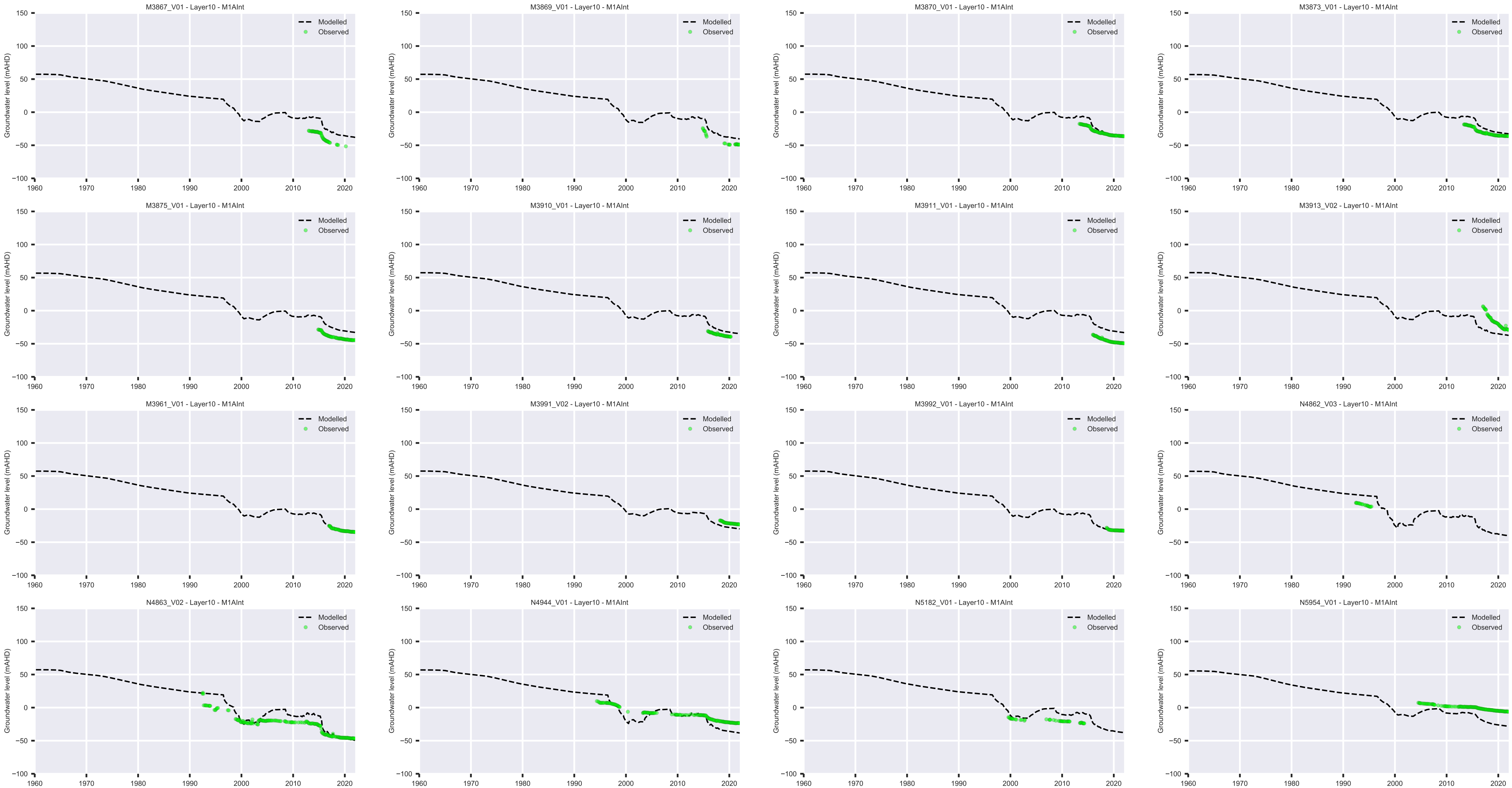
M3867_V01 - Layer10 - M1AInt
M3869_V01 - Layer10 - M1AInt
M3870_V01 - Layer10 - M1AInt
M3873_V01 - Layer10 - M1AInt
M3875_V01 - Layer10 - M1AInt
M3910_V01 - Layer10 - M1AInt
M3911_V01 - Layer10 - M1AInt
M3913_V02 - Layer10 - M1AInt
M3961_V01 - Layer10 - M1AInt
M3991_V02 - Layer10 - M1AInt
M3992_V01 - Layer10 - M1AInt
N4862_V03 - Layer10 - M1AInt
N4863_V02 - Layer10 - M1AInt
N4944_V01 - Layer10 - M1AInt
N5182_V01 - Layer10 - M1AInt
N5954_V01 - Layer10 - M1AInt
Modelled
Observed
Groundwater level (mAHD)
150
100
50
0
−50
−100
1960
1970
1980
1990
2000
2010
2020

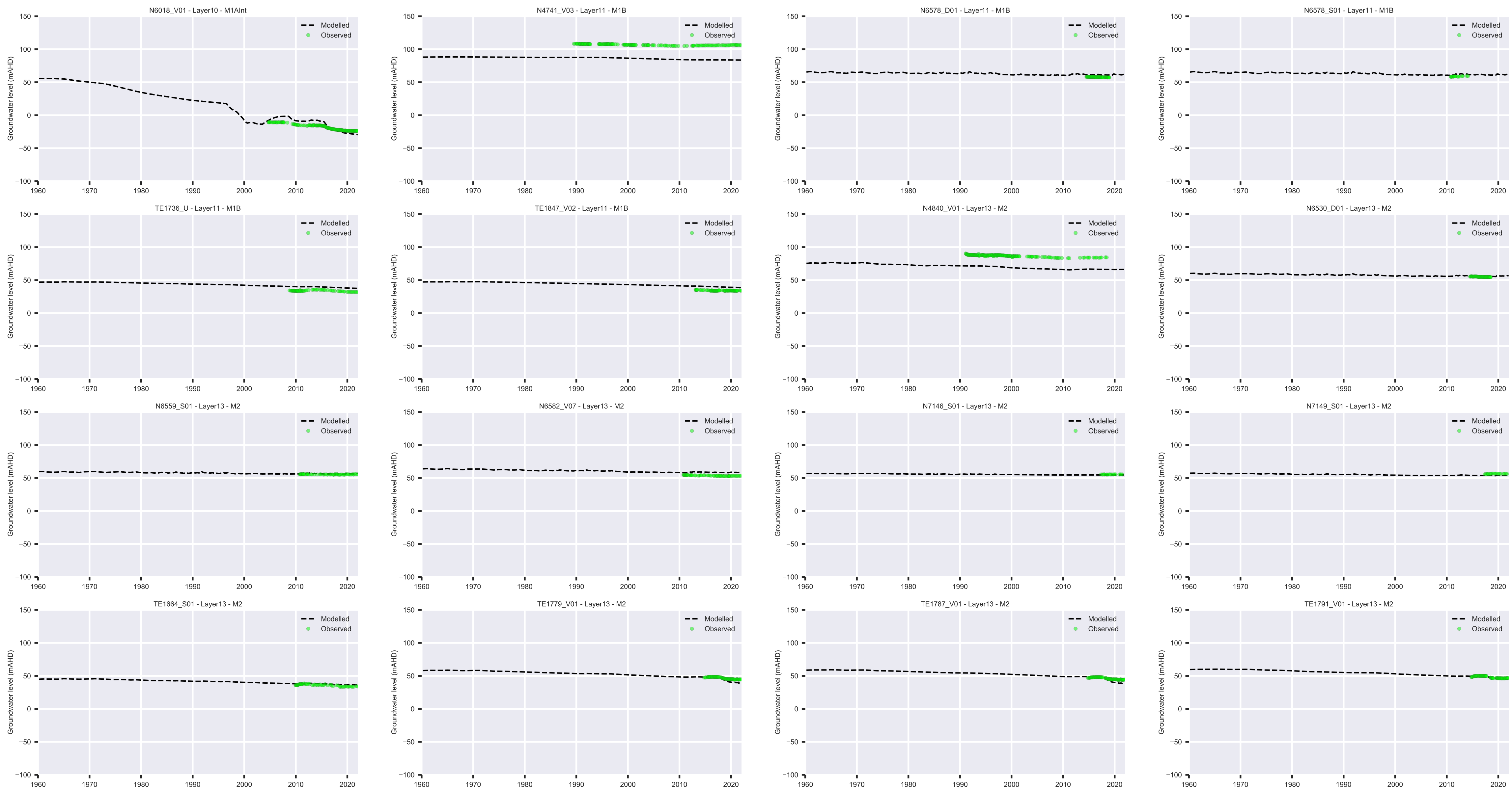

N6018_V01 - Layer10 - M1AInt
N4741_V03 - Layer11 - M1B
N6578_D01 - Layer11 - M1B
N6578_S01 - Layer11 - M1B
TE1736_U - Layer11 - M1B
TE1847_V02 - Layer11 - M1B
N4840_V01 - Layer13 - M2
N6530_D01 - Layer13 - M2
N6559_S01 - Layer13 - M2
N6582_V07 - Layer13 - M2
N7146_S01 - Layer13 - M2
N7149_S01 - Layer13 - M2
TE1664_S01 - Layer13 - M2
TE1779_V01 - Layer13 - M2
TE1787_V01 - Layer13 - M2
TE1791_V01 - Layer13 - M2
Modelled
Observed
Groundwater level (mAHD)

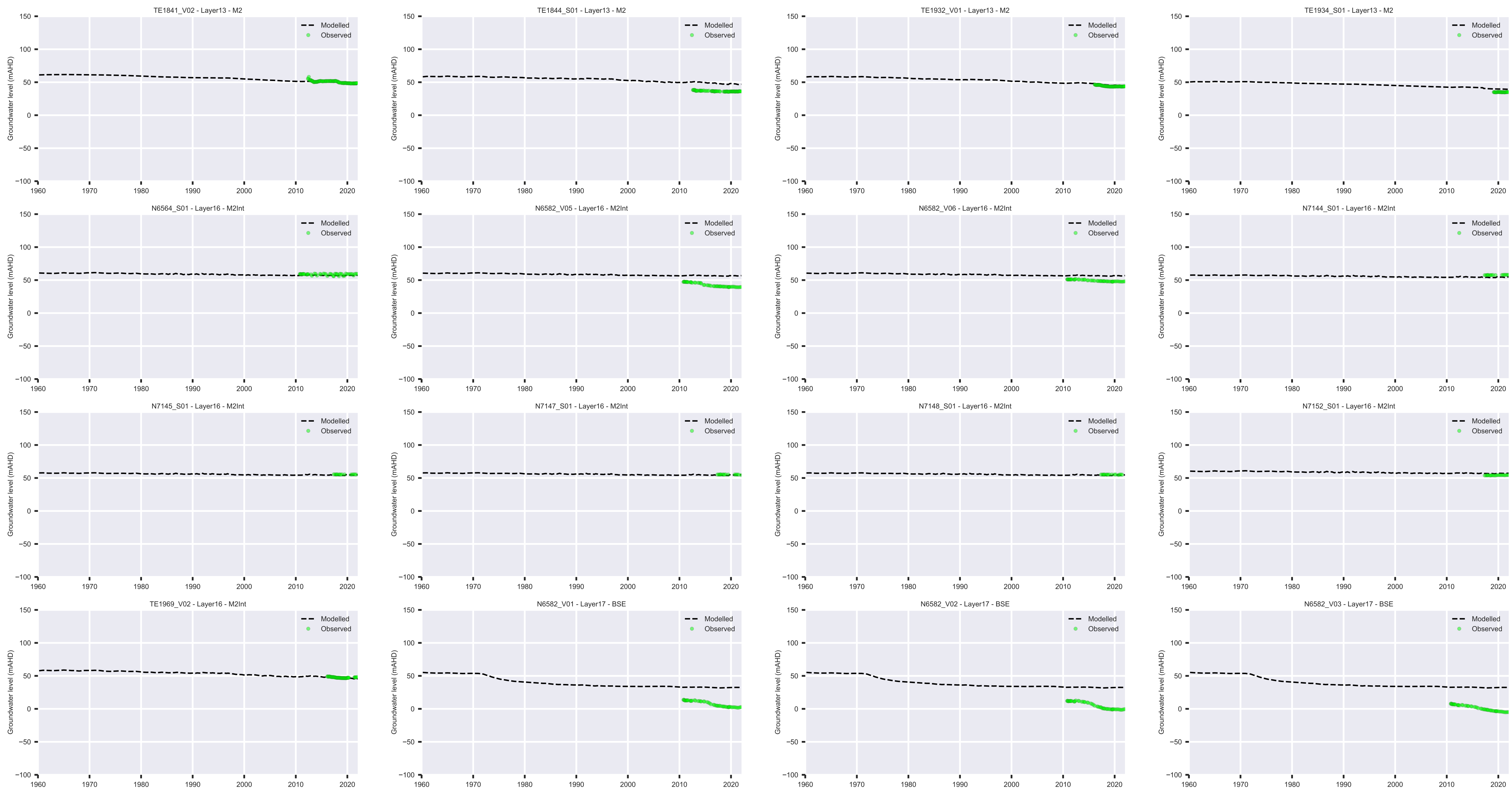
TE1841_V02 - Layer13 - M2
TE1844_S01 - Layer13 - M2
TE1932_V01 - Layer13 - M2
TE1934_S01 - Layer13 - M2
N6564_S01 - Layer16 - M2Int
N6582_V05 - Layer16 - M2Int
N6582_V06 - Layer16 - M2Int
N7144_S01 - Layer16 - M2Int
N7145_S01 - Layer16 - M2Int
N7147_S01 - Layer16 - M2Int
N7148_S01 - Layer16 - M2Int
N7152_S01 - Layer16 - M2Int
TE1969_V02 - Layer16 - M2Int
N6582_V01 - Layer17 - BSE
N6582_V02 - Layer17 - BSE
N6582_V03 - Layer17 - BSE
Modelled
Observed
Groundwater level (mAHD)
150
100
50
0
−50
−100
1960
1970
1980
1990
2000
2010
2020

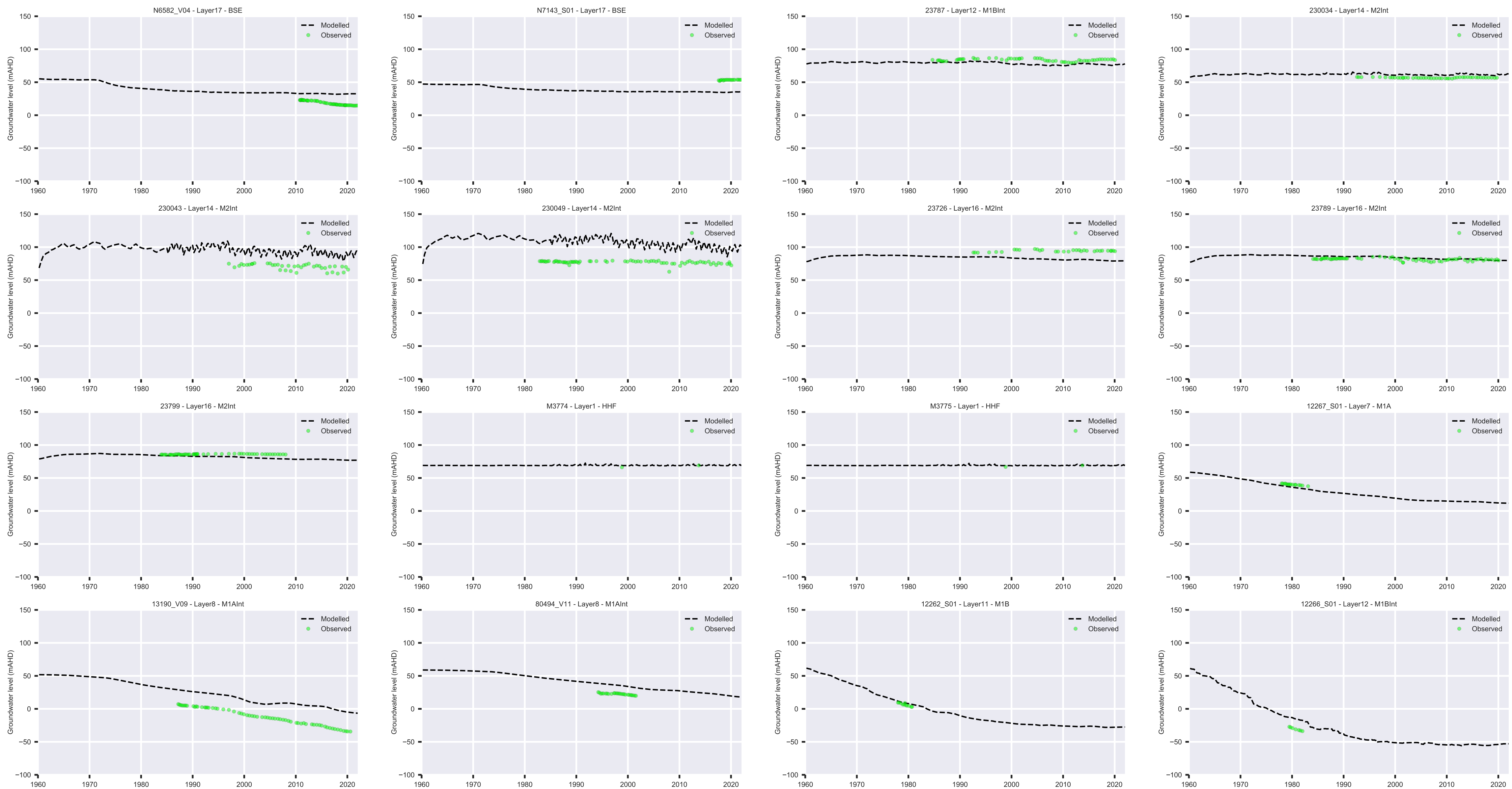
N6582_V04 - Layer17 - BSE
N7143_S01 - Layer17 - BSE
23787 - Layer12 - M1BInt
230034 - Layer14 - M2Int
230043 - Layer14 - M2Int
230049 - Layer14 - M2Int
23726 - Layer16 - M2Int
23789 - Layer16 - M2Int
23799 - Layer16 - M2Int
M3774 - Layer1 - HHF
M3775 - Layer1 - HHF
12267_S01 - Layer7 - M1A
13190_V09 - Layer8 - M1AInt
80494_V11 - Layer8 - M1AInt
12262_S01 - Layer11 - M1B
12266_S01 - Layer12 - M1BInt
Modelled
Observed
Groundwater level (mAHD)

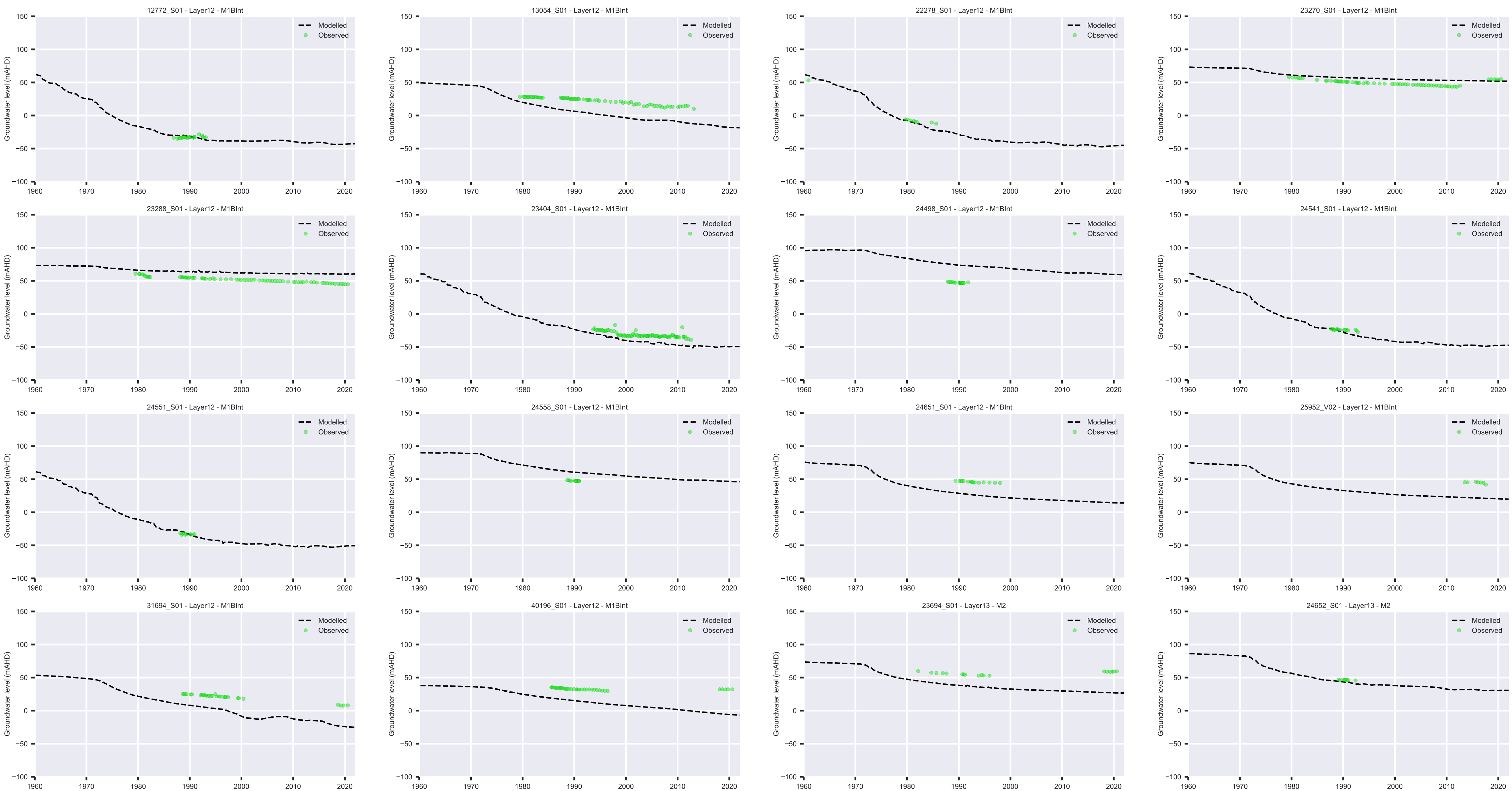

12772_S01 - Layer12 - M1BInt
13054_S01 - Layer12 - M1BInt
22278_S01 - Layer12 - M1BInt
23270_S01 - Layer12 - M1BInt
23288_S01 - Layer12 - M1BInt
23404_S01 - Layer12 - M1BInt
24498_S01 - Layer12 - M1BInt
24541_S01 - Layer12 - M1BInt
24551_S01 - Layer12 - M1BInt
24558_S01 - Layer12 - M1BInt
24651_S01 - Layer12 - M1BInt
25952_V02 - Layer12 - M1BInt
31694_S01 - Layer12 - M1BInt
40196_S01 - Layer12 - M1BInt
23694_S01 - Layer13 - M2
24652_S01 - Layer13 - M2
Modelled
Observed
Groundwater level (mAHD)

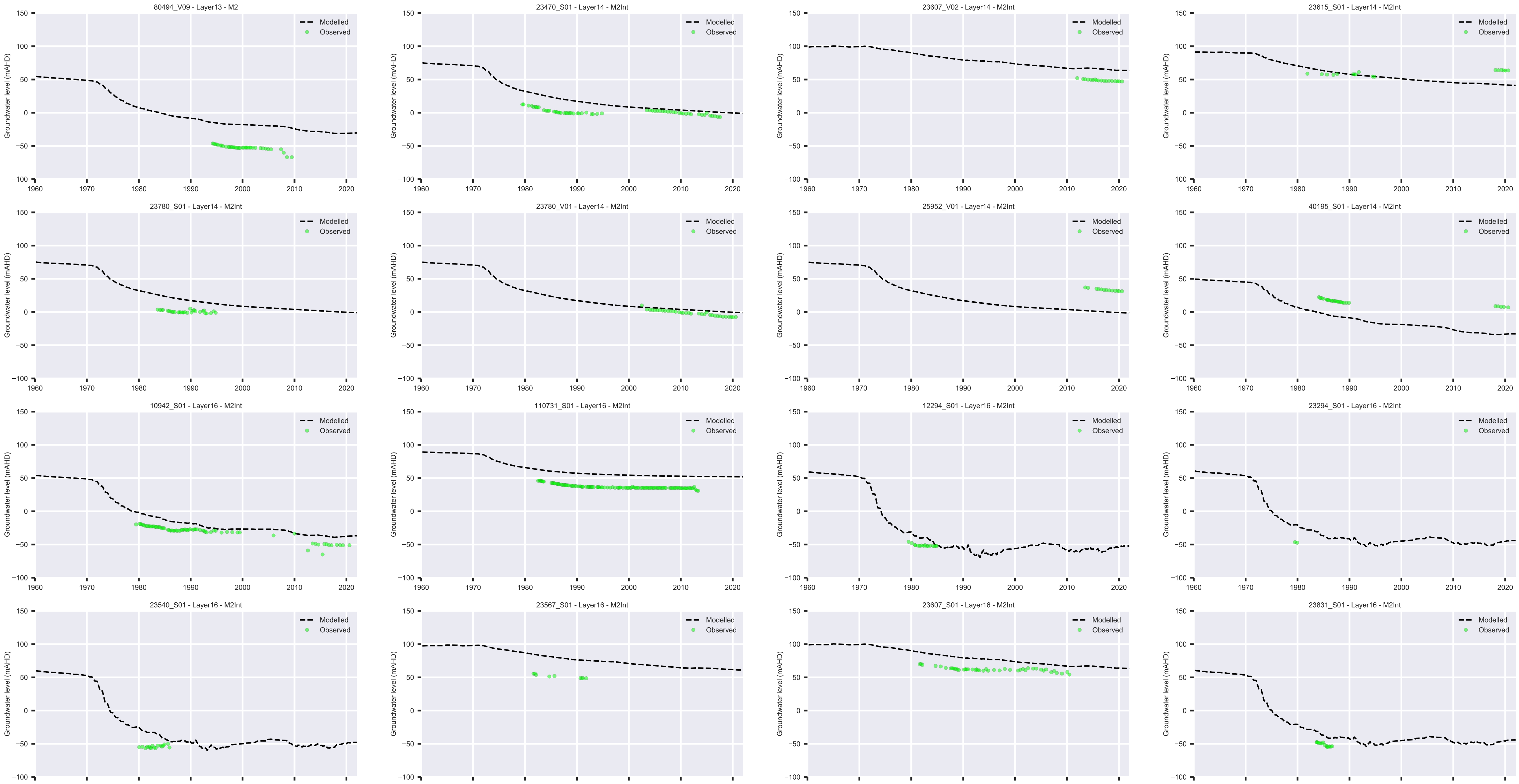
80494_V09 - Layer13 - M2
23470_S01 - Layer14 - M2Int
23607_V02 - Layer14 - M2Int
23615_S01 - Layer14 - M2Int
23780_S01 - Layer14 - M2Int
23780_V01 - Layer14 - M2Int
25952_V01 - Layer14 - M2Int
40195_S01 - Layer14 - M2Int
10942_S01 - Layer16 - M2Int
110731_S01 - Layer16 - M2Int
12294_S01 - Layer16 - M2Int
23294_S01 - Layer16 - M2Int
23540_S01 - Layer16 - M2Int
23567_S01 - Layer16 - M2Int
23607_S01 - Layer16 - M2Int
23831_S01 - Layer16 - M2Int
Modelled
Observed
Groundwater level (mAHD)

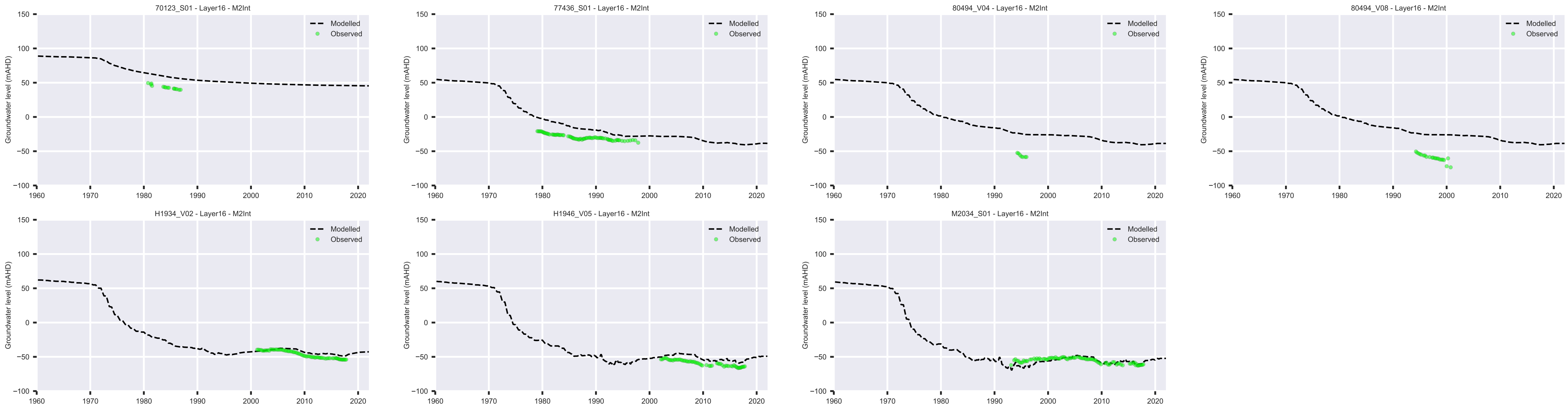
70123_S01 - Layer16 - M2Int
77436_S01 - Layer16 - M2Int
80494_V04 - Layer16 - M2Int
80494_V08 - Layer16 - M2Int
H1934_V02 - Layer16 - M2Int
H1946_V05 - Layer16 - M2Int
M2034_S01 - Layer16 - M2Int
Modelled
Observed
Groundwater level (mAHD)
150
100
50
0
−50
−100
1960
1970
1980
1990
2000
2010
2020

ghd.com

The Power of Commitment